UNIVERSITAT DE BARCELONA

Development of electrochemical platform for DNA sensing

Thesis dissertation to qualify for Ph. D. in Nanoscience

Presented by:

Wilmer Alfonso Pardo

Supervised by:

Dr. Mònica Mir Llorente **Dr. Josep Samitier**

Departamento de Electrónica
Facultad de Física
Barcelona, 2016

UNIVERSITAT DE
BARCELONA

UNIVERSITAT DE
BARCELONA

Development of electrochemical platforms for DNA sensing

A la sangre de mi sangre, porque somos fuego y fluidez
A ti, Madre
A ti, Hijo
A ustedes, Hermanos
A ustedes, Familia
Al universo, por ser fuego y fluidez

A.M.G.D.

Plasmar unas letras en muchas hojas de papel, es solo un pequeño reconocimiento del largo y gran trabajo que mucha gente realizó durante este proyecto. Es difícil establecer el alcance de la ayuda y del trabajo mutuo de las muchas personas que estuvieron en mi camino durante la realización de esta tesis doctoral.

Miles de agradecimientos a:

El profesor Josep Samitier, agradezco su confianza y el brindarme la oportunidad de pertenecer a este instituto, fue mi casa durante mi estadía en Barcelona, una buena casa.

A la gente del grupo de nanobioingeniería por su compañía, aún a pesar de mi poca participación en muchos de sus eventos. Especial mención a Miriam, gran trabajo y ¡¡¡mucho orden!!! A David, gracias por toda tu ayuda, ustedes dos son el alma del laboratorio.

Los que ya no están, Reyes y Javier, por sus aportaciones a este trabajo; Rossella por su humor negro y exageradamente crítico; Bogachan, gran amigo y compañero de tertulias. A José Luis, siempre era bueno reír contigo. A las chicas de máster Ana y Raquel, me veía en ustedes cuando empecé.

Erika, fue bueno tener a otra colombiana en casa… por y para todo lo que se vivió.

Las personas de Genomica S.A.U. comprometidas con la causa.

Samuel y Judit, porque ¿quién dijo que el trabajo no es divertido?

Las personas externas al laboratorio, a ellos y ellas, pilares y apoyos en cada cambio estacional.

Alexa, por tu bonita compañía.

Harold, con especial cariño, después de todo, somos lo que hacemos.

Ximena, que me da lo mejor que puede una persona dar a otra, su tiempo… ¡Infinitas Gracias! … por todo lo que significas y edificas. Un beso eterno.

Barcelona, casi casi, otra Bogotá…y yo amo Bogotá.

Mi familia…Lo son todo.

Mònica… podría decir muchas cosas sobre ella, pero como ella lo sabe, no soy de escribir mucho, más bien conciso y certero…usted, profe: mi***ÁNGEL*** en Barcelona. Por siempre agradecido.

A todos los anteriores y los que hicieron falta, gracias totales.

Index

Acronyms

CDTI: Centro de Desarrollo Tecnológico Industrial

CENIT: Consorcios Estratégicos Nacionales de Investigación Técnica

IBEC: Institute for Bioengineering of Catalonia

UB: Universitat de Barcelona

POC: Point-of-care

LOC: Lab-on-a-chip

PCR: Polymerase Chain Reaction

DNA: Deoxyribonucleic acid

ssDNA: single strand DNA

dsDNA: double strand DNA

RNA: Ribonucleic acid

PNA: Peptide Nucleic Acid

CAU: Central Automatized Unit

OECD (OCDE): Organization of Economic Cooperation and Development

GMO: Genetically Modified Organism

IUPAC: International Union of Pure and Applied Chemistry

SELEX: Systemic Evolution of Ligands by Exponential Enrichment

SPR: Surface Plasmon Resonance

SPRi: Surface Plasmon Resonance imaging

eSPR: Electrochemical Surface Plasmon Resonance

RM: Resonant mirror

TIRF: Total Internal Reflection Fluorescence

GNP: Gold Nanoparticle

FET: Field Effect Transistors

PVC: Polyvinyl Chloride

ISFET: Ion Selective Field Effect Transistor

QCM: Quartz Crystal Microbalance

WE: Working Electrode

RE: Reference Electrode

CE: Counter Electrode

CV: Cyclic Voltammetry

DPV: Differential Pulse Voltammetry

SST: Single Surface Technique

DST: Double Surface Technique

ITO: Indium Tin Oxide

ASV: Adsorption Stripping Voltammetry

HRP: Horseradish Peroxidase

ALP: Alkaline Phosphate

MEMS: Microelectromechanical Systems

PDMS: Polydimethylsiloxane

NSA: Nonspecific adsorption

ALD: Atomic Layer Deposition

CVD: Chemical Vapor Deposition

PVD: Physical Vapor Deposition

MSA: Molecular Self-assembly

SAM: Self-assembled Monolayer

UHV: Ultra High Vacuum

PEG: Polyethylene Glycol

MCH: Mercaptohexanol

CP: Capture probe

Fc: Ferrocene

CP-MCH: Capture probe-Mercaptohexanol SAM

LAM-PEG: Lipoic Acid Maleimide-Polyethylene glycol SAM

MalPEG: Maleimide-Polyethylene glycol disulphide SAM

XPS: X-ray Photoelectron Spectroscopy

PSI: Phase Shift Interferometry

STM: Scanning Tunneling Microscopy

ECI: Electronic Control Interface

CEMIC: Centro de Ingeniería de Microsistemas para Instrumentación y Control

COP: Cycle Olefin Polymer

COC: Cycle olefin Copolymer

PC: Polycarbonate

PEEK: Polyether ether ketone

LOD: Limit of detection

Motivation and work objective

This thesis is framed within a research and development (R & D) project in collaboration with the industry. This project was funded by Centro de Desarrollo Tecnológico Industrial (CDTI) with a CENIT under the name of "New strategies based on biomarkers for the detection and prognostic of cancer, and novel treatments development and response prediction (ONCOLOGICA)". Our part of the project was established jointly with the molecular diagnostics company Genomica S.A.U., the Nanobioengineering group in the Institute for Bioengineering of Catalonia (IBEC), and the University ofBarcelona (UB). The main objective within the project was the development of a commercial point-of-care (POC) diagnosis system for cancer detection. For this purpose, a lab-on-a-chip (LOC) device was developed, integrating a polymerase chain reaction (PCR) to amplified and label the DNA sequences specific for this illness and an electrochemical DNA biosensor, to specifically hybridize and detect the illness sequences in the LOC. The LOC functionality requires electronics to move the fluidic pumping, the heating for the PCR and the read-out for the electrochemical detection.

Four units integrate the overall device,a PCR thermocycler, a microfluidic system of channels and confinement liquids chambers, an electrochemical biosensor array, and a central automatized unit (CAU) to control previous described units. See scheme 1 to whole system.

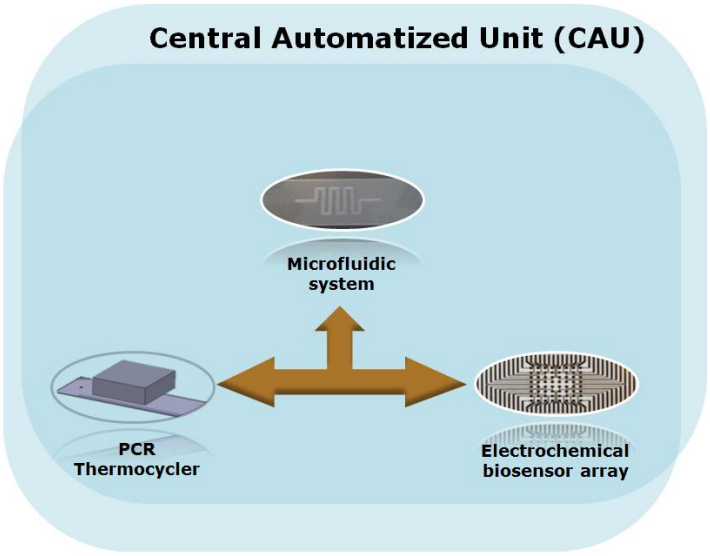

Scheme 1: POC device schematic

Regarding the processes of design, manufacture and development of the central unit containing the electronics for the automatization of the heating with a peltier, control of fluidic pumping and electrochemical read-out were in charge the group of Dr. Manuel Puig of the UB. All information, corresponding to the development of these systems belongs to other parallel doctoral thesis. Consequently, those results are not shown in this thesis. Genomica Company has a commercialized colorimetric macroscale kit for cancer detection where the PCR has been already optimized and they adapt their PCR to the mini-PCR integrated in the cartridge. We developed part of the characterization of the product obtained from the integrated PCR in the cartridge. Confidential information about the details of the PCR developed by the Genomica Company cannot be included in this thesis due to the private nature of the project. The design of the microfluidic cartridge that integrates the PCR unit and the biosensor unit was performed by our group, but supervised by Dr. Antoni Homs. We developed the fabrication and characterization of the microfluidics related with the electrochemical cell. We performed the design and fabrication of the electrochemical biosensors integrated in the LOC. For this purpose, different biosensors interfaces and biosensor configurations were studied based on the better efficiency of the biosensor sensitivity and selectivity.

During the five years of development of this project, significant progress was achieved. So, after hundreds of tests on materials, manufacturing techniques, detection strategies and prototypes with different architectures, among other items, it was decided to follow with the project and engage a company with the technology for mass production of electronics and microfluidics of a similar device based on the developments achieved so far. In the final part of the development of this LOC, the German company Microfluidics ChipShop GmbH was incorporated into the new project. The objective of this new project was the same that the above, but with the main direction of obtaining a final commercial device.

ChipShop is contributing with their extensive experience in microfluidic issues and so are responsible for the design that integrates alow-cost easy to fabricate microfluidic systems and electrodes array, integrated with an affordable electronic device that controls fluidics, heating and electrochemical readout, but based on the results obtained so far.

At light of the new commercial nature of the final goal, the new changes proposed by ChipShop are essential to reduce the manufacturing costs. They proposed a change in the structure of the microfluidic cartridge and a reduction of the electro-array size and geometry setting. We have characterized the microfluidics related

with the electrochemical cell and optimized the performance of the different fabricated and designed electrochemical arrays. From these characterizations, we collaborate in the improvement of the designs and fabrication techniques for the fluidics and the arrays. We integrated and optimized the developed electrochemical biosensors for the new electrochemical cell. The IBEC, Genomica S.AU., Microfluidics ChipShop GmbH and UB collaboration is even today.

Outline of the thesis

To achieve a better understanding of this document in each chapter we present an order of definition, advantages and applicability of the concepts. In this manner,chapter one presentsa biosensor and LOC definition and some generalities and trends in the field of biosensors for medical diagnosis. The DNA sensors are introduced especially those that working with electrochemical techniques. Then, the hybridization event and the different strategies of duplex formation detection in biosensors are described, followed by the state of the art of commercial DNA arrays.

Chapter 2 is about the DNA biosensor interfaces, due to its importance in the efficiency of the sensitivity and selectivity of these devices. The molecular organization of the self-assembledDNA bioreceptor is studied under different type of linkers. The optimization and characterization of the electrochemical biosensing interface (BSI) for the functionalization of the gold surface electrodes on an ultraflat surface and on the LOC is also reported.

Chapter 3is focused in the design, materials, fabrication, and characterization of the microfluidic cartridge and the electrochemical array as well as its integration. The evolution of the different designs, the fabrication techniques used for theseand the differences observed in all the prototypes are explained.

Chapter 4 contains the integration of the biosensor interface optimized in chapter 2 with the fabricated cartridge introduced in chapter 3. The different optimizations of the electrochemical DNA biosensor array obtained with the hybridization of the amplified DNA sample are shown in this chapter.

Chapter 5 is dedicated to summarize all the work presented and general concluding remarks.

Finally, chapter 6 is a summary in Spanish of the work.

Chapter one

1.1 Introduction

During the last decades the convergence of the pure sciences (biology, physicsand chemistry, among others) and technology (engineering, electronics, computing) results in extraordinary achievements in various sectors, which have increased their use over time.In general this union is called biotechnology or bioengineeringand one of the best definition of this new field of study is given by the Organization of Economic Cooperation and Development (OECD); "the application of scientific and engineering principles to the processing of materials by biological agents"[1]. More simply, biotechnology makes use of biological systems and processes to manufacture useful products and provide services. Production may be carried out by using intact organisms, such as yeasts and bacteria, or by using natural substances (e.g. enzymes or nucleic acids) from organisms.

The new tools provide an approach to problem solving and these are considered as a collection of essential outfits in the advancement of products in the pharmaceutical, medical, chemical, biological and clinical industries, as well as in research fields.

Within the field of research in biomedical applications, the current trend is to develop point-of-care devices. These new technologies involve materials and procedures capableof interact with living tissue or biomolecules.Most of the designsand materials used in these platforms arealso mimickingbiosystems. Taking advantage that offers millions of years of nature evolution, the use of biomoleculesoffervery high selectivity to specific target for the functionality of the biomaterial under study.

In this way, analytical chemistry is one of the fields benefited bybiotechnology. The ability to detect bioanalytes on inorganic material opens fields for many applications:

- Disease diagnosis
  - Cancer, Diabetes, viral infections[2-4]
- Genetically Modified Organism(GMO) and food
  - Transgenic food, gene determination[5-7]
- Medicaland Forensic sciences
  - Drug detectors, organic or inorganic traces, genetic identification, and paternity[8-12]
- Environmental issues

- Pollution, heavy metal identifications in air or water, toxins concentration in aquatic ecosystems[13-18]

❖ Industrial process control
- Gases detection, microorganism detection[19-23]

❖ Veterinarian issues
- Parasite control, viral detections[24-26]

❖ Military Security
- Biosecurity and biodefense, detection of dangerous chemical and biological agents, explosive detection[27-30]

For this purpose,it is necessary to have a versatile tool. Biosensors are the most recent and relevant platformsto build up a low cost, portable, selective and sensitive analytical devices[31-37].

1.2 DNA molecule

The deoxyribonucleic acid (DNA) is one of the most widespread biomolecules used in biosensors, due to its easy synthesis, stability but mainly because of the large information that can be extracted from their sequences of bases.

DNA molecule is a polyelectrolyte chain and joint with the RNA formed the called nucleic acids. DNA is an organic compound containing carbon, hydrogen, oxygen and nitrogen and has a double helix structure, this mean that the DNA molecule is really a molecule composed of two strands. Each one of these strands is a polymeric compound of nucleotide subunits. Each nucleotide is composed of three units: a sugar molecule called deoxyribose, a phosphate group and one of four nitrogenous compounds called bases: adenine (A), thymine (T), cytosine (C) and guanine (G). The deoxyribose molecule occupies the center of the nucleotide and in its flanks there is a phosphate group (to a side) and a base (on the other side). The phosphate group is in turn attached to the adjacent deoxyribose nucleotide chain. Nucleotides of each of the two chains that form DNA establish a specific association with the corresponding of the other strand. Due to the chemical affinity between the bases, nucleotides containing adenine always engage with those containing thymine, and cytosine containing those containing guanine (see Fig 1.1)[38].

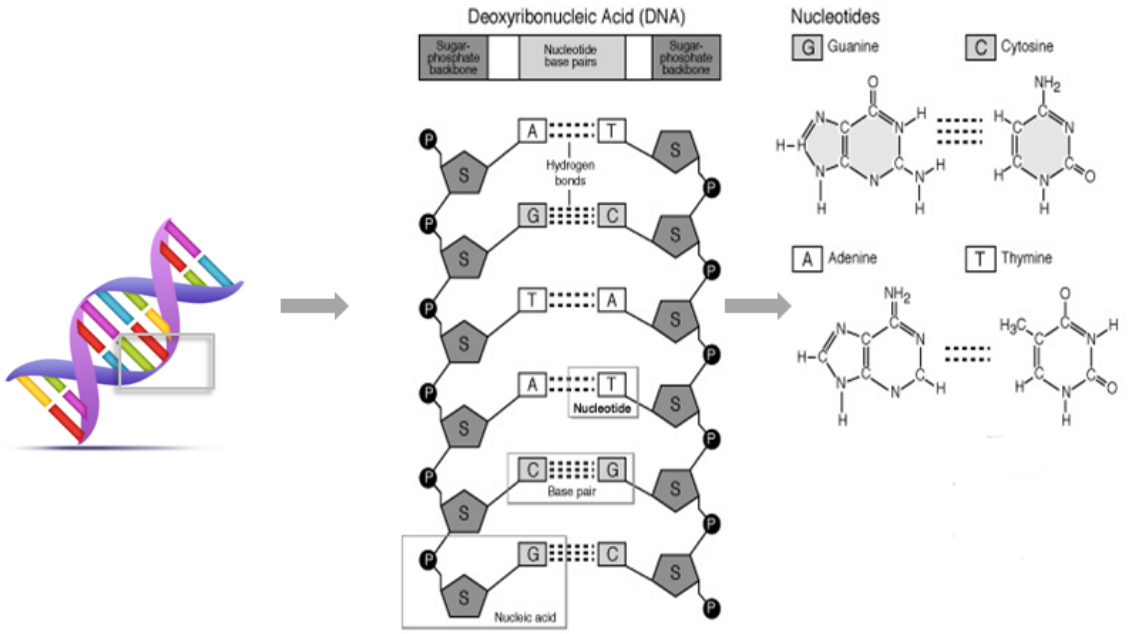

Figure 1.1: DNA structure

The complementary bases are joined together by weak chemical bonds called hydrogen bonds and these interactions are those that give the DNA its spiral shape. This specific attraction between nucleotides is the base of hybridization process. A single strand of DNA (ssDNA) will hybridize to another single strand of DNA if their nucleotides sequences are complementary(figure 1.2). Besides, the complementarity of nitrogenous bases responds to a specific order of consecutive matching nucleotides. Electrochemical detection of the hybridization event (duplex DNA formation) is based on changes of electrochemical behaviors. The detection can be due to changes in the nucleic acids electroactivity, or labeling of the target or the probe with electroactive species by covalently bounds, or nanoparticles functionalized probes, or changes in various electrochemically detectable DNA properties, which are related to changes in the DNA structure resulting from the hybridization step[39]. For this work, the detection of this event is possible due to the redox label that contains the DNA target in their structure.

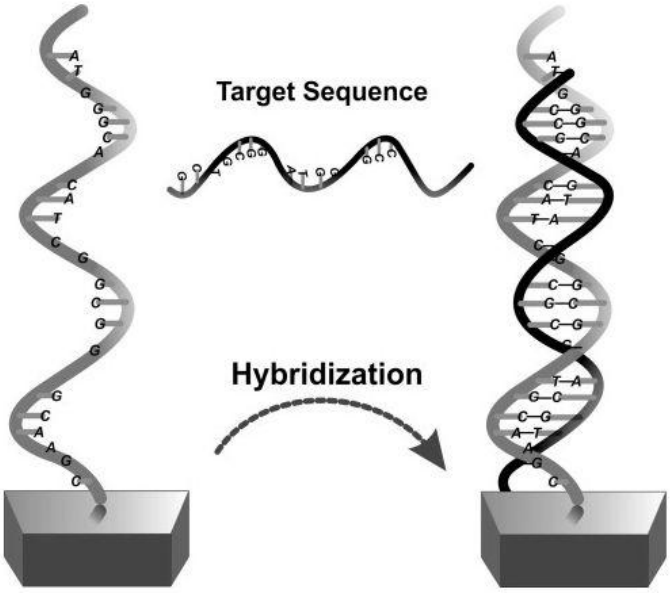

Figure 1.2: Hybridization event

1.3 Biosensors

Biosensors arise as tools capable of producing continuous signals that are proportional to the amount of binding molecules that react on the surface of a sensor. Biosensors according withthe IUPAC (International Union of Pure and Applied Chemistry) definition done in1999 are: "A device that use specific biochemical reactions mediated by isolated enzymes, immunosystems, tissues, organelles or whole cells to detect chemical compounds usually by electrical, thermal or optical signals" [40].

In the literature, there are as many biosensor definitions as authors. There are those who argue that a biosensor involves only bio-supramolecular structures [41, 42]; others include in their definition all systems involving any molecules related with the life [43-47]. There are also those who take off this group to those devices having electronic parts and/or integrated fluidic [48, 49], to name a few cases.

However, still out of this definitions are the non-enzymatic proteins and complex biomolecules such as DNA and RNA types. For this reason, the scientific community involved many more features to this definition as it advances in the use of these devices. We can get a more complete definition based on new materials, structures

and techniques used today. Thus, an integral and current definition of biosensor is this one: biosensors are devices that detecting, monitoring and transmitting information of biophysical and/or biochemical specific reactions with high specificity, that occurring before, during and after over interfaces that involving a bioelement (or several) as recognition element and one transducer (or more). This transducer would be capable of transforming those changes in electrochemical, electrical, optical, thermal, heat or sound output signals, among others, for further processing of data [50, 51].

Inside this maelstrom of definitions, there is unanimity on the constituent components of a biosensor, a recognition element and a transducer. The recognition element or bioreceptor is a biomolecule able of recognizing, in a very selective and sensitive way,the target analyte in a complex matrix. These biomolecules are usually attached on the sensor surface, although in some cases can be found in solution, performing a bulk detection. The transducers are tools that transform this biological interaction event into a quantifiable output signal[52]. The particularity of a biosensor is that these two components are integrated into a single device as shown in scheme 1.1. This combination allows the detection, measurement and quantitation of the analyte without previous separation.

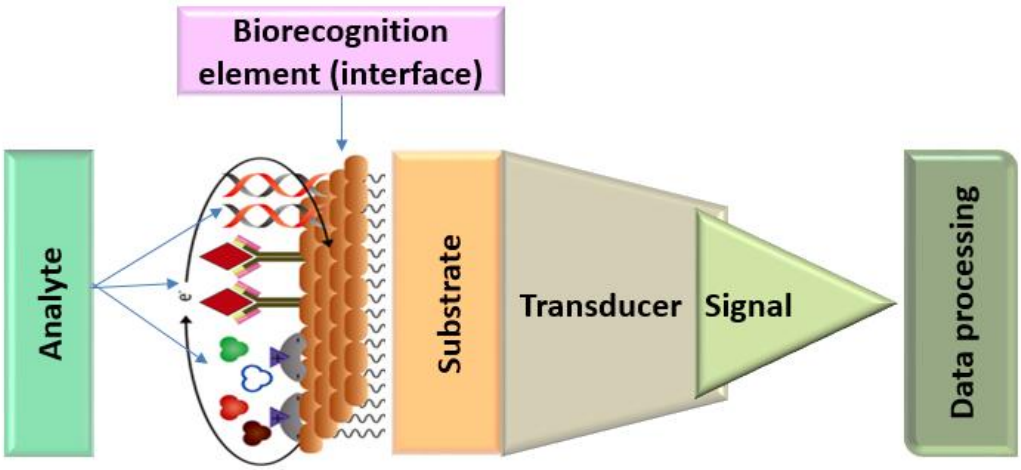

Scheme 1.1:Scheme of the different biosensor parts

Therefore, there are classifications of biosensors depending on the nature of its constituent components. Considering the bioreceptor, the systems that use antibodies as recognition element are called immunosensors [53], and are one of the most widespread types of biosensors, with many applications mainly when it is involved a biomarker protein.

Among this classification, are included the enzymatic sensors, that uses enzymes as intermediaries of a chemical process. In this category are the famous glucose sensors [3]. These biosensors have been so commercially successful that represent 85% of the global market. However, they are not the only sensors that use enzymes. There are transferases sensors for determining xenobiotics [54, 55], with hydrolases for sucrose [56, 57], containing liasas for analysis of citric acid [58] and isomerases for detecting hormones or their precursors [59], among others.

Also with the great knowledge offered by the Genome Project, made that nucleic acidenjoyed a successful spread to this field.Inside these types of biosensors, the bioreceptor is either ribonucleic acid (RNA) or deoxyribonucleic acid (DNA). There are those that using natural or its synthetic forms of DNAs and RNAs. Ordinations as varied as plasmids and peptide nucleic acid (PNA) are present as synthetics bioelements [60-63]. The success of these biosensors is given by the extraordinary affinity of the nitrogenous base pairs of the polyelectrolyte chains of these acids. Furthermore, using amplified DNA fragments techniques, like Polymerase Chain Reaction (PCR),makes this molecules easy to detect in a very sensitive way and so the applications of DNA arrays or genosensors, as they are also called, are countless [64-69].In addition, DNA is being used also for detecting any type of analytes, besides ssDNA complementary strands, called in this case aptamers. Using genomic libraries techniques and in vitro selection techniques, like Systemic Evolution of Ligands by Exponential Enrichment (SELEX), the sequences of these DNA molecules can be structured to link specifically to any kind of molecule..

The type of reaction that can be generated between the analyte and the bioelement it can lead to other classification also. So, regarding the type of interaction if the bioreceptor binds the analyte, the sensor is classified as an affinity sensor. On the other hand, if the bioelement and analyte result in a chemical change that can be used to measure the concentration of a product, the biosensor is called metabolic sensor. Another possibility is that the bioreceptor is combined with the analyte and it does not change chemically but converts it to a sub-product, then the biosensor is called catalytic sensor [70, 71].

Furthermore, from the point of view of the transducer the classification of biosensors are based on the type of reading of the output signal generated. So, the thermometric biosensors are those involving a temperature sensor and it measures the amount of heat generated in bioreactions. This is mainly employed in the food and cosmetic industries [72-74].

Piezoelectric materials such as quartz have a stable vibration frequencywhen an electrical signal at certain frequencies is applied in the quartz disc. Thereby, a defined mass and shapes of the piezoelectric transducer, brings a known oscillation frequency that depends on the intensity of the electrical signal input. Thus, an addition of tiny mass on the surface transducerproduces a change of the oscillation frequency that can be measured electrically. It is the principle under acoustic biosensors work[75, 76]. Another example of piezoelectric biosensor isthe microcantilevers. In this case, a mechanical change is detected when the tip of the cantilever bend with themicro-weight provided by the attached biomolecules after the interaction with the bioreceptor attached on the cantilever [77-79]. Its applications are mainly in the foodindustry and clinical analysis.

From the standpoint of optics, the common principle of these biosensors is the behavior of light within the limits of two media with different refractive index. Some fundamental properties such as intensity, phase and the reflected light angle are measured directly and used to calculate the mass of analyte integrated in the biosensor. The refractive index at the interface changes in proportion to the mass changes at the surface, that is, upon binding of molecules [80]. Techniques such as Surface Plasmon Resonance (SPR), Optical wave guiding or Resonant Mirror (RM) and Total Internal Reflection Fluorescence (TIRF), Optical fibers, evanescent wave-based sensor or fluorescence spectroscopy, DNA-gold nanoparticles (GNPs), among others [81] are used to detect these changes.

An example of these optical sensors is the optical fiber, which is a dielectric physical entity that carries information by electromagnetic waves, such as light.These waves must have a direction parallel to the axis of the fiber core. Generally, optical fiber sensors have the capture probe at one end. After hybridization with the target DNA, measured changes in fluorescence intensity between the duplex and a fluorescent label [82, 83]. SPR and evanescent wave genosensors measure changes in superficial optical parameters of a metal-dielectric interface caused by a chemical or biochemical reaction due to the hybridization event [84, 85].Optical biosensors based on a change of color due to a chemical reaction, can be read out with absorbancespectrophotometer, such enzyme linked oligonucleotide array or directlywith the eyes as the pregnancy test biosensor based on GNP. In this last case, the GNP has its fundament on the color change undergone by the gold nanoparticle dispersed (red) when passing to larger aggregates (blue). These platforms used a sandwich system of three single DNA strands. Two of them are capture probes, which are functionalized respectively with GNP or on latex microparticles and on the nitrocellulose substrate. The third target is the DNA

target, which has the two complementary sequences of the capture probes on its ends. When a double hybridization occurs, GNP or latex microparticles aggregates, with a subsequent change on solution color [86].

Fluorescence spectroscopy is based on the use of fluorophores as a label directly to the DNA target or indirectly in the case of the more voluminous quantum dots. These nanocrystals are excellent labels for biomolecules because they are most stable, monochromatic and brighter than other fluorophores[87]. Depending on its size, onceare excited releases a very characteristic wavelength in the visible spectrum. Thus, the labeled analyte is easily detectable. These quantum dots can be incorporated to other optical techniques as SPR [88]. Besides the label of the target, this fluorophores can be attached to the capture probe forming a beacon platform, see figure 1.3. For this purpose, a specific shape of the capture probe is required in a single strand DNA hairpin fashion. This capture probe is labeled in an end with a fluorophore and in the other end with a quencher. The hairpin configuration makes that fluorophore and quencher keep closer avoiding fluorescence emission. When DNA target hybridize and duplex formation occurs, the hairpin shape disappears, lifting far the fluorophore (or dye) from the quencher and so,the fluorophore emits its fluorescence [89].

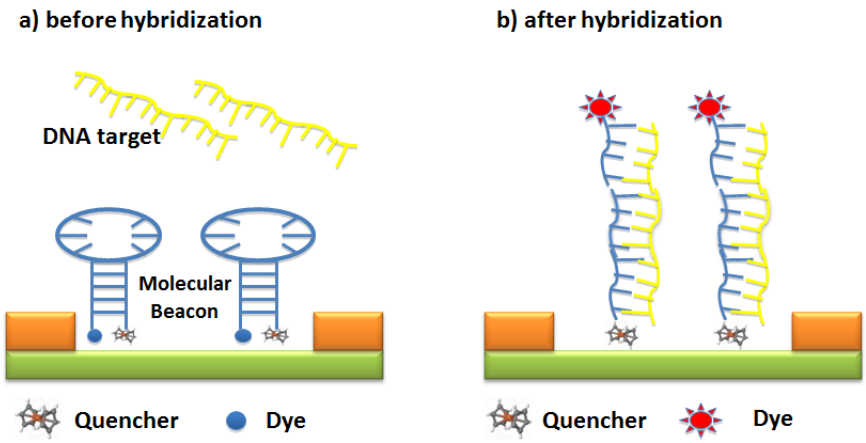

Figure 1.3: Molecular beacon platform a) fluorophore not excited, b) fluorophore excited

Although the optical biosensors are widespread, those have some limits. The big disadvantage of the optical DNA biosensor is the high cost of labels and the transductors, besides the difficulty for its miniaturization limited its applicability. This has prevented its use beyond of the research or in laboratory analysis, where

voluminous and expensive equipment are used by experimented technician to perform genomic arrays.

Electrochemical biosensors overcome the limitations of cost and miniaturization presented in optical biosensors and opens the possibility to apply these devices to POC and home diagnosis as happened with electrochemical glucose sensors. Biosensors with electrochemical transducers are based on the principle of production or consumption of electrons or ions, from a redox solution, from a label or even directly from the biomolecules. According the IUPAC definition (1999), these biosensors may be potentiometric, amperometric, voltammetricsurface charge using Field Effect Transistors (FET), see figure 1.4, and conductimetric. The applications of them are in many branches of science, engineering and medicine.

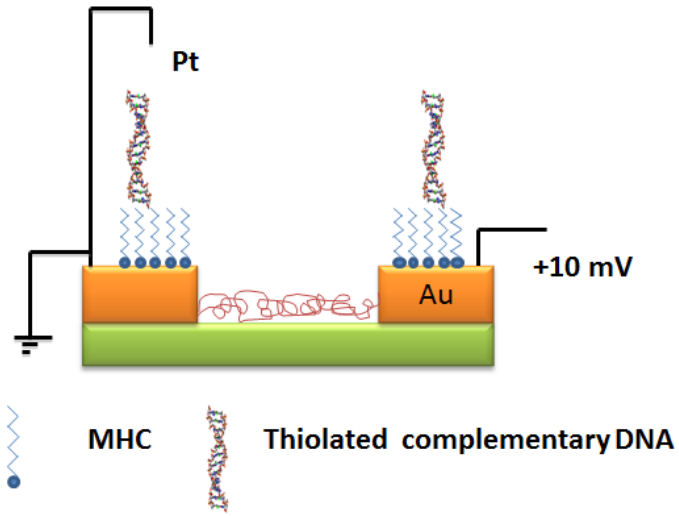

Figure 1.4: Field Effect Transistors platform

1.3.1 Biosensor evolution

The majority of biosensors involve an immobilization step of the bioelement recognition on the sensor area. Paradoxically, the first biosensor based on enzymatic detection of glucose described in 1962 by Clark and Lyons[90]had no enzyme immobilized directly on the electrode. This consisted of confining a solution of glucose oxidase (bioreceptor) between two semipermeable dialysis membranes connected to a platinum electrode (transducer) in order to detect the concentration of glucose in a blood sample. They measure the oxygen concentration surrounding to the electrode surface, which was proportional to the amount of glucose in the sample. Thereafter several authors have marked the evolution of these devices. In 1962 Guilbault *et. al.* shows the first analytical application of a biosensor with an

immobilized enzyme [91]. Guilbault and Montalvo in 1969 announced the first potentiometric sensor based on the detection of urea using an ion selective electrode to determine change of NH_4^+ions concentrations [92]. In 1975, first immunosensor on a potentiometric transducer was presented byJanata. In this system, he detected Concanavalin A through covalent attachment between the lectin and a polyvinyl chloride (PVC) membrane on a platinum electrode [93]. In 1979,the first amperometric immunosensor showed by Aizawa analyzed human chorionic gonadotropin by an amperometric oxygen electrode [94]. Bergveld showed the first ion selective field effect transistor (ISFET) sensor in 1972 [95]. During the 80s electro-polymerization techniques [96]and biosensors improvements such as flow injection and optical fibers were introduced. During this decade (1983), the SPR biosensing principles were described [97-100], and the first gas phase biosensor based on a quartz crystal microbalance (QCM) was reported [101]. During the 90s, the boom in biosensors increased due to the introduction of nucleic acids as biorecognition elements. Consequently, the knowledge of decades of development with enzymosensors and immunosensors were applied to this new world of biosensors.

The use of nucleic acids in biointerfaces not only promoted the development of analytical techniques with higher resolution but also paved the way for research into new materials and processes. However, the greatest contribution of these was made in the genomics area in both biological and clinical field. Techniques such as PCR and bioinformatics tools have become inseparable in the construction of DNA microarrays [48,102,103].

Compared to immunosensors, the introduction of smaller biomolecules, such as nucleic acids, made more relevant the interface use. The chemical structure of DNA also makes the functionalization of sensor surfaces more challenging. DNA works excellently as biorecognition element because of its high physical and chemical stability. In addition, its inherent specificity, which is the primary characteristic in the detection of analytes, achieved by the specific hybridization of a DNA sequence attached onto the sensor surface complementary to the sequence of the analyte.

The applications of DNA biosensors have their main role in identifying target sequences for the medical diagnostic. However, it is not the only field in which is can apply. Identifying different strains of microorganisms makes the genosensors powerful tools in the field of biosafety. Moreover,it does not mean biosafety only in the bioterrorism protection waybut to identify potential crop pests or pathogens in the food production chain[104-106]. Moreover,they serve as an analytical tool in the quality analysis of reservoirs of water for human and animal consumption. DNA

biosensors are also powerful tool in clinical diagnosis to even to formulate the most suitable treatment of each patient in a personalized medicine. Likewise, serve as platformto aid in evolutionary biology to determine the similarities between taxa at the genetic level or to evaluate the paternity of a child.

1.4 Electrochemical DNA biosensors

In the market of the DNA sensors, the optical sensors have a high influence in many applications. However, the electrochemical biosensors have been gaining ground due to its better advantages. The bioelectroanalysis in DNA biosensors systems is an area than rapidly expanding because of its great benefits. Electrochemical techniques offer a high specificity; high selectivity; fast results; low costand application to portable systems. These are desirable characteristics in every industry and area of expertise. The synergy of considering the great possibilities of many applications that offers DNA detection in addition to the excellent benefits of employing electrochemical transduction makes a powerful platforms for successfully face the challenges that are ahead in this field. Others advantages of electrochemical techniques instead of optical techniques are the easier data management due to no special imagine transduction is required. Other plus is the possibleposterior automation in combination with other types of the assays such as microfluidic and/or thermoblocks.

The basic elements of thiselectrochemical system are atransducer which serves asworking electrode (WE) or a system with multiple WEs functionalized with only one or different DNA capture probes, a reference electrode (RE) and a counter electrode (CE). In these biosensors,the capture probes are single strands DNA (ssDNA) and its sequences are predefined depending on the target that we want to detect.The target (analyte) is another ssDNA complementary to the capture probe sequence. The hybridization between both chains of DNA produces a physical-chemical change that is detected with the transductor. The varieties of electrochemical techniques that can be used with these devices offer them great flexibility and open fields to manypossible applications.

Electrochemical biosensors are commonly composed by three electrodes WE, RE and CE. This configuration was introduced in the 50s, by the revolutionary approach of Clark, that modifies the polarography technique of Czech Jaroslav Heyrovsky, introducing other electrode than working like REto calibrate the main

electrode, resulted in the polarographic electrode Clark type. In this system, the accuracy increased and oxygen consumption was reduced when both electrodes were coated with plastic and glass down to the tip. This allowed the measurement of the oxygen partial pressures in blood and Clark could improve theirblood oxygenation detection system[90].The electrochemicaltechnique that used Clark was an amperometric technique connecting WEand RE in an electrolytic cell [107]. Afterwards, another electrode was also considered,anauxiliary or CE, in order to pass the current through CEinstead of the REthat makes more stable this last electrode.

The WE is generally the electrode where reactions take places and the surface of this electrode is functionalized with the recognition bioelement. In the RE, no current flows and it has a fixed potential and known in order to determine a potential difference between this one and the WE. The CE balances the overpotentials on the WE[108].Usually, with this three-electrode system operates the different types of DNA electrochemical biosensors, although in some cases can be used a pseudo reference-counter and use this electrode for both functions, but it gives less stability to the readout.

There are different electrochemical techniques to monitor DNA hybridization.Main ones are amperometry, voltammetry, potentiometry, and conductimetry; in all cases, the sensor takes the name of the technique used.

Amperometric sensors are based on measuring a resulting current of a chemical process of oxidation or reduction of an electroactive species. These oxidation-reduction processes, also called redox, are usually carried out at constant potential on the working electrode and it is monitored the current versus time[109]. This type of detection usually involves enzymatic labelling of the target.

Voltammetric sensors are based on the potential-current response of a polarizable electrode in a solution.In these techniques, current changes, as a function of the potential applied in the system, are studied[110]. The process involves redox reactions, of one or more electroactive speciesat the electron and mass transfer mechanisms. The latter may be due to migration (movement of species by charge difference), convection (movement of matter by physical changes) and diffusion (species movement by concentration gradient). In most cases, the redox is carried out under conditions such that diffusion mechanism is the fundamental process in the transport of the electroactive species. In this way, the migration and convection are minimized by the addition of an excess of supporting electrolyte and preventing movement of agitation and temperature gradients.Within the numerous techniques

used in voltammetry, the techniques of cyclic voltammetry (CV) and Differential Pulse Voltammetry (DPV) are the most used[111].

Potentiometric systems involve the detection of a potential difference between the WEand theRE.This difference of signal is created due to the increase of charges from the attached and hybridized DNA on the WE. In order to improve the sensitivity PNA capture probes are used for these applications, since these bioreceptors have uncharged nature[112].One type of potentiometric sensors are the ISFETs and as potentiometric, are sensors that react to changes in the activity of a specific ion.However, due to its design the measuring principle is the transistor channel modulation by the voltage difference that exists between the electrolyte solution and the device gate [113].

The conductimetric system usually uses two pair of electrodes called interdigitated electrodes and between the electrodes are immobilized the DNA capture probes. The device measures the conductivity across the pair of electrodes in turn with a fixed frequency. In presence of hybridized DNA, local changes of conductivity in the electrodes neighborhood are registered. These changes are depending on the DNA concentration and a quantitative analytic system can be developed, as in previous electrochemical techniques[114].

As shown, many of these systems measure the electron dynamics in the solutions where DNAisembedded. For this, there must be an ionic or electronic exchange near the surface of the working electrode. For this reason, the suitable choosing of bioreceptor and electrolyte as well as the electrodes is vital to select the adequate detection technique.

1.5 DNA electrochemical sensing strategies

Electrochemical biosensorsto detect the DNA duplex formation started with rather primitive methods using carbon and gold electrodes in combination with redox indicators.This type of biosensors are considers an indirect, since the hybridization event is detected through a third molecule, a redox label. In addition, the fact that this interaction was performed on the transductor sensors makes them a single surface technique (SST). On the other hand, to improve the abilities of the electrochemical analysis of DNA in biological matrices, about 10 years ago the double surface technique (DST) was proposed. In this system, the DNA hybridization was performed at one surface (usually magnetic beads, optimized for capturing target DNA or RNA from biological materials) and

electrochemicaldetection of the DNA hybridization was done at the WEsurface.. DST offered very high sensitivity and specificity in the analysis of real DNA samples, but it required more manipulation than usual SST or an efficient microfluidic system.

On a more easy way, there are the direct DNA electrochemical biosensors, were the detection of the DNA hybridization event is done in a label-free manner.

1.5.1 Direct DNA electrochemical detection

The direct DNA detection relies in the detection of the hybridization event without require any external label. There are many approaches reported in the literature for the direct electrochemical detection of DNA. One of the first examples was based on the direct reduction and oxidation of DNA in a mercury electrode. Hence, the amount of reduced or oxidized DNA reflects the amount of DNA captured by tensiometric processes [115]. Alternatively, label-free detection based on guanine oxidation signals at carbon electrodes, or later G oxidation with a mediator at Indium Tin Oxide (ITO) electrodes, was used[116]. At gold electrodes, DNA was attached to the surface by an attachedterminal −SH group (thiol), forming an interface with standing-up DNA molecules. At carbon electrodes, unlabeled probe DNA was lying flatly at the electrode surface attached through electrostatic by the amine groups in the DNA bases. These techniques worked relatively well with synthetic oligos targets. They were, however, mostly poorly efficient in the analysis of real DNA samples. There are also methods to discriminate between single strand and double strand of DNA through the direct reduction of DNA. One of them is an accumulation of DNA strands on the electrode surface by electrostatic induction before the detection step. This accumulation and detection is done by adsorption stripping voltammetry (ASV)[117]. The purine bases of DNA, adenine and guanine, can be oxidized electrochemically, and this process is more clearly detected using carbon or ITO electrodes among other metals, or with polymer-coated electrodes [116]. The problems with these DNA biosensors are the high potentials needed for direct oxidation of nucleic acid and thehigh background currents. To eliminate these interferences, researchers have developed physical separation techniques. An example of this, it is the use of magnetic beads functionalized with capture probes. After hybridization, the beads are separated with a magnetic field and the DNA strands are depurinated in an acidic solution. In this way, free adenines and guanines are easilydetected [118].

But the wider spread approaches are the ones in which the hybridized DNA strands are detected indirectly, and done through the use of chemical electromediators,

that can be diffusional solutions or redox labels attached directly or indirectly to the DNA. In previousexample,in order to reduce the high voltages observed, a potential that oxidizes a diffusional electromediator to contact the DNA strand is applied. Guanine present in the polyelectrolyte DNA chain come into play and it reduces again the electromediator, producing a regeneration of it. The difference of the electrochemical mediator signal before and after oxidation gives us an estimation of the amount of guanine available in the system [119].The above approachis highly sensitive, in the order of femtomoles, but its main problem is that its use represents the destruction of the sample, and after adding the mediator is not anymore a direct system.

1.5.2 Indirect DNA electrochemical detection

1.5.2.1 Label-based systems with redox molecules or enzymatic complex

Due to the weakness of the direct methods, the approaches involving electroactive labeling techniques into the target DNA strand took boom. To mention a few, these labels can be ferrocene redox species or enzymatic labels such as horseradish peroxidase (HRP) or alkaline phosphatase (ALP), which are attached through a biotin for its subsequent reaction with enzyme-streptavidin [120]. In these systems, the signal of the redox species or redox enzyme complex is the hybridization evidence. There also indirect labels, where unlabeled DNA target, after hybridize with immobilized capture probe, has a second hybridization in a different sequence in its chain with a third strand of labelled DNA. The advantage of this is that the labelled synthetic chain can carry multiple labels of the same or different redox species with different redox potential. If there are two distinct redox species, the double peak of detection allows a multidetection of DNA in the same electrode[121]. This method is called the sandwich method and has countless variations.

1.5.2.2 Redox indicators

Other electrochemical approach worth noting is the detection of hybridization using redox reporter molecules or redox indicators. These techniques use an additional step subsequent to hybridization to introduce non-covalently electroactive molecules, which behave in three ways. The first of them are positively charged molecules and are accumulated on the surface where hybridization occurs, taking

advantage of the high density of negative charges of DNAthat exists to increase its redox capacity. The $Co(phen)_3^{+3}$ and Ru $(NH_3)_6^{+3}$ are examples thereof. In a contrary way, the negatively charged $[Fe(CN)6]^{4-}$ is expelled from the electrode surface when the DNA concentration increases. In the third case, are those molecules that are intercalated within the duplex DNA and exploit redox electrochemistry of purine bases for itself electroactive activity. The methylene blue is a typical example [122].

1.5.2.3 Nanostructure-based electrochemical amplification

One of the great challenges in detecting DNA hybridization is the magnification of the signal. For this purpose there are many strategies involving nanostructures of different materials and shapes. The uses of gold nanoparticles, carbon nanotubes, dendrimers, magnetic nanoparticles, electroactive polymers, nanoporous membranes and others are the order of the day. These platforms can be functionalized with capture probes and have their greatest strength in increasing the area available for the immobilization of capture probes. It is simple, to larger area more immobilized capture probes, more hybridization events and electrochemical reading signal improved [123-128]. The above different electrochemical sensing strategies are summarized in table 1.1.

Electrochemical sensing system	Example	Advantages	Disadvantages	Label	Habitual applications
Direct Intrinsic DNA electroactivity	Guanine oxidation	High sensitivity	Sample destruction High background signals	No	Hybridization detection; DNA damage
Indirect DNA electrochemistry	Guanine reduction	High sensitivity	Sample destruction	No	Hybridization detection; DNA damage
Labels-based in redox molecules or enzymes	Organometallics like ferrocene; Horseradish peroxidase; Metal chelates	Unaltered samples; Multiple target detection; Moderate to high sensitivity	Additional chemical steps required	Yes	Hybridization detection; Primer extension; Mismatch detection
Redox indicators	Methylene blue $Co(phen)_3^{+3}$ Ferrocyanide	High sensitivity Multiplexing	Additional Biochemical preparation steps required	No	Hybridization detection; DNA damage; Host-guest interactions
Nanostructure-based amplification of the electrochemical signal	Gold nanoparticles Carbon nanotubes Dendrimers	Multiple target detection Extremely sentivity	Several additional steps Sample destruction usually	Yes/No	Hybridization detection

Table 1.1: DNA electrochemical sensing summary

The versatility of biosensors allowed its application in many and varied platforms with these features. In addition, easy integration with microelectronic systems

allowed the incorporation of other technologies around them [129-131]. Depending on the application, these portable biosensor system requires its integration with other sample processing for separation of certain compound, sample concentration or/and amplification, among others. For this purpose, it is required biosensor integration in fluidic-electronic systems, resulting in the creation of new devices, the LOCs.

1.6 Lab-on-a-chip

LOC refers to technologies that allow operations, which normally require a laboratory on a much-miniaturized scale, within a portable or handheld device (see figure 1.5). In this scale, the analysis of samples can take place in situ, exactly where the samples are generated, rather than being delivered to a laboratory.This in turn, reduces manufacturing cost and increases the high performance capability. Because the benefits of low cost, high performance and miniaturization, this technology isa fundamental and powerful tool for clinical research, diagnostics, drug development, toxicology studies and the selection of patients for trials clinicians. The criterion of miniaturization, that has given the push for continuous progress of microelectronics technology, opens these devices to a wider range of applications. From the first mechanized microsensors on silicon in the 70s and microelectromechanical systems (MEMS), scientific improvements are focused on developing new platforms that offer advantages such as portability, speed of results, measurement accuracy, selectivity among other features. For these reasons, and many others, the LOCs and other variations such as, cell-on-a-chip, organ-on-a-chip, and tissue-on-a-chips were created [132].

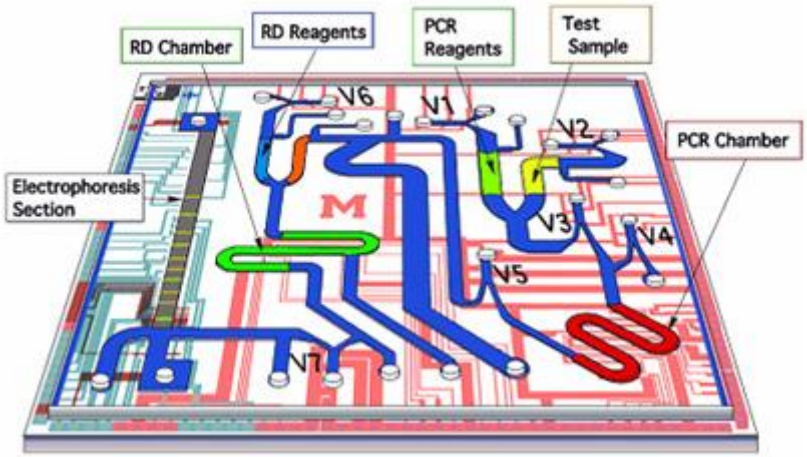

Figure 1.5: Schematic of the "Genotyper" LOC device, developed by researchers at the University of Michigan, which could identify different strains of flu

These microsystems for analysis or laboratories mounted on a microdevices are taking importance in chemical, biological, pharmaceutical and medical fields to name a few. The LOCs can perform all the functions of conventional laboratory equipment, with the advantages of made analysis in parallel and in multiplexed portable systems.The possibility of separation and quantification of these molecules on a single platform is the main advantages of LOCs. Because of this compartmentalization of functions, these microlabs need lower sample volumes, generating less waste and reducing costs in the purchase of expensive reagents. When working with smaller volumes also we reduce the reaction times for getting faster answers in biochemical reaction systems. Also, being contained in sealed chambers the risk of biological contamination is less [132, 133].

With these specialized techniques, the traditional approaches of analytical measurements are undergoing a fundamental transition. These changes are driven by scientific advances that are creating micro and nano sensors closer to the biomolecules size, making trend towards detection of multiple molecules [132, 133]. The idea of isolate individual molecules in confined spaces is more seductive than conventional techniques; often focus on the behavior of a large number of molecules.More and detailed information aboutchemical and physical events is extracted in studies on micro and nanosensors that involves high volume of bulk molecules.

Because of this, the miniaturizations of the basic components of the LOCs are very relevant and are being designed using numerous strategies and materials [134, 135]. The microelectronic component, which is the integration of electrochemical microcells in those devices for using electronic readouts,is mainly fabricated by standard photolithographic process, inkjet printing or screen-printing. The materials used for the fabrication of the electrodes are as varied as the applications: gold, silver and platinum,different forms of carbon, among others. These materials are ableof generating an output signal of a biochemical process while this occurs in its surface. Regarding the microfluidic component, the materials used for these platforms are usually inert polymers such as polydimethylsiloxane (PDMS)[136]. However, new trends are directed to the use of non-silicon-based polymers such as halogenated vinyl, styrenic, acrylics and polyolefins [137, 138]. The techniques used to manufacture the microchannels and compartments are going from traditional photolithography to revolutionary 3D imprinting methods [139, 140] This without leaving aside all microengineering that makes possible the integration, separation and subsequent mixing of the sample. In addition to the flow conditions,

pumps and valves, sealing cameras and other features of these small airtight devices.

There are many applications for LOCs such as microfluidic dispenser, electrophoretic separator, lysis of cell, DNA amplification by PCR, concentration gradient generator, micro bioreactor for immunoassay, integration of a real-time PCR, fluid samples preparation, cellular analysis, and biochips with protein or DNA microarrays.

1.7 Trends in biosensors

Since 20 years ago, with the introduction of new technologies, the advances in detection techniques are even more specific and with higher resolution. With the new generation of materials and the revolutionary techniques of micro and nanofabrication, the tendency of the scientific community and the market is clear: to develop low cost smart devices capable of detecting, with highly selectivity and sensitivity, many analytes in one shot of any type of compounds. We talked about three key words in the historical context of the biomicro or bionanotechnological development: biosensors, miniaturization and integration. Each one defines what is and what will be the main scientific research around the world. In addition, the three joined the hopeless offered by the romantic idea of the perfect tool for the new technological revolution. As result among these three words, a tradeoff is created and when the field of research in biosensors is stagnant, the other features picking up the reins for bringing a higher degree of complexity and smallness.

For the biosensors its future development and research depends on producing advantageous characteristics as specificity, portability, economy, simplicity and robustness. The specificity offers precision and the certainty that we will detect what we want in a complex matrix, decreasing the probabilities of errors in our conclusions. This has been achieved through the creation of nanostructures accompanied by multiple geometries of various materials from amorphous nanomagnetic iron particles to some very definite, as carbon nanotubes, or gold, silicon, supramolecular systems and, of course, more complex biomolecules, among others. Moreover, the portability of these devices and the economy in its manufacturing process guarantees their mass use, as well as their access to remote areas with difficult environments and economies. The miniaturization of these devices guarantees the success in the use of resources, the smaller amounts of reagents and sample required and its portability. Also, improve of device robustness opens new possibilities of use. To the success of biosensors

development, the suitable choice of biorecognition element and the best transduction system are the first steps to determine.

1.8 Biochips

A biochip is a biosensor whose recognition element is DNA or antibodiesin a multiple matrix of biosensors. In this way, a miniaturized device that contains DNA or antibodiesbiosensing matrix or microarray is a strict definition of the biochip. The array matrix is a network of specific binding sites where hundreds of chemical reactions can occur simultaneously. These platforms have been developed to allow genomic, proteomic and large-scale functional analysis. In general, there are two types of biochips: DNA microarrays and protein microarrays, both integrated in microfluidic chips. These devices are platforms with multiple channels and the integration of these systems with arrays of biomolecules confined to a substrate is called LOC. The protein microarrays are the platform used mainly for expression of protein profiles. These microarrays can be used to examine protein-protein, protein-ligand or enzyme-substrate interactions on a single biochip. In contrast to DNA chips, protein microarrays require more steps for its manufacture. They are also much more chemically unstable because proteins may lose its tertiary or quaternary structure. Regarding the DNA arrays, its main advantages are the great facility to anchor the DNA molecule over the substrate; its chemical stability; the high specificity of the hybridization event, among others. Its versatility popularized its use, and allowed the resolution of initial problems. In recent years, advances in the DNA biochips have overcome the problems of low hybridization efficiency, poor sequence discrimination, low signal detection and tedious procedures inherent in the previous technologies. Now is possible to produce miniaturized arrays that use small volumes of reagents. Besides, the ability to perform multisequence detection with optical and electrochemical techniques makes that this field continues to growth[141].

1.9 Commercial DNA biochips and microarrays

Major pharmaceutical, technology and medical companies have been realized about the huge market behind DNA arrays. For this reason, the most powerful international companieshave bet for their creations, each having a relative successful. In the market, there are several designs of devices involving DNA biosensor technologies. The applications are diverse, food, drugs, cosmetics,

environmental, etc. Our commercial summary is focused to devices with biological and medical diagnostic applications using DNA biosensors.

There is a difference in the definition of the terms DNA Chip and DNA microarrays. Usually DNA chips have a much lower density per unit area of bioreceptor whereas DNA microarrays are highly dense. This differencearises from the different methods of immobilization of the capture probes. In the DNA microarrays, the syntheses of oligonucleotides are made in situ.

Affymetrix is the flagship company of the manufacture of DNA microarrays. They use a photolithography method for in situ synthesis of probes. This method involves a series of steps of light exposure dependent on where each nucleotide selectively added to the chain loses its protection training to lead to elongation of the sequence to be built [142]. The disadvantages of this method are several, the method is costly and time consuming and the different steps may introduce errors in the bioreceptor sequences[141, 142]. Meanwhile, in DNA chips, pre synthesized oligonucleotides are spotted on the electrode for its immobilization mainly with nanoplotting or inject printing.Genometrics, Inc. with VistaMorph and VistaExpressand Hyseq, Inc. with its HyChipGenosensor are companies producing with this method. A different way of DNA bioreceptor attaching is the one commercialized by Nanogen, which anchor the capture probes on the substrate byelectronic attraction of the negatively charged DNA molecules, generating an electric field at the desiredelectrodes in the array and so that the DNA molecules aredrive and adhered specifically in the streptavidinactivated electrodes[141, 142].

There is another method developed by Agilent, to fabricateDNA microarrays. This involves transporting phosphoramides and activators to specific sites of the substrate by inkjet printing, of any single base of the bioreceptor sequence. Here, through traditional chemistry, the elongation of the probe is produced, which can be up to 60 base pairs [143, 144]. Other companies with similar devices are Clontech Laboratories and Rosetta Inpharmatics[145, 146].

The pin-based fluid transfer methods are developed primarily by BioRobotics, Ltd. (MicroGrid II); Gene Machines (OmniGrid); Gentix, Ltd. (Q Array). The pin-based technology use pins with a micro-capillary channel that contains the liquid that will be deposited on the substrate. For a more detailed review of techniques and companies, see following references[141, 142]. The common to all these explained methods is that none used electrochemical techniques to detect their targets. The majority of them use fluorescent scanners and in some cases such as; Millenium Pharmaceuticals and Biocore (General Electric division) have SPR DNA chips and

Sequenom, Ltd. uses DNA spectrochips for mass spectrophotometry detection. Nevertheless, all this equipment are extremely costly and voluminous, where is required a trained personnel for their use, only affordable for few analytic laboratories in the world.

Regarding the electrochemical detection there are some biodevices available commercially[147, 148]. Some examples are:

- E-Sensor XT-8

  GenMark Diagnostics offers e-Sensor XT-8 technologiesto detect a respiratory viral DNA.This technology integrates microfluidics and electrochemical detection. The signal indicating hybridization event is generated by voltammetric technique using a reporter probe with label of ferrocene. Like general summary of the system, the real sample is obtained and then the target DNA is separated and amplified by PCR outside of the final cartridge. In this way, the platform is not an integrated LOC. The DNA is subject to exonuclease reaction to create ssDNA. Then, the ssDNA is injected in the XT-8 electrochemical-microfluidic system cartridge. This cartridge contains a solution with the reporter probe. Once inside the specific viral reporter probe is hybridized with the target DNA. Through of pumping system the mix is introduced in microfluidic chamber wherein the target DNA will have a second hybridization with the pre-assembled capture probe. Finally, the electrochemical reading is carrying out. Figure 1.6 shows us a schematized procedure for this typical sandwich system.

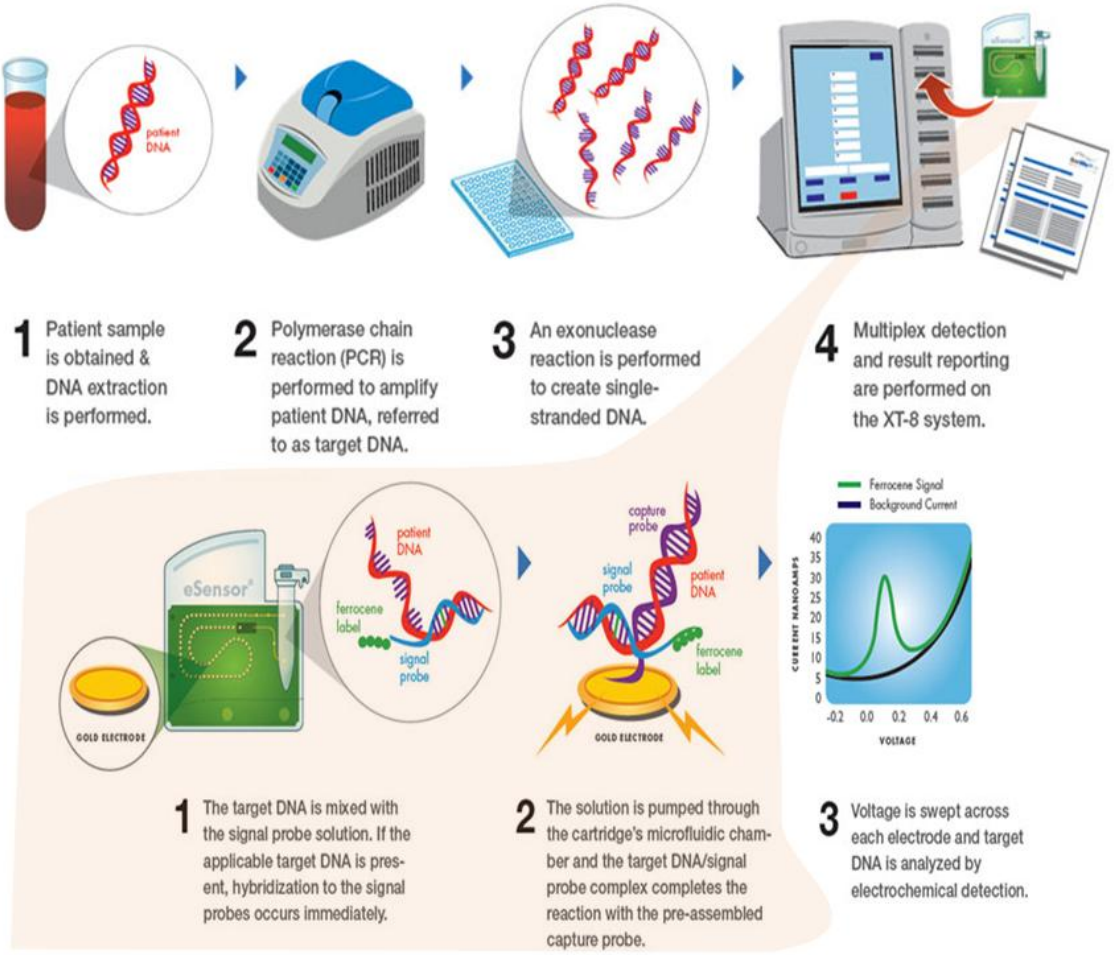

Figure 1.6:GenMark e-Sensor technology schematic

Source: http://www.genmarkdx.com/technology/esensor.php

The technology developed by this company is not integrating the PCR in the device, it requires a laboratory and trained personal and the part of the sensing integrated in the cartridge is quite tricky with many steps and reagents, such as the use of exonucleases and three ssDNA to form the sandwich complex.

- CombiMatrix Diagnostics has developed oligonucleotide microarray platform containing 12544 individually addressable microelectrodes in a semiconductor matrix. This approach requires labeling of the target DNA with biotin, which (after hybridization with immobilized capture probe) binds Horseradish peroxidase (HRP) streptavidin conjugate. The HRP-catalyzed enzymatic reaction involves an oxidation of 3,3',5,5'-tetramethylbenzidine (TMB), followed by amperometric determination of the product. CombiMatrix core technology is

based on a specially modified semiconductor adapted for biological applications, which contains arrays of platinum microelectrodes. The CombiMatrix system has the ability to measure the signal present at that electrode site. The two main components are ElectraSense™ Reader and ElectraSense™ microarray with hybridization cap. The figure 1.7 was taken and modified of [148] and show the CombiMatrix assembly.

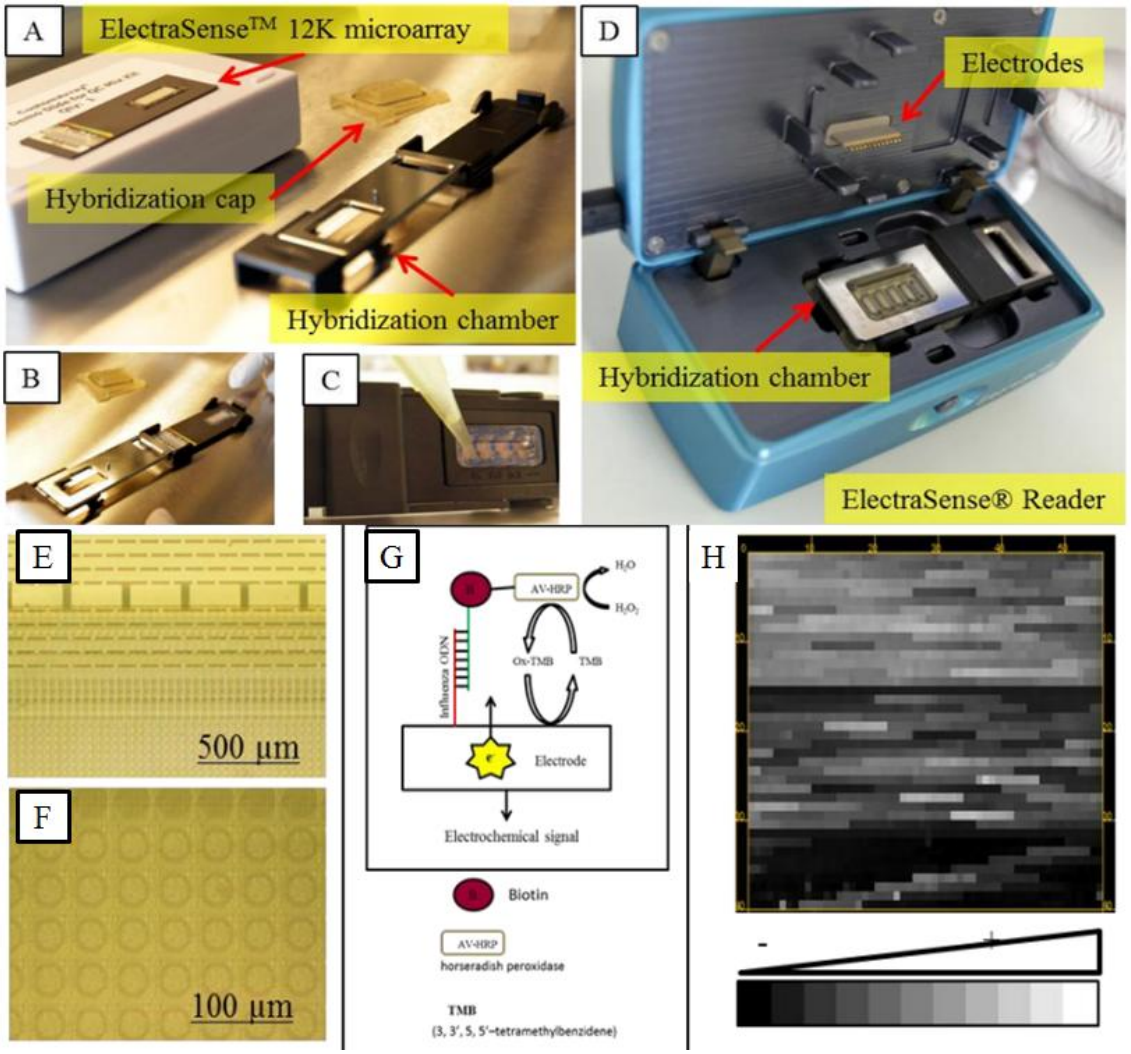

Figure 1.7:CombiMatrixElctroSense™, A) B) C) Microarray assembly of ElectraSense™, D) ElectroSensor™ reader unit, E) F) microphotos of the electrodes and spots with oligonucleotide probes,G) HRP-TMB reaction for electrochemical detection scheme, H) Image of microarray and the position and intensity signal of probes from ElectraSense™ reader

This company, as previous, does not integrates the PCR, which leave far from a POC application both devices.

Others studies developed in research groups,and not commercialized yet,are focused in the creation of functional DNA chips or LOC devices that are summarized in table 1.2.

System Chip	Electrochemical technique	target Nucleic Acid	LOD
16 gold WE	CA	rRNA	8 fM
8 gold WE	CA	miRNA	2 pM
4 gold WE	DPV	herpes virus	5 aM
48 gold WE array	SECM	*Samonella ssp*	100 fM
Silicon chip 16 gold WE	CV	*Alu 1* restriction enzyme site	N/A
16 Pt microdisk electrode	CV	microbial rRNA	<100 pM
Integrated microfluidic Ti/Au sensor	ACV	*Salmonella enterica*	10 aM
ITO-coated Si glass microchip	DPV	Bacteriophage M13	$\approx 10^3$ copies/μL
Capillary electrophoresis-based microfluidic device with Au microelectrodes	HDV	8-hydroxy-deoxyguanosine	100 nM
Conducting polymer/AuNP on Pt microelectrode array	LSV	100-bp DNA ladder	113 fM

WE, working electrode; CA, chronoamperometry; DPV, differential pulse voltammetry; SECM, scanning electrochemical microscopy; CV, cyclic voltammetry; ACV, AC voltammetry; HDV, hydrodynamic voltammetry; LSV, liner sweep voltammetry; LOD, limit of detection; ITO, indium tin oxide

Table 1.2: No commercial LOC devices reported in literature

1.10 Summary

As we can see from published report and reviews, the current trend in biosensors is the integration of multiple systems within a single platform. However, despite the miniaturization of some components many commercial systems still need to perform procedures outside the LOC. The treatment sample steps are often the main problem to achieve a complete small-integrated laboratory. For example, the DNA amplification by PCR is necessary to label the DNA sample and to increase the number of ssDNA target and so to amplify the detection signal. However, in several commercial devices this step is still done externally from the cartridge in the traditional thermocyclers. Besides, almost all systems are able to analyze numerous probes of the same type, but still there is a lack in the development of different types of probes in the same test. Techniques in multi-probe array would discriminate between different types of samples in a single assay. Even more important is the evident lack of electrochemical devices on the market, which

provides many advantages to the LOC and makes it more competitive in the market.

The device presented in this study overcome the limitations observed in the diagnosis market devices with the development of an electrochemical multi-probe DNA array for detection of different specific DNA sequences related with cancer. The device integrates all the required steps to obtain in an easy way a direct response after the sample introduction. The use of this equipment does not require any other laboratory equipment or specialized personal, and can be use in POC applications by the family doctor in medical centers.

1.11 References

1. Azzam, W., A. Bashir, and O. Shekhah, *Thermal study and structural characterization of self-assembled monolayers generated from diadamantane disulfide on Au(111).* Applied Surface Science, 2011. **257**.
2. Farjami, E., et al., *"Off-on" electrochemical hairpin-DNA-based genosensor for cancer diagnostics.* Analytical chemistry, 2011. **83**(5): p. 1594-1602.
3. Wang, J., *Glucose Biosensors: 40 Years of Advances and Challenges.* Electroanalysis, 2001. **13**(12): p. 983-988.
4. Amano, Y. and Q. Cheng, *Detection of influenza virus: traditional approaches and development of biosensors.* Analytical and bioanalytical chemistry, 2005. **381**(1): p. 156-164.
5. Feriotto, G., et al., *Biosensor Technology and Surface Plasmon Resonance for Real-Time Detection of Genetically Modified Roundup Ready Soybean Gene Sequences.* Journal of Agricultural and Food Chemistry, 2002. **50**(5): p. 955-962.
6. Tichoniuk, M., M. Ligaj, and M. Filipiak, *Application of DNA hybridization biosensor as a screening method for the detection of genetically modified food components.* Sensors, 2008. **8**(4): p. 2118-2135.
7. Viswanathan, S., H. Radecka, and J. Radecki, *Electrochemical biosensors for food analysis.* Monatshefte für Chemie - Chemical Monthly, 2009. **140**(8): p. 891-899.
8. Neuži, P., et al., *Revisiting lab-on-a-chip technology for drug discovery.* Nat Rev Drug Discov, 2012. **11**(8): p. 620-632.
9. Ojanperä, I., M. Kolmonen, and A. Pelander, *Current use of high-resolution mass spectrometry in drug screening relevant to clinical and forensic toxicology and doping control.* Analytical and bioanalytical chemistry, 2012. **403**(5): p. 1203-1220.
10. Scannell, J.W., et al., *Diagnosing the decline in pharmaceutical R&D efficiency.* Nat Rev Drug Discov, 2012. **11**(3): p. 191-200.
11. Kuczynski, J., et al., *Experimental and analytical tools for studying the human microbiome.* Nat Rev Genet, 2012. **13**(1): p. 47-58.
12. Hou, Y., et al., *Microbial Strain Prioritization Using Metabolomics Tools for the Discovery of Natural Products.* Analytical chemistry, 2012. **84**(10): p. 4277-4283.
13. Looser, M.O., A. Parriaux, and M. Bensimon, *Landfill underground pollution detection and characterization using inorganic traces.* Water Research, 1999. **33**(17): p. 3609-3616.

14. Mattiasson, B., *MIPs as Tools in Environmental Biotechnology*, in *Molecularly Imprinted Polymers in Biotechnology*, B. Mattiasson and L. Ye, Editors. 2015, Springer International Publishing. p. 183-205.
15. Alam, A. and V. Sharma, *Environmental Biotechnology-A Review.* Researcher, 2013. **5**(4): p. 71-93.
16. Xie, J., et al., *Analytical and environmental applications of nanoparticles as enzyme mimetics.* TrAC Trends in Analytical Chemistry, 2012. **39**: p. 114-129.
17. Golet, E.M., et al., *Trace Determination of Fluoroquinolone Antibacterial Agents in Urban Wastewater by Solid-Phase Extraction and Liquid Chromatography with Fluorescence Detection.* Analytical chemistry, 2001. **73**(15): p. 3632-3638.
18. Malon, A., et al., *Potentiometry at Trace Levels in Confined Samples: Ion-Selective Electrodes with Subfemtomole Detection Limits.* Journal of the American Chemical Society, 2006. **128**(25): p. 8154-8155.
19. Berger, R.G., *Aroma biotechnology*. 2012: Springer Science & Business Media.
20. Omasa, K., et al., *Air pollution and plant biotechnology: prospects for phytomonitoring and phytoremediation*. 2012: Springer Science & Business Media.
21. Koutinas, M., et al., *Bioprocess systems engineering: transferring traditional process engineering principles to industrial biotechnology.* Computational and structural biotechnology journal, 2012. **3**(4): p. 1-9.
22. Nikačević, N.M., et al., *Opportunities and challenges for process control in process intensification.* Chemical Engineering and Processing: Process Intensification, 2012. **52**: p. 1-15.
23. Wijffels, R.H., O. Kruse, and K.J. Hellingwerf, *Potential of industrial biotechnology with cyanobacteria and eukaryotic microalgae.* Current opinion in biotechnology, 2013. **24**(3): p. 405-413.
24. Tu, Z. and H. Zhang, *[Controlled Veterinary Drug Delivery Systems against Parasitic Infection].* Zhongguo ji sheng chong xue yu ji sheng chong bing za zhi= Chinese journal of parasitology & parasitic diseases, 2015. **33**(1): p. 58-63.
25. Amarante, M., et al., *Species-specific PCR for the identification of Cooperia curticei (Nematoda: Trichostrongylidae) in sheep.* Journal of helminthology, 2014. **88**(04): p. 447-452.

26. Silva, M.V.B., et al., *Identification of quantitative trait loci affecting resistance to gastrointestinal parasites in a double backcross population of Red Maasai and Dorper sheep.* Animal Genetics, 2012. **43**(1): p. 63-71.
27. Piorek, B.D., et al., *Free-Surface Microfluidics/Surface-Enhanced Raman Spectroscopy for Real-Time Trace Vapor Detection of Explosives.* Analytical chemistry, 2012. **84**(22): p. 9700-9705.
28. Peng, L., et al., *On-site Rapid Detection of Trace Non-volatile Inorganic Explosives by Stand-alone Ion Mobility Spectrometry via Acid-enhanced Evaporization.* Scientific reports, 2014. **4**.
29. Ma, Y., et al., *Highly selective and sensitive fluorescent paper sensor for nitroaromatic explosive detection.* Analytical chemistry, 2012. **84**(19): p. 8415-8421.
30. Yagur-Kroll, S., et al., *Detection of 2, 4-dinitrotoluene and 2, 4, 6-trinitrotoluene by an Escherichia coli bioreporter: performance enhancement by directed evolution.* Applied microbiology and biotechnology, 2015: p. 1-12.
31. Carrascosa, L.G., et al., *Nanomechanical biosensors: a new sensing tool.* TrAC Trends in Analytical Chemistry, 2006. **25**(3): p. 196-206.
32. Minunni, M., et al., *Biosensors as new analytical tool for detection of Genetically Modified Organisms (GMOs).* Fresenius' journal of analytical chemistry, 2001. **369**(7-8): p. 589-593.
33. Bagni, G., et al., *Electrochemical biosensors as a screening tool of in vitro DNA-drug interaction.* Current Pharmaceutical Analysis, 2005. **1**(3): p. 217-224.
34. Bertók, T., et al., *Electrochemical lectin based biosensors as a label-free tool in glycomics.* Microchimica Acta, 2013. **180**(1-2): p. 1-13.
35. Kociketal, J., *Biosensors-The tool for fast detection.* Preparedness Against Bioterrorism and Re-emerging Infectious Diseases, 2004: p. 191.
36. Mutlu, M., *Biosensors in Food Processing, Safety, and Quality Control*. 2010: CRC Press.
37. Higson, S., *Biosensors for medical applications*. 2012: Elsevier.
38. Bruce Alberts, A.J., Julian Lewis, David Morgan, Martin Raff, Keith Roberts, Peter Walter, *Molecular Biology of the Cell*. 6th edition ed. The Structure and Function of DNA. 2002, New York: Garland Science.
39. Paleček, E. and M. Bartošík, *Electrochemistry of Nucleic Acids.* Chemical reviews, 2012. **112**(6): p. 3427-3481.

40. Labuda, J., et al., *Electrochemical nucleic acid-based biosensors: Concepts, terms, and methodology (IUPAC Technical Report).* Pure and Applied Chemistry, 2010. **82**.
41. Wang, L., et al., *Recent advances in biocompatible supramolecular assemblies for biomolecular detection and delivery.* Chinese Chemical Letters, 2013. **24**(5): p. 351-358.
42. Piccinini, E., et al., *Chemical Communications c5cc05837f.*
43. Sukhorukov, G.B., et al., *Multilayer films containing immobilized nucleic acids. Their structure and possibilities in biosensor applications.* Biosensors and bioelectronics, 1996. **11**(9): p. 913-922.
44. Takaoka, Y., A. Ojida, and I. Hamachi, *Protein Organic Chemistry and Applications for Labeling and Engineering in Live-Cell Systems.* Angewandte Chemie International Edition, 2013. **52**(15): p. 4088-4106.
45. Yang, H., *Enzyme-based ultrasensitive electrochemical biosensors.* Current opinion in chemical biology, 2012. **16**(3): p. 422-428.
46. Nöll, T. and G. Nöll, *Strategies for "wiring" redox-active proteins to electrodes and applications in biosensors, biofuel cells, and nanotechnology.* Chemical Society reviews, 2011. **40**(7): p. 3564-3576.
47. Kotanen, C.N., et al., *Implantable enzyme amperometric biosensors.* Biosensors and bioelectronics, 2012. **35**(1): p. 14-26.
48. Wang, J., *Survey and summary from DNA biosensors to gene chips.* Nucleic acids research, 2000. **28**(16): p. 3011-3016.
49. Park, M., S.-L. Tsai, and W. Chen, *Microbial biosensors: Engineered microorganisms as the sensing machinery.* Sensors, 2013. **13**(5): p. 5777-5795.
50. Yang, M., M.E. McGovern, and M. Thompson, *Genosensor technology and the detention of interfacial nucleic acid chemistry.* Analytica Chimica Acta, 1997. **346**(3): p. 259-275.
51. Zhou…, M., *Bioelectrochemical Interface Engineering: Toward the Fabrication of Electrochemical Biosensors, Biofuel Cells, and Self-Powered Logic Biosensors.* Accounts of Chemical Research, 2011.
52. Monošík, R., M. Streďanský, and E. Šturdík, *Biosensors-classification, characterization and new trends.* Acta Chimica Slovaca, 2012. **5**(1): p. 109-120.
53. Luppa, P.B., L.J. Sokoll, and D.W. Chan, *Immunosensors—principles and applications to clinical chemistry.* Clinica Chimica Acta, 2001. **314**(1–2): p. 1-26.

54. Andreou, V.G. and Y.D. Clonis, *Novel fiber-optic biosensor based on immobilized glutathione S-transferase and sol–gel entrapped bromcresol green for the determination of atrazine.* Analytica Chimica Acta, 2002. **460**(2): p. 151-161.
55. Choi, J.-W., et al., *Optical biosensor consisting of glutathione-S-transferase for detection of captan.* Biosensors and bioelectronics, 2003. **18**(12): p. 1461-1466.
56. Soldatkin, O., et al., *Novel sucrose three-enzyme conductometric biosensor.* Materials Science and Engineering: C, 2008. **28**(5): p. 959-964.
57. Surareungchai, W., et al., *Dual electrode signal-subtracted biosensor for simultaneous flow injection determination of sucrose and glucose.* Analytica Chimica Acta, 1999. **380**(1): p. 7-15.
58. Prodromidis, M., et al., *Bioelectrochemical determination of citric acid in real samples using a fully automated flow injection manifold.* Analyst, 1997. **122**(10): p. 1101-1106.
59. Sheu, J.-T., et al., *A possibility of detection of the non-charge based analytes using ultra-thin body field-effect transistors.* Biosensors and bioelectronics, 2008. **23**(12): p. 1883-1886.
60. Palchetti, I. and M. Mascini, *Electrochemical Nucleic Acid Aptamer–Based Biosensors.* Electrochemical Biosensors, 2015: p. 75.
61. Radi, A.-E., *Electrochemical Aptamer-Based Biosensors: Recent Advances and Perspectives.* International Journal of Electrochemistry, 2011. **2011**.
62. Ananthanawat, C., et al., *Surface plasmon resonance study of PNA interactions with double-stranded DNA.* Biosensors & bioelectronics, 2011. **26**(5): p. 1918-1923.
63. Wang, J., *DNA biosensors based on peptide nucleic acid (PNA) recognition layers. A review.* Biosensors and bioelectronics, 1998. **13**(7): p. 757-762.
64. Mousa, S., *Biosensors: the new wave in cancer diagnosis.* Nanotechnology, Science and Applications, 2010.
65. Liao, J.C., et al., *Use of electrochemical DNA biosensors for rapid molecular identification of uropathogens in clinical urine specimens.* Journal of clinical microbiology, 2006. **44**(2): p. 561-570.
66. MacKay, S. and J. Chen. *Biosensor systems and applications in genomics, proteomics and metabolomics: A review*. in *Circuits and Systems (ISCAS), 2014 IEEE International Symposium on*. 2014: IEEE.
67. Kuralay, F. and A. Erdem, *DNA Biosensors*, in *Environmental Analysis by Electrochemical Sensors and Biosensors*. 2014, Springer. p. 313-330.

68. Liang, H., et al., *Functional DNA-containing nanomaterials: cellular applications in biosensing, imaging, and targeted therapy.* Accounts of Chemical Research, 2014. **47**(6): p. 1891-1901.
69. Ligaj, M., et al., *Electrochemical DNA biosensor for the detection of pathogenic bacteria Aeromonas hydrophila.* Electrochimica Acta, 2014. **128**: p. 67-74.
70. Turner, A.P., *Biosensors--sense and sensitivity.* Science, 2000. **290**(5495): p. 1315.
71. Kang, Q., L. Yang, and Q. Cai, *An electro-catalytic biosensor fabricated with Pt–Au nanoparticle-decorated titania nanotube array.* Bioelectrochemistry, 2008. **74**(1): p. 62-65.
72. Mohanty, S.P. and E. Kougianos, *Biosensors: a tutorial review.* Potentials, IEEE, 2006. **25**(2): p. 35-40.
73. Bhand, S.G., et al., *Fructose-selective calorimetric biosensor in flow injection analysis.* Analytica Chimica Acta, 2010. **668**(1): p. 13-18.
74. Vermeir, S., et al., *Microplate differential calorimetric biosensor for ascorbic acid analysis in food and pharmaceuticals.* Analytical chemistry, 2007. **79**(16): p. 6119-6127.
75. Länge, K., B.E. Rapp, and M. Rapp, *Surface acoustic wave biosensors: a review.* Analytical and bioanalytical chemistry, 2008. **391**(5): p. 1509-1519.
76. Lec, R.M. and P. Lewin. *Acoustic wave biosensors*. in *Engineering in Medicine and Biology Society, 1998. Proceedings of the 20th Annual International Conference of the IEEE*. 1998: IEEE.
77. Abad, J., et al., *Determination of organophosphorus and carbamate pesticides using a piezoelectric biosensor.* Analytical chemistry, 1998. **70**(14): p. 2848-2855.
78. Tsai, J.-Z., et al., *Resonant efficiency improvement design of piezoelectric biosensor for bacteria gravimetric sensing.* Bio-medical materials and engineering, 2014. **24**(6): p. 3597-3604.
79. Faegh, S., N. Jalili, and S. Sridhar, *Ultrasensitive Piezoelectric-Based Microcantilever Biosensor: Theory and Experiment.* Mechatronics, IEEE/ASME Transactions on, 2015. **20**(1): p. 308-312.
80. Piliarik, M., H. Vaisocherová, and J. Homola, *Surface plasmon resonance biosensing.* Methods in molecular biology (Clifton, N.J.), 2009. **503**: p. 65-88.
81. Teles, F. and L. Fonseca, *Trends in DNA biosensors.* Talanta, 2008. **77**.

82. Ko, S. and S.A. Grant, *A novel FRET-based optical fiber biosensor for rapid detection of Salmonella typhimurium.* Biosensors and bioelectronics, 2006. **21**(7): p. 1283-1290.
83. Liu, X. and W. Tan, *A fiber-optic evanescent wave DNA biosensor based on novel molecular beacons.* Analytical chemistry, 1999. **71**(22): p. 5054-5059.
84. Hutchinson, A.M., *Evanescent wave biosensors.* Molecular biotechnology, 1995. **3**(1): p. 47-54.
85. Homola, J. and S.S. Yee…, *Surface plasmon resonance sensors: review.* Sensors and Actuators B: Chemical, 1999.
86. Saha, K., et al., *Gold nanoparticles in chemical and biological sensing.* Chemical reviews, 2012. **112**(5): p. 2739-2779.
87. Leutwyler, W.K., S.L. Bürgi, and H. Burgl, *Semiconductor clusters, nanocrystals, and quantum dots.* Science, 1996. **271**(5251): p. 933-937.
88. Robelek, R., et al., *Multiplexed hybridization detection of quantum dot-conjugated DNA sequences using surface plasmon enhanced fluorescence microscopy and spectrometry.* Analytical chemistry, 2004. **76**(20): p. 6160-6165.
89. Huang, K. and A.A. Martí, *Recent trends in molecular beacon design and applications.* Analytical and bioanalytical chemistry, 2012. **402**(10): p. 3091-3102.
90. Clark, L.C. and C. Lyons, *Electrode systems for continuous monitoring in cardiovascular surgery.* Annals of the New York Academy of sciences, 1962. **102**(1): p. 29-45.
91. Guilbault, G.G., D.N. Kramer, and E.B. Hackley, *New substrate for fluorometric determination of oxidative enzymes.* Analytical chemistry, 1967. **39**(2): p. 271-271.
92. Guilbault, G.G. and J.G. Montalvo Jr, *Urea-specific enzyme electrode.* Journal of the American Chemical Society, 1969. **91**(8): p. 2164-2165.
93. Janata, J., *Immunoelectrode.* Journal of the American Chemical Society, 1975. **97**(10): p. 2914-2916.
94. Aizawa, M., et al., *Enzyme immunosenser: Ill. Amperometric determination of human cherienic gonadotropin by membrane-bound antibody.* Analytical biochemistry, 1979. **94**(1): p. 22-28.
95. Bergveld, P., *Development, operation, and application of the ion-sensitive field-effect transistor as a tool for electrophysiology.* Biomedical Engineering, IEEE Transactions on, 1972(5): p. 342-351.
96. Finkenstadt, V.L., *Natural polysaccharides as electroactive polymers.* Applied microbiology and biotechnology, 2005. **67**(6): p. 735-745.

97. Kretschmann, E., *Die bestimmung optischer konstanten von metallen durch anregung von oberflächenplasmaschwingungen.* Zeitschrift für Physik, 1971. **241**(4): p. 313-324.
98. Kretschmann, E. and H. Raether, *Notizen: Radiative Decay of Non Radiative Surface Plasmons Excited by Light.* Zeitschrift für Naturforschung A, 1968. **23**(12): p. 2135-2136.
99. Liedberg, B., C. Nylander, and I. Lunström, *Surface plasmon resonance for gas detection and biosensing.* Sensors and actuators, 1983. **4**: p. 299-304.
100. Pockrand, I., et al., *Surface plasmon spectroscopy of organic monolayer assemblies.* Surface Science, 1978. **74**(1): p. 237-244.
101. Guilbault, G.G. and J.H. Luong, *Gas phase biosensors.* Journal of biotechnology, 1988. **9**(1): p. 1-9.
102. Tothill, I.E., *Biosensors for cancer markers diagnosis.* Seminars in Cell & Developmental Biology, 2009. **20**(1): p. 55-62.
103. Khlebodarova, T.M., et al., *Application of bioinformatics resources for genosensor design.* Journal of bioinformatics and computational biology, 2007. **5**(02b): p. 507-520.
104. Ward, E., et al., *Plant pathogen diagnostics: immunological and nucleic acid-based approaches.* Annals of Applied Biology, 2004. **145**(1): p. 1-16.
105. Mousavi, S.R. and M. Rezaei, *Nanotechnology in agriculture and food production.* J Appl Environ Biol Sci, 2011. **1**(10): p. 414-419.
106. Bott, N.J., et al., *Toward routine, DNA-based detection methods for marine pests.* Biotechnology advances, 2010. **28**(6): p. 706-714.
107. CLARK JR, L.C. and E.W. CLARK, *A personalized history of the Clark oxygen electrode.* International anesthesiology clinics, 1987. **25**(3): p. 1-29.
108. Dietze, W., H.-P. Haar, and W. Obermeier, *Electrochemical analysis system*. 1994, Google Patents.
109. Roussel, T., et al., *Amperometric Techniques*, in *Encyclopedia of Microfluidics and Nanofluidics*, D. Li, Editor. 2008, Springer US. p. 39-47.
110. Bard, A.J., M. Stratmann, and P. Unwin, *Encyclopedia of Electrochemistry volume 3: Instrumentation and Electroanalytical Chemistry*. 2003: Wiley-VCh.
111. Protti, P., *Introduction to modern voltammetric and polarographic analisys techniques.* Editorial AMEL, 4ta. edición, Italia, 2001: p. 2-37.
112. Bockris, J.O.M. and A.K. Reddy, *Modern electrochemistry: an introduction to an interdisciplinary area*. 2012: Springer Science & Business Media.
113. Wang, J., *Analytical electrochemistry*. 2006: John Wiley & Sons.

114. Stradiotto, N.R., H. Yamanaka, and M.V.B. Zanoni, *Electrochemical sensors: a powerful tool in analytical chemistry.* Journal of the Brazilian Chemical Society, 2003. **14**(2): p. 159-173.
115. Tomschik, M., et al., *Reduction and oxidation of peptide nucleic acid and DNA at mercury and carbon electrodes.* Journal of Electroanalytical Chemistry, 1999. **476**(1): p. 71-80.
116. Palecek, E., *Oscillographic polarography of highly polymerized deoxyribonucleic acid.* Nature, 1960. **188**: p. 656-657.
117. Paleček, E., *Adsorptive transfer stripping voltammetry: Determination of nanogram quantities of DNA immobilized at the electrode surface.* Analytical biochemistry, 1988. **170**(2): p. 421-431.
118. Wang, J. and A.-N. Kawde, *Amplified label-free electrical detection of DNA hybridization.* Analyst, 2002. **127**(3): p. 383-386.
119. Fan, Y., et al., *TiO 2-graphene nanocomposite for electrochemical sensing of adenine and guanine.* Electrochimica Acta, 2011. **56**(12): p. 4685-4690.
120. Alfonta, L., A.K. Singh, and I. Willner, *Liposomes labeled with biotin and horseradish peroxidase: A probe for the enhanced amplification of antigen-antibody or oligonucleotide-DNA sensing processes by the precipitation of an insoluble product on electrodes.* Analytical chemistry, 2001. **73**(1): p. 91-102.
121. Vercoutere, W. and M. Akeson, *Biosensors for DNA sequence detection.* Current opinion in chemical biology, 2002. **6**(6): p. 816-822.
122. Zhu, L., et al., *Electrochemical Behaviors of Methylene Blue on DNA Modified Electrode and Its Application to the Detection of PCR Product from NOS Sequence.* Sensors, 2008. **8**.
123. Cai, H., et al., *Electrochemical detection of DNA hybridization based on silver-enhanced gold nanoparticle label.* Analytica Chimica Acta, 2002. **469**(2): p. 165-172.
124. Du, P., et al., *Electrochemical DNA biosensor for the detection of DNA hybridization with the amplification of Au nanoparticles and CdS nanoparticles.* Bioelectrochemistry (Amsterdam, Netherlands), 2009. **75**(1): p. 37-43.
125. Zanoli, L.M., R. D'Agata, and G. Spoto, *Functionalized gold nanoparticles for ultrasensitive DNA detection.* Analytical and bioanalytical chemistry, 2012. **402**(5): p. 1759-1771.
126. Zhang, Q., et al., *Applications of carbon nanotubes to electrochemical DNA sensors: a new strategy to make direct and selective hybridization detection*

from SWNTs. Advances in Natural Sciences: Nanoscience and Nanotechnology, 2011. **1**.

127. Zhang, Y., et al., *An electrochemical DNA sensor based on a layers-film construction modified electrode.* The Analyst, 2011. **136**(20): p. 4204-4210.
128. Astruc, D., *Electron-transfer processes in dendrimers and their implication in biology, catalysis, sensing and nanotechnology.* Nature chemistry, 2012. **4**(4): p. 255-267.
129. Chin, C.D., V. Linder, and S.K. Sia, *Lab-on-a-chip devices for global health: past studies and future opportunities.* Lab on a chip, 2007. **7**(1): p. 41-57.
130. Nyholm, L., *Electrochemical techniques for lab-on-a-chip applications.* The Analyst, 2005. **130**.
131. Rackus, D.G., M.H. Shamsi, and A.R. Wheeler, *Electrochemistry, biosensors and microfluidics: a convergence of fields.* Chemical Society reviews, 2015.
132. Temiz, Y., et al., *Lab-on-a-chip devices: How to close and plug the lab?* Microelectronic Engineering, 2015. **132**: p. 156-175.
133. Zhao, Y., et al., *Lab-on-a-chip technologies for single-molecule studies.* Lab on a Chip, 2013. **13**(12): p. 2183-2198.
134. Herold, K.E. and A. Rasooly, *Lab on a Chip Technology: Fabrication and microfluidics*. Vol. 1. 2009: Horizon Scientific Press.
135. Giannitsis, A.T., *Microfabrication of biomedical lab-on-chip devices. A review.* Estonian Journal of Engineering, 2011. **17**.
136. Sia, S.K. and G.M. Whitesides, *Microfluidic devices fabricated in poly (dimethylsiloxane) for biological studies.* Electrophoresis, 2003. **24**(21): p. 3563-3576.
137. Taberham, A., et al., *The fabrication of lab-on-chip devices from fluoropolymers.* Journal of Micromechanics and Microengineering, 2008. **18**(6): p. 064011.
138. Nunes, P.S., et al., *Cyclic olefin polymers: emerging materials for lab-on-a-chip applications.* Microfluidics and nanofluidics, 2010. **9**(2-3): p. 145-161.
139. Fiorini, G.S. and D.T. Chiu, *Disposable microfluidic devices: fabrication, function, and application.* BioTechniques, 2005. **38**(3): p. 429-446.
140. Comina, G., A. Suska, and D. Filippini, *PDMS lab-on-a-chip fabrication using 3D printed templates.* Lab Chip, 2013. **14**(2): p. 424-430.
141. Chang Ming Li, H.D., Qin Zhou, and Kai H. Goh, *Electrochemical Sensors, Biosensors and their Biomedical Applications*. First Edition ed, New York: Academic Press.
142. Heller, M.J., *DNA microarray technology: devices, systems, and applications.* Annual review of biomedical engineering, 2002. **4**(1): p. 129-153.

143. Van Swearingen, A.E.D., et al., *Combination therapy with MEK inhibition is efficacious in intracranial triple negative breast cancer models.* Cancer Research, 2015. **75**(15 Supplement): p. 2579-2579.
144. Siggers, T., et al., *Characterizing the DNA Binding Site Specificity of NF-κB with Protein-Binding Microarrays (PBMs).* NF-kappa B: Methods and Protocols, 2015: p. 609-630.
145. Srivastava, M., et al., *Reduced PARP1 as a Serum Biomarker for Graft Rejection in Kidney Transplantation.* J Proteomics Bioinform, 2015. **8**: p. 031-038.
146. Nakayama, S., et al., *FOXD1 Expression Is Associated with Poor Prognosis in Non-small Cell Lung Cancer.* Anticancer research, 2015. **35**(1): p. 261-268.
147. Castillo-León, J., *Microfluidics and Lab-on-a-Chip Devices: History and Challenges*, in *Lab-on-a-Chip Devices and Micro-Total Analysis Systems*. 2015, Springer. p. 1-15.
148. Rodrigo, M.A.M., et al., *Electrochemical Microarray for Identification Pathogens: A.* Int. J. Electrochem. Sci, 2014. **9**: p. 3431-3439.

Chapter Two

2.1 Interfaces

In electrochemical biosensors, the interface is the nanometric monolayer that links the electrode with the bioreceptor, so it is a relevant connection from the micro (the electrode) to the nanoscale (biomolecule)[149].

In electrochemical devices, the interface is the region where electron transfer occurs from the solution bulk to the electrode surface. In this area occurs desorption or absorption of molecules, diffusion of reagents, chemical reactions among others.

In biosensors, the main objective of the interfaces is focused on the conception and elaboration of functionalized surfaces of materials for biosensing. The idea is to develop surface modification strategies to improve physical and chemical parameters of the electrodes materials that are reflexed in a better performance of the biosensors. In this way, the sensibility, efficiency and hardiness of the biosensor are heightened. With this purpose, the interface is fundamental in creating an antifouling sensor surface to reduce non-specific adsorption (NSA) of undesired molecules, to help in the electron transfer forenhancing electrochemical signal detection, to create a high surface anchoring area to link the bioreceptors, among others[150]. Therefore, the biosensors interface is one of the main pillars in the fabrication of these devices[151, 152].

Biosensor interfaces include the use of the nanostructures of diver materials and shapes also. For electrochemical biosensing applications, the layer or multilayer designs for the interface would include the specific biomolecule recognition to posterior integration in microdevices that use electrochemical transducers[153]. One fundamental pillar of the biosensors is its behavior in the modern bioelectronic circuits. The wide range of applications that involve the use of these microdevices has led to rethink the old approaches for the bioelement immobilization. Besides, with the advance in the nanofabrication techniques and the incorporation of new materials, it has been possible design new architectures and 3D scaffolds[154, 155].

Bottom Up techniques are the principal methods for fabrication of self-organizing functional systems in a nanometric scale from down, the transducer in our case, to up, the whole layers of the biosensor [156-158]. For that, different techniques are used such as Atomic Layer Deposition (ALD); excellent to produce core-shell nanostructures and sol–gel nanofabrication; relevant to obtain functional metal

oxide materials and some alloys. Moreover, Chemical Vapor Deposition (CVD) and Physical Vapor Deposition (PVD) are vapor phase deposition techniques frequently used in the synthesis of carbon nanostructures like nanotubes or sheets. One of the most important bottom up technique due to its simplicity and low cost is the molecular self-assembly technique (MSA)[159, 160]. These nanofabrication methods are based in the spontaneous self-assembly of molecules without the presence of outside interactions. Because of their spontaneous nature and ease of manufacturing procedures, the self-assembly approach is widespread and currently many researchers still consider it. However, the biophysics behind self-assemblyit is still poor understood[161]. Its applications are mainly in biosensors, biotechnology and biomedicine.

The self-assembly involves the term of self-organization and this is defined as the spontaneous formation of hierarchical complex structures from predesignedmolecules [162]. Molecular self-assembly mechanism has notable implications in nanofabrication processes since its reducethe costly processes and because does not require other techniques and difficult manufacturing steps[163]. Besides, it permits to create supramolecular structures susceptible to preset patterns. This technique can be used for both biological molecules and biological supramolecular structures as an integral part of the interface. This allows the formation of thermodynamically stable structures more complex and functional. Other advantage of MSA structures is their capacity of self-repair offering very homogeneous interfaces.

2.2 Self-assembled Monolayers (SAMs)

SAMs are a type of MSA to the fabrication of single molecules layers on the substrate. SAMs represent new fabrication mechanisms of structures and forms at nanoscales, which traditional techniques do not include. They are in many fields of technology and their study resulted in a multitude of learning about the interfacial mechanics at the atomic level[164-166]. Although not represent the last frontier of nanotechnology development, we can say that its use significantly expanded research in surface science and materials. The SAMs are highly ordered and low-dimensional molecular assemblies. These are formed spontaneously by adsorption on different single crystal surfaces of different materials. Some authors

considerSAM like dynamic nanostructures. Table 2.1 shows a summary of type of moleculesand its counterpart substrates for its immobilization.

Molecules	Carboxilic Acids	Alcohols	Amines	Alkane-silanes	Thiocyanates	Disulfides	Thiols
Substrates	Cu, Ag, NI, Pd, Al_2O_3	Pt, graphite	Pt	SiO_2, SnO_2, TiO_2	Au	Au	Au, Ag, Cu and Pt

Table 2.1: Different self-assembled systems

The idea of self-assembled monolayers was in the mind of Jacob Sagiv in 80s early. The adsorption of silane molecules on glass surface, offered a highest versatility on the traditional Langmuir-Blodgett films. Then many researches introduced new molecules on new materials to find self-assembled systems different to the silanes. Nuzzo and Allara at Bell laboratories were the first in reporting the disulfide molecules behavior on gold[167]. It is the most typical SAM system and it has been the center of numerous studies. However, the complete physic-chemical processes of the self-assembly is not clear yet. Scheme 2.1 shows some example of the interactions chemistry and the different interface possibilities behinds SAMs.

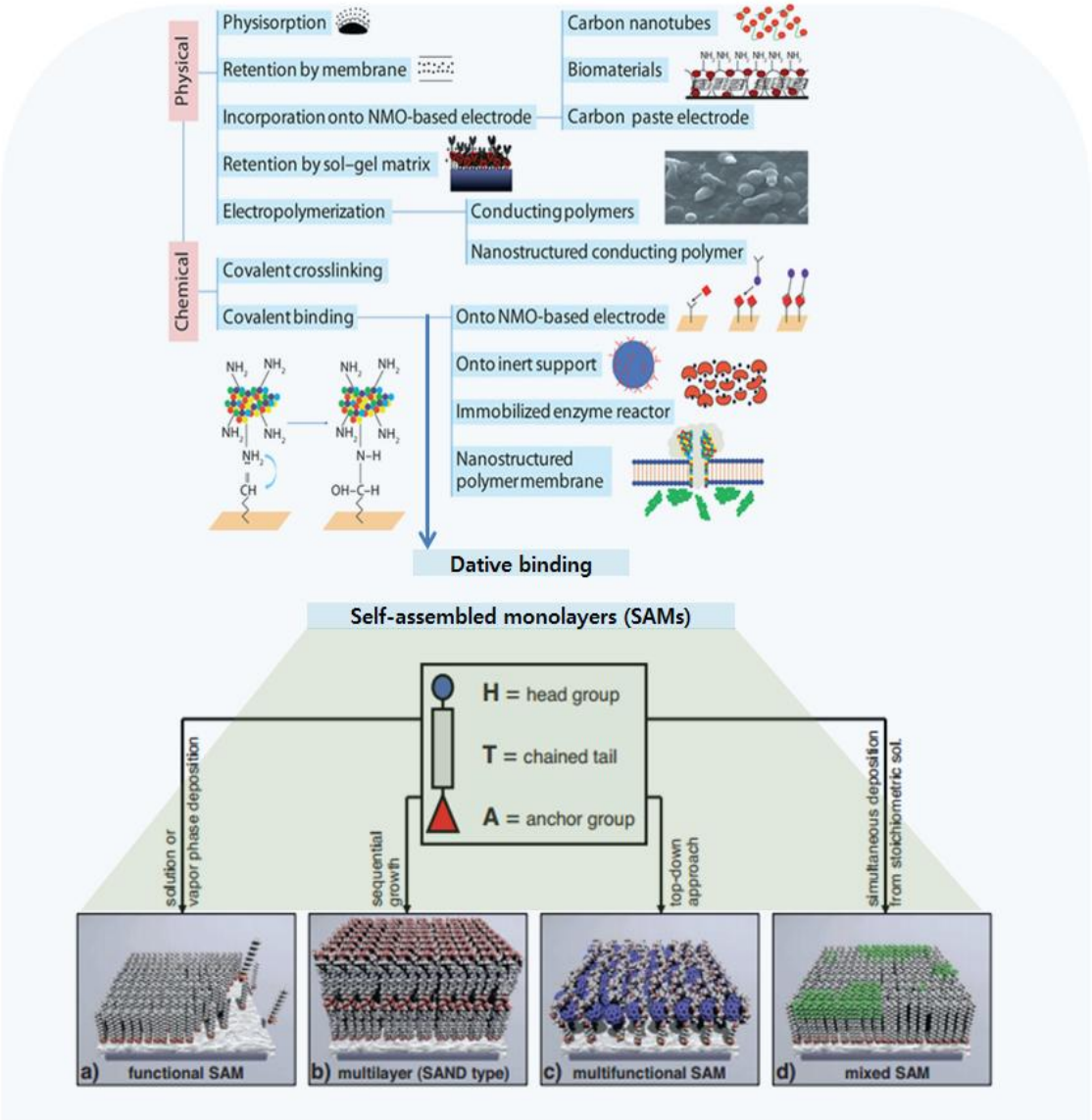

Scheme 2.1: Some Bottom Up interfaces and schematic sketch of SAM examples, a) n-alkylphosphoric acid SAM, b) multilayer SAM nanodielectric (SAND), c) PEG-phosphoric acid SAM, d) mixed SAM.

In general, SAMs have two principal components a crystalline substrate –generally a metal or glass- and one molecule with both a "head group" in one end and a "functional group" in the other end. The head group should have specific affinity for the substrate and the functional group offers a reactive group for its interaction with other molecule or biomolecule. In figure 2.1, we can see a most simplified scheme of the structure of SAMs.

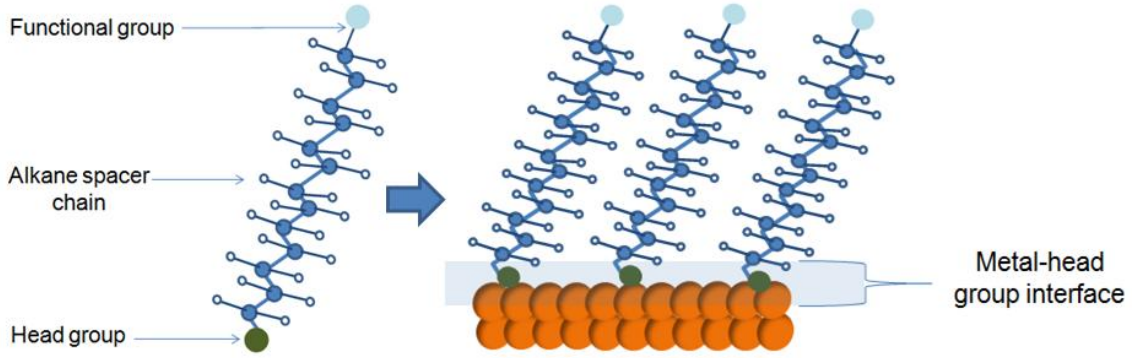

Figure 2.1: Typical representation of self-assembled monolayer

2.3 Thiol Self-assembled Monolayers

Nowadays the alkylthiolate monolayers are the most widespread SAMs used in biological applications[168-170]. The strong dative binding gives high stability of gold-sulphur interactions and allows the functionalization of many different nanostructures. The strong adsorption of sulphur-based compounds like thiols, disulphides, sulphides, and other related molecules on crystalline metals, especially gold (Au) and silver (Ag) make of these systems tools friendly which electronics and easy to use in laboratories[171-174]. The ability to control the interface modifications with a molecular level approach and the capacity to characterize the molecular buildings are other advantages of the alkylthiolate SAMs[175-179].

In this project, we chose the thiol-SAMs due to its big advantages exposed above and its notorious applications in DNA biosensors. Different types of SAM were tested to compare its performance in the development of biosensor.

2.3.1 Chemistry, kinetic and structure of thiol SAMs

During the SAM formation, alkanethiols chemisorption takes place on gold surface. This process can be considered as an oxidative addition of the S-H bind to the gold surface and posterior elimination of hydrogen byreductive procedure. When a clean gold surface is used, the hydrogen of the thiolated group is removed as a hydrogen molecule (H_2). It must be noted that in this reaction, the molecule chemisorpted on gold is an alkane-thiolate and the exact behavior is currently unknown[180-183]. However, the most accepted theory is that the shared pair of electrons to form this

type of covalent bond, called dative bond, are coming from the same atom, the thiol in this case, that interacts strongly with the two vacant of the gold atoms on the substrate. Regarding other sulphur-based molecules, the chemisorption mechanisms have been little studied. However, many proposals incorporates Au-adatom model[184-188]. Besides, this studies generally working with ultraplanar gold with perfect hexagonal unit cells. This model proposes a continuous interaction between the adsorbates and the gold surface. The dynamical reconstruction of the surface involves the formation of thiolate–adatom moieties. In this way, thiolate–Au complexes have been proposed as the building blocks of SAMs not only for planar surfaces, but also for the case of thiol-capped Au nanoparticles. Regarding (111) crystalline organization the model is valid but the amorphous geometries not.

The SAM structure depends of several factors and their kinetic of formation also[189, 190]. The size of the adsorbed molecule, the alkyl chain length, the crystal organization of gold, temperature, pressure, surface clean among others, are factors to take into account during the SAM formation[191-193]. The most common kinetic of SAM formation consist in many steps; the first one of them involves the physisorption of molecules followed by chemisorption of these. Then, with the molecules in parallel configuration to substrate surface, the ordered domains appear on the substrate. Therefore, to add more molecules we obtain a tilted transition in the configuration of alkyl chains. Finally, the defect correction is carrying out due to the movement and reorganization of these molecules on the substrate. For further information about the SAM formation, we can see ref [152, 194-200]

2.3.2 Self-assembled monolayers preparation

The SAMs formation can be done by spontaneous adsorption from a liquid medium or gaseous phase. The gas method is used under conditions of ultra-high vacuum (UHV) when the application requires. In other hand, the assembly from a solution is an effective method for most applications, especially those requiring contact with crystalline solid surfaces. Due to the nature of the project, the immobilization method from solution was chosen. The protocol to follow is simple; the substrate used to form the monolayer is dipped in a solution containing the thiolated molecule. To achieve reproducibility in the manufacture of the SAM, the preparation and clean conditions should be optimal.

2.3.3 Self-assembled monolayers test

Considering the information in the literature, three different self-assembling systems were tested in order to choose the one that offer the best results in our platform. In order to reduce NSA two interfaces were chosen with polyethylene glycol (PEG) integrated in the linker, since these molecules is a well-recognized antifouling molecule. Two different anchored thiolated molecules were used in each system, a disulphide molecule in one case and a thioctic acid in the other case. These two linkers are including a maleimide group at one end for labelling with the capture probe. Both systems were compared with the most widespread interface reported in biosensors, a mixed monolayer of 6-mercapto-1-hexanolmercaptohexanol (MCH) and thiolated-DNA. The working oligos used in the experimental part of this work are common elements in the three SAMs. The first one is the 23-mercapture probe (CP), and it has in the 5' end a thiol group. In all these platforms, this thiolated-DNA capture probe is used for its direct attachment on gold, in the case of the mixed monolayer with MCH, or for the interactions of the thiol moiety with the maleimide group at the end of the surface-attached linker.

The second oligo is the PCR amplified target DNA. It has different lengths, depending on the different sequences that will be detected in the array.The 5' end of the target is labelled with ferrocene (Fc) redox molecule, by means of a Fc-labelled primer used in the PCR,that gives the electrochemical signal required to detect the hybridization event. For the full detection of the cancer, there were fourteen different CPs with their corresponding target DNA.

Another molecule in common, in each one of the monolayer tested, is the MCH. In one case because it is part of the monolayer and in the case of the interfaces based in PEG, because it is the molecule used to block the free maleimide groups still unreacted with the thiolated-CP. MCH is a short alcohol molecule of six carbon with a sulfhydryl group at its end (see figure 2.2). Generally is used to avoid the non-specific adsorption (NSA) and like antifouling agent over the gold surface. This NSA can interfere with detection measures either concealing them or giving false positives. NSA is one of the major problems in biosensing interfaces and so it is very relevant the study of an appropriate interface. Other function of the MCH is to serve like spacer between bigger molecules. Because of its small size the kinetic of reaction with the gold surface is often faster that the longer molecules and it could be used as a spacer between the bioreceptors on the sensor surface, for improving its next interaction with the target.

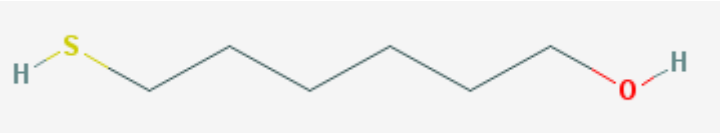

Figure 2.2: 6-Mercapto-1-hexanol structure

Table 2.2 shows the conditions involved in each interface. For each immobilized layer. The distinct immobilization times tested gave us crucial information about possible reorganizations in the SAMs formation dynamics. Some of the buffers, times PCR conditions and temperature settings were in the original confidential protocol of the company Genomica S.A.U, and so there are not introduced in this thesis. There were washing steps after each immobilization step in order to avoid NSA, the formation of disulfide bonds and to clean the SAM surrounding environment. After having the particular SAM interface, the target DNA was immobilized under flow. The idea was to detect the hybridization event and to observe the kinetic behavior. Electrochemical measurements were done before target DNA injection to discard possible contaminations. The electrochemical reading performed after hybridization permit us to detect the duplex formation. Moreover, SPR optical technique was parallel used to characterize all the immobilization steps on the biosensor.

IMMOBILIZATION PHASE	
Immobilization method	Batch and flow
Immobilization time	overnight / 2 hours/ 1 hour
Immobilization buffer and pH	Tris-HCL 10 mM, NaCl 1M, EDTA 1 mM, ClMg 5 mM
Electrochemical buffers	KCl 10 mM / Ferrocyanide 1 mM
HYBRIDIZATION PHASE	
Hybridization buffer	Hybridization solution pH 7.38
Temperature	59ºC
Hybridization time	1 hour
Electrochemical buffers	NaCl 10 mM

Table 2.2: Fixed features during the molecular self-assembly of the biosensor

2.3.4 Capture probe and mercaptohexanol SAM (CP-MCH)

The first interfacetested was the most typical SAMreported[201]; the CP-MCH mixed monolayer. Both molecules have a thiol in one of its end and these functional groups are anchorage on the gold surface. The concentrations used for both molecules were 1 μM in a ratio of 1:9 for CP and MCH respectively. For this SAM formation was necessary only one-step, being just necessary the immersion of the gold substrate where was done only one time.

2.3.5 Lipoic acid maleimide-Polyethylene glycol SAM (LAM-PEG)

One of the two PEG-based linker is a 5-[(3R)-dithiolan-3-yl] pentanoic acid-C4-NHCO-EG6-C2-maleimide (LAM) where EG is ethylene glycol unit. The LAM molecule (see figure2.3) has a thioctic acid (lipoic acid derivate) with two sulfur atoms in a pentagonal cycle binding between them by disulfide bond, these two atoms are gold anchor. This linker has a PEG arm in its alkyl chain, as we introduced before, the PEG inclusion was to decrease the NSA. Finally, this linker has a maleimide group in the other end. The maleimide group is very reactive with single thiolated molecules and in this way we are anchored the thiol of capture probe on the sensor surface. This SAM has three formation steps. The initial level consists in a SAM of the LAM in 1 μM concentration. The second level has two molecules and two immobilization steps, one for each molecule added. First the thiolated CP (1 μM) was interacted with the maleimide moiety. Then the 1 μM MCH was added to block the remaining maleimide and gold surface still unreacted.

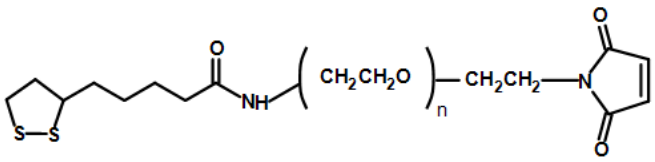

Figure 2.3: Lipoic acid maleimide structure

2.3.6 Maleimide-PEG disulphide SAM (MalPEG)

The other PEG-based linker tested is a HO-EG6-C11-S-S-C11-EG6-NHCO-Maleimide (MalPEG). This molecule has a maleimide disulphide with two PEG arms. Each arm has an alkyl chain and then a six PEG subunit. One arm ends with hydroxyl group and the other with maleimide group (see figure 2.4). Like in the above molecule, this group will reacted with the thiol group of the CP and/or the thiol of the MCH. The SAM formation process is similar than LAM-PEG SAM, the monolayer immobilization consists in three steps also. In a similar way, first the monolayer of MalPEG was immobilized, then the CP and finally the MCH molecule is introduced into the double layer system. The concentration used for each molecule was 1 μM.

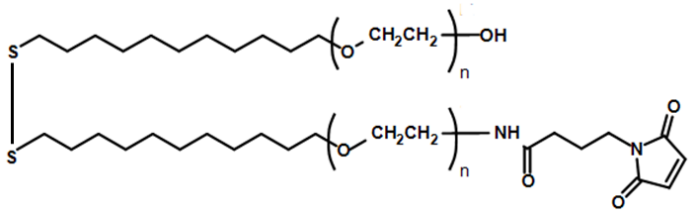

Figure 2.4: Maleimide-PEG disulphide structure

Figure 2.5 schematize each of the SAM systems used during the experimental sets. It is notorious the double level of the SAMs that uses the PEG based linkers. There are few reported articles related with these two PEG linkers and these papers are focused on the formation of monolayers but without any practical application. In this project, we used a biosensor interface and we studied its effect in the biosensor performance.

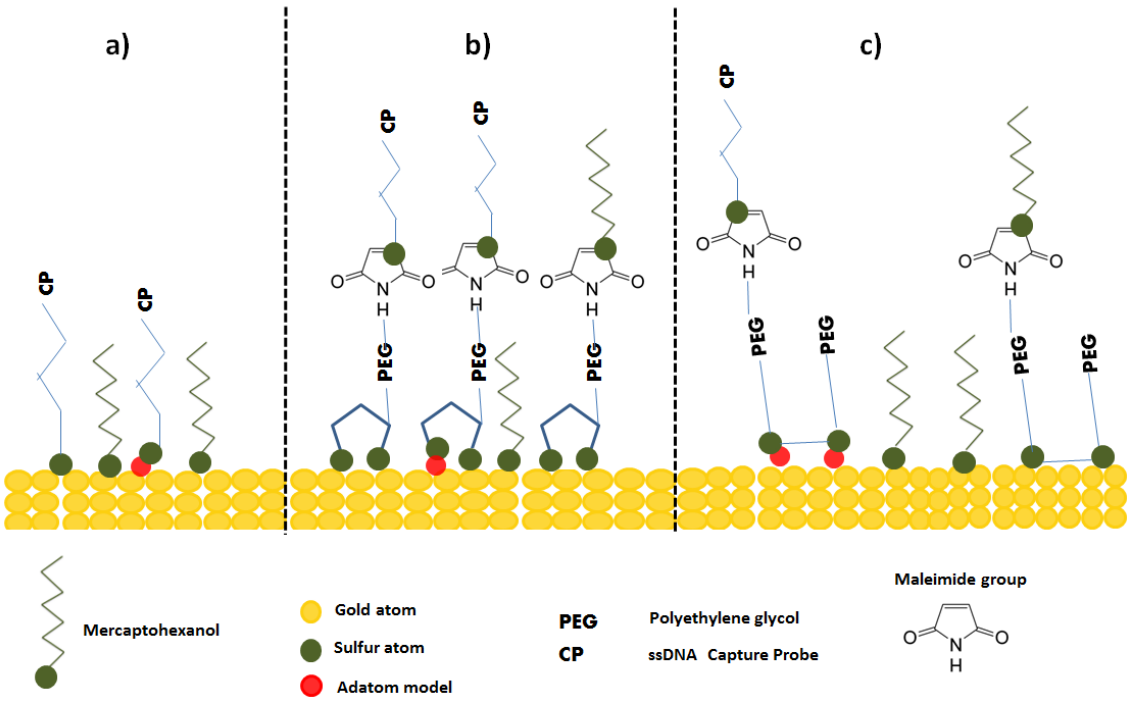

Figure 2.5:Three SAMs system tested, a) CP-MCH, b) LAM-PEG, c) MalPEG

2.4 Techniques for SAM characterization

Even though the self-assembly process is far from being completely controlled, we can monitor whether certain characteristics during their formation process. SAM characterization is important in the development of an optimal biosensing platform, as we introduced before. There are several techniques to characterize a SAM. In literature, we found infinity of studies, depending of the work aim. We summarized some of them in table 2.3. In this work, we do not contemplate deep structural organization study of the monolayer, but in the benefits that different types of interfaces bring to our electrochemical DNA biosensor. In this sense, we have studied optically and electrochemically the surface coverage, stability and NSA of different interfaces to check the improvements on the selectivity and sensitivity in the electrochemical DNA sensor. In practical terms, we optimize optical and electrochemically a sensing interfaces for subsequent integration into a LOC device (see chapter three for more detail)

Techniques for SAM characterization	
Experimental technique	Extracted information
Electronic techniques	
X-ray photoemission spectroscopy (XPS)	Elemental composition, chemical state
Auger electron spectroscopy (AES)	Surface elemental composition, coverage
X-ray absorption near edge spectroscopy (XANES)	Molecular orientation, bonding nature
Structural techniques	
Low energy electron difraction (LEED)	Atomic distances, surface symmetry
Infrared spectroscopy (IR)	Molecular tilt, adsorption site
Ions scattering spectroscopy (ISS)	Surface structure and composition
Optical techniques	
Surface plasmon resonance (SPR)	Coverage, adlayers molecular interactions
Microscopic techniques	
Scanning tunneling microscopy (STM)	Surface topography, surface structure (periodicity)
Atomic force microscopy (AFM)	Surface topography, surface structure (periodicity)
Electrochemistry techniques	
Cyclic voltammetry (CV)	Molecular interactions, electroactivity, impurities
Differential pulse voltammetry (DPV)	Molecular interactions, electroactivity
Amperommetry	Molecular interactions, electroactivity

Table 2.3: Techniques for SAM characterization

The techniques used for the characterization of the SAMs in this work are explained following.

2.4.1 Surface Plasmon resonance (SPR)

One of the optical techniques more efficient in the study of surface-interface interactions is SPR[202-204]. The mechanism of surface plasmon is well known today and we can found several publications discussing their properties in detail.

Surface Plasmons are surface electromagnetic waves that propagate parallel along a metal/dielectric interface. They are sensitive to small changes at interface, as the adsorption of molecules on the surface. Plasmon excitation requires polarized light and it occurs when plane-polarized light is reflected under flat angles from a thin metal film deposited on a glass substrate. At a specific angle (θ) the photons interact with the free electron cloud in the thin metal film, causing a drop in the intensity of the reflected light. When a layer is added in the substrate, this angle shifts due to changes in the refractive index of the interfacial surrounding of the SPR metal substrate.

Thus in a multilayer interface, the change in properties of the dielectric layer requires a change in the conditions of surface plasmon excitation for each layer. This indicates a change in the incidence light angle for the plasmons excitation, which depend on the optical thickness (refractive index) of the layers involved. That

angle shift is just the base for monitoring the molecules attachment on the SPR sensor. In this way, we can determine the molecules surface coverage in each adlayer.

The typical SPR optical sensor comprises a system which contains a source of optical radiation and an optical structure in which plasmon is excited, a transducing medium which interrelates the optical and biochemical domains, and an electronic system supporting the optoelectronic components of the sensor and allowing data processing.

The method used for surface plasmon optical excitation in this work is the Kretschmann configuration[97] show in figure 2.6a. The technique is sensitive to molecular events occurring in an interaction volume defined by the extension of the evanescent electric field of the surface plasmon, extending a few hundred nanometers into the surrounding medium.

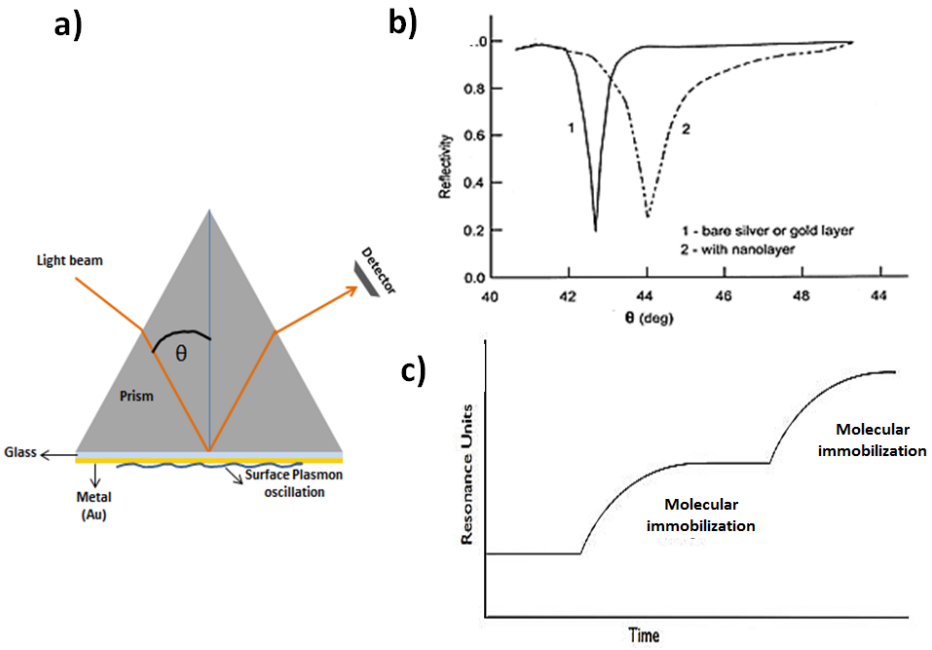

Figure 2.6: a) Scheme of Kretschmann configuration SPR b) scan method measure c) kinetic method measure

There are two measurement modes in SPR technique. One of them is the scan method (figure 2.6b) and involves measurement of reflectivity in function of incidence angle that allows having the minimum reflectivity angular position. Measuring θ shift produced by the adlayer adsorption, and having as input the refractive index of the same, the thickness of the immobilized layers can be fitted and calculated. The second method is a kinetic measurement (figure 2.6c). The aim

of this reading is to monitor the growth of a film in function of time and so, the progress and the kinetics of surface adsorption process.

For this work, we used the ResTec (RT-2005) spectrometer, with a custom-made setup, developed by Prof. Wolfgang Knoll (Material Science) at the Max-Planck-Institute for Polymer Research in Mainz, Germany (see figure 2.7). In this apparatus the plasmon excitation is achieved with a standard 633 nm He (Helium)-Ne (Neon) laser. A sensitive silicon detector senses the reflected light. The software used to control the SPR and to monitor the results is Wasplas. The software used to data processing was Winspall that it is based on the Fresnel equations and the matrix formalism. The characterization results obtained with these experiments are usually the optical thickness [nm] and/or surface coverage [ng/cm2] of each adlayer.

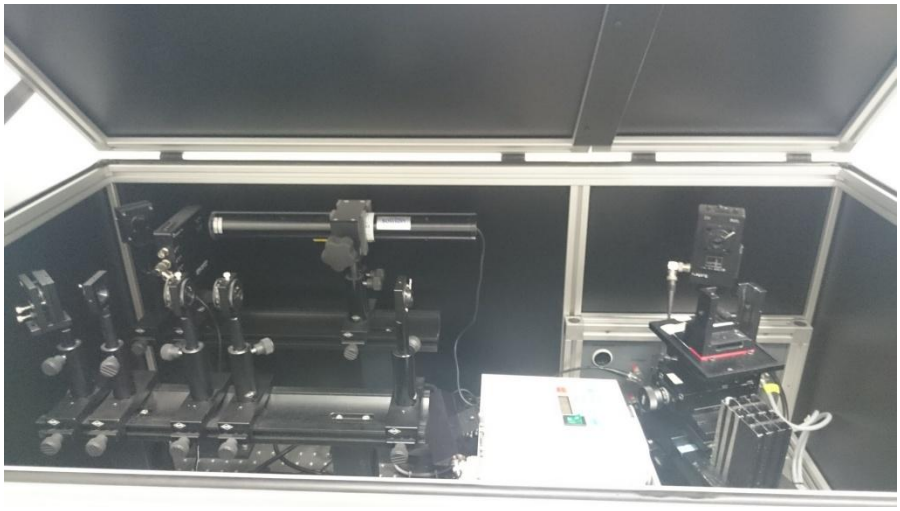

Figure 2.7:Restec SPR picture

2.4.1.1 SPR imaging

During the first optimization stages of the different SAMs systems, the SPR imaging (SPRi) platform of GWC technologies was used[205]. Comparing with the previous SPR introducedtheimaging SPR permits the visualization of the whole chip through a video CCD camera. This design enables to analyze the array, or chip, in each

active spot providing information simultaneously, see figure 2.8. In this system, a broad-beam monochromatic polarized light from a laser diode (at a specific wavelength) illuminates the completely functionalized area of the SPRi chip surface (which is mounted within the instrument detection chamber). The high-resolution CCD video camera provides real-time difference images across the array with up to 16active sites distributed on thegold spots. As the above SPR system, it captures all of the local changes at the surface of the chip providing detailed information on molecular binding, biomolecular interactions and kinetic processes. The main advantage of this equipment is that we can to perform until 16 different measurements at the same experiment.

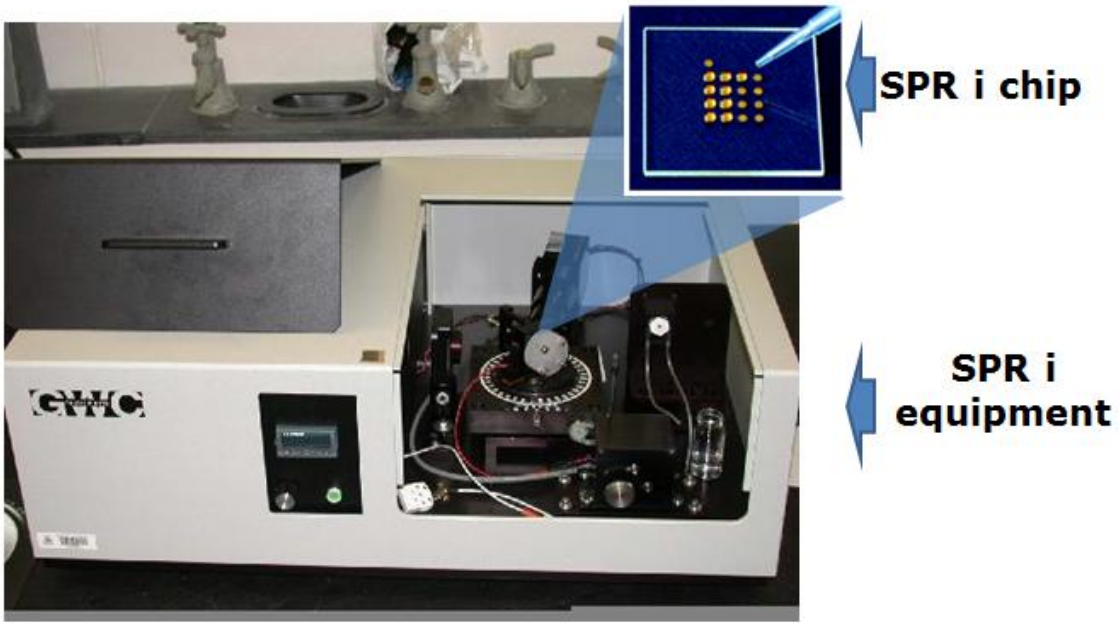

Figure 2.8: SPRi equipment and chip picture

2.4.1.2 Electrochemical SPR (eSPR)

The e-SPR cell was designed exclusively for this project to perform the SPR measurements in the RESTECequipment but also to carry out electrochemical measurements on the same gold SPR chip[206]. Two pieces of different materials, Teflon and Polyether ether ketone (PEEK) were used for this purpose. Both are thermoplastic materials and are unreactive to almost any organic molecule. Some molecules adsorption tests were conducted and the results were optimal for each case. Figure 2.9 show the design and final product. The final cell works like usual electrochemical cells, three electrodes were included inside theoptical SPR cell. For

this purpose, it was integrated into the cell an Ag/AgCl RE screw up into the cell and a platinum wire as CE was inserted into the cell with external connection. The gold chip substrate was used for plasma excitation in SPR and as WE in the electrochemical cell. It was externally connected with a spring pin connector.

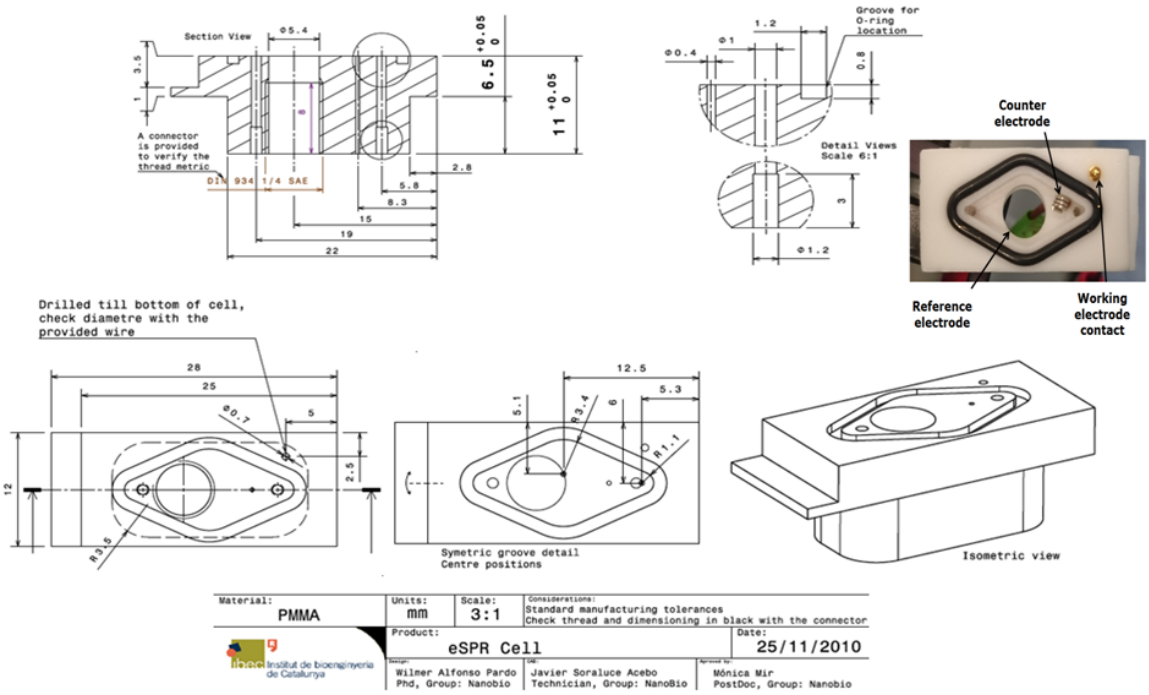

Figure 2.9: e-SPR cell schematic

2.4.2 Electrochemical techniques: Cyclic Voltammetry

Electrochemical techniques were used in this work to characterize the immobilization biosensor interface but more importantly, to readout the signal from the electrochemical DNA biosensor developed in this project. For the electrochemical detection of target, the PCR amplified DNA labeled with Fc was used. The cyclic voltammetry (CV) technique is used to determine the diffusion coefficients and redox potentials of electroactive species. This technique is based on applying a sweep potential to the working electrode in both the forward direction and the reverse. This means that a triangular potential sweep is performed (figure 2.10a). This potential sweep begins at an initial value ($E_i$or E_0) to a final value (E_f). In this type of techniques, the slope of the variation of potential is known as scan rate. It is clear that not necessarily the end of the potential sweep has to match the initial value, so it would be more appropriate to mention that there are three important potential values, the initial potential, cutting anode potential (E_a) and cutting cathode potential court (E_c). The sweep can be initiated in either direction

(anode or cathode) and this technique allows repeating this cycle as timesas necessary. Figure 2.10b show a schematic diagram of this technique.

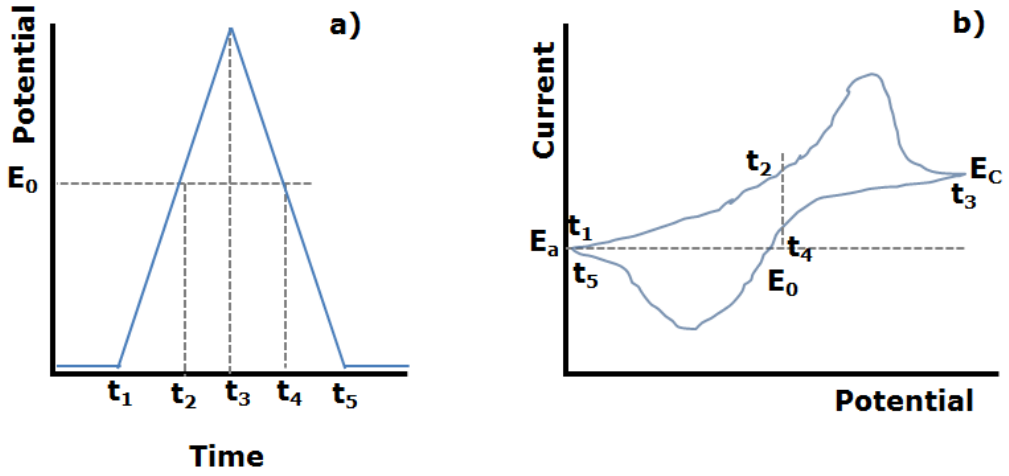

Figure 2.10: a) Potential change as a function of time. b) Typical curve obtained in CV

For a reversible system, like ferrocene (see figure 2.11), the current-potential response obtained is similar to that presented in figure 2.10b.Whereas the sweep starts at the anode sense, we see that to the reaching the appropriate potential value for starting the oxidation reaction, the current increases notoriously to a certain current peak value. Then the voltage is going to where the oxidation is not favored, and so the current decline as the potential is increased. Once it reaches the anodic potential value, the potential scan is reversed and the cathodic current increases and so the corresponding reduction reaction is obtained. The cycle ends in the cathodic potential value cutting, where in the majority of cases this value coincides with the initial potential value. Two important values into this oxidation-reduction process analysis are the current values obtained at the maximums, called anodic peak current (ep_a) and cathodic peak current (ip_c) respectively. For these experiments, CH660C potentiostat from CH Instruments was used.

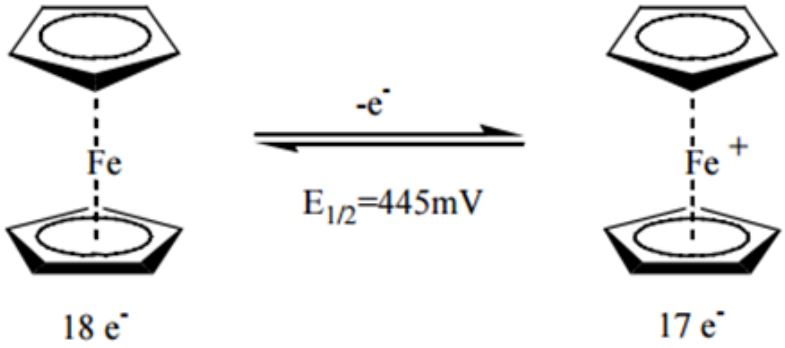

Figure 2.11 Ferrocene redox process

2.4.3 X-ray Photoelectron Spectroscopy (XPS)

Also known as ESCA (Electron Spectroscopy for Chemical Analysis), the XPS is a technique to determine the chemical composition of surfaces[207-211]. For comprehend the XPS technique we should understand the photoelectric photoemission effect. So, when a photon of the incident radiation used in the XPS encounters an atom, three things may happen: that the photon passes through it without interaction; that the photon is scattered by an electron with its respective energy loss and, finally, the photon interacts with an electron transferring all its energy and emitting the electron (see figure 2.12). Normally, when a surface is bombarded with X-rays, core level electrons are first emitted. The energy used in the X-ray may vary according to the application. The emitted electrons kinetic energy can be measured by the analyzer. In this way, the difference between the used photon energy (in our case Al K_α 1486.6 eV) and the kinetic energy recording in the analyzer, give us the binding energy and this parameter is like a fingerprint of an element. This technique working in the first 5 nm of the surface and each photoemission peak area is proportional to the number of emitters in the sample analysis.

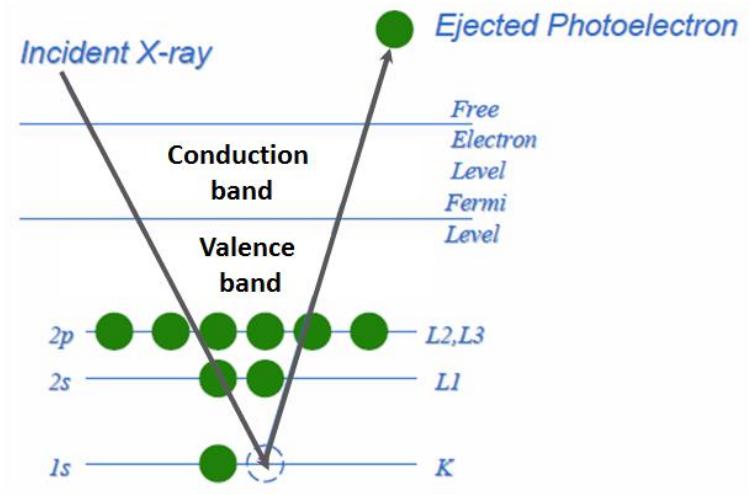

Figure 2.12: Energy transfer scheme of XPS

This characterization technique was used to perform an elemental chemical analysis of the atoms of our immobilized sensor surface.

2.4.4 Laser optical interferometry

Interferometry is a technique that uses the superposition of light waves in order to produce interference. The physical principle used is that two light waves coincide in phase are amplified while two waves in phase opposition are canceled. The difference between these fringes interference patterns gives information about some properties of the original state of the waves. These patterns of interference can be constructive or destructive and the image obtained is called interferogram. Interferometry is an important research technique in the fields such as astronomy, seismology, plasma physics, biomolecular interactions, surface profiling, and microfluidics among others. A variant of this technique is the Phase Shift Interferometry (PSI), based on optical phase shifting, which uses the difference in intensity as an alternative to fringes patterns. It also uses filtered light, and the reference surface is translated instead of the objective. PSI takes advantage of the wave properties of light to analyze surface characteristics, in particular surface height variations. For evaluation of areal surface topography, the source light beam is separate in two, so that it follows two independent paths, one of which includes a reference surface and the other the object surface. Then, the separated light beams are recombining again and directed to a digital camera that measures the resultant light intensity over multiple image points simultaneously. The intensity of the recombined light exhibits high sensitivity to the differences in path lengths, effectively comparing the object surface (surface under study) with the reference

surface (integrated in the apparatus) with nanometer resolution. The interferometer used for these experiments was the Wyko NT 9300 by Veeco Instruments, shows in figure 2.13, which use the Mirau interferometer configuration instead the typical Michelson configuration. For additional information about this technique, see the references.This technique provides a complete topographic profile of gold surface.

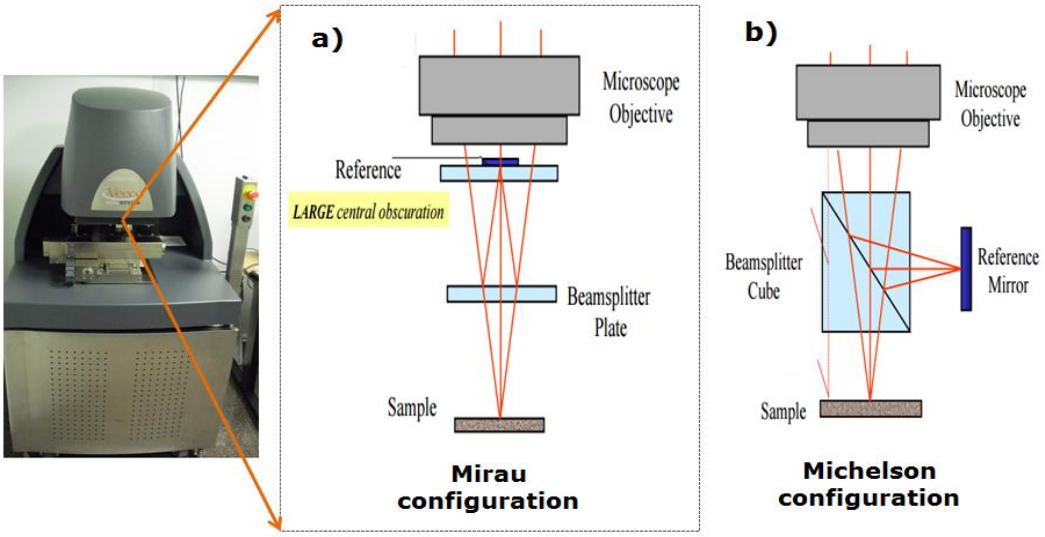

Figure 2.13: Interferometer configurations, a) Mirau, b) Michelson, image takes and adapted of Veeco Instruments brochures

2.4.5 Scanning tunneling microscopy (STM)

In the early 1980's two IBM scientists, Binnig & Rohrer developed a new technique for studying surface structure, scanning tunneling microscopy (STM)[212-214]. The technique is based upon scanning a conducting tip just above a surface. A bias applied between the two can allow electrons to tunnel through the vacuum between them, monitoring some interaction between the tip and the surface. The name of the technique arises from the quantum mechanical tunneling-type mechanism by which the electrons can move between two surfaces (see figure 2.14). The resulting tunneling current is a function of tip position, applied voltage, and the local density of states (LDOS) of the sample. Information is acquired by monitoring the current as the tip's position scans across the surface, and is usually displayed in image form. The STM with atomic resolution requires a well-defined, atomically flat electrode surface, ultra-high vacuum (UHV), extreme conditions of cleanness, sharp tips, excellent vibration control, and sophisticated electronics.

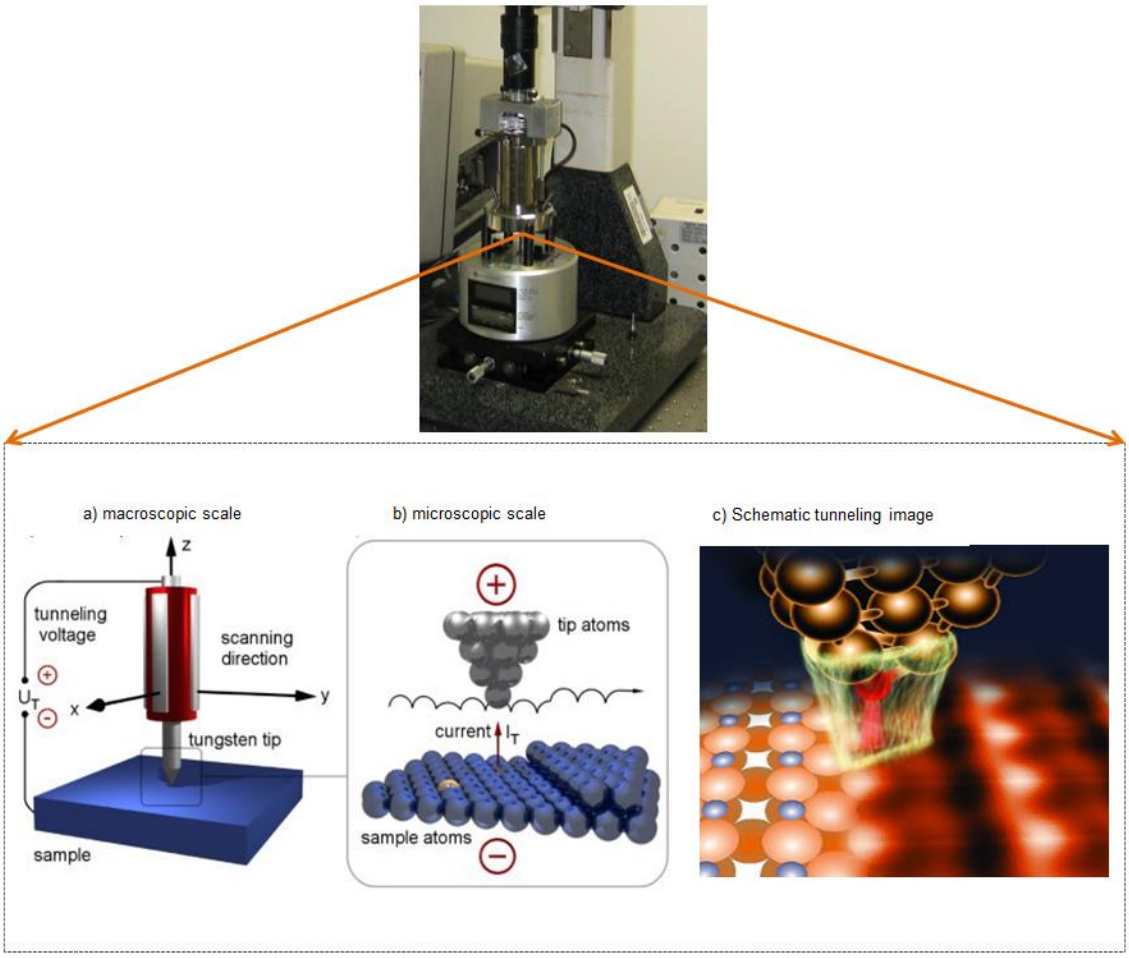

Figure 2.14: STM equipment (upper) with tip-surface detailed a) macroscale, b) microscale c) tunneling effect schematic

2.5 Experimental sets

The goal of this part of the project is to establish a thiol linker optimal interface that maximize the hybridization efficiency and subsequent detection of specific target DNA (amplified by mini-PCR) on a DNA electrochemical biosensor integrated in a LOC cartridge. In order to optimize and characterize the sensor interface, it was performed on alternative single gold chip instead of the biosensor matrix cartridge. SPR technique was chose to characterize the gold substrate and the SAM formation processes. However, the sets of experiments were established thinking in the final device. In this way, two methods of immobilization were conducted. The first was by immersion or stationary phase (batch) of the monolayer and the second immobilization by flow or dynamic phase (flow). For each experiment set three replicates are performed. All chips were measured first in bare (without adsorbate)

by SPR, for determining the state of the gold substrate. The flow chips were measured by the same technique after each added layer.

The batch chips were removed from the SPR cell for its functionalization and placed again after SAM attachment for following with the monitoring of subsequent steps. Prior to hybridization, the batch chips were measured in the SPR cell to determine the change in the reflective angle regarding the bare measurement. All hybridizations were done at 59º C and under flow to discard uncertainties in the comparisons.

2.5.1 Gold surface characterization

The first stage in the development of this interface is the gold surface characterization. The substrates used to optimize our biosensing platform were evaporated planar gold chips (see figure 2.15). The different shapes of chips have not relevant in this study and only depended of the company wherein were purchased. The common features of the chips were a BK7 glass substrate, evaporated with a layer of 2 nm of chrome and finally a layer of 50 nm gold. The BK7 glass is used in optical detectiondue to its low refractive index and its low dispersion. The chrome is used like intermediate layer for binding strongly the gold on the glass surface. The gold is used in electrochemical biosensors due to its conductive properties and its reactivity with the thiolates molecules and in SPR for its excitation of the plasmon. At difference of the typical studies in literature focused in SAM characterization, our gold is not monocrystalline. This means that we have an amorphous and rough surface, instead of an ultraplanar surface with crystalline structure.

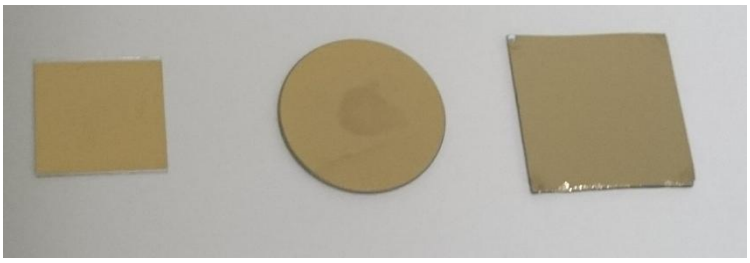

Figure 2.15: Different gold chips used to SAM optimization

The first characterization of the chips was to determine the correct thickness of each metal layer in the substrate. The right metal thickness is required to have an exact fitting of the thickness of subsequent interface immobilized layers. An angle scan measure was made and compared with Winspall software simulation (version 3.0.2.0).

Table 2.4 shows the values of different optical constants where *n* is refractive index and *K* is extinction coefficient of each material of the chip required for the simulation of each independent layer. The ε' and ε'' optical parameters are not used during simulations.

Material	Thickness (nm)	n	K	$\varepsilon' = n^2 - K^2$	$\varepsilon'' = 2nK$
Prism BK7	0	1,5151	0		0
Prism LaSFN9	0	1,8448	0	3,403	0
Cr (20-25ºC)	2	3,129 3,139	3,308 3,316	-1,096	20,786
Au (20-25ºC)	50	0,174 0,2 0,197	3,419 3,32 3,0901	-12,3	1,29
Thiol-CHx	1.5	1,5	0	2,25	0
DNA	0.34 x base	1,3748	0	1,8903	0
Air	0	1	0	1,77	0
PBS/water	0	1,332	0	1	0

Table 2.4: Simulation values for fitting SPR, the values in blue or red corresponding at different temperatures

In order to have a homogeneous and reproducible interface, the substrate has to be perfectly cleaned. To remove impurities from the gold surface, different cleaning treatments were performed. Solutions as piranha, super-piranha, ethanol and sulfuric acid were used, as well as sonication methods in ethanol and UV exposure also. After many trials, the best cleaning method that was found is described in the following protocol.

2.5.2 Surface gold cleaning protocol

- Wash the gold surface with liquid soap directly under running water in order to remove possible fat from the skin
- Immersion of the gold chip in a piranha solution in ratio 5:1 (5 ml of sulfuric acid: 1 ml of hydrogen peroxide) for 5 minutes
- Wash it in distilled water

- ❖ Immersion of the gold chip in a solution of absolute ethanol and sonicate for 10 minutes
- ❖ Dried with nitrogen
- ❖ Exposure the chip to UV for 5 minutes

The results of the optical scan after cleaning and its corresponding simulation can be seen in figure 2.16. We can note the similar behavior between the simulation and the measurements and the decrease minimum reflective angle value after cleaning.

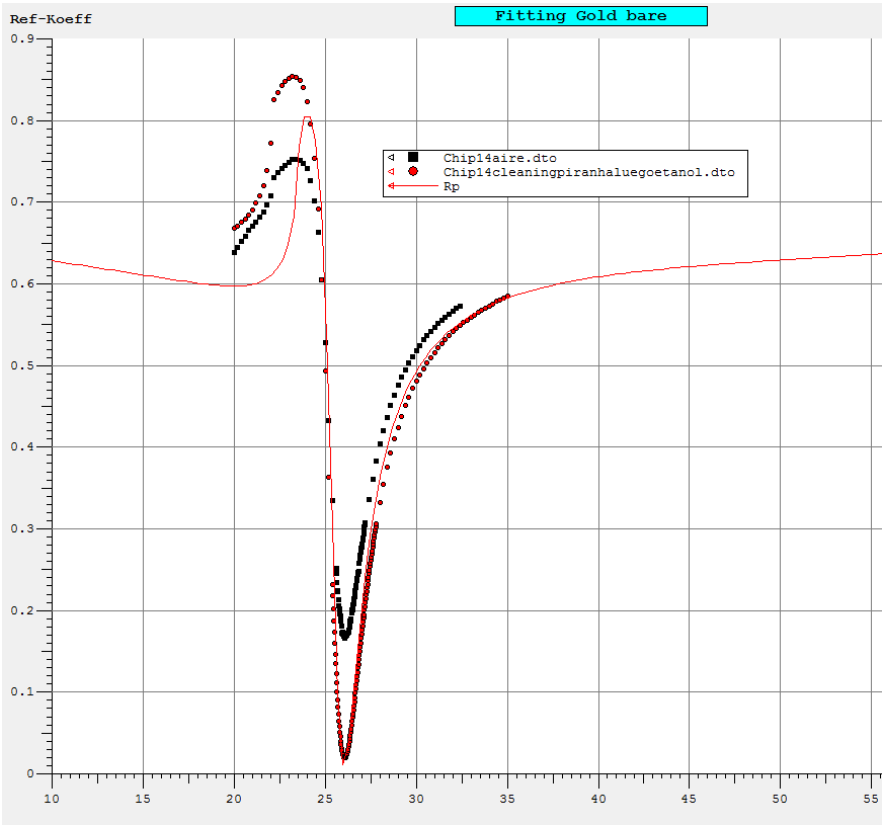

Figure 2.16: SPR angle scan of: (black squares) surface gold without cleaning treatment; (red spots), gold surface after cleaning treatment; (red line), simulation fitting

2.6 Results

2.6.1 SPR characterization

The optical optimization of the biosensor interface was performed with SPR.As we already introduced, the technique is sensitive to changes in the optical properties in

a solid-liquid interface, and any interaction between the sensor and the interface and between the probe and the target is detected.

The SPR kinetic measurement was monitored during the SAM formation at a fixed angle, following the increase of intensity (R(%)) versus time. Figure 2.17 show the normal behavior during the distinct immobilizations steps.

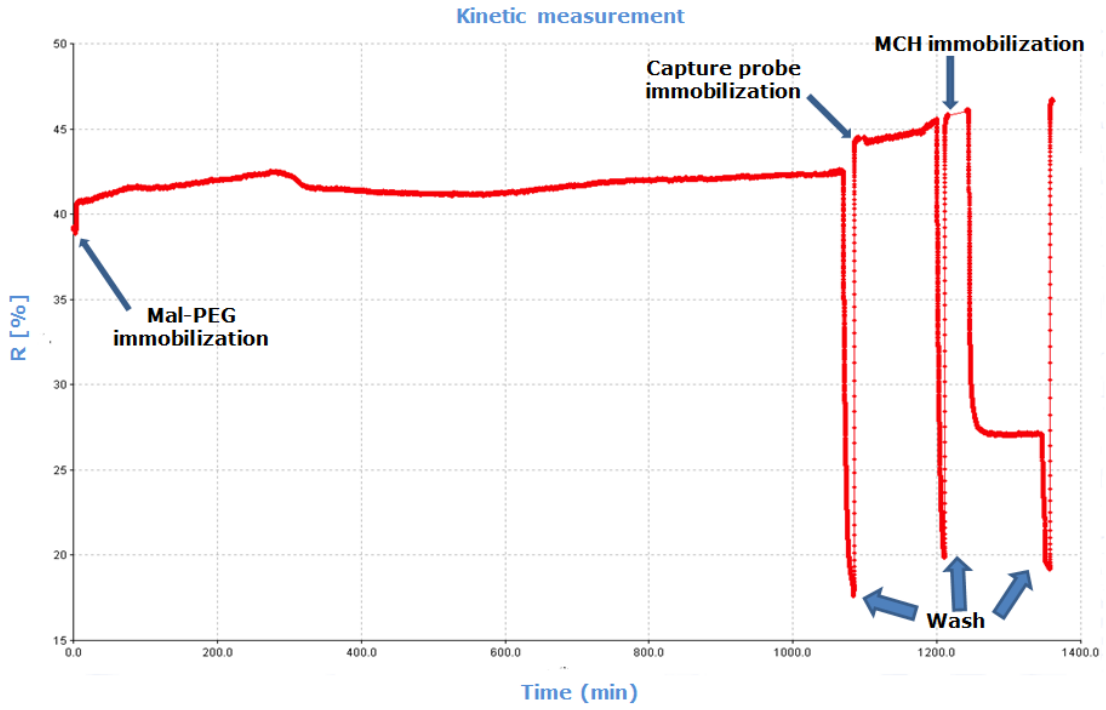

Figure 2.17:SPR kinetic measurement of the biosensor formation

The comparison of the SPR angle shift due to capture probe immobilization and its hybridization with the PCR DNA amplified sample is summarized in figure 2.18. We can see the angle shift, which implies a change in the refractive index of the gold-solution interface, due to the adhesion of the molecules on the SPR sensor. The blue columns give us information about the immobilization of the CP over the respective interface. The red columns show us the average of the angle shift due to the amount of duplex formation between the immobilized CP and the target. The errors bars showed the irreproducibility within each system. In the immobilization of CP-MCH interface the shift was not significant in comparison with the others systems and it is more irreproducible than the other platforms. The small size of the MCH molecule may bring to this molecule a faster reaction kinetic with the gold surface, diminishing the available places to anchor the CP. The low hybridization efficiency results observed in this platform support this hypothesis. On the other hand, LAM-PEG interface shows high amount of CP immobilized perhaps due to the

higher hydrophilicity compared with MCH and also due to its stronger thioctic acid anchoring molecule. The same hydrophilic chemistry applies in the MalPEG interface. However, unlike this, the MalPEG linker has two PEG branches, having a higher spacing between functional maleimide groups and so less places to attach the CP. Therefore, the unbranched LAM linker has less charge interaction between linkers and steric restrictions for immobilization of the linker.

However, during the hybridization process we observed much lower hybridization efficiency in the LAM platform, where the CP immobilization was much higher. Meanwhile the contrary is observed in the MalPEG platform. The reason for that may be the higher CP molecules density in the sensor with LAM could prevents the duplex formation due to steric or charge hindrance from the negative charged CP to the negative DNA target. Contrary to LAM-PEG interface, the MalPEG system offer good hybridization efficiency. The two arms of this molecule give a sufficient spacing between maleimide molecules and so CP, avoiding possible electrostatic repulsion and dodging steric hindrances successfully. The MalPEG SAM was chosen as functionalization biointerface due to its high hybridization efficiency and good reproducibility.

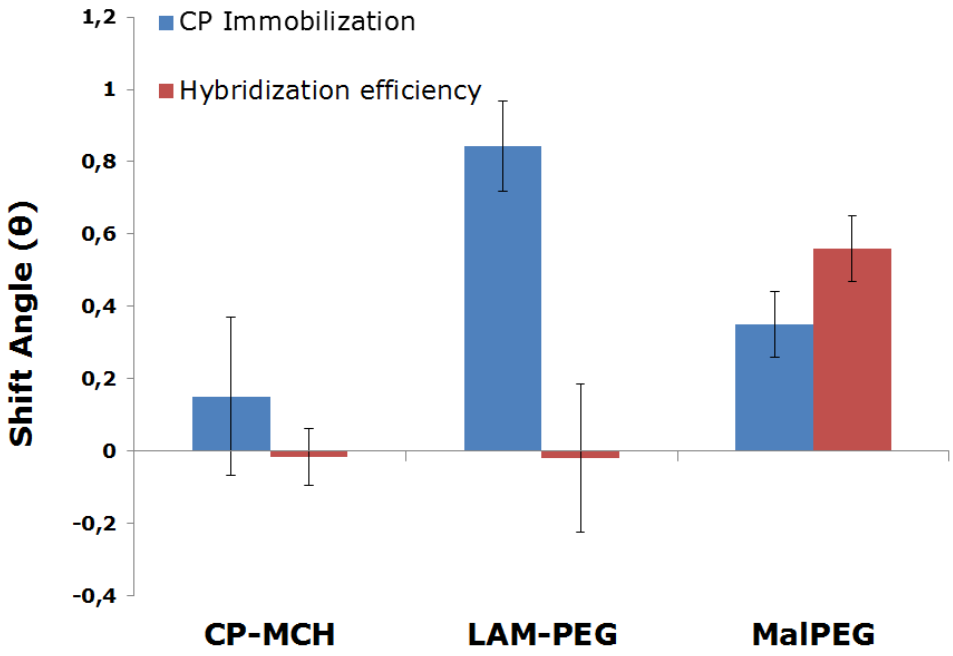

Figure 2.18: Shift angle (θ) of SPR results with different interfaces

2.6.2 i-SPR Maleimide layer optimization

The second stage in the interface optimization is the determination of the critical concentrations of the components of the chosen SAM, with the purpose of improving the hybridization efficiency. Maleimide-PEG layer is the first component to optimize. The assay would include a hybridization efficiency test with a fixed CP concentration (1 μM) and different maleimide concentrations. For these test five concentrations of maleimide-PEG were used; 1 μM, 5 μM, 10 μM, 20 μM, 100 μM. Each concentration has three repetitions. In this case, the SPR sensor used is SPRi that permits a multidetection ofSPR spots at the same time (figure 2.19). The immobilization procedure was the same as the used in the above assays. The MalPEG layer was immobilized first. Then we immobilized the CP layer, followed by 5 μM MCH. Finally, the target DNA was injected in the system. Between each immobilization layer a cleaning step was performed.

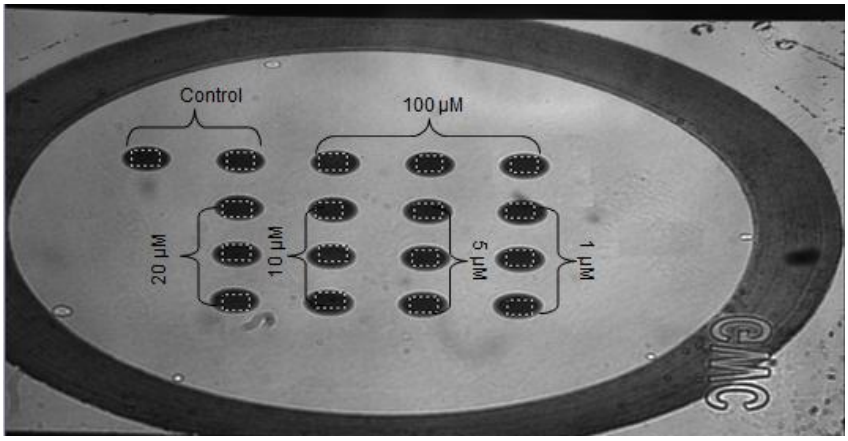

Figure 2.19:SPRi chip with different maleimide-PEG concentrations

The results are shows in figure 2.20. The lowest concentrations (1 and 5 μM) show problems during the CP immobilization due to low amount of maleimide reactive groupson the surface. Besides, the great irreproducibility into the spots in these concentrations is shown in its negative average of CP immobilization. The 100 μM concentration has a similar irreproducibility that the lowest concentrations in the CP immobilization. Is not until the 10 and 20 μM concentrations of maleimide that the results shows a good behavior, being 20 μM the one that has lower irreproducibility in the CP immobilization. It is also under this concentration where the hybridization of the target has a saturated signal. Therefore, we used 20 μM of MalPEG for next experiments.

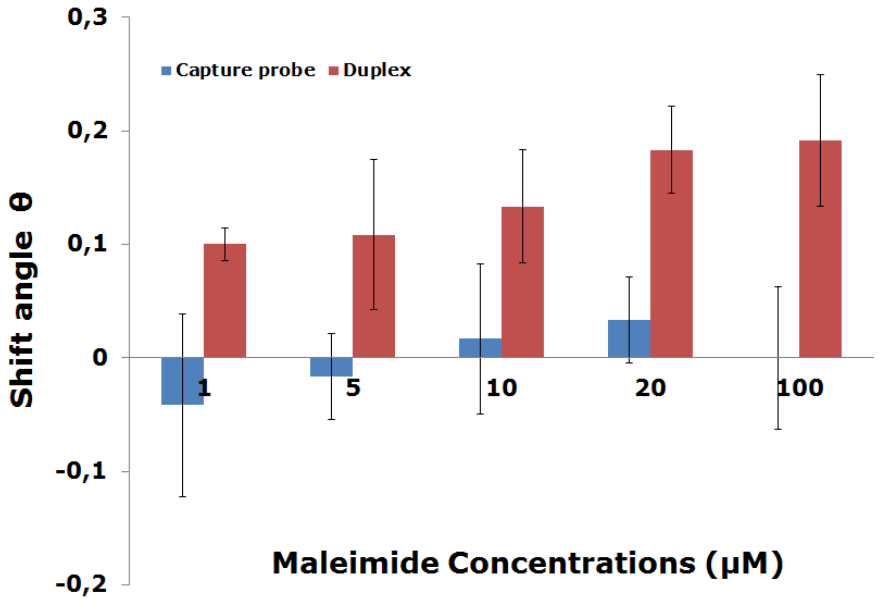

Figure 2.20: Maleimide-PEG concentration optimization with SPRi

2.6.3 Nonspecific adsorption test

Several checks were performed in order to test the selectivity of the measured hybridization and discard that the measured signal is not coming from NSA. The trials consist in immobilizing a CP and hybridize it with a non-complementary DNA, and with complementary target DNA over a gold surface with and without MalPEG linker.

The figure 2.21 represents the results of these NSA test. Is notorious the NSA in the control without MalPEG. In this case, without the attachment of the MalPEG linker what we have on the sensor surface is the direct interaction of the SH group of the thiolated CP and the subsequent blocking with MCH; it is, basically, the mixed MCH-CP platform immobilized in two steps. As can be appreciates in the graph this interface is giving high irreproducibility as in previous results and high NSA, that does not allow to detect differences between the complementary and not-complementary hybridization. In fact, it is surprising the bad results presented by the mixed SAM of CP-MCH, being one of the most reported interfaces. However, we should be noted that the majority of reported works are done with short synthetic DNA target, without any extra molecules. Nonetheless, in this work, we are hybridizing long DNA target amplified by PCR and so it contains a large mixture of other molecules, such as the primers, Taq polymerase, free nucleotides, and DNA

strands bits, among others, being our system more closed to a real sample and then with more probabilities of attachment of undesired molecules.

On the other hand, the platform with MalPEG linker shows again good hybridization response and negligible NSA, which demonstrates the good performance of the PEG chain in the linker.

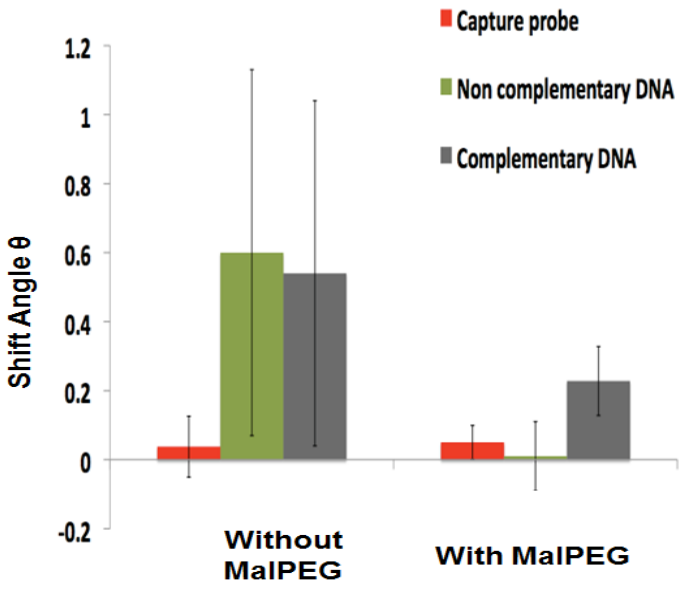

Figure 2.21: MalPEG SAM non-specific adsorption results

2.6.4 e-SPR Capture probe layer optimization

2.6.4.1 CP concentration

To optimize the CP layer a 20 μM fixed MalPEG concentrations was used. We tested three concentrations of CP; 5, 7.5, 10 μM. The immobilization protocol was the same used in previous experiments. This optimization was already performed in the e-SPR, so, both electrochemistry and SPR readouts were done at the same sensor chip. Figure 2.22 shows the results obtained with both characterization techniques. It is notorious the higher sensibility obtained from the same SPR sensor with electrochemistry than with SPR. In low concentrations of CP, 5 and 7.5 μM the SPR is just able to detect low hybridization signal, meanwhile electrochemical detection given already a saturated signal at 5 μM. The concentration of 10 μM is chosen for its good results in both techniques.

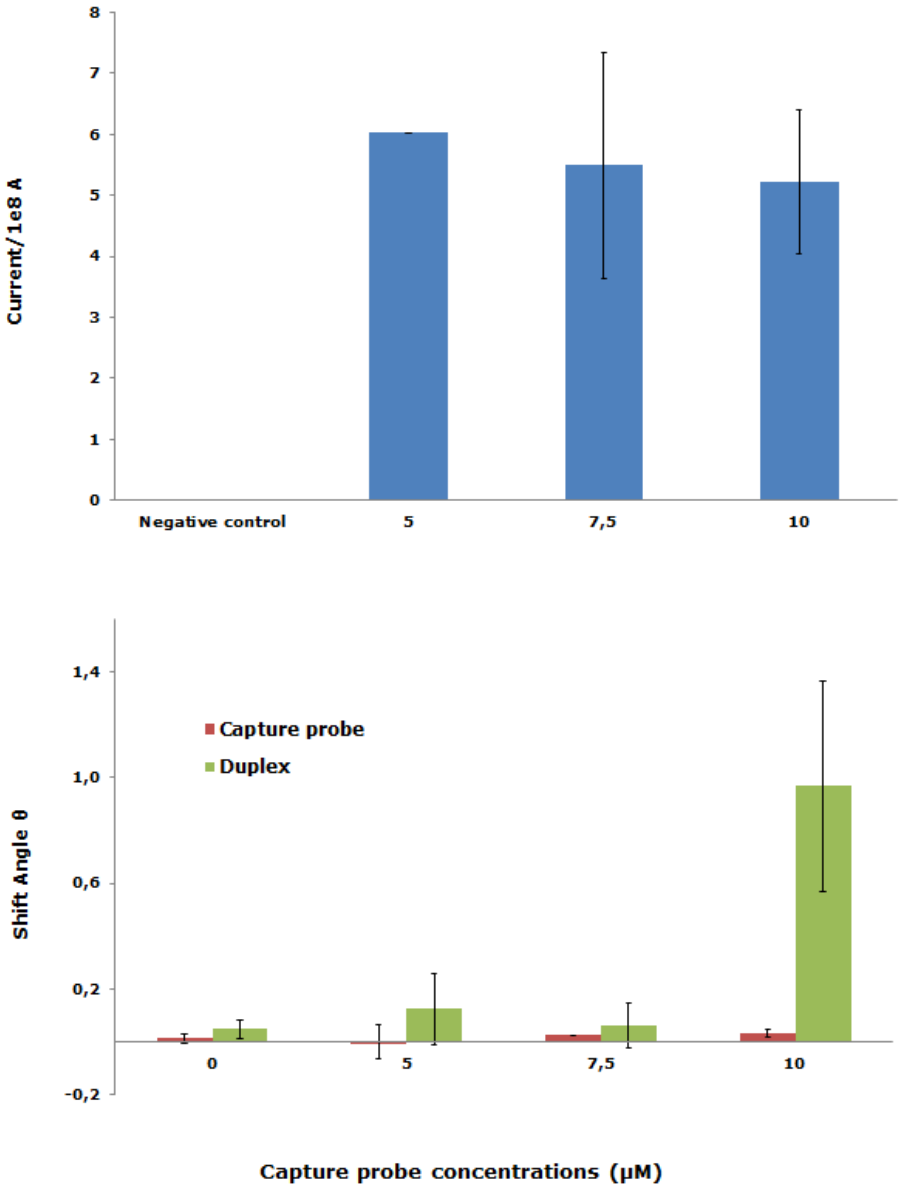

Figure 2.22: Electrochemical (up) and optical (down) results for CP layer optimization after hybridization with Fc-DNA target

2.6.4.2 Target orientation

Due to the length of our Fc-labeled targets DNA, the complementary sequence of the capture probe into them is not equidistant from the 5'and 3' ends of the target. In this way, depending on the end in which CP was functionalized with the thiol group, the target hybridize in a complete different configuration respect to the WE and the Fc moiety. Because this translocation, the sequence that has the ferrocene

molecule, which is even in the 5’ end of target DNA, can be closer or farther away to sensor surface, see figure 2.23. To improve the electrochemical response, different assays were performed with thiolated capture probes in both 5’ and 3' ends. When the hybridization is done with 3’ thiolated CP, the ferrocene label is closer to surface, this mean that the electron transfer is faster and efficient and facilitates the duplex detection. In contrary way, when we use the 5’ thiolated CP, the redox label is further from the surface and the electron flow is lower. The electrochemical difference between both thiolated CPs is more than twice. Regarding SPR characterization, the CP 5’ thiolated hybridization efficiency is higher because of the lower steric hindrance given by the short number of residues rearranged on the surface, while that the hybridization is more difficult in the 3’ thiolated CP due to the higher steric hindrance. Figure 2.24 summarizes the results obtained. Due to a higher electrochemical signal, and thinking in the next step of SAM integration with the electrochemical cartridge, the capture probe 3‘ thiolated is selected as working oligonucleotide hereafter.

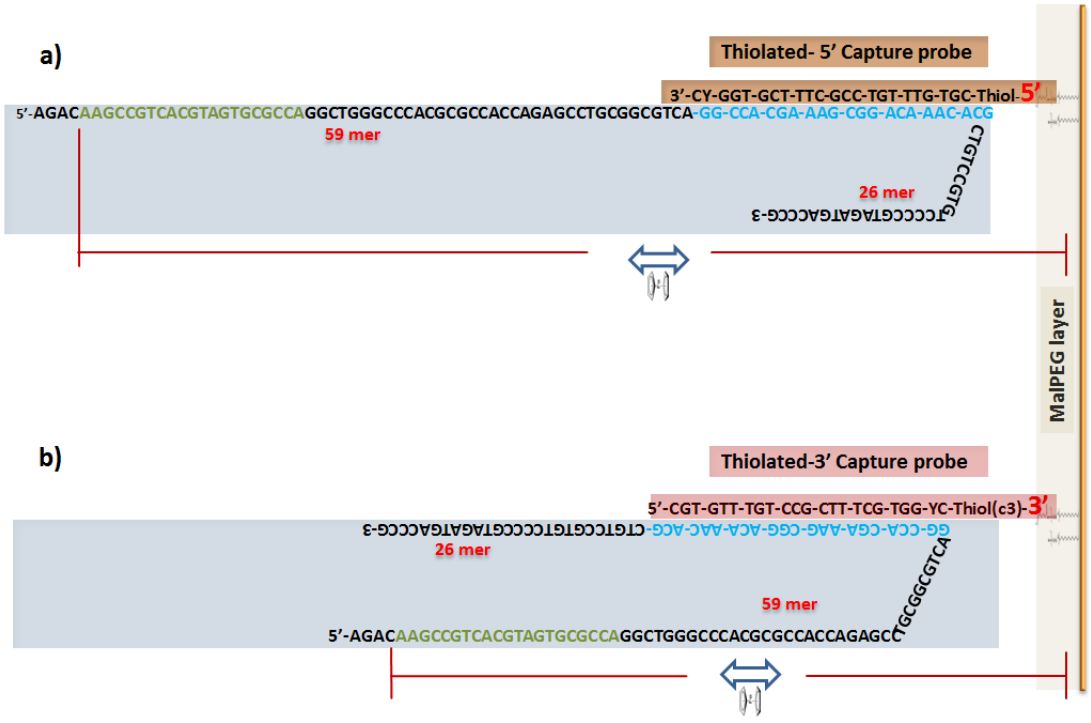

Figure 2.23: Different configurations of Fc-labeled DNA hybridization with a) 5’ thiolated CP and b) 3’ thiolated CP. The green sequence is the Fc label site and the blue sequence is the complementary sequence of CP. Red line indicates the distance of the redox molecule regarding the surface. The number of mer indicates the not equidistant position of the complementary CP sequence regarding to the ends

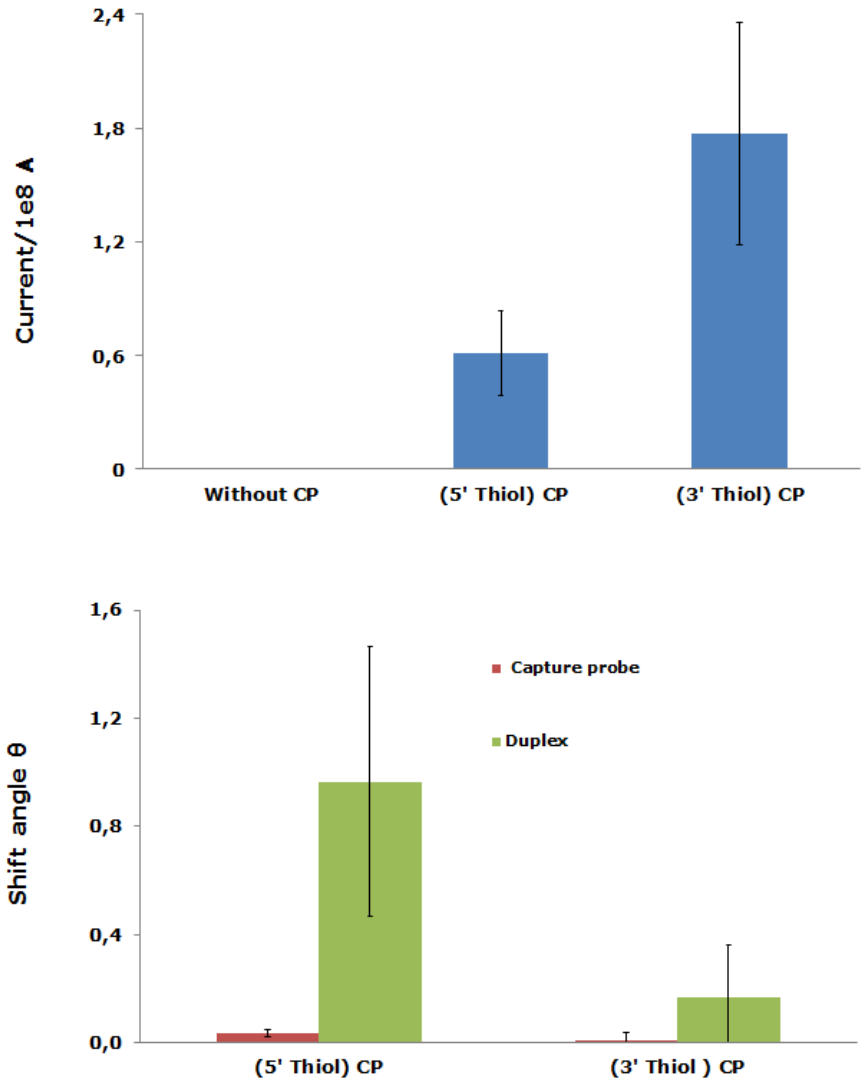

Figure 2.24: Electrochemical (up) and SPR (down) response of 5' and 3' thiolated CP

2.6.5 XPS characterization

Once chosen the MalPEG SAM as the best option for the interface, the interaction of each layer with the sensor was studied with XPS. Therefore, a chip with only MalPEG layer, a second chip with MalPEG and CP layers, and finally a third chip with MalPEG, CP, and MCH layer were analyzed with XPS. The figures 2.25, 2.26 and 2.27 show the different atomics percentages in each adlayer. Elements like hydrogen (H), gold (Au) and carbon (C) were discarding in the analysis due to its high percentages in each chip. We focused in oxygen (O), sulphur (S), nitrogen (N), and phosphorous (P) atoms because these elements are fundamental parts and characteristic objectives of each immobilized layer.

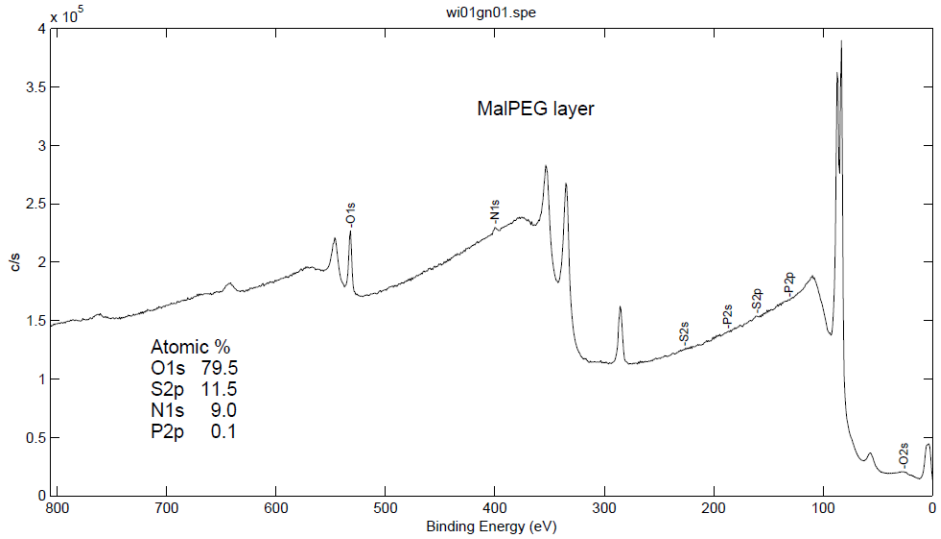

Figure 2.25: XPS analysis of MalPEG layer with atomic percentage

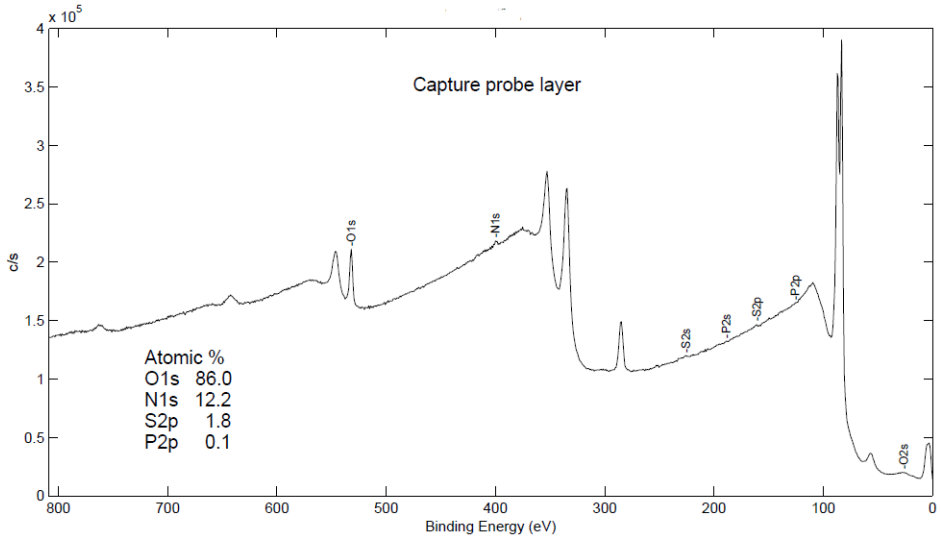

Figure 2.26: XPS analysis of MalPEG + CP layer with atomic percentage

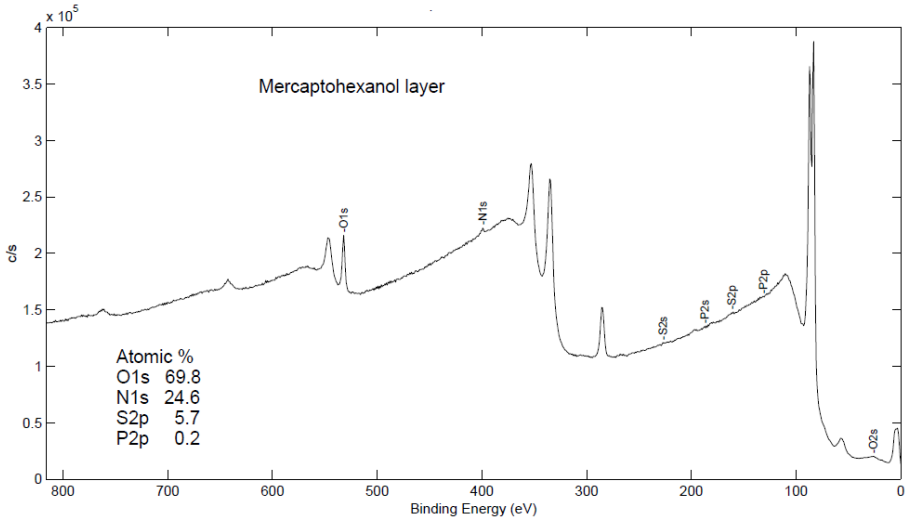

Figure 2.27: XPS analysis of MalPEG + CP+ MCH layer with atomic percentage

Figure 2.28 summarizes the results of the XPS analysis obtained with the different added layers. In the MalPEG layer, we found that the O and S percentages are higher. This result reinforces the correct MalPEG linker immobilization on the sensor surface. The amount of oxygen represents the PEG chain on each arm of the linker molecule and the sulphur element indicates the presence of the gold-sulphur bond. When the CP is introduced in the next layer, the N percentages increase due to the presence of nitrogenous bases from the DNA in the interface.

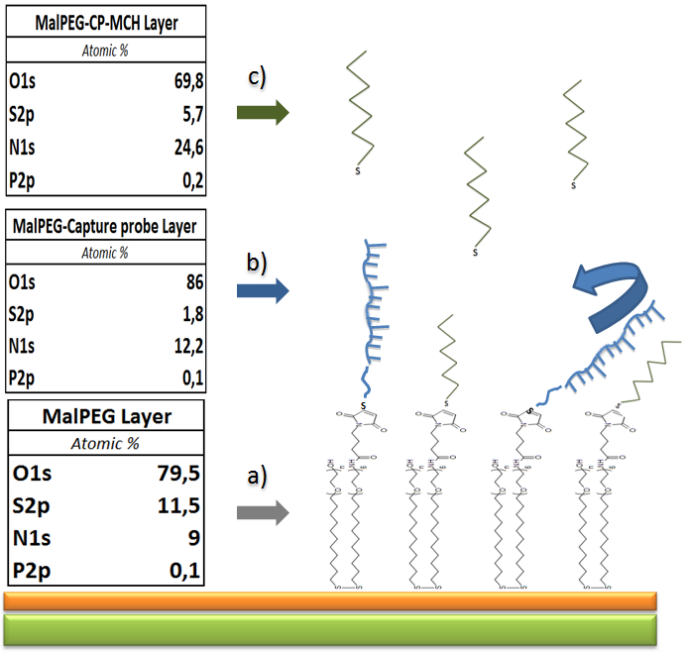

Figure 2.28: Schematic summary of the XPS analysis a) MalPEG layer immobilization, b) CP layer immobilization, c) MCH layer immobilization

Furthermore, the S percentage decreases maybe due to the shielding effect of the CP chain tilt on the first layer. When MCH is introduced in the sensor, the idea is that this molecule block the maleimide unreacted and the empty gold surface, but this molecule helps in the reorganization of the CP position lining up this DNA molecule. This effect has been already observed and reported in mixed monolayer of MCH and thiolated CPs. The XPS results observed after MCH show this hypothesis because the percentage of sulphur is increased due to the disappearance of the shielding effect. In addition, due to the lineup of the CP chains, the nitrogenous and phosphorous percentages is the double, because the DNA bases are more exposed, reinforcing our predictions.

Finally, the figure 2.29 shows a scheme of the definitive SAM components and its possible interactions. The materials used for this interface were the maleimide-polyethylene glycol disulfide supplied by ProChimia; 6-Mercapto-1-hexanol was purchased in Sigma-Aldrich; all aqueous solutions were prepared in double distilled water. The DNA capture probe was manufactured by Metabion International AG. The DNA target complementary was amplified by polymerase chain reaction (PCR) with Qiagen PCR reagents.

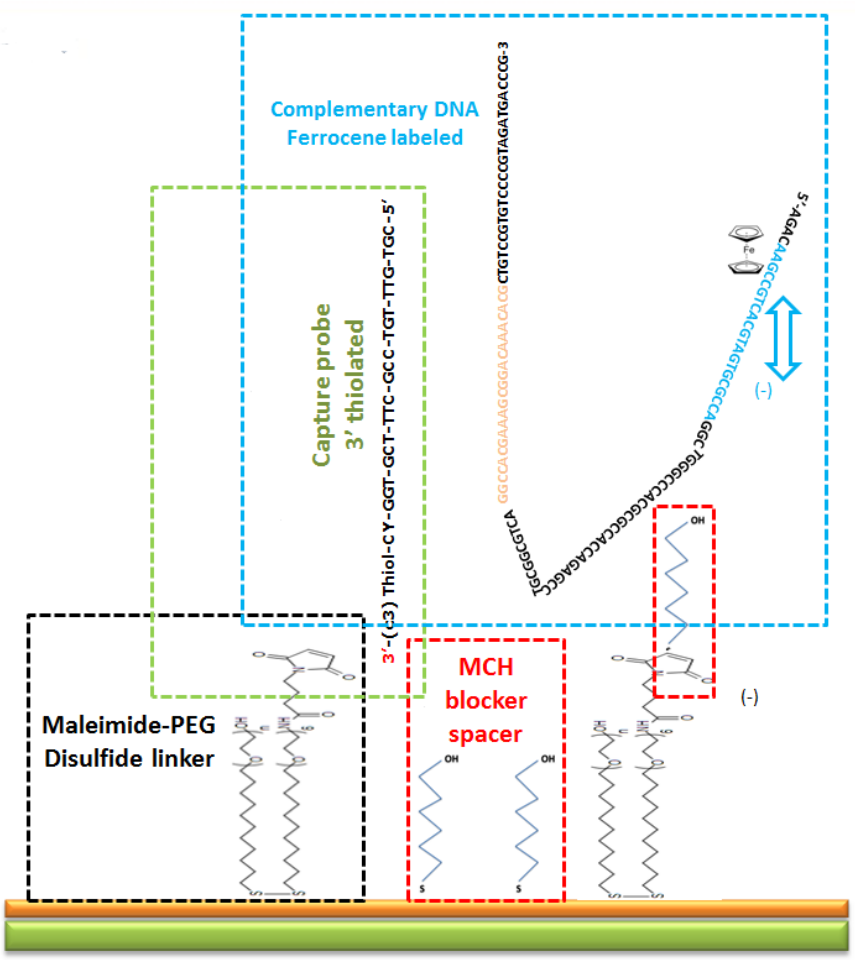

Figure 2.29: Final components of biosensing interface in immobilization order, Maleimide-PEG disulfide linker (black box), CP 3' thiolated (green box), and MCH molecule like blocker and spacer agent (red box); target DNA (blue box). Boxes overlays show the interactions between molecules

2.7 Gold substrate annealing

In order to have a more ordered SAM of the biosensor interface and so enhance the electrochemical detection, another improvement introduced in the MalPEG platform was the gold surfaces flattening by means of annealing. This method is a heating treatment wherein a material changes some of its properties such as crystallography organization, strength, hardness, and roughness. The heating of the apparently gold surface, melted the gold grains and produces terraces hypothetically unilamelars. The effect of the annealing on gold substrates has been characterized with scanning tunneling microscopy (STM) and optical interferometry (OI). Like in previous experiments, SPR and electrochemical techniques have been

used to characterize the monolayer distribution of the bioreceptors and to measure the target hybridization efficiency on annealed substrate to compare with untreated substrates.

2.7.1 Annealing treatment

The gold substrates purchased from Menzel-Gläser consist in BK7 glass square chips of 2 cm^2 with refraction index (*n*) 1.5151 and coated with 2 nm of chromium and 50 nm of gold, which were deposited by evaporation with an Edwards Auto 306 evaporator. This is a common method for thin film deposition, but the obtained surfaces have pebble-type structures with high roughness and contain gold islands. The annealing treatment on these substrates restructures the crystallographic organization of gold, leading the formation of flat terraces with a pronounced (111) texture. For the annealing treatment, it was used a butane flame for 5 minutes at a distance of 3 cm from the chip, making a zigzag movement onto gold surface. The chips were cooled under argon atmosphere at room temperature. For its cleaning, it was sonicated in ethanol for 5 minutes and then it was dried with nitrogen. Finally, the chip was placed in UV for 10 minutes. Annealing is a widespread method to obtain ultra-flat surfaces for nanometric characterizations methods, but it has never been applied in biosensor applications. This transition is temperature dependent [215], and influenced by the distance between the flame and the gold surface and the heating time [216].It is reported that the gold layer thickness also influences the quality of the new flat terraces [217].

2.7.2 STM results

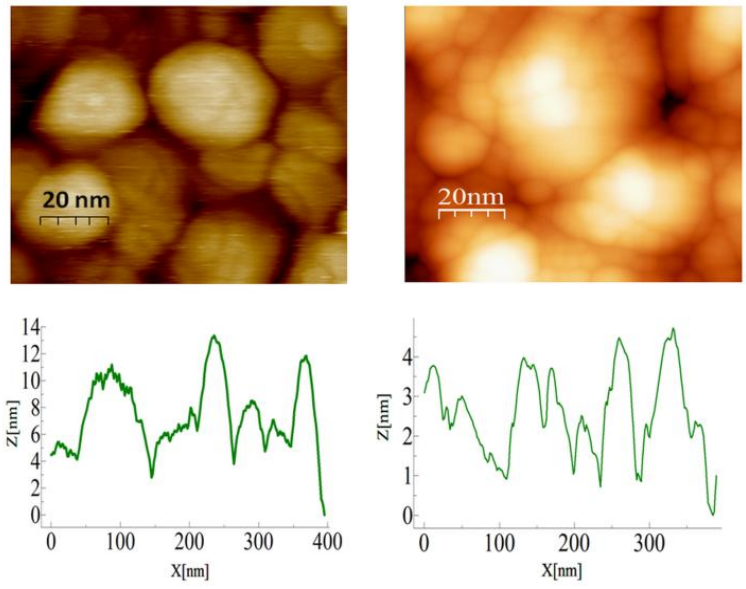

Figure 2.30: Images of STM characterization of un-treated (left side) and annealed substrates (right side)

The typical gold evaporated SPR chips are no truly flat. A quick look on the STM characterization (figure 2.30) reveals the differences in shape, size and the condition of the gold grains before (left) and after (right) surface heating treatment. The fusion of the gold islands found on the un-annealed substrates, generates after heating grain enlargement organized as flat terraces, giving homogeneity to the surface nanostructure. The gold grain size average in the pebble-type un-treated substrate is 14 nm, while it is reduced to 4 nm after the gold restructuration by the annealing process, reducing the surface roughness of the substrate.

2.7.3 Interferometry characterization

Nanoscale characterization blinds us to another important surface characteristic, the waviness. It is a broader view of roughness and its measurement permits to observe periodic irregularities, whose spacing is greater than the roughness length. The roughness and waviness of gold surface does not depend exclusively on the method in which is deposited the metal on the substrate, but also strongly depends on the nature of the solid support. It is commonly believed that the supports are stable solids. However, high temperatures and frequent shelling during the processes of gold deposition have effects on them. Some of the consequences of thisprocessare the waviness and roughness.

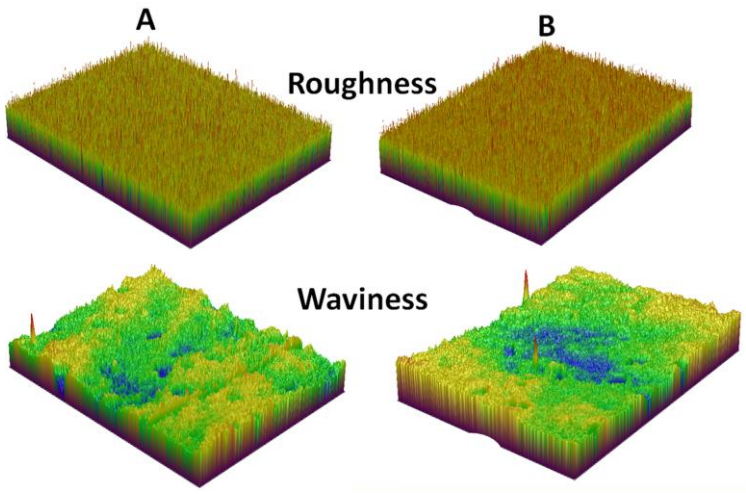

Figure 2.31 Roughness and waviness factors measured by optical interferometry of un-treated surface (A) and annealed surface (B).

Figure 2.31 shows the differences between the arithmetic average of absolute values (Ra factors) in both roughness and waviness. The interferometry results show a decrease of four times on roughness of the annealed surface versus the untreated gold (0.04 nm vs. 0.16 n, respectively). Large-scale measures allow us to say that annealing is not only a method for forming flat terraces of low roughness but also masked glass support defects. This heating treatment helps to reduce the waviness of the glass substrate from 0.66 nm to 0.37 nm.

2.7.4 Electrochemical characterization of effective surface

To measure the effective conductive area in both type of nanostructure gold electrode surface, cyclic voltammetries were carried out in sulfuric acid for measuring the experimental active area. For its mathematical calculation, this formula reported in literature [218] was used:

$$Area = Q_{Au} * (r_{Au}/r_{O2})^2 / n\ Q^0$$

Where Q_{Au} is the area under the curve of the sulfuric acid reduction peak; $(r_{Au}/r_{O2})^2$ is the square of the atomic radius ratios between the gold substrate and the adsorbed oxygen; n is the number of electrons involved in oxygen oxidation and Q^0 is the reference charge for reduction of an oxide monolayer on polycrystalline gold. For these experiments, Q^0 equal to 390μC cm^{-2} was considered [219].

Table 2.5 shows the results obtained with this electrochemical characterization. The variations of the real active area of gold after annealing and un-treated are compared with the geometric theoretic area of the electrode. From this results, it can be observed that the electrochemical roughness factor (ρ= experimental area/ theoretical area) [220]in un-treated surface is 2.4; while in the annealed electrode is only 1.2. Thus, the decrease of the roughness and the effective area after annealing treatment is nearly 50%, which approaches annealed surfaces to the theoretical value of ultra-flat surfaces.

Surface coverage (Γ= molecules/mm^2)			
Monolayer	**Theoretical values**	**Experimental Values without annealing**	**Experimental Values with annealing**
Electrode area	**0,567 (cm^2)**	**1,353 (cm^2)**	**0,661 (cm^2)**
Bioreceptor	**9,3x10^{11}**	**1,21x10^{12}**	**9,9x10^{11}**
Capture probe	**3,2x10^{11}**	**1,05x10^{10}**	**5,6x10^{10}**
Target DNA	**1,9x10^{11}**	**2,78x10^{10}**	**6,1x10^{10}**
DNA hybridization efficiency	**100%**	**14%**	**32,10%**

Table 2.5: Experimental and theoretical values of electrode areas characterized by CV and surface coverage (Γ) for the different immobilization stages for annealed and un-treated surfaces measured with SPR.

2.7.5 Surface coverage characterization with SPR

Once the nano-structuration of both studied substrates, pebble-type un-treated gold and annealed flat terraces-type gold, has been characterized. The effect of the substrates roughness was studied in the performance of DNA biosensors.

SPR offers a deep understanding about the amount of biomolecules attached on the chip surface in each step of the biosensor set up.

The theoretical values proposed in the table, were calculated taking into account shielding diameters of the MalPEG (1.17 nm) [221]as the basement of the bioreceptor immobilization and dsDNA diameter (2.55 nm) to consider the hybridized DNA in a perfect geometrical distribution of the biomolecules on the surface.

The differences observed on the roughness and effective area, are reflected in the adsorption rates of molecules in each type of substrate. The experimental values measured in the ultra-flat annealed substrate shows a very similar bioreceptor surface coverage compared with the theoretical one. It was assumed that the theoretical values are calculated under a virtual flat surface, and the closer surface coverage values obtained on the annealed surface reveals that the treatment helps to achieve this goal, giving well-ordered and packed monolayers. On the other side, the grainy surface of the un-treated gold has larger area of gold for the immobilization of bioreceptor interface.

The visible differences between the monolayer immobilization efficiency reflect structural changes of the gold surface (see figure 2.32). The reorganization of the

crystalline structure formed on flat terraces of gold, decreases the available places, also observed on the reduction of the effective area of the gold surface. For this reason, the bioreceptor molecules diminish its surface coverage on the annealed treated surfaces, comparing with un-treated substrate that has higher roughness and so higher effective area and bioreceptor immobilization.

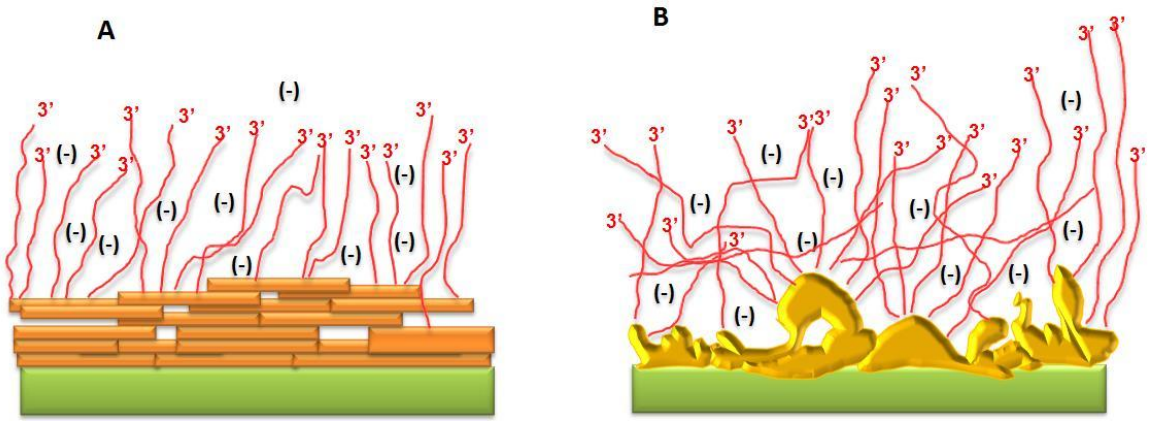

Figure 2.32: SAM immobilization schemes from annealed (A) and un-treated (B) substrates. Note a well ordered system in annealed surface

However, although more receptors site were deposited on the pebble-type surface, the amount of hybridized DNA molecules are lower comparing with the annealed flat chip, being the double of targets detected on the annealed one. Considering the theoretical value calculated for the covering of ds DNA molecules, in the case of ultra-flat substrate was observed 32% of efficiency, while this percentage is reduce to 14% in the case of the rough surface.

Dates show in figure 2.33 confirmed the varied distribution of biomolecules on the different nanostructured substrates. This figure shows the increase of intensity due to the SPR chip covering. The change of intensity is measured under equal refractive index conditions on the chip before and after biomolecules incubation. Therefore, the shift of intensity is only due to the modification of the resonant oscillation of excited plasma with the adsorbed molecules on the gold chip. As it was commented in the previous table, higher adsorption of the bioreceptors is observed on the rough un-treated surface. However, higher hybridization is detected on the ultra-flat chip.

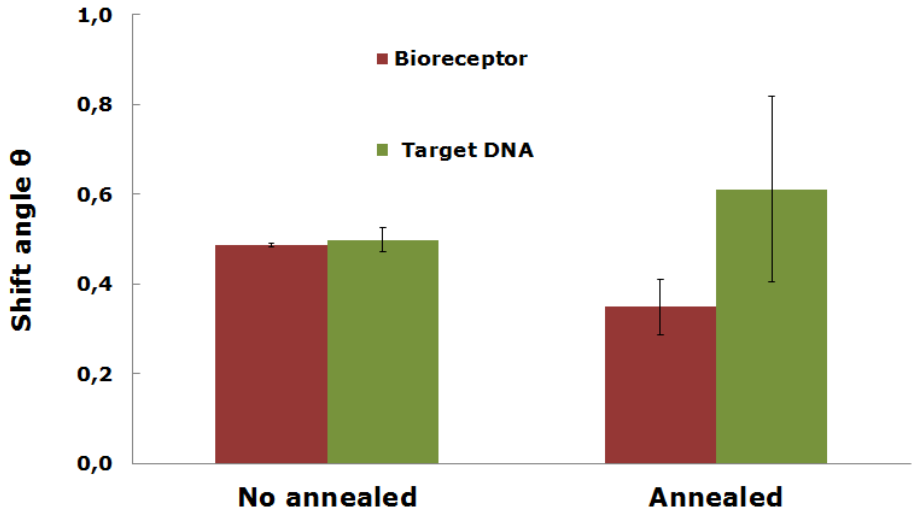

Figure 2.33: SPR responses from bioreceptor and target DNA layer on annealed and untreated substrates.

The new surface organization on the ultra-flat substrates turns out in the formation of immobilization patterns that reduce both steric hindrances and electrostatic repulsion. The monolayer formation has been studied to form the thiol chains approximately $(\sqrt{3}x\sqrt{3})R30°$ angle titled to the gold surface [222].In a planar annealed surface, the deposited molecules have the similar angle. However, in the case of a pebble-type surface the monolayer follows the distortions of the flat surface. Thus, the well-ordered and organized distribution, in similar direction of the bioreceptors, in the planar configuration, contrast with the random orientation of the highly packed linking sites on the un-treated substrate. This chaotic distribution of the negatively charged bioreceptors hinders the entrance of the negatively charged DNA target.

Moreover, many of the features of the SAMs depend directly of the crystalline organization substrate where they are deposited. By changing this surface organization also changes the thermal stability and kinetics of chemisorptions of the head groups on gold and thus its distribution, covering and angle with respect to the surface are different [223].

These small but important changes greatly enhance the hybridization efficiency, being the increase in more than twice in surface coverage DNA hybridization, although annealed substrate contains lower amount of bioreceptors.

2.7.6 Electrochemical DNA sensor characterization

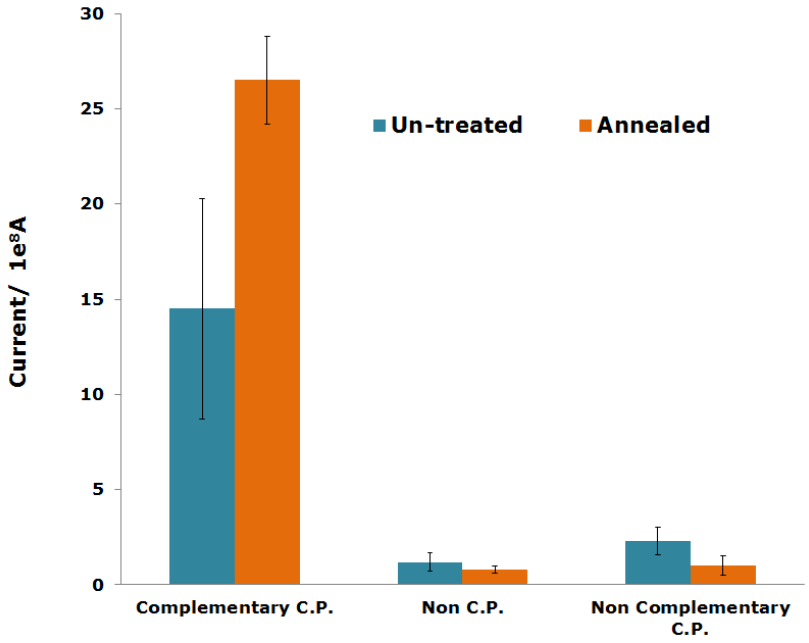

Figure 2.34: Electrochemical responses from the sensor immobilized and hybridized with target-Fc on annealed and un-treated substrates.

From the electrochemical point of view, pebble-type electrodes have some drawbacks comparing with ultra-flat substrates. The ions adsorbed on the rough electrodes have a larger area for adsorption, and so higher capacitance effect [224]. In this way, the electron transfer from the ferrocene label to the electrode becomes more difficult, thus decreasing the signal obtained. Moreover, the charge redistribution between molecules in the ordered assembled interface has a beneficial effect on electron transport and charge transfer [225], helping in the transport of the electrons from the redox label to the electrode, and thus in the sensitivity of the electrochemical biosensor [224].The distance between oxidation and reduction peaks, the reversibility of a redox reaction and reproducibility of electrochemical measurements, are affected by the state and nature of the substrate [226].

Besides the fact that the flat electrodes have beneficial effects on the electrochemical read-out, the well-ordered distribution of the bioreceptors on annealed electrodes, as surface coverage characterization with SPR, demonstrate higher efficient hybridization of the target DNA.

Also the electrochemical characterization of the DNA biosensor on evaporated wrinkled gold electrodes and on annealed flat gold surfaces, shown higher

hybridization efficiency in the sensor previously treated with annealing (see figure 2.34). In electrochemical sensors, the improvement is much clearer than in optical detection, being more than twice in magnitude the current observed in the annealed system. These results are due to the synergy effects on annealed substrates of both factsless steric hindrance for the target hybridization in a more ordered distribution of the bioreceptors, and easier transfer of the charge and less capacitance on the electrode.

The selectivity and the low non-specific fouling achieved by the biosensor interface is demonstrated with the low signal obtained in the controls without capture probe and with mutated capture probe in both type of substrates.

2.8 Summary

In summary, the three interfaces compared the most successful one was the MalPEG, which contains two branches of PEG and a better spacing for the target hybridization. The optimization of each biosensor layer resulted in; 20 μM MalPEG SAM, 10 μM of CP, and the MCH like blocking and spacer agent presented the best results of hybridization detection during the optimization and characterization of the SAM. In addition, it was demonstrated that the annealing treatment on commercial gold evaporated substrates has a beneficial effect on the biosensor performance. The transition between the nanoparticulate substrate to the laminar-annealed surface has deep consequences over the biomolecules distribution, interaction, and so in the sensitivity of the sensor. The heating treatment causes the molecular rearrangement of the gold, forming ultra-flat terraces. The pebble-type un-treated substrates, with higher surface area demonstrate broader bioreceptor coverage. However, the flat annealed surface favors improved and well-ordered bioreceptors patterns with its subsequent lower steric hindrance for the hybridization of the DNA target. The organization, more homogeneous of the monolayers in annealed substrates, results in a high quality monolayers and sensors. Moreover, an ordered charged bioreceptors interface facilitates the transfer of electrons from the redox label to the electrode and reduce the capacitance effects. This involves improvements in both the hybridization efficiency and electrochemical reading, making the annealing a powerful tool in the optimization of biosensors interfaces. However,annealing gold pre-treatment is just limited to substrate that could handle the high temperatures required. As will be presented in next chapter, the cost

required for the fabrication of the cartridge limit the type of materials used for this project and the polymers used are not compatible with annealing.

2.9 References

149. Gill, A., et al., *Biocompatible interfaces for biosensors.* International Journal of Environmental Analytical Chemistry, 2005. **85**.
150. Oliveira, O.N., et al., *Nanomaterials for Diagnosis: Challenges and Applications in Smart Devices Based on Molecular Recognition.* ACS Applied Materials & Interfaces, 2014. **6**(17): p. 14745-14766.
151. Kim, P., et al. *An electrochemical interface for integrated biosensors*: IEEE.
152. Wong, E.L., E. Chow, and J.J. Gooding, *DNA recognition interfaces: the influence of interfacial design on the efficiency and kinetics of hybridization.* Langmuir : the ACS journal of surfaces and colloids, 2005. **21**(15): p. 6957-6965.
153. Kim, D. and D. Kang, *Molecular Recognition and Specific Interactions for Biosensing Applications.* Sensors, 2008. **8**.
154. Gao, T., et al., *Assembly of Selective Biomimetic Surface on an Electrode Surface: A Design of Nano–Bio Interface for Biosensing.* Analytical chemistry, 2015. **87**(11): p. 5683-5689.
155. Gao, Y., L.K. Wolf, and R.M. Georgiadis, *Secondary structure effects on DNA hybridization kinetics: a solution versus surface comparison.* Nucleic acids research, 2006. **34**(11): p. 3370-3377.
156. Philp, D. and J.F. Stoddart, *Self-assembly in natural and unnatural systems.* Angewandte Chemie International Edition in English, 1996. **35**(11): p. 1154-1196.
157. Shimomura, M. and T. Sawadaishi, *Bottom-up strategy of materials fabrication: a new trend in nanotechnology of soft materials.* Current Opinion in Colloid & Interface Science, 2001. **6**(1): p. 11-16.
158. Zhang, Y., et al., *Bottom-Up Molecular Tunneling Junctions Formed by Self-Assembly.* Israel Journal of Chemistry, 2014. **54**(5-6): p. 513-533.
159. Huie, J.C., *Guided molecular self-assembly: a review of recent efforts.* Smart Materials and Structures, 2003. **12**(2): p. 264.
160. Barth, J.V., G. Costantini, and K. Kern, *Engineering atomic and molecular nanostructures at surfaces.* Nature, 2005. **437**(7059): p. 671-679.
161. Chen, D. and J. Li, *Interfacial design and functionization on metal electrodes through self-assembled monolayers.* Surface Science Reports, 2006. **61**.

162. Whitesides, G.M., J.P. Mathias, and C.T. Seto, *Molecular self-assembly and nanochemistry: a chemical strategy for the synthesis of nanostructures*. 1991, DTIC Document.
163. Khoo, H., et al., *Self-Assembly in Micro- and Nanofluidic Devices: A Review of Recent Efforts.* Micromachines, 2011. **2**.
164. Ulman, A., *Formation and Structure of Self-Assembled Monolayers.* Chemical reviews, 1996. **96**(4): p. 1533-1554.
165. Gooding, J.J. and S. Ciampi, *The molecular level modification of surfaces: from self-assembled monolayers to complex molecular assemblies.* Chemical Society reviews, 2011. **40**(5): p. 2704-2718.
166. Gooding, J.J., et al., *Self-assembled monolayers into the 21st century: recent advances and applications.* Electroanalysis, 2003. **15**(2): p. 81-96.
167. Nuzzo, R.G. and D.L. Allara, *Adsorption of bifunctional organic disulfides on gold surfaces.* Journal of the American Chemical Society, 1983. **105**(13): p. 4481-4483.
168. Arya, S.K., et al., *Recent advances in self-assembled monolayers based biomolecular electronic devices.* Biosensors & bioelectronics, 2009. **24**(9): p. 2810-2817.
169. Frasconi, M., F. Mazzei, and T. Ferri, *Protein immobilization at gold-thiol surfaces and potential for biosensing.* Analytical and bioanalytical chemistry, 2010. **398**(4): p. 1545-1564.
170. Wei, F., P.B. Lillehoj, and C.-M.M. Ho, *DNA diagnostics: nanotechnology-enhanced electrochemical detection of nucleic acids.* Pediatric research, 2010. **67**(5): p. 458-468.
171. Love, J.C., et al., *Self-assembled monolayers of thiolates on metals as a form of nanotechnology.* Chemical reviews, 2005. **105**(4): p. 1103-1169.
172. Ferretti, S., et al., *Self-assembled monolayers: a versatile tool for the formulation of bio-surfaces.* TrAC Trends in Analytical Chemistry, 2000. **19**(9): p. 530-540.
173. Delamarche, E., B. Michel, and H.A. Biebuyck…, *Golden interfaces: The Surface of Self-Assembled Monolayers.* Advanced …, 1996.
174. O'Dwyer, C., G. Gay, and B.V. de, *The nature of alkanethiol self-assembled monolayer adsorption on sputtered gold substrates.* Langmuir, 2004.
175. Badia, A. and R.B. Lennox…, *A dynamic view of self-assembled monolayers.* Accounts of chemical research, 2000.
176. Canaria, C.A., *Self-assembled monolayers for the study of biological targets.* Self-assembled monolayers for the study of biological targets, 2008.

177. Carrascosa, L.G., et al., *Understanding the role of thiol and disulfide self-assembled DNA receptor monolayers for biosensing applications.* European biophysics journal : EBJ, 2010. **39**(10): p. 1433-1444.
178. Durmaz, F., *A modular approach to functional self-assembled monolayers.* A modular approach to functional self-assembled monolayers, 2006.
179. Lud, S.Q., et al., *Controlling surface functionality through generation of thiol groups in a self-assembled monolayer.* Langmuir : the ACS journal of surfaces and colloids, 2010. **26**(20): p. 15895-15900.
180. Aponte, M.I., *Effect of alkanethiol self-assembled monolayers on the plastic and elastic deformation of gold (111) films.* Effect of alkanethiol self-assembled monolayers on the plastic and elastic deformation of gold (111) films, 2010.
181. Bashir, A., *Growth and structural characterization of self-assembled monolayers (SAMs) on gold made from functionalized thiols and selenols.* Growth and structural characterization of self-assembled monolayers (SAMs) on gold made from functionalized thiols and selenols, 2008.
182. Edinger, K., et al., *Formation of self-assembled monolayers of n-alkanethiols on gold: a scanning tunneling microscopy study on the modification of substrate morphology.* Langmuir.
183. Lee, S., et al., *The influence of packing densities and surface order on the frictional properties of alkanethiol self-assembled monolayers (SAMs) on gold: a comparison of SAMs ….* Langmuir, 2000.
184. Yu, M., et al., *True nature of an archetypal self-assembly system: mobile Au-thiolate species on Au(111).* Physical review letters, 2006. **97**(16): p. 166102.
185. Torres, E., P.U. Biedermann, and A.T. Blumenau, *The role of gold adatoms in self-assembled monolayers of thiol on Au(111).* International Journal of Quantum Chemistry, 2009. **109**.
186. Maksymovych, P., et al., *Gold adatom as a key structural component in self-assembled monolayers of organosulfur molecules on Au(111).* Progress in Surface Science, 2010. **85**.
187. Maksymovych, P., D.C. Sorescu, and J.T. Yates, *Gold-adatom-mediated bonding in self-assembled short-chain alkanethiolate species on the Au(111) surface.* Physical review letters, 2006. **97**(14): p. 146103.
188. Cortés, E., et al., *Enhanced stability of thiolate self-assembled monolayers (SAMs) on nanostructured gold substrates.* Langmuir : the ACS journal of surfaces and colloids, 2009. **25**(10): p. 5661-5666.

189. Addato, M.a., et al., *Alkanethiol Adsorption on Platinum: Chain Length Effects on the Quality of Self-Assembled Monolayers.* The Journal of Physical Chemistry C, 2011. **115**.
190. Chaudhuri, A., et al., *(2√3×3)rect. phase of alkylthiolate self-assembled monolayers on Au(111): A symmetry-constrained structural solution.* Physical Review B, 2009. **79**.
191. Gannon, G., et al., *Molecular dynamics study of naturally occurring defects in self-assembled monolayer formation.* ACS nano, 2010. **4**(2): p. 921-932.
192. Hamoudi, H., et al., *On the self assembly of short chain alkanedithiols.* Physical chemistry chemical physics : PCCP, 2008. **10**(45): p. 6836-6841.
193. Wolf, H., H. Ringsdorf, and E. Delamarche…, *End-group-dominated molecular order in self-assembled monolayers.* The Journal of …, 1995.
194. Schwartz, D.K., *Mechanisms and kinetics of self-assembled monolayer formation.* Annual review of physical chemistry, 2001. **52**: p. 107-137.
195. Millone, M.A., et al., *Self-assembly of alkanedithiols on Au(111) from solution: effect of chain length and self-assembly conditions.* Langmuir : the ACS journal of surfaces and colloids, 2009. **25**(22): p. 12945-12953.
196. Pensa, E., et al., *The Chemistry of the Sulfur-Gold Interface: In Search of a Unified Model.* Accounts of chemical research, 2012.
197. Vericat, C., et al., *Thiol-capped gold: from planar to irregular surfaces.* Journal of Physics: Condensed Matter, 2008. **20**.
198. Vericat, C., et al., *Self-assembled monolayers of thiols and dithiols on gold: new challenges for a well-known system.* Chemical Society reviews, 2010. **39**(5): p. 1805-1834.
199. Vericat, C., et al., *Surface characterization of sulfur and alkanethiol self-assembled monolayers on Au(111).* Journal of Physics: Condensed Matter, 2006. **18**.
200. Vericat, C., M.E. Vela, and R.C. Salvarezza, *Self-assembled monolayers of alkanethiols on Au(111): surface structures, defects and dynamics.* Physical chemistry chemical physics : PCCP, 2005. **7**(18): p. 3258-3268.
201. Gong, P., et al., *Hybridization behavior of mixed DNA/alkylthiol monolayers on gold: characterization by surface plasmon resonance and 32P radiometric assay.* Analytical chemistry, 2006. **78**(10): p. 3326-3334.
202. Wijaya, E., et al., *Surface plasmon resonance-based biosensors: From the development of different SPR structures to novel surface functionalization strategies.* Current Opinion in Solid State and Materials Science, 2011. **15**.

203. Willander, M. and S. Al-Hilli, *Analysis of biomolecules using surface plasmons.* Methods in molecular biology (Clifton, N.J.), 2009. **544**: p. 201-229.
204. Willets, K.A. and R.P. Van Duyne, *Localized surface plasmon resonance spectroscopy and sensing.* Annual review of physical chemistry, 2007. **58**: p. 267-297.
205. Malic, L., T. Veres, and M. Tabrizian, *Nanostructured digital microfluidics for enhanced surface plasmon resonance imaging.* Biosensors & bioelectronics, 2011. **26**(5): p. 2053-2059.
206. Kang, X., G. Cheng, and S. Dong, *A novel electrochemical SPR biosensor.* Electrochemistry Communications, 2001. **3**(9): p. 489-493.
207. Bourg, M.C. and A. Badia…, *Gold-sulfur bonding in 2D and 3D self-assembled monolayers: XPS characterization.* The Journal of Physical …, 2000.
208. Lee, C.-Y.Y., et al., *Fluorescence, XPS, and TOF-SIMS surface chemical state image analysis of DNA microarrays.* Journal of the American Chemical Society, 2007. **129**(30): p. 9429-9438.
209. Vance, A.L., et al., *XAS and XPS characterization of monolayers derived from a dithiol and structurally related disulfide-containing polyamides.* Langmuir, 2002.
210. Techane, S.D., L.J. Gamble, and D.G. Castner, *Multi-technique Characterization of Self-assembled Carboxylic Acid Terminated Alkanethiol Monolayers on Nanoparticle and Flat Gold Surfaces.* The journal of physical chemistry. C, Nanomaterials and interfaces, 2011. **115**(19): p. 9432-9441.
211. Shen, G., M.F. Anand, and R. Levicky, *X-ray photoelectron spectroscopy and infrared spectroscopy study of maleimide-activated supports for immobilization of oligodeoxyribonucleotides.* Nucleic acids research, 2004. **32**(20): p. 5973-5980.
212. Lüssem, B., et al., *STM study of mixed alkanethiol/biphenylthiol self-assembled monolayers on Au(111).* Langmuir : the ACS journal of surfaces and colloids, 2006. **22**(7): p. 3021-3027.
213. Azzam, W., et al., *Combined STM and FTIR characterization of terphenylalkanethiol monolayers on Au(111): effect of alkyl chain length and deposition temperature.* Langmuir : the ACS journal of surfaces and colloids, 2006. **22**(8): p. 3647-3655.
214. Wang, W., T. Lee, and M.A. Reed, *Electron tunnelling in self-assembled monolayers.* Reports on Progress in Physics, 2005. **68**.

Chapter three

In previous chapter, we show the development and optimization of an electrochemical DNA biorecognition interface. As we already introduced in the motivation of this thesis, this biosensor interface is an integral part in the development of a high-tech device within an industrial project with the company Genomica S.A.U. The main objective of this project is the construction, commissioning and validation of a LOC device ableof detecting various polymorphisms in cancer DNA samples on a single platform and its subsequent introduction by the company into the diagnosis market. The new device is a portable cartridge that incorporates mechanical, electrical and heating elements with electronic and microfluidic systems. The multisystem device will be able to amplify DNA by PCR and detect real DNA samples electrochemically. The main idea is that the device will be an effective tool in the diseases diagnostic in early stages of those and directly used in the medical center by the doctor, to give to the patient a direct and faster diagnosis. It not intended to replace traditional techniques but to complement them and to expedite their diagnosis. The main components of this LOC are:

- Electrochemical detection system or potentiostat
- Electrochemical DNA biosensor array
- Automatized system of temperature ramps to perform amplification of DNA by PCR
- Microfluidic platform cartridge

An Electronic Control Interface (ECI) provides acquisition and data processing software and involves the potentiostat, the mini-PCR and the fluidics components. This ECI will be in contact through a fluidic cartridge that integrates the mini-PCR chamber and the electrochemical biosensor detection area.

The aim of this chapter is to show the various stages of manufacture of the biosensor platform part. This device consists of two main blocks: the PCR block involving microfluidic designs and biosensing block involving electrochemical designs and hybridization chamber.

The conceptual framework in which the work takes place is given by a joint interest between a biotech company and a scientific institute. Today, the market of electrochemical DNA biosensors for the detection of diseases is a fertile field for the advancement of interdisciplinary research. For this fundamental reason, the commercial-academic background of this project becomes relevant within the development thereof.

The biotechnology company that propels the project is Genomica SAU, who optimized the multi-PCRDNA amplification to be performed in the mini-PCR, and the scientific research institute that provides the nanobiotechnological support is the Institute for Bioengineering of Catalonia (IBEC), where we developed the optimization, fabrication, integration and validation of the electrochemical biosensor. In another area of our group, supervised by Dr. Antoni Homs, it was performed the fluidics part. The aforementioned interdisciplinary of the project involves also staff from other groups like CEMIC, in the Electronics Department of the Faculty of Physics of the University of Barcelona. This group is where was developed the electronics for the controls of the temperature ramps in the Peltier, required for the PCR, and the electrochemical multi-read-out of the biosensors in the arrays and the software to control both equipment, which was supervised by Prof. Manel Puig.

The final LOC device should be able to manipulate the sample and reproduce the complete sensing protocol including the PCR and the hybridization and detection steps in a closed package. It is interesting to be able to manufacture the complete device in a short number of steps and materials in order to make its final fabrication cheaper and easier, and so more efficient its commercialization.

Most of the microfluidical structures and LOC parts are desired make in a low cost polymeric material due to its high resistance comparing with glass, and its qualities for mass production.To accomplish this objective, a study to determine the desired material properties has been conducted. As a result, several issues have been designated as critical in order to choose the proper material. These include:

Considering the cartridge manufacturing, we should take into account:

- Material affordable for mass production
- Suitable for molded (milling, hot embossing or injection molding)
- Thermal or plasma activated and/or solvent sealing between LOC parts achievable
- Material with low impurities (reduction of material variability)
- Chemical resistance during cleaning procedures
- Chip surface modification availability
- Possibility of patterning metals on top of it
- Resistance to casual impacts (in hospital and other critical environments it is important to reduce the risks of the cartridge breaking down)
- Gamma ray and hot steam sterilization possible
- Disposability (low environmental impact), ecological reasons and commercial advantage in front of environmental friendly policies

The points to consider in the cartridge material for reagents and electrodes preparation are the next:

- High heat resistance (up to 100ºC is desired for PCR and for target denaturation)
- Chemical resistance to acid compounds, alkali solutions, and soft solvents, among others is important for the handling of reagents, electrodes cleaning.

To consider in the cartridge in relation to the reagents storage;

- Material with low biomolecules fouling
- Low permeability (reduction of LOC properties changes during storage)
- Chemical resistance (especially important for on-chip reagent storage)

3.1 Materials test

3.1.1 Experimental material test

In order to suit to above requirements, or most of them, some proposed materials were cycle olefin polymer (COP), cycle olefin copolymer (COC) and some types of polycarbonate (PC). COP shows superior optical properties and this could be an advantage to use fluorescent markers for the setup of some parts of the assay, such as the PCR, in the initial prototypes. Biocompatibility tests based on nucleic acid absorbance were done to further support the material choice.

The COP films tested were:

- Zeonor 1060R
- Zeonor 1420R
- Zeonex 330R
- The COC films tested were:
- TOPAS 5013
- TOPAS 6013
- TOPAS 6015
- TOPAS 8007
- The PC films tested were:
- TECANAT Ensinger
- Makrolon 2458 Bayer

For biocompatibility test of these polymers was done with pieces of 2x2 cm^2withsix wells of 2 mm of diameter and 1 mm in depth, fabricated with hot embossing. The

study was conducted by depositing about 3000 copies of DNA in each well of the different plastic samples and incubates for30 minutes. The recovered sample was evaluated by RT-PCR to compare with the original sample amount, and so to determine the genetic material absorbed in each one. No significant differences between the polymers evaluated were observed and all can be applicable to our device from the viewpoint of biocompatibility.

Regarding the properties related to permeability, chemical resistance and possible surface modifications, the COP and COC films gave better response.

Because of the high variability in the optical properties of COCs films, it was discard. In this way, and considering that all prerequisites were fulfilled the COP Zeonor 1420R was chosen as main material to manufacture the disposable cartridge.

Besides COP, other materials like gold, silver, silver chloride, different glues and Teflon among the most important, were used for the LOC fabrication.

3.2 Electrodes microfabrication techniques

3.2.1 Photolithography

Photolithography is the process of transferring nano and micrometric geometric shapes on a mask to the working surface. The steps involved in the photolithographic process (explained in more detail below) are substrate cleaning, metallic coating, photoresist application (positive and negative), mask alignment,exposure and finally the development.

3.2.1.1 Substrate cleaning

In the first step, the COP substrate is chemically cleaned to remove particulate matter on the surface as well as any traces of organic, ionic and/or metallic impurities. The cleaning consist in submerge the COP sheet into the Piranha solution for 30 minutes and then expose it to UV light for 10 minutes.

3.2.1.2 Metallic coating

The better adhesion of the metal layer on COP plastic was achieved with sputtering than evaporation. Sputtering is a technique used to deposit thin films of material

onto a substrate surface. There are two traditional sputtering techniques: the physical vapor deposition (PVD) and chemical vapor deposition (CVD), based on physical interactions and chemical reactions respectively. The first step that follows these techniques is to create gaseous plasma and then acceleratethe ions ofthis plasma into the material source, gold in our case. The gold is eroded by the plasmaions, via energy transfer, and it is ejected in particle clusters or atoms. These particles travel in a straight line unless they encounter something, in our case, the COP surface. In this way, the COP surface is coated by a thin gold film, where the gold thickness is time dependent.

3.2.1.3 Photoresist Application

After gold deposition, the photoresist is applied on the gold surface. High-speed centrifugal whirling or "spinning" of the photoresist is the standard method for applying the coatings. This technique produces a thin uniform layer of photoresist on the gold, with thickness dependent of rpm (revolutions perminute) and time.

3.2.1.4 Positive and Negative Photoresist

There are two types of photoresist: positive and negative (see figure 3.1). For positive resists, it is exposed with UV light wherever the underlying material wants to be removed. In these photoresists polymers, the exposition to the UV light, changes the chemical structure of the resist so that it becomes more soluble in the developer. The exposed resist is then washed away by the developer solution, leaving windows of the bare underlying material. The mask, therefore, contains an exact copy of the pattern that wants to beremained on the surface. In this work, we used the positive approach.

Negative photo resists polymer behaves in the opposite manner. Exposition to the UV light causes the polarization of the negative photoresist polymer, and so it is more difficult to dissolve. Therefore, itremains on the surface wherever it is exposed, and the developer solution removes only the unexposed portions. Masks used for negative photoresists, therefore, contain the inverse (or photographic "negative") of the pattern to be transferred. Negative resists were popular in the early history of integrated circuit processing, but positive resist gradually became more widely used since they offer better process controllability for small geometry features.

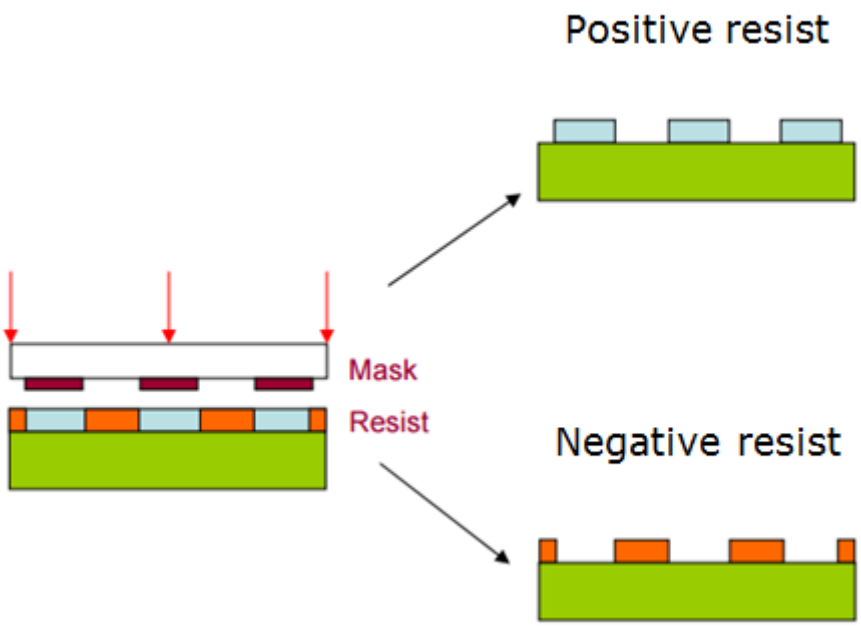

Figure 3.1: Scheme showing the two different types of photoresist

3.2.1.5 Mask Alignment and Exposure

The basic principle behind of a photoresist coating is the change in solubility of the resist in a developer upon exposure to light (or other types of exposing radiation). Thus, a spatial variation in light energy incident on the photoresist will cause a spatial variation in solubility of the resist in the developer. In this step, the mask, which contains the required pattern, is accurately aligned with the pattern on the working surface. For this purpose, mask aligner equipment is used to control the right position of the mask on the substrate and its distance. The photoresist is exposed through the pattern on the mask with a high intensity ultraviolet light.

3.2.1.6 Development

The last step in the photolithographic process is the development. At low-exposure energies, the negative resist remains completely soluble in the developer solution. As the exposure is increased above threshold energy, more of the resist film remains after development. At exposures two or three times the threshold energy, very little of the resist film is dissolved. For positive resists, the resist solubility in its developer is finite even at zero-exposure energy. The solubility gradually increases until, at some threshold, it becomes completely soluble. In this procedure

the developer solution, remove the exposed or unexposed photoresist, leaving this area of the substrate opened for the next step.

3.2.1.7 Etching

During this step, a chemical agent removes the metallic surface of the substrate in the areas that are not protected by photoresist. This procedure can be done in two ways, with a liquid called wet etching, or with plasma called dry etching. Following this step is necessary to remove the remaining photoresist on the covered gold.

3.2.2 Screen printing technique

The process of screen-printing is used for array fabrication and it does not requirethe use of clean room that makes faster, cheaper and more simple the process. However, the resolution obtained with this technique is much lower than photolithography. The procedure consists of transferring a conductive or dielectric ink or paste through a patterned screen or mash onto a substrate held on the reverse of the screen. The ink passage is blocked in areas where no image are patterned, instead allowing the passage of the ink in the areas of drawing, since they have the open mesh, see figure 3.2. This technique allows drawings of electrodes of the order of micrometers.

Successive layers can be deposited by this procedure on different ink layers and repeat patterns can be designed onto the same screen to enhance production speed. The most common substrates are the polycarbonate, polyester, glass fiber or ceramic. Each ink layer is deposited through the corresponding mask providing a specific pattern. These masks are prepared by photolithographic techniques.

In our case the conductive ink are made of gold and give rise to the formation of the array and the conductive tracks on the COP substrate. Functional materials can also be part of the formulation and more recently, nanosized metals and carbon nanotubes were used for this purpose.

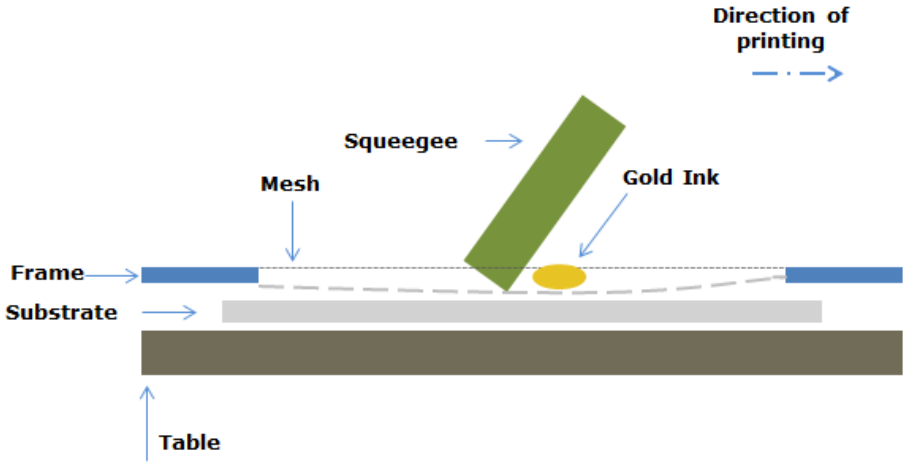

Figure 3.2: Screen printing process scheme

3.3 Cartridge design

The entire structure of the cartridge is conceived in a sandwich format. The constituents parts were optimized independently but considering the entire device to facilitate their eventual integration[227]. Many advantages were observed in this sandwich format, compared with the usual planar cartridge, where all the components of the LOC are in the same level. In this case, gravity helps in the flow of the liquids; the same Peltier may be used for heating the PCR and for the hybridization temperature in the detection area. and the electrochemical cell leave at the same distance the counter electrode to all the working electrodes that forms the arrays, having the same reproducible entrance of the current to all the working electrodes. However, this sandwich platform brings more challenges than the planar LOCs in the fabrication of the vertical fluidic channels and in the two layers connections in the electrochemical cell.

Microfluidic of the miniaturized PCR system and the hybridization-detection chamber were the first elements made in parallel. It took into account parameters of electrical connectivity, fluidic complex and thermal behavior in the whole cartridge in order to minimize possible changes during the final integration with the external actuation device, wherein will be held the electrochemical reading and the fluidic control. Figure3.3 shows the cartridge structure. To facilitate the reading of this design, the different layers were separated and numbered with roman numerals. The development of the device is explained layer by layer in next section. In each layer description, we found the design and material evolution as

well as the different fabrication techniques. Thus, first we explain the fabrication process of the biosensing block followed by the layers corresponding to the PCR block.

The steps that will carry out this LOC are the next; first, a blood sample will be extracted from the patient and inserted in a tube with the PCR reagents. This mix will be inserted by the fluidic pump until the PCR chamber. There will be performed all the amplification steps with the PCR temperature cycles to obtain millions of copies of the initial DNA sample labelled. Details about this process are introduced in the next PCR block section. This DNA labelled sample is dehybridized at 100 ºC in a mix 1:1 ratio with hybridization solution and flow it to the hybridization-detection chamber. There will be incubated this mixture at 59ºC for 1 hour and then the hybridized duplex will be electrochemically detected.

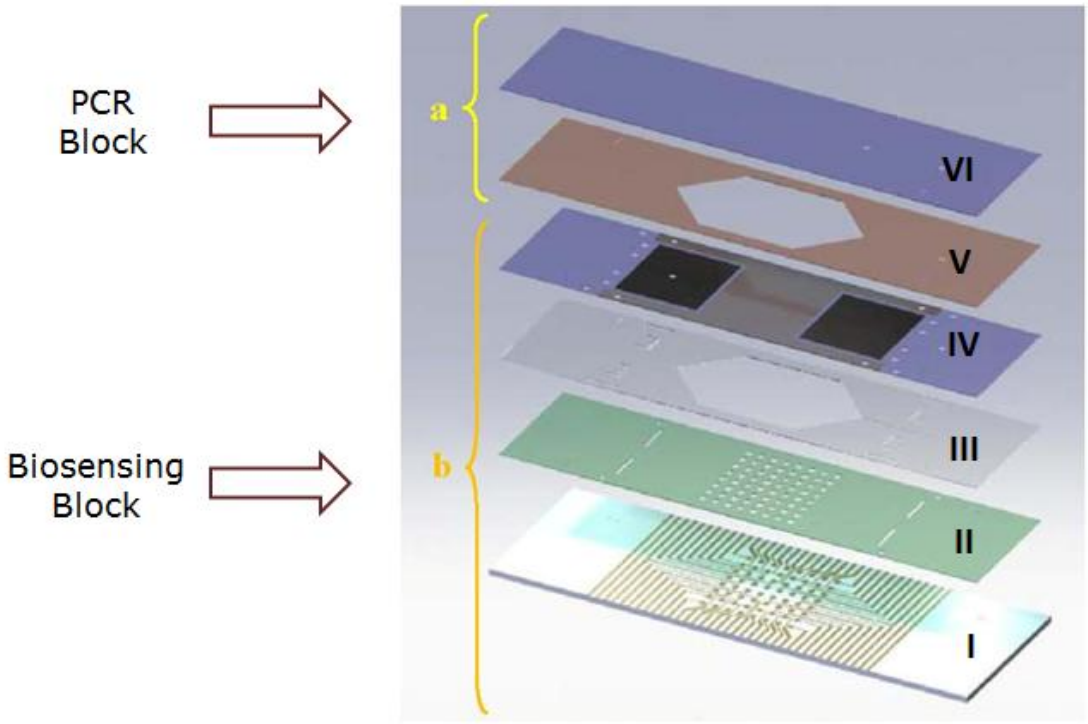

Figure 3.3: Cartridge sandwich components scheme

3.3.1 Biosensing Block

This block constitutes the part where the biorecognition electrochemical interface presented in chapter two is integrated. Therefore, it contains the electrochemical sensing platform that is functionalized with the specific DNA capture probes of interest. It serves as both hybridization chamber and electrochemical cell for detection of target DNA. It contains four layers (I, II, III, IV) listed below.

3.3.1.1 Layer I: biosensors matrix

The first layer contains the 64 gold working electrodes required for the immobilization of the 14 capture probes selective for the detection of the target of interest as well as negative or internal controls to check, considering three repetitions for each immobilized capture probe. Also the pattern include all the pad for the connection of the WE with the potentiostat and REand CE pads, that will be connected from the upper layers by means of a conductive vertical channel.

This layer is a COP sheet of 188 μm thick that contained all the electronic paths and the WE on an 8x8 matrix. This is a rectangular pattern of circular electrodes that connect with lines of gold to the ends of the sheet. This layer is wider that the other layers because have exposed in each lateral sides the gold paths for its connection with the potentiostat. The first two golden paths of the right and left ends have not direct connection to the central points. These lines are connecting by conductive silver ink with both the REand CE in layer IV. The rest of gold paths are direct connections at WE or gold spots in the biosensors array matrix. Figure 3.4 shows us the dimensions in mm of the original gold pattern in a) and the general parts in b).

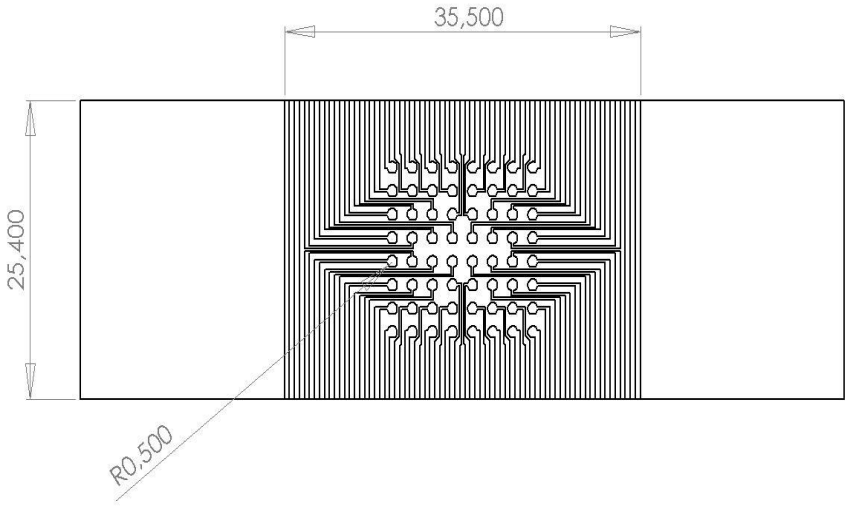

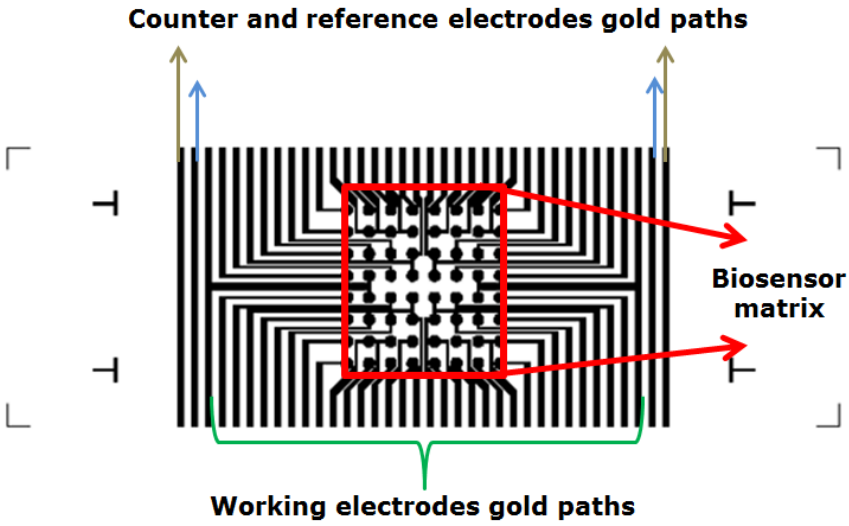

Figure 3.4: a) Original gold pattern mask dimension. b) Main parts of the layer I

The fabrication of the gold electrodes pattern on layer I was performed with two techniques; photolithography, in our IBEC installations, and by screen printing technique, fabricated in Atic S.A. Company. For the fabrication of these screen-printing arrays, DEK 248 equipment was used. The mask used in this fabrication is showing in figure 3.5.

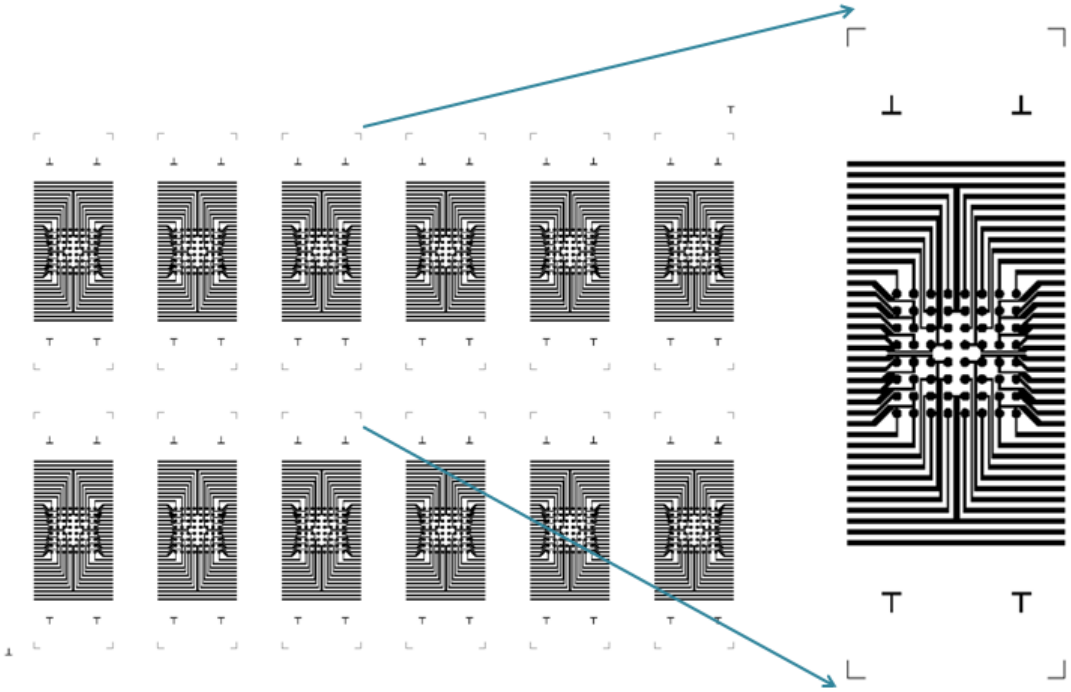

Figure 3.5: Screen-printed layer I mask detail

During the first tests, these chips made by screen-printing showed that the resolution of the technique was less than initially expected. Because of this, many of the conductive tracks were short-circuited, disabling its use as a biosensor. Therefore, we proceeded in two directions: the first was to change the arrangement of the electrodes of the array spacing more the conductive tracks and second,was manufactured the arrays by another technique, photolithography. The first option (figure 3.6) involved changes in more than one layerof full biosensing block. The two alternatives were developed in parallel by not excessively delay the fabrication of the full biosensor block. Due to the good results obtained with the photolithographic technique, the fabrication with screen-printing was dismissed.

Figure 3.6: Screen-printed redesigned mask to increase the distances between pads and spots

In the photolithographic approach, gold deposition was conducted with sputtering processes. This method is performed on completely clean COP sheets. The fabrication was made in theIBEC clean room under controlled temperature and humidity conditions of the clean room. The equipment used forthis fabrication can be seen in figure 3.7.

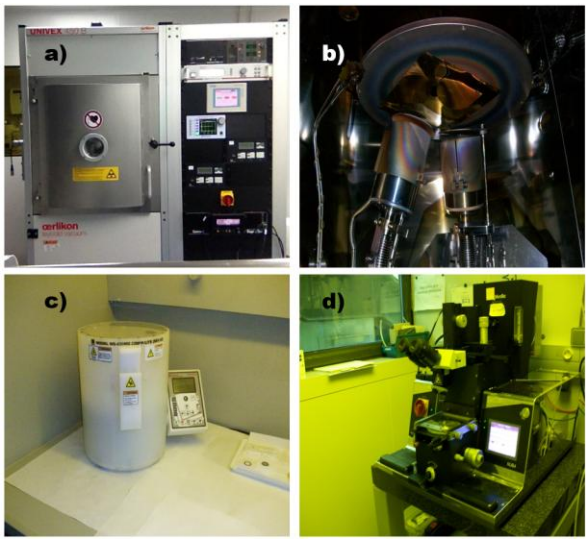

Figure 3.7: IBEC photolithography equipment, a) Sputtering, b) Sputtering cell, c) spinner, d) mask aligner

It should be noted that the metal deposition by sputtering over COP sheets is not a standardized process and optimum conditions were obtained after a long process of optimization. At the end of optimized process, COP sheet that contain a gold face completely covered tightly adhering was obtained (figure 3.8).

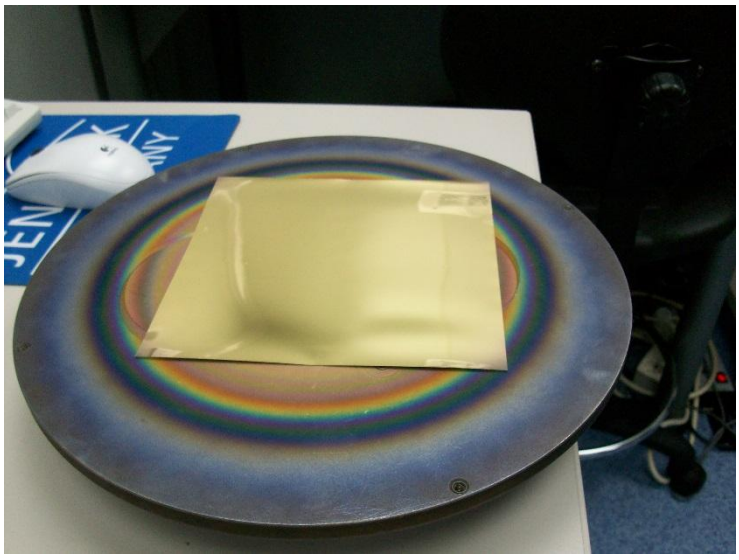

Figure 3.8: COP sheet covered with thin gold film

Once deposited the gold this must be selectively removed to uncover the structure of desired electrodes. To achieve this, areas corresponding to the electrodes

pattern are protected and then harsh chemicals baths are applied to the COP. The selective protection is made by depositing a thin uniform photoresist film by spinning over all gold layer. This resist is exposed to selective treatment of UV light through a mask containing the electrode design (figure 3.9). UV light sensitizes the resist layer in a selective form and it allows protecting only a certain gold areasduring development step.

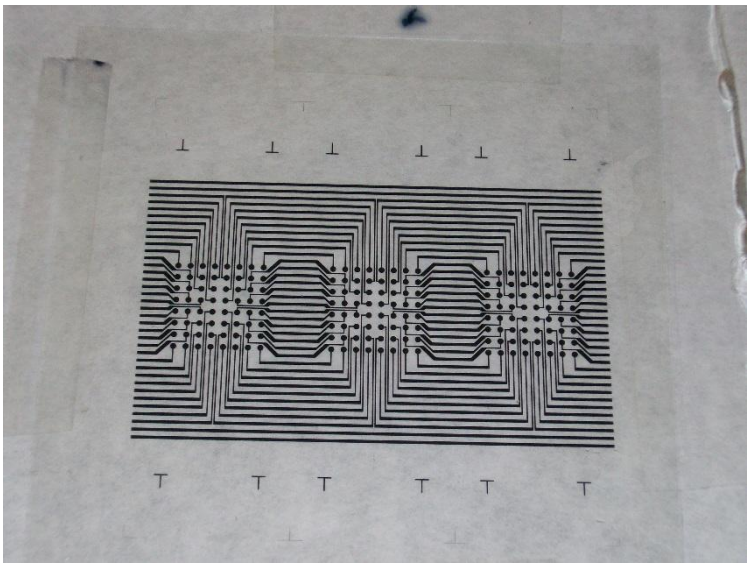

Figure 3.9: Photolithography mask of the WEs array

The resulting COP is subjected to a harsh chemical treatment for gold. At the end, we only had a gold protected by the resin previously revealed. The last step was done to remove the resin remaining on gold paths with other specific dissolvent, getting the gold matrix on completely clean COP. The resolution of this process based on photoresists depends on the resolution of the light and the quality of the mask used. Low cost masks (fabricated in acetone) used for this process allows resolutions of up to 10 μm, well below 200 μmobtained by screen printing technique initially used. The resulted array with this technique is shown in figure 3.10. We can see that is obtained a more shine gold because this gold sputtering deposition method gets much less rough metal surfaces than screen printing. Furthermore, conductive tracks present no short circuit between them, being a better resolution in the whole pattern.

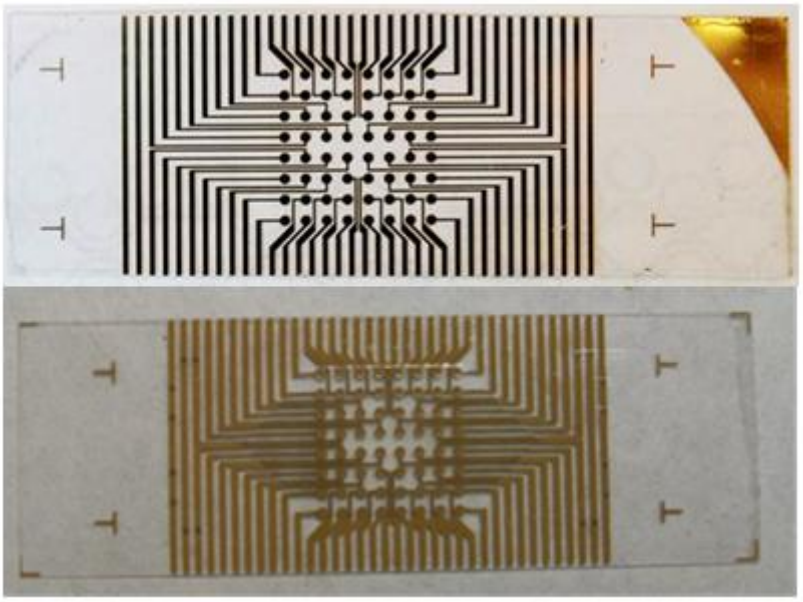

Figure 3.10: Fabrication of biosensor matrix by (up) photolithography and (below) screen-printed comparison

3.3.1.2 Layer II: Passivation layer

The function of this layer is to define the area of the WEspotsand separate those from the gold pads. We can see the dimensions of layer II in figure 3.11. In the original design, the idea was to make passivation pattern in a sheets of COP and then fuse them together with layer I and layer III by pressure-temperature techniques combined with solvents. However, after several assays with different chemical treatments, pressures and temperatures the adhesion of this layer was not strong enough and leaks of the liquid was observed between layer I and layer III. Because of this, to facilitate manufacturing and reduce costs of the device the COP mask of layer IIwas changed to a new insulating layer of resin, fabricated with SU8, above the layer I. The photolithographed mask used in this occasion can be seen in figure 3.12.

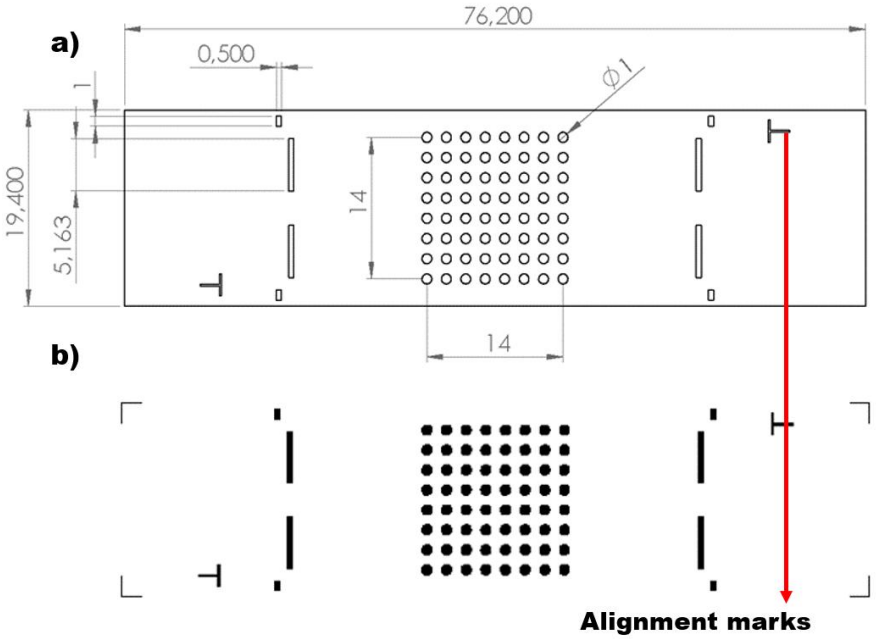

Figure 3.11: Original COP layer I design, a) dimensions of the mask, b) mask where the black regions represents the laser mechanized positions

This layer was deposited by photolithography, that allows stick this film directly above layer I by selective deposition of an insulating material. As a result it is also facilitated the alignment of the layers II, and I but difficult the fusion between layer III and layer I due to material incompatibilities. Therefore, the design of the photoresist mask of layer II was changed to left more free COP area to bind with layer III. The new design solved this problem (figure 3.13); the new photoresist material layer was maximized to leave discovered the biggest surface area of COP in layer I. This allows keep using the technique of sealing layers by fusion with pressure, temperature and solvents, between layer I and III.

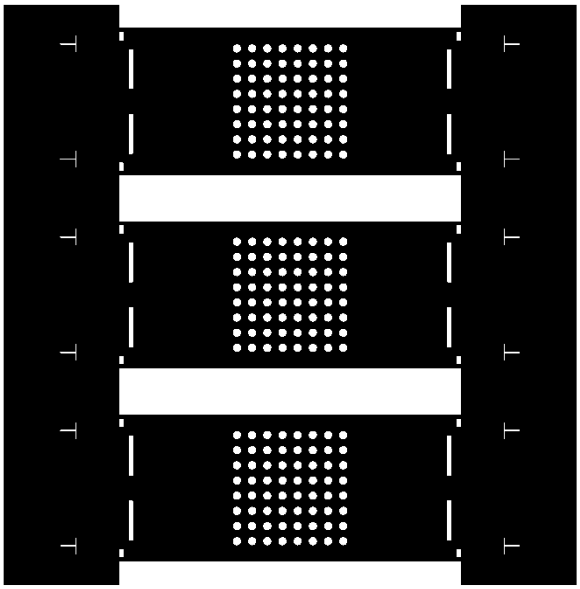

Figure 3.12: Photoresist mask in acetate of layer II used for the passivation fabrication on layer I. Black represents the desired pattern

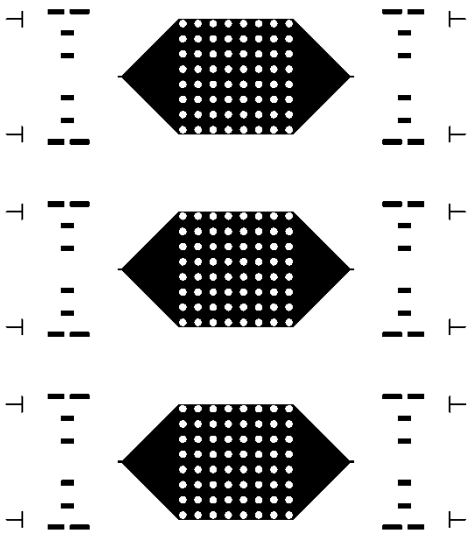

Figure 3.13: Final layer II photoresist mask used for the passivation fabrication on layer I. Black represents the desired pattern

The process for depositing the insulating resin and subsequent development is analogous to that used to define the gold electrodes in layer I. To cover the desired areas with the electrical insulator we used photolithographic techniques. These are based on the selective illumination of resins that react to specific wavelengths, changing its polymeric structure, and making them more or less resistant to

solvents. For this passivation, the substrate is the biosensor array of layer I that previously has been cleaned to delete superficial impurities. Subsequently, working in a pristine environment of controlled light, a thin layer of 2.5μm thickness ofSU8photosensitive resin compatible with biomolecules is deposited.

Spin-coating speed is selected according to the viscosity of the resin to obtain desired SU8 thickness at the end of the process. After the deposition, the resin is fixed by a thermal cure at 95 ° C for 2 minutes. At that point, the mask of figure 3.13 is aligned with the biosensor array by means of the mask aligner machine and the alignment marks patterned in layer I. The assembly is subjected to a controlled ultraviolet light exposure. Note that the masks have been made in three sets of chips to maximize the utilization of the manufacturing process and to minimize prototyping costs. This number is the maximum of arrays that can be done atonce with the sputteringand photolithography equipment in IBEC clean room.

The alignment between the sheets and passivation mask is crucial. Microscope control in the photolithographicprocess was performed to check the positioning of both sheets controlling the points (T-shaped and L) reference. Once aligned, they are subjected to light exposure that will make the exposed parts of the resin alter their polymeric structure. Finally, a bath was given with a specific relatively weak solvent for the resin. The parts of the resin that through the mask were subjected to ultraviolet light were detached from the plates, releasing areas of desired electrical contact.

In figure 3.14, we can see the final detail of the passivation by photolithography near the circular electrodes and gold tracks as well as the different steps during this procedure.

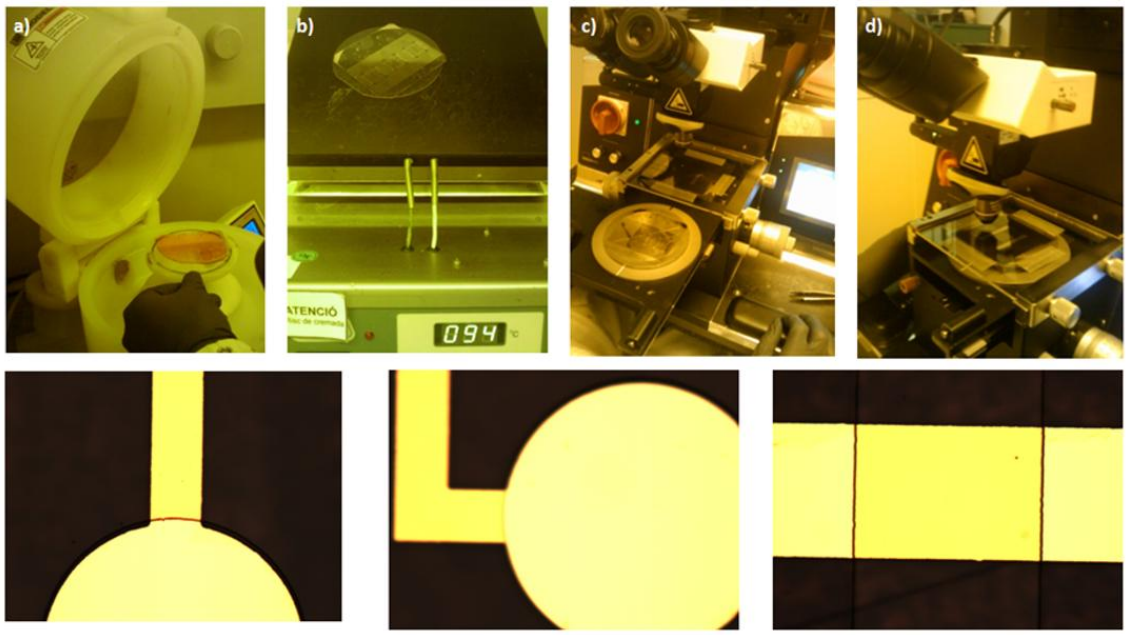

Figure 3.14: Layer II photolithography procedure steps a) spinning, b) thermal cure, c) ultraviolet light calibration, d) layer alignment, in lower figures show a passivated electrodes details

To optimize the photolithographed passivation layer, several passivates were tested. The main reason of this comparison was the unusual electrochemical behavior after fabrication processes, of certain polymer tested. The initial photoresist was the AZ5214 and presented some reactivity in the electrochemical measurements. So, other materials like as AZ3750, Epoxy resin, SU8 and SiO_2 were tested also. After deposition of each one on the biosensors array, we followed the same cleaning protocol to performelectrochemical test. A CV for each fabrication sets was performed. Four cycles with potential values from +0.35 V to +0.90 V at a scan rate of 0.05 mV/s were recorded measuring on the fabricated array the redox response of ferrocyanide 100 µM in 10 µM of NaCl. After of some tests, the SU8 was chosenasmaterial to fabricate the layer II due to its low electroactivity and high chemical resistant. The final protocol to passivate the arrays was:

- COP substrate with a thin film of 200 nm of gold
- Spinner the SU8 in two stages:
  - ✓ 5 minutes to 500 rpm - Acceleration - 500 rpm
  - ✓ 30 minutes to 2000 rpm - Acceleration - 1000 rpm

With these parameters, we obtain a height of approximately 2.4 µm.

- Soft hotplate bakes for1minute at 65ºC and 2 minutes at 95°C.

- ❖ UV light exposure, with acetate passivation mask, in mask aligner for4.1 seconds
- ❖ Post hotplate bake for 1minute at 65°C and 1 minute at 95°C.

The sample is developed with a liquid developer prescribe by manufacturer of Developer SU8 resin for 1 minute and then rinsedwith isopropanol and dry with N_2.

3.3.1.3 Layer III: Hybridization chamber

It is an intermediate layer with a central hexagonal hole, which matches the space occupied by the gold electrodes array matrix in layer I and has to be aligned with the hexagonal shape of the passivated SU8 pattern in layer II. Besides, also contains microchannels, where a conductive ink connects both the REand CE in layer IV with their respective gold paths in layer I (see figure 3.15)

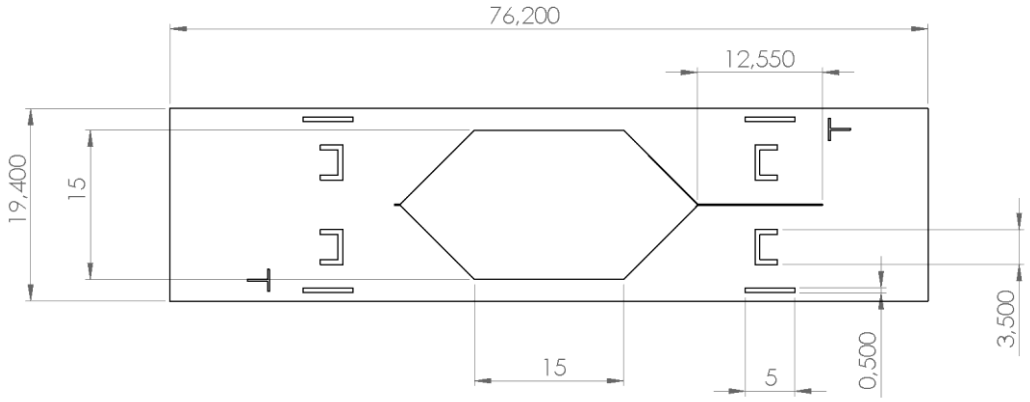

Figure 3.15: Layer III dimensions

Like the previous layer, it also was made of COP and its assembly would be through the same technique of surface modification solvent (cyclohexane) and then apply pressure at a certain temperature. Again, this technique had problems. Trends to deform and detached after the sealing treatment were constant. For that reason, the manufacturing strategy was changed for this layer.

As a solution to the problem, it was decided to replace the layer III of COP by a double-sided adhesive layer of 200 μmin height. The adhesive is called Scapa and withstands temperatures of 110°C. This change facilitates the assembly of the layers II, III and IV. The main drawback added to this change was the impossibility to use the cutting process performed with laser high precision technique used for COP sheets (figure 3.16).

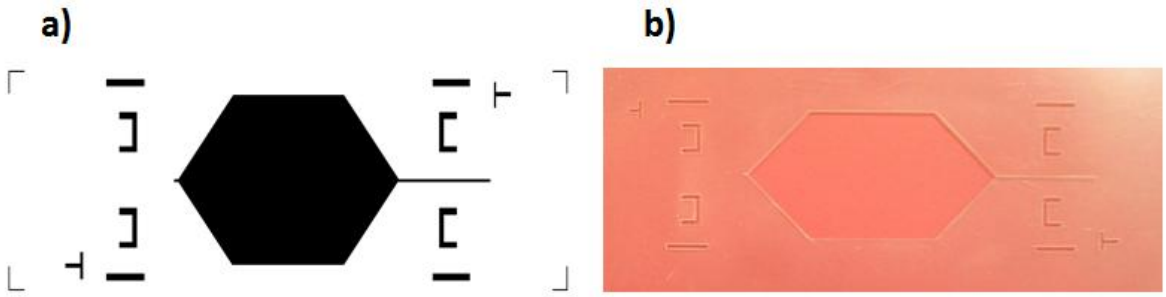

Figure 3.16 a) COP laser positions mask. b) COP layer III by laser

In this way, many methods were tested and finally it was chosen a cutting plotter for cost-benefits reasons. The machine used for this cutting pattern is a plotter Craft Robo CE 5000-40-CRP, performed in IBEC laboratory.

Regarding the mask design for layer III fabrication, figure 3.17 shows the introduced changes in the connection microchannels and hybridization chamber.

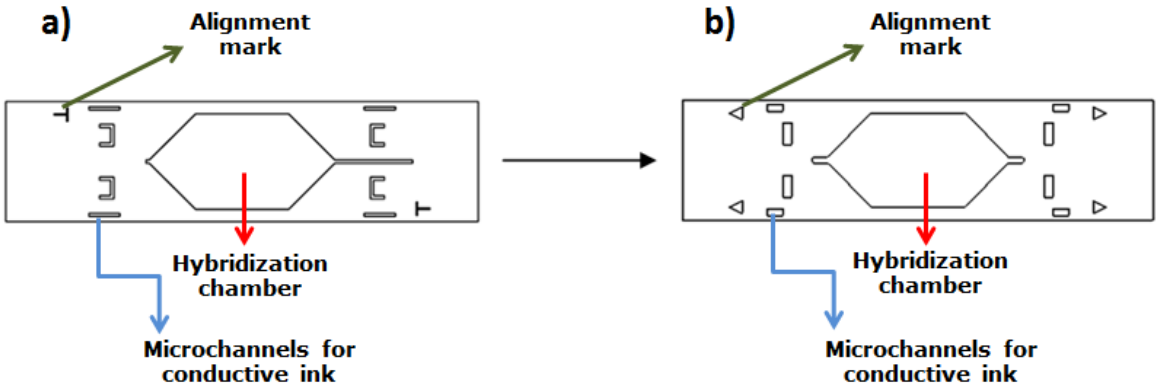

Figure 3.17: Layer III design evolution, a) original COP/Laser design, and b) final double-sided adhesive/plotter design

After optimization of the techniques and material for layer III, we proceeded to unify it with the other layers. So, with the new design of this layer, the layers I, II and III were assembled. During assembly the alignment of the connecting microchannels of the layer III with the gold paths in layer I was complicated. It was decided to test the old mask layer II presented the figure 3.12. In this way, two assemblies of the first three layers schematized in figures 3.18 and 3.19 were tested.

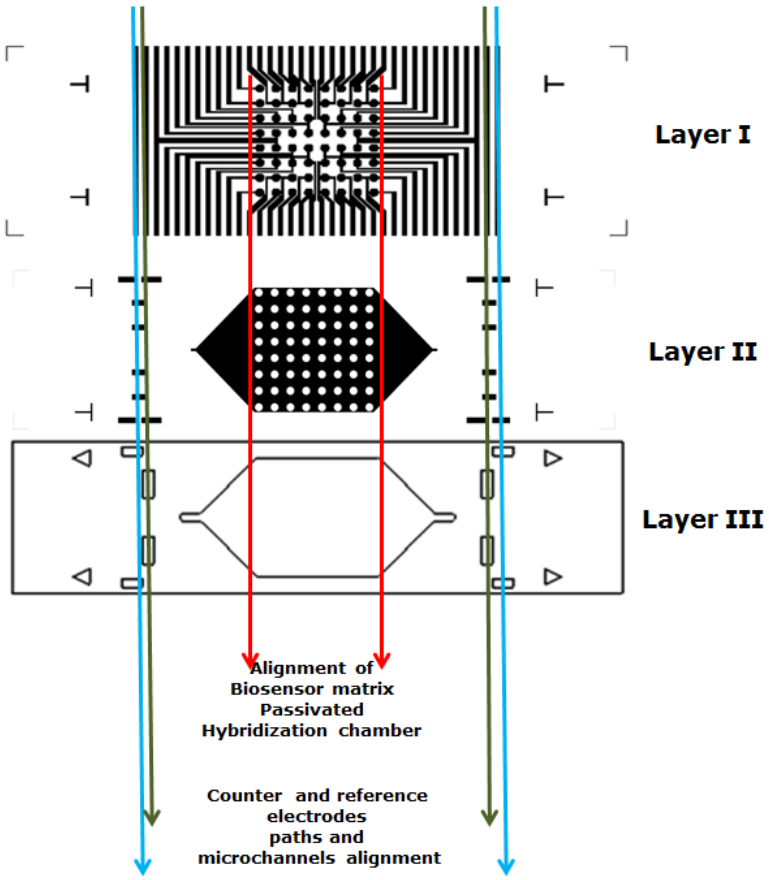

Figure 3.18: Layers I, II, and III first assembly design, can be note the mask used for layer II.

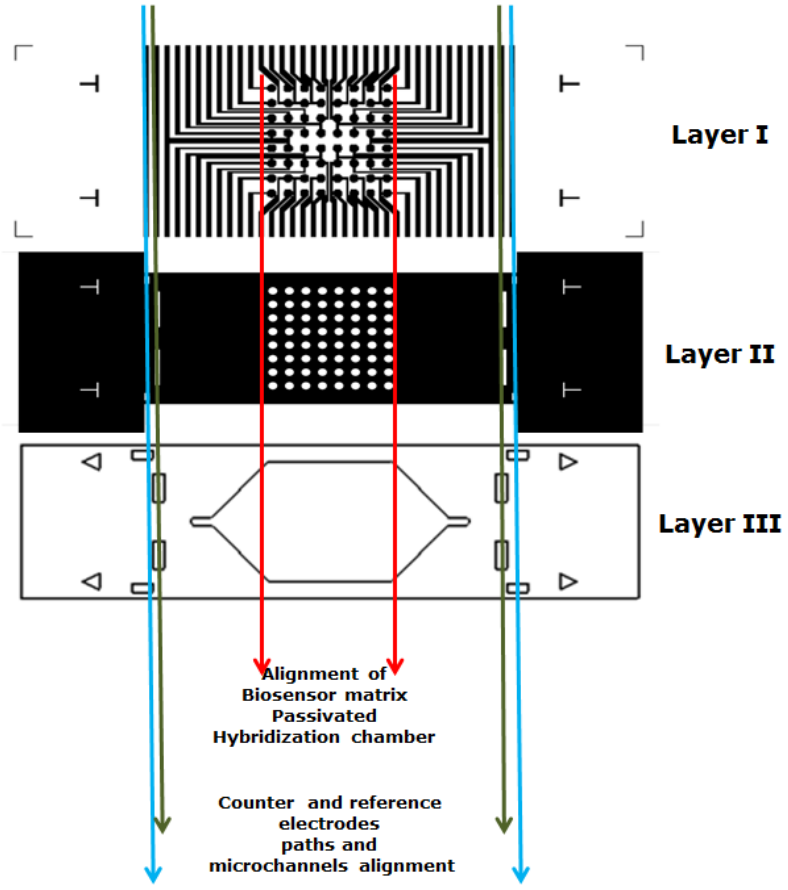

Figure 3.19: Layers I, II, and III, second assembly design, can be note the other mask used for layer II.

Complications presented in the assembly of figure 3.18, arose after injecting the silver conductive ink in the connection microchannels. The ink was spread on other gold paths in the layer I creating short circuits. However, due to a larger area of passivation on the gold of layer II used in the second assembly, this problem was solved. Because of the change in the material of the layer III, the sticking problem that generated this mask of the layer II disappeared, and so it is not a problem to use with this configuration.

3.3.1.4 Layer IV: Reference and counter electrodes

The layer IV (figure 3.20) was made in COP of 188 μmand has printed the REandCE. This printing is done by screen-printing of the Ag/AgCl (Dupont 5874) and carbon (Dupont 7105) for RE and CE respectively, using masks shows in the figures 3.21 and 3.22. The machine used for this fabrication was a DEK printer and the arrays were fabricated by Atic S.A.

The conductive parts of the layer IV are connected with gold paths in layer I, through the vertical microchannels, in layer III. To achieve this connection those channels are filled with liquid silver paint or conductive silver epoxy and then dried. Layer IV also contains two holes (numbers 1 in figure 3.20) corresponding to the input and output of the test sample.

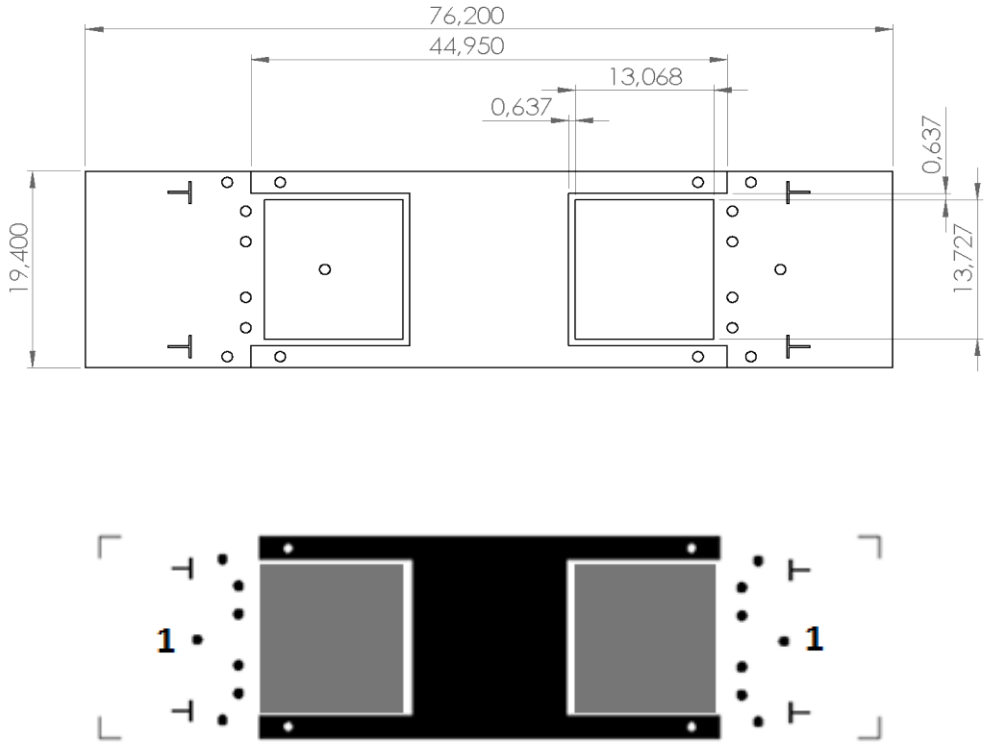

Figure 3.20: Screen-printed counter (H black shaped) and reference electrode (gray squares) dimensions of the whole piece

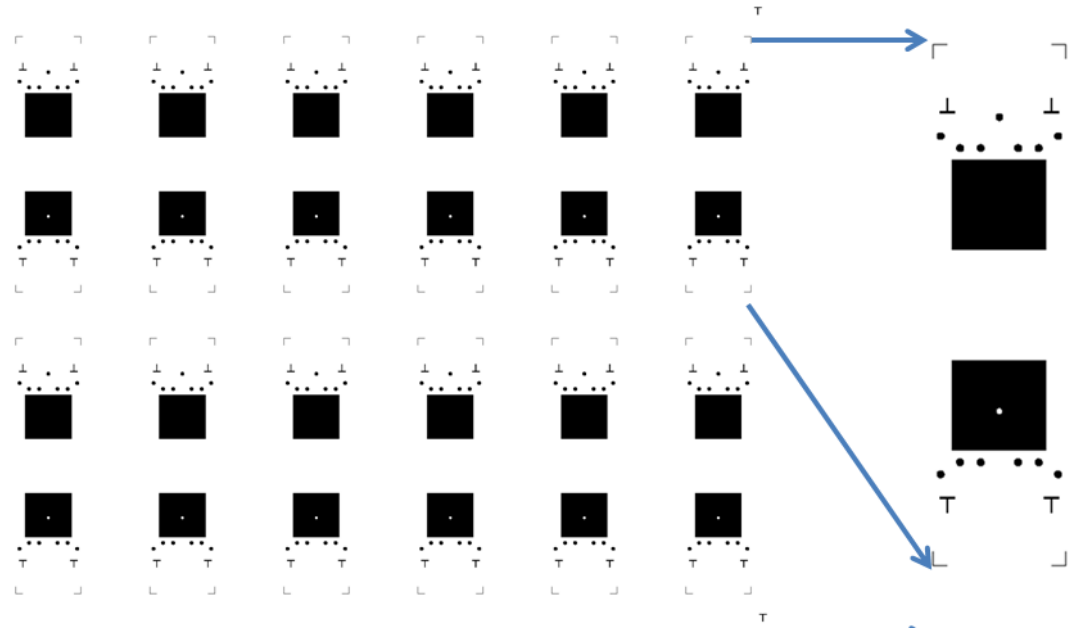

Figure 3.21: Screen-printed for Ag/AgCl reference electrode mask

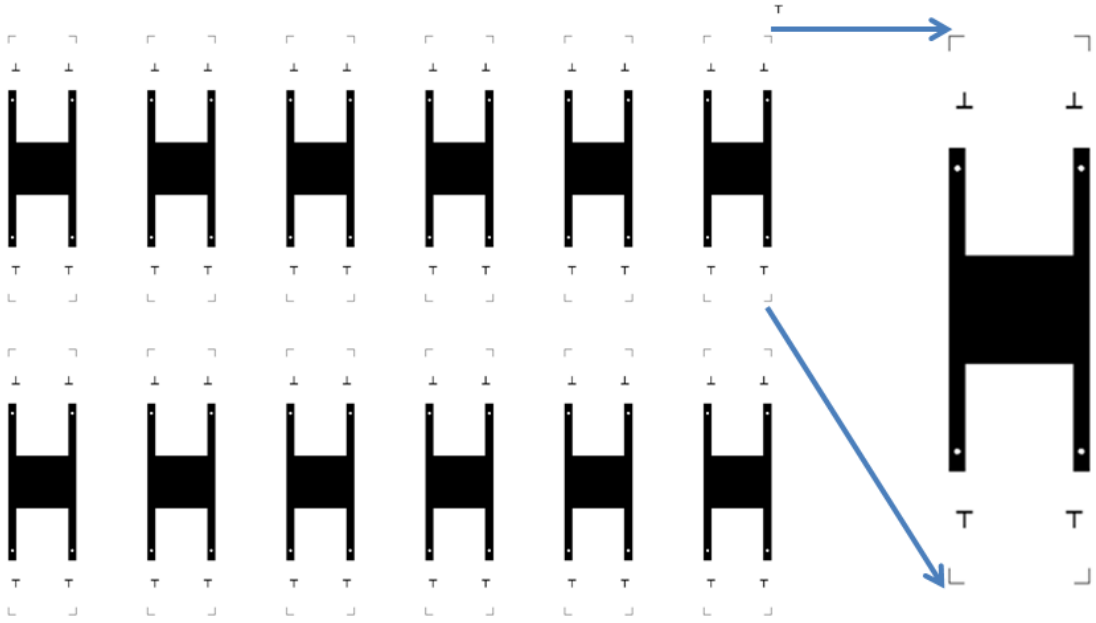

Figure 3.22: Screen-printed for carbon counter electrode mask

3.3.2 Biosensor block assembly

A scheme of the complete assembly of this block is shows in figure 3.23. To correct alignment of each one of the layers, there are alignment marks in T or triangle (Δ)

shape. The vertical channel to connect the RE and CE with layer I is shows also in this figure through the difference layers where this vertical channel cross.

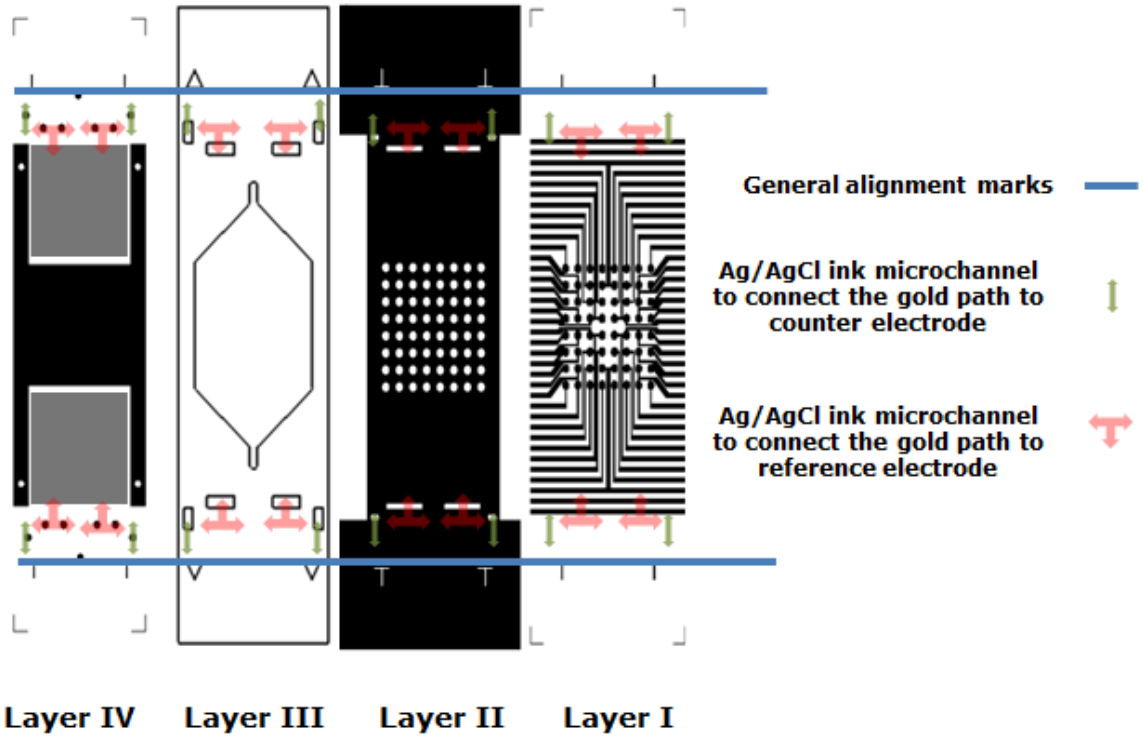

Figure 3.23: Lateral disaggregated scheme of layers I, II, II, and IV, complete assembly. Note the alignment marks and the conductive silver ink microconnections

After of fabrication of the different layers, the standard joint procedure consisted of a series of steps detailed below. The layer I and layer II were united by the same photolithographic manufacturing process. Then, layer I was immobilized with the different DNA CPs following the protocol optimized in chapter two and with the use of nanoploter as detailed in the next section. The layer III, made of adhesive material on both sides of the layer, was aligned and bonded by one side in the layer I/layer II. Then, the silver conductive ink is placed directly into the microchannels of the layer III before sealing with the layer IV. This is done without removing the protective double-sided adhesive on the side of the sheet adhesion with layer IV (see figure 3.24a). Thus, the protection of the same adhesive serves as guide of the ink. Once the liquid (paint or epoxy) begins to dry the protection of the adhesive is removed,leaving perfectly defines its shape(see figure 3.24b). The ink chosen was Conductive Epoxy CW2400 of CircuitWorks.

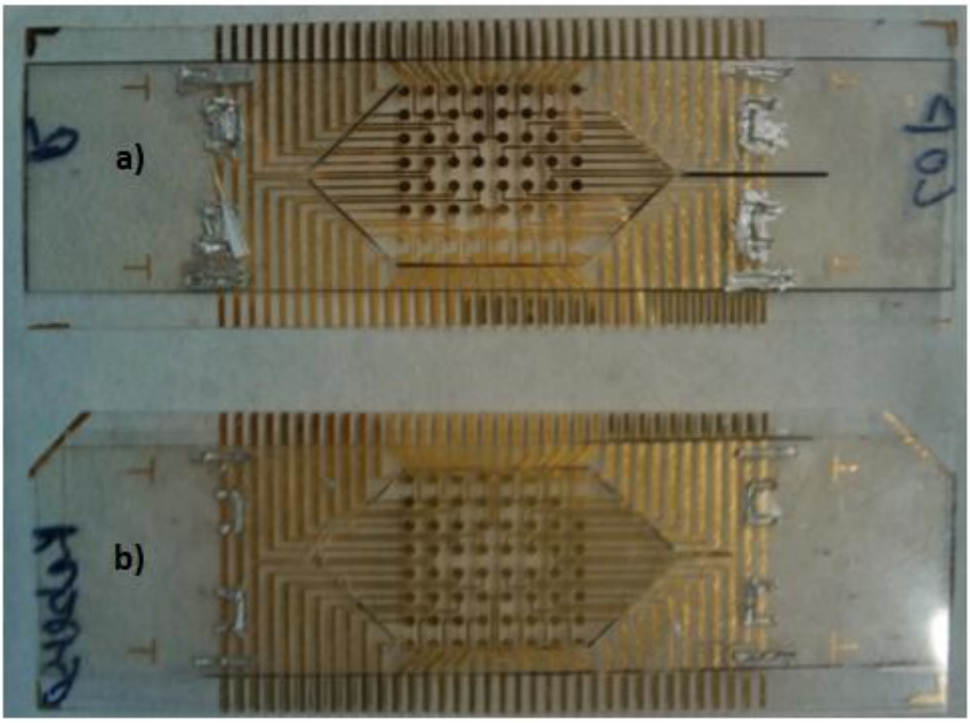

Figure 3.24: Microchannels filled with silver ink, a) with side up adhesive. b) Without side up adhesive, note the well-define shape of the microchannels

Finally, the layer IV aligns and adheres to the adhesive, sealing the cartridge. This method is especially useful when conductive epoxy is used instead of silver paint due to their higher viscosity. The complete assembly of biosensing part of the cartridge can be seen in the figure 3.25. All the electrical connections of the chip can be accessed from one single side. In this sandwich structure can be incorporate other operations placing with planar structures on top of this one. This could facilitate the use of a smaller peltier or PCR systems. Besides, this shape allows that the sample preparation can be done in similar planar structures around this one.

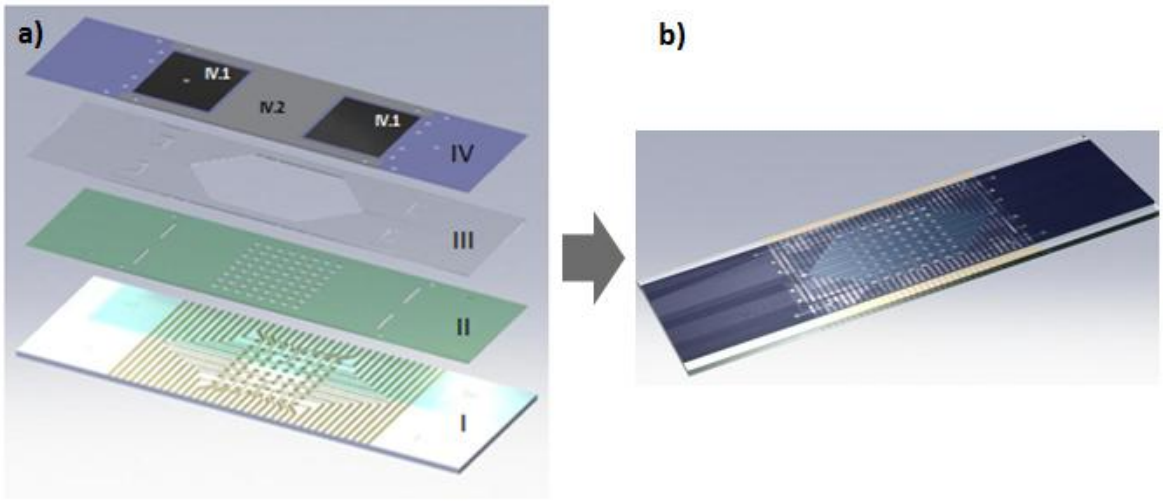

Figure 3.25: Schemes of a) Layers of biosensor block. b) Whole biosensor block

To finish the part of the electrochemical cell fabrication is necessary to put luer-lock connectors in the microfluidic inputs and outputs holes in layer IV to facilitate the insertion of liquid into the cell. Each connector wasjoined using epoxy adhesive. See figure 3.26.

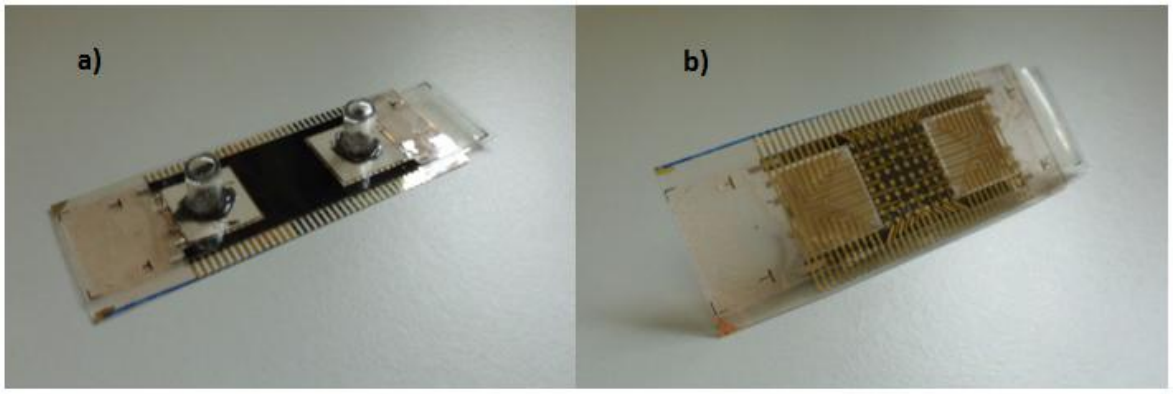

Figure 3.26: Biosensor block a) Top side view with luer-locks in input and output holes. b) down side view

3.3.3 DNA spotting by nanoploter

To perform the deposition of the capture probes on the gold arrays with volumes in nanoliters, automated equipment Nanoplotter NP 2.0 GeSiM with a nano-Tip STMP 0148 was used (seen figure 3.27).

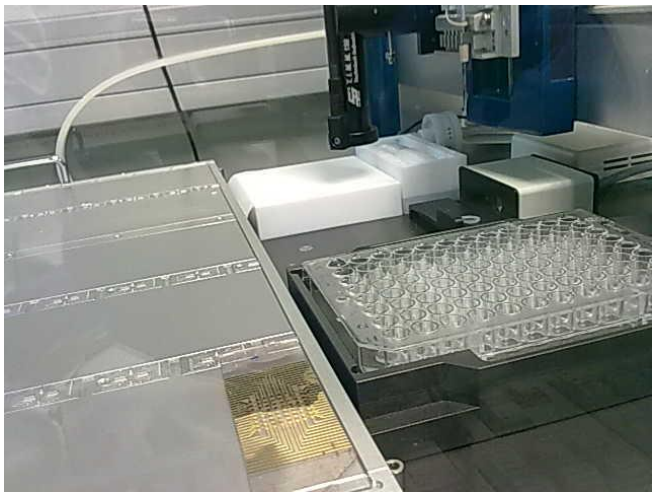

Figure 3.27: Nanoplotter use for the capture probes immobilization

The main parameter to be optimized for this deposition is the drop volume necessary to cover completely each circular gold electrode avoiding that the liquid expands into the adjacent electrodes. This volume depends on the hydrophobicity of the substrate, so in the case of a hydrophobicsubstrate, lower volume is necessary to cover each spot. The hydrophilic nature of the substrate was established through an oxidation process with Piranha solution.

The equipment dispenses a drop volume of 0.4 nL in each deposition. Since a volume of 0.4 nL does not completely cover the surface of each spot, it is necessary to increase the number of drops deposited in each electrode. Therefore, the parameter optimized really was the number of drops needed to cover adequately each one of the 64 god spots. The optimization is carried out with concentrated black ink soluble in water, since the test of the drop covering of the spot was done by naked eyes(see figure 3.28).

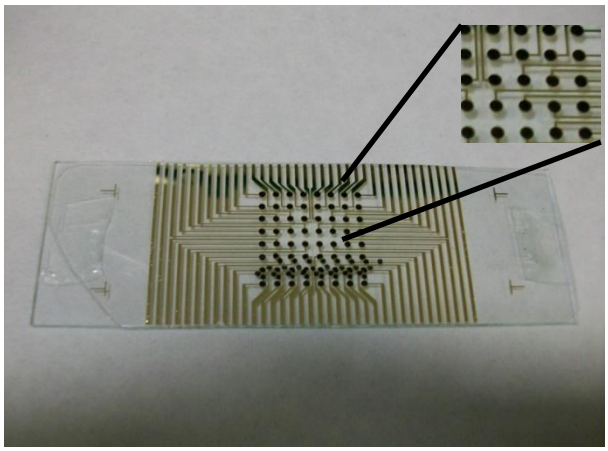

Figure 3.28: Detail of a black ink spotting during the optimization of protocol for immobilization nanoploter

The substrate surface was cleaned before deposition of the probes, making that acquire a hydrophilic nature by chemical treatment. This last consistson immersing the array in deactivated Piranha (5:1) for 10 seconds, and then wash with MilliQ, dry with N_2, sonicate in absolute ethanol for 5 minutes, dry with N_2, expose in UV cleaner for 5 minutes, and keep under argon atmosphere until measurement. During the optimization, parameters of the nanoplotter,such as pulse width, voltage and frequency, were adjusted to achieve a single drop of more rounded shape (see figure 3.29). The optimized values for these parameters were 17 µs, 80 V and 200 Hz, respectively.

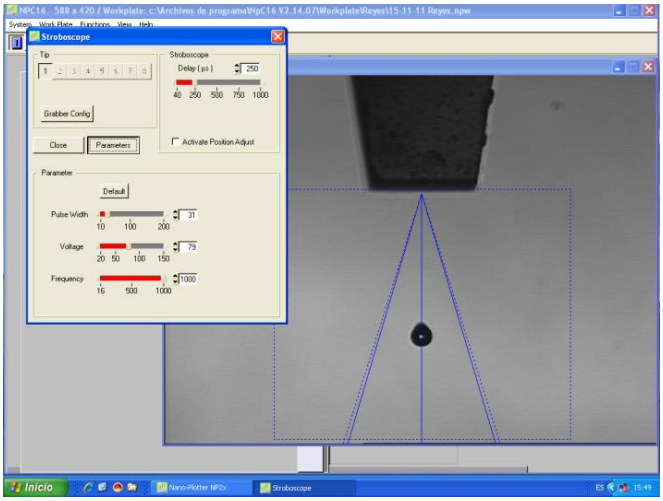

Figure 3.29: Image of NPC16 software in the stroboscope section wherein the drops is observed

After many tests with different numbers of drops, a number of 180 drops were optimized to cover completely the surface of each spot. At a frequency of 200 Hz, the time needed to deposit 180 drops was 0.9 seconds/spot. Therefore, the total time required to cover the full array of spots was 57.6 seconds, regardless of the time of the tip transfer from one spot to another.

3.3.4 PCR Block

The function of this block is to contain biological samples and other reagents during the PCR amplification process. The PCR is a technique used to make multiple copies of a segment of the DNA of interest, usingcontinuous cycles of heating and cooling to make many copies of a specific region of DNA, generating a large amount of copies from a small initial sample. First, two short DNA sequences called primers are designed to bind to the start and end of the area of DNA target that want to be amplified. Then, the DNA template that contains the target sequence to amplify is added to a tube that contains primers, free nucleotides, and an enzyme called Taq polymerase. Then, the mixture is heated until 100 ºC approximately, to denature or separate the double-stranded DNA template intwo single strands. Then, when the temperature is decreased, the primers anneal to the complementary matches on the DNA target template. At a slightly higher temperature, the enzyme Taq polymerase begins to bind to the primer sequences and adds nucleotides to extend the new second strand. Following the synthesis and at the end of the first cycle, each double-stranded DNA molecule consists of one new and one old DNA strand. In subsequent cycles, the process of denaturing, annealing and extending are repeated to make additional DNA copies (see figure 3.30). After a determined number of cycles, as many as billion copies of the target DNA sequence are produced from a single starting molecule.

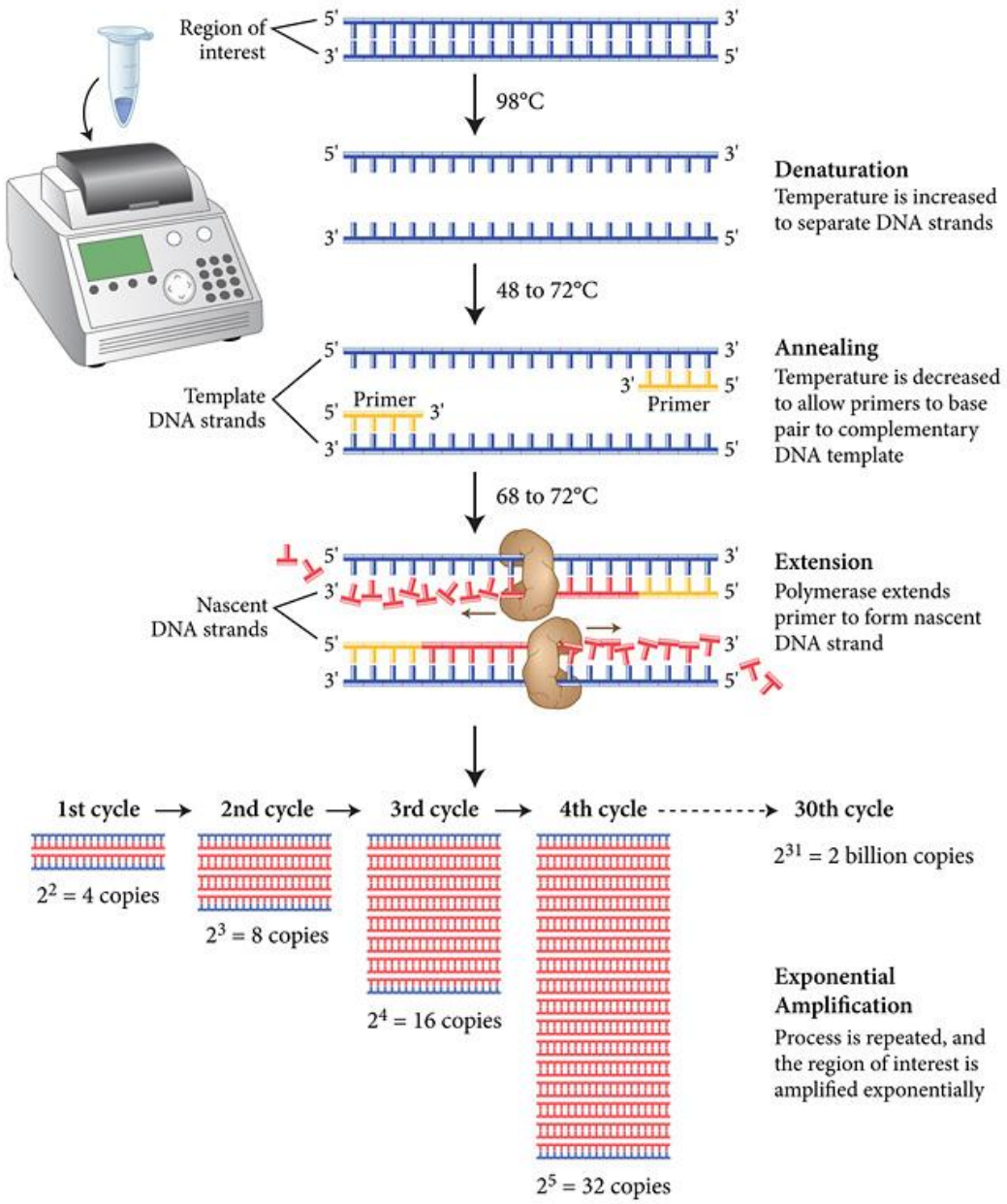

Figure 3.30 PCR process whole schemes. Image taken of https://www.neb.com/

In the scheme of figure 3.31, we can see the different layer that made up the part corresponding to the PCR block in this LOC. This block will be joined to the Peltier-heating device during the complete system integration. This cartridge component was divided in layers also, like the biosensor block. All layers would be done of COP and coupled by solvents, pressure and thermal techniques. The layers that constituted this block were the layer IV, layer V and layer VI.

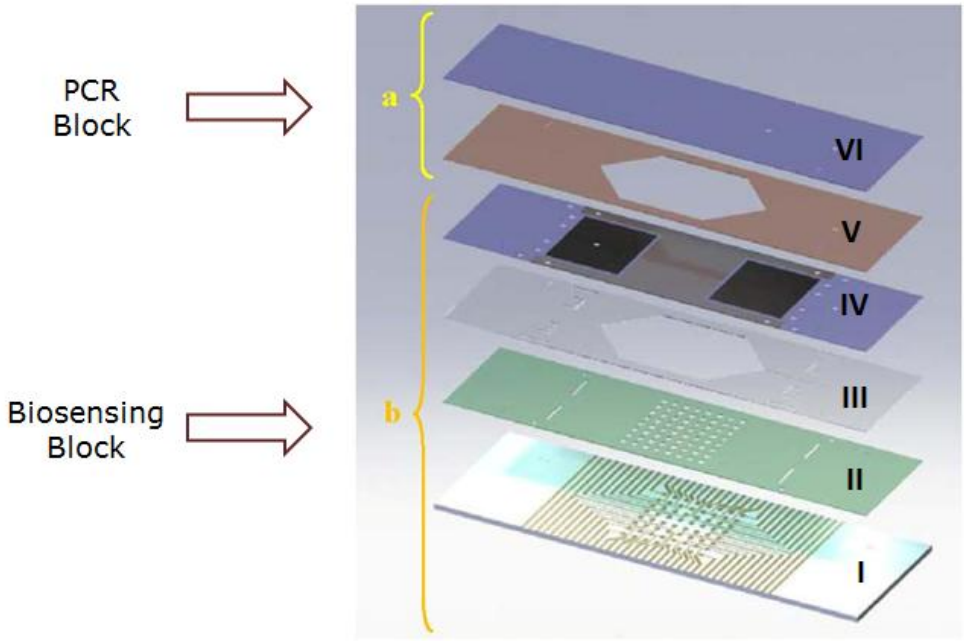

Figure 3.31: Initial design of the whole cartridge components scheme

3.3.4.1 Layer IV

In original design, the layer IV belonged to both constitutive cartridge blocks. In its downside, include the pattern of the RE and CE, and its upside is in contact with the biological sample, worked like inert surface floor in the PCR chamber. This layer contains the in/outlet holes that will contact the flow of the liquid from the PCR to the electrochemical cell. Due to that, the development of this block was done in parallel with the biosensor block, and so the layer IV was replaced by other layer of COP of 188 µm while the complete assembly was accomplished.

3.3.4.2 Layer VI

As the up side of layer IV, layer VI is very simple with the only aim of contain the liquids injected in layer V. As other layers this is made of COP and has the same lateral dimensions that the layer IV;188 µm. The sheet has two machined holes that serve as input and output sample. In figure 3.32, the outline of the different dimensions of the layer VI prototype is shown.

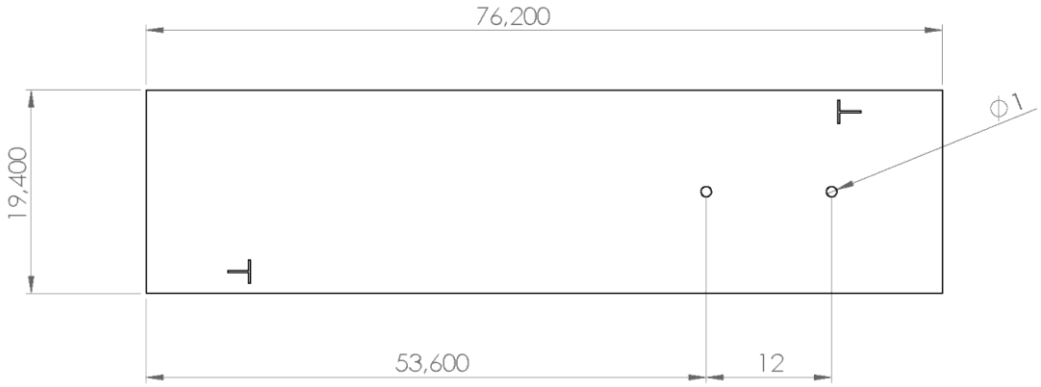

Figure 3.32: Original design of layer VI

3.3.4.3 Layer V: PCR chamber

This layer is what defines the fluidic cell containing the liquid during the PCR. It is an intermediate sheet with a central hollow and very similar to layer III. The design of this layer can see in figure 3.33. The layer was made in COP with a thickness of 188 µm.

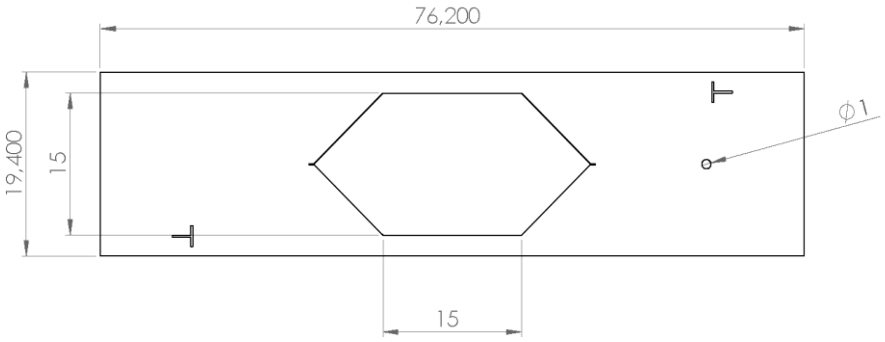

Figure 3.33: Original design and dimensions of layer V

In early test versions, the hole of 1 mm of diameter to communicate the PCR chamber with the hybridization chamber was removed, because the PCR and detection blocks were not yet together. The COP cuts were made with laser technique as in previous layers.

During the assembly of the three layers (IV, V, and VI) of this block, the fusion of COP presents many problems. The main two problems were, in several cases the temperature applied in the hot-embossing seal on the central part of the hexagonal area in layer VI with the layer IV, due to the tiny thickness inside the cell that were melted together. Similar problems were also observed in the first trials in biosensor

block sealing. Another important problem were the leaks observed during the PCR, the high temperature need it for the PCR, produce high pressure inside the cell, breaking the sealing between layers.

Contrary to what was done with the biosensor block, where the layer III was replaced by an adhesive double sided sheet, layer V should continue to be made with COP, or alternatively in a material compatible with PCR.

As a solution to the problem, it was decided to change the design of PCR block and replace the V and VI of COP layers by a micromachined sheet. This design avoids one sealing step and increase the sealing area with the layer IV. For this purpose, the hexagonal cell was changed to a loop shape cell. The design is shown in figure 3.34. In this new layer, the channel is machined directly onto a 1 mm COP sheet with a channel depth of 0.5 mm.

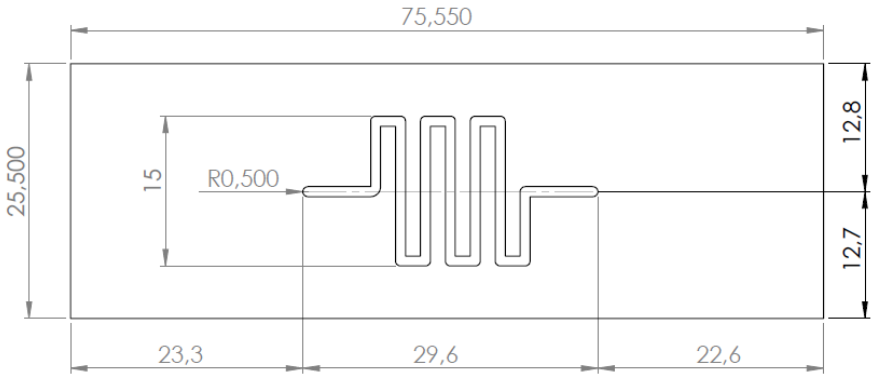

Figure 3.34: New design of PCR block

A theoretical simulation study was performed to optimize the new loop design for the PCR cell in order to dismiss the risk of turbulence (figure 3.35). In this study was tested a correct filling of the liquid and the pressure during filling. The pressure observed was not more than 0.05 bars that ensure the tightness of the PCR block. Moreover, during the process of cell redesign, the volume of 50 µl of sample was remained at all times to maintain the specifications set in the beginning.

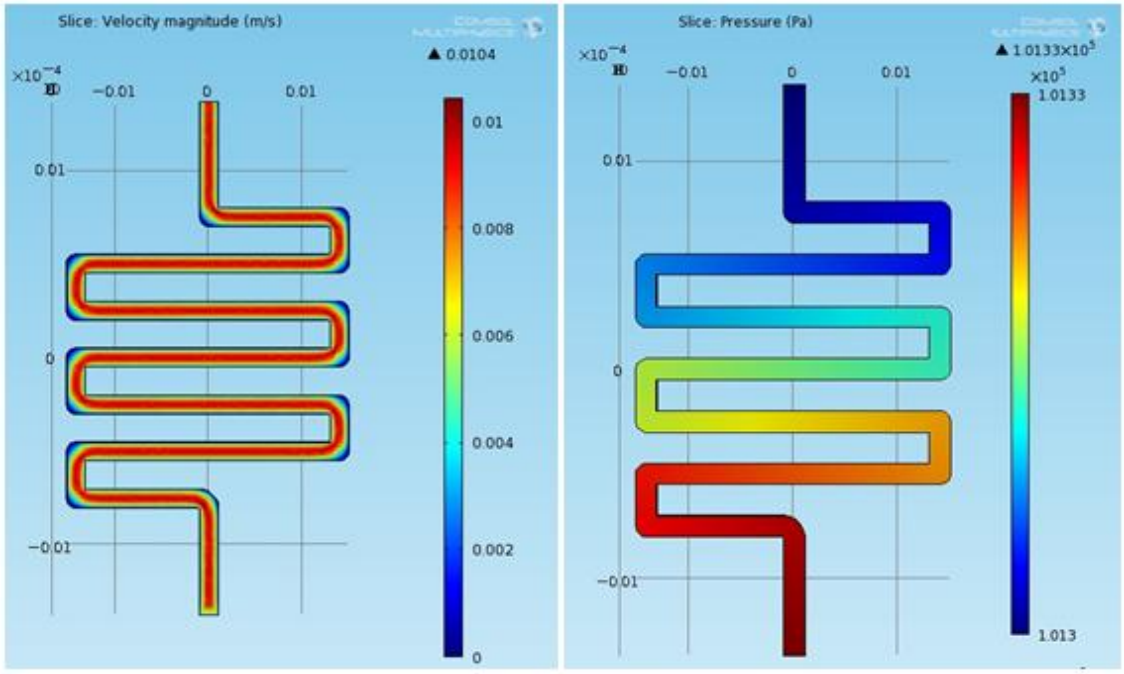

Figure 3.35: Liquid flow simulations in the new PCR block, velocity (left) pressure (right)

Manual microfluidic tests for checking the filling and emptying speed of the channel and thermal conductivity for establishing possible deformations of the cell were performed. All this optimization and simulation as well as the integration of the two blocks were supervised and conducted by Dr. Antoni Homs. The final PCR block is showed in figure 3.36.

Figure 3.36: New PCR block with loop channel like PCR chamber

3.4 Final cartridge: assembly

Microfluidic optimization tests of biosensor and PCR blocks were successful and so, we proceeded to the assembly both blocks. After the replacement of the original hexagonal PCR chamber for the loop channel, the prototype manufacture was greatly simplified. Now, the sealing between layers IV with the new PCR block was performed in one-step. This seal was much easier, since it was the union of only two structures of COP-COP surfaces. In addition, the channel to seal was much narrower and deeper than the original hexagonal chamber, and so no problem of sealing the two covers was encountered.

The seal between the blocks was made with the technique of surface modification using cyclohexane. The surfaces under cyclohexane were the upside layer IV of the biosensor block and downside of the PCR block. Then, the surfaces were aligned and subjected to pressure at a certain temperature. After a lapse, we gained the complete cartridge.

In the first experiments to test the integrated cartridge with the electrochemical detection systems (potentiostat) and mini-PCR, some design faults were detected. The most important observation was the complicated architecture that should arm

the electronic device to integrate the fluidics, Peltier and array connectors in the small area of the cartridge. It should be recalled that the connection pads in layer I are face up and needs to be connected from the top part of the cartridge, where the Peltier and the fluidic inlet are placed, and this left short space for the Peltier and the heating of it affected the electrochemical readout.

In order to solve the inconvenient and future problems is decided modify the layer LOC order.

The new assembly architecture of the two blocks was thought to change the electrochemical connections to the contrary side of the peltier position. Changes introduce in the LOC allowed eliminate minor but remaining problems during manufacture. Besides, the number of layer decreases from six to five. The new modifications incorporates a principal COP layer (200 μm) that has, at the same time, the loop channel PCR chamber and the biosensor array matrix patterned on the other side of the COP. Thus, the PCR block and biosensor block is joined by layer I now.

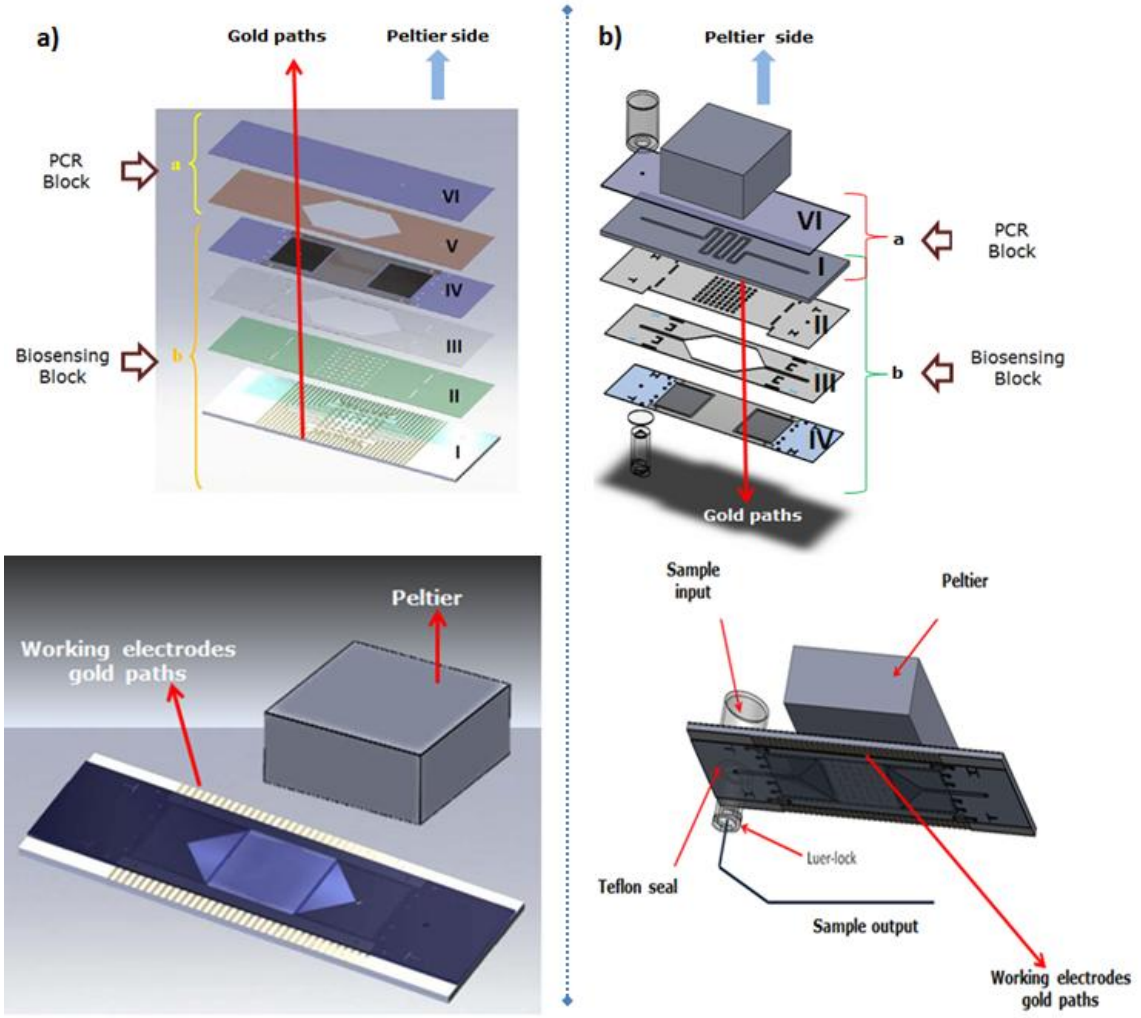

Figure 3.37: Biosensor cartridge evolution of two blocks. a) Old layer disposition. b) Final assembly disposition

In the disaggregate layer schemes of figure 3.37 the changes during the development of the project are clear. We can note the disappeared of the layer V, since it was merged with the old layer I. In addition, we can see the sensing block turn down in order to have the connections on the contrary side of the Peltier. This positional change of the gold paths for electrochemical readings facilitates the mechanical contact between the potentiostat pins holder with the working electrodes and reduce reading noise from the peltier. Also, the upside-downside flow direction system facilitates the sample injection. Moreover, this new disposition of the layers permits us to have the mini-PCR system and the electrochemical holder in two different sides, which facilitates the electronics.

3.5 Summary

Studies ofdifferent materials and microfabrication techniques were performed to design and fabricated a sandwich type cartridge that integrates in a small size and sample volume; DNA amplification and labelling with a mini-PCR and DNA hybridization detection with an electrochemical array. The prototype was designed on different layers that were joined in a sandwich manner. This chapter explains the different testsand redesigns of some of the layers presented in the overall development of the cartridge. The PCR and biosensing blocks were optimized first separately,in a parallel way, and then integrated. Thinking even about of the future integration of the systems, as well as in the low cost character of the cartridge, the improvements introduced were done to overcome problems encountered and to allow a good handling of the elements during the array functionalization process. The assembly of the materials chosen like COP and the double-side adhesive was successful, and allowing to develop a new concept of sandwich cartridge for integrating a mini-PCR and a multiarray in a LOC for medical diagnosis.

3.6References

227. Sin, M.L., et al., *System Integration - A Major Step toward Lab on a Chip.* Journal of biological engineering, 2011. **5**: p. 6.

Chapter 4

4.1 Electrochemical assays in microfluidic cartridge

After optimization of the electrochemical interface or SAM on the single electrode gold presented in chapter 2, and the optimization of materials and manufacturing processes for the LOC cartridge reported in chapter 3, we proceed to integrated both techniques to perform electrochemical testing in the final prototype cartridge in order to establish an effective protocol for both hybridization and detection.

The characterization and commissioning of the electrochemical cartridge was performed at all stages with each one of the probes of the study. Nevertheless, the showed results are the obtained only with the target4 for confidentiality reasons. The CV is the technique used for the array characterization and hybridization detection.The main objective of this chapter is to present the protocols evolution of some procedures such as gold surface functionalization, electrochemical characterization, and hybridization detection strategies on the final array cartridge and results obtained with the electrochemical array cartridge prototype with one of the targets under study.

4.2 Electrochemical cell assembly

As a quick summary, the cartridge for electrochemical detection is the cornerstone in the development of point-of-care device. This cartridge contains the biosensor matrix, which is a photolithographed 64 working electrodes made of gold. Each electrode is connected to the outside by means of gold path in order to establish physical contact with a multipotentiostat system. The cartridge also contains the REand CE in the hybridization chamber. Figure 4.1 shows both sides of the layer containing the RE and CE. In figure 4.2 can be appreciate the assembly of the electrochemical cell, containing the three different layers

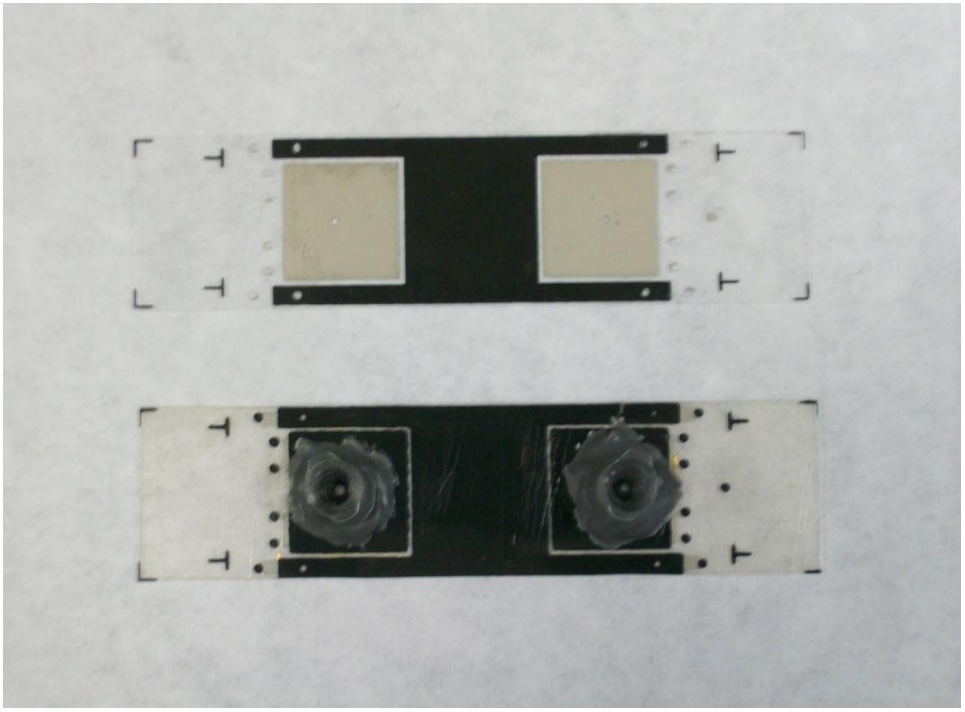

Figure 4.1: CE and RE layer upside and downside views

Before sealing the electrochemical cell, all the WE in the array are functionalized with the specific bioreceptor.

Many immobilization tests were performed with different strategies according to the experiments performed. For this reason, it was sometimes the formation of the SAM conducted with closed electrochemical cell and sometimes with an open cell.

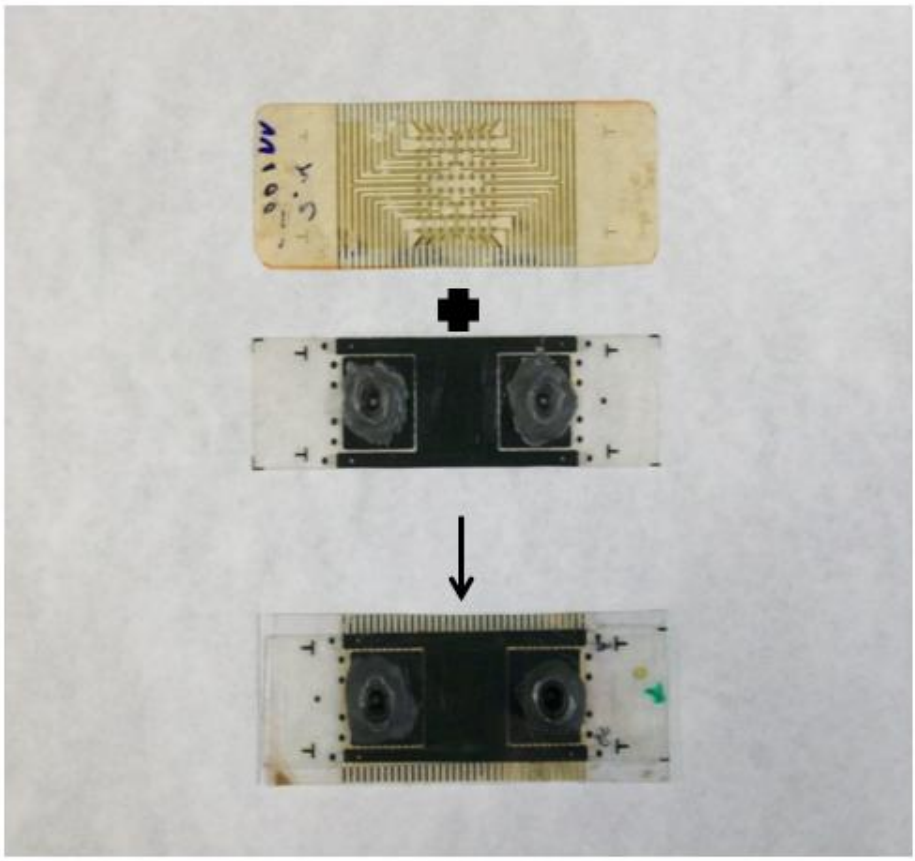

Figure 4.2: Electrochemical cell assembly, Top, open chamber. Down, closed chamber

4.3 Cleaning Array

Depending on the electrodes fabrication technique the gold surface of the fabricated electrodes in the array presented waste of the materials or reagents with which these were in contact. Some of these residues showed electrochemical activity during a measurement test. In addition, the dirtiness may avoid monolayer formation processes on the gold surface. To characterize this problem, electrochemical tests on bare array were performed.

The technique used for this purpose was CV with buffer 10 mM sodium chloride (NaCl). We tested several cleaning protocol that involved the use of sulfuric acid, for electrochemical desorption of impurities on gold, piranha solution to eliminate organic traces, UV exposition to oxidase all organic compound on the surface, and sonication in ethanol, among others. After each cleaning procedure, the array was tested electrochemically again to test the cleaning method efficiency, but also considering the degradation of the array pattern and the plastic substrate. After

several test, piranha solution method was choose. The procedure is simple; the Piranha solution is prepared with sulfuric acid and hydrogen peroxide in a ratio of 5:1 respectively. This mixture is then left at room temperature for 30 minutes to obtain deactivated piranha. Then the array is washed in a Petri dish rinsing it with a Pasteur pipette with the deactivated Piranha solution for 2 minutes.

4.4 Gold electrode characterization

The electrochemical characterization of each one of the 64 gold spots represented a challenge due to the multi-readings of the array that requires a stable multi-connector. In the absence of the final microfluidic-electrochemical cartridge, due to its parallel construction, other measurement platforms were created and built.

Figure 4.4a show one of these alternative models composed of two parts of PEEK material, the bottom piece served as support and anchors of the cartridge, the upper piece contained a number of contact pins for each gold path on the electrode array (figure 4.4b). Regarding the microfluidic-electrochemical cartridge (figure 4.4c), a new PDMS layer containing a hold with hexagonal shape of the electrochemical cell between the RE/CE layer and the WE-array layer was introduced, to function as sealant between the other two layers. For the fabrication of the PDMS layer, a Teflon mold (Figure 4.3) was fabricated with the negative cell pattern into the mold. The PDMS was prepared mixing Sylgard 184 elastomer, which consists of pre-polymer and curing agent, a plastic cup in a ratio 10:1 (w/w) respectively. Then, the mix was shaken vigorously for five minutes until the entire mixture is place in a desiccator to degas for 30 minutes approximately. Finally, the mixture was placed slowly into a Teflon mold that has the patterned structure.

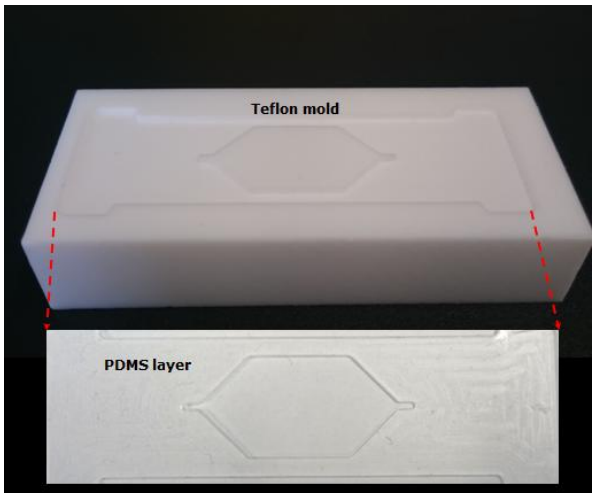

Figure 4.3 Teflon mold and PDMS layer

The three pieces of the cartridge, 2 electrode layers and PDMS layer, were holded with four screws sandwiched with the PEEK layers, which pressure the PDMS layer and contain the liquid inside the cell (figure 4.4b). The idea with this structure was to help during the electrochemical measure since was easier to controls de cell liquid and connect each WE with the commercial potentiostat wires (figure 4.5).

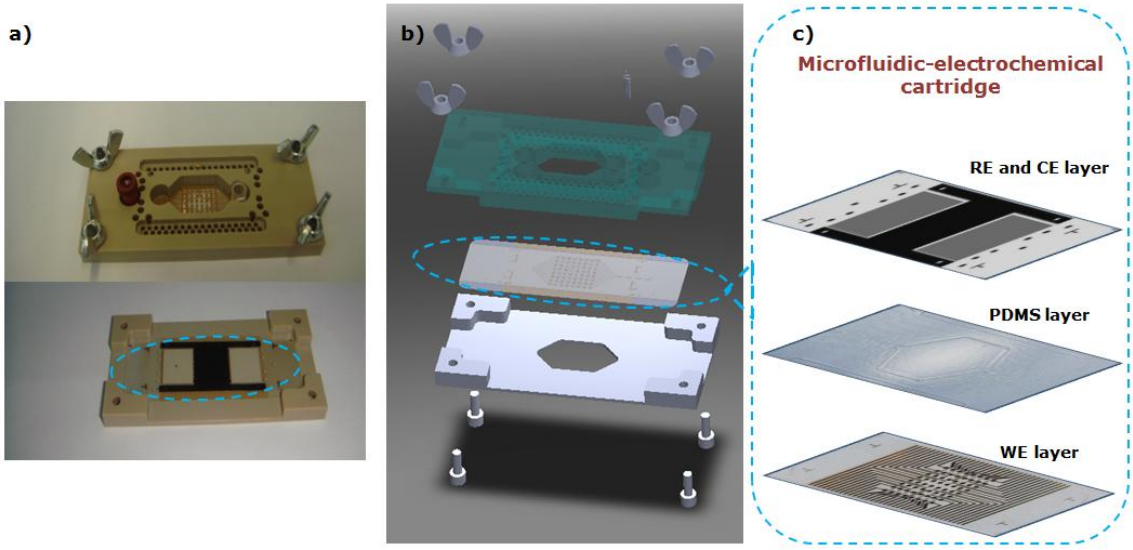

Figure 4.4 Alternative platform to electrochemical measures, a) PEEK pieces photography, b) general assembly scheme, c) Cartridge layers

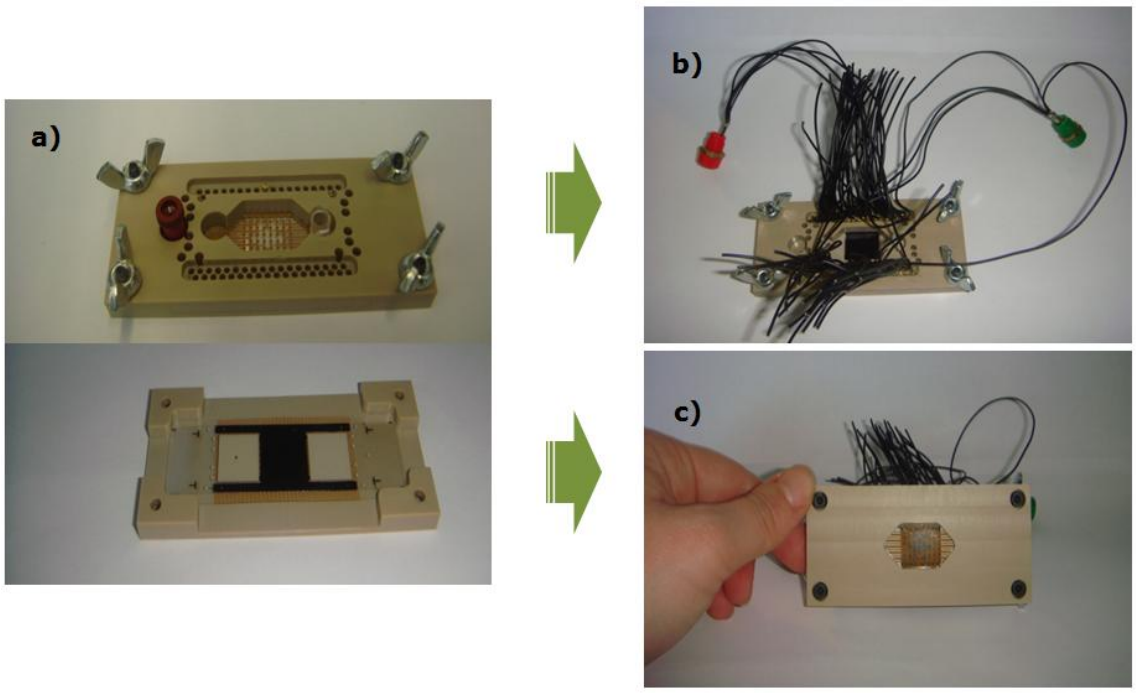

Figure 4.5: Alternative multi-connector by electrochemical measurements, a) pieces in PEEK material, b) complete multi-connector system, c) hybridization chamber windows in down view

The results with this platform were not satisfactory. The cable tangle was difficult to handle and brought confusion in the electrochemical connections. In addition, the stiffness of the cables pulled the pins of its place and the gold paths contact losing touch. Considering also that at this point of the project we need to measure with a 8 channels commercial potentiostat and so it was not required to connect the whole 64 WE at the same time, a smaller easier to use connector was developed. Therefore, the next tool to perform multiple electrochemical measurements was the electrochemical caliper. The figure 4.6 shows us the homemade multiplexer contacts.

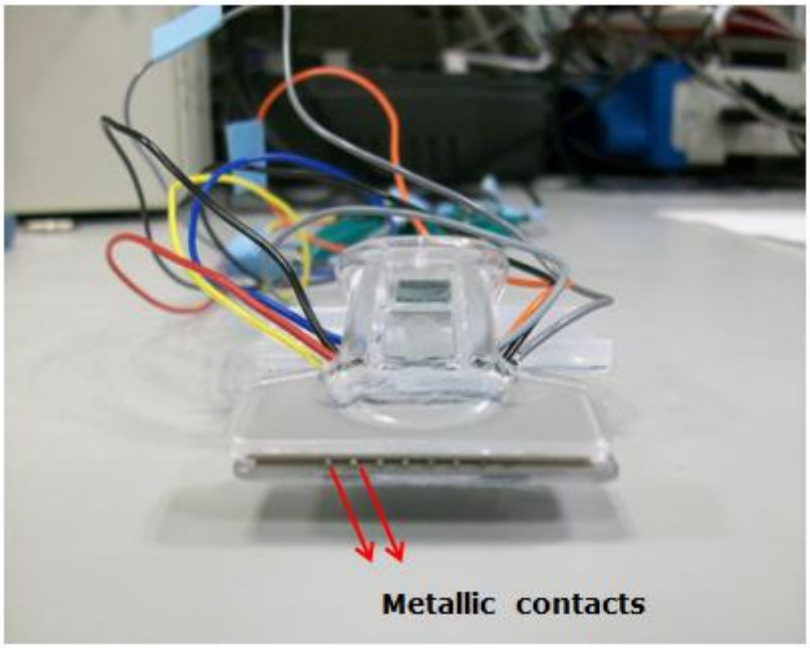

Figure 4.6: Homemade electrochemical caliper

With this tool, we perform easily electrochemical measurements and allowing us to measure eight electrodes at the same time with a commercial eight multi-channel CH instruments potentiostat. This improvement significantly decreased the time spent during the array characterization and the irreproducibility of the results.

The next step was to generate a current map of the electrode matrix to establish possible differences in the electrochemical readouts in the whole array. Figure 4.7 shows us distinct current zones in the array. This characterization was performed with 5 mM of $K_4[Fe(CN)^6]$ / PBS solution. The CV measurements were done from -0.23 to +0.55 V with a scan rate of 0.05 mV/s. The map is obtained from the oxidation peak of third CV cycle of the four performed.

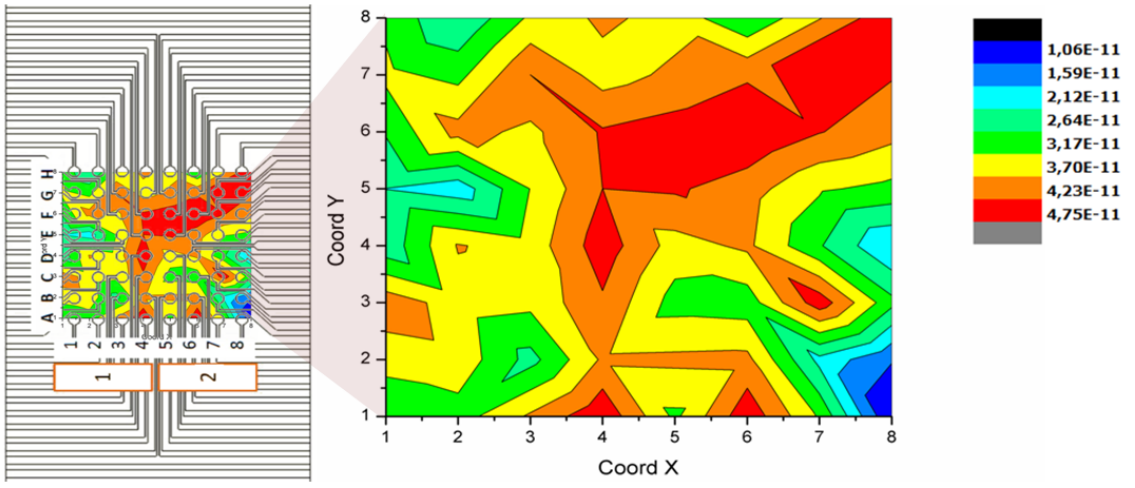

Figure 4.7: Electrode matrix current map

From the reading of the 64 spots that comprise the array, the map of currents could be established. All areas of the matrix are represented and despite the differences between the peripheral and the central area, these do not become significant, being just a difference of 3.4 $*10^{-11}$ (A) between the most different areas.

During the electrochemical characterization of the array some fabrication problems were found, figure 4.8 summarizes the observed damages. Some of the harms were on the gold parts of the biosensing platform, probably, due to the continuous and extensive use of the electrochemical connections. The scratched is another problem that appears after setting up the cell by the friction between layers. Moreover, in other cases appear after fabrication due to an incorrect adsorption of the metal on the plastic. To solve these problems, the thickness of gold layer was increased from 100 nm to 200 nm inthe array fabrication. In posterior test with the new arrays, there were not damages over the gold after electrochemical analyses.

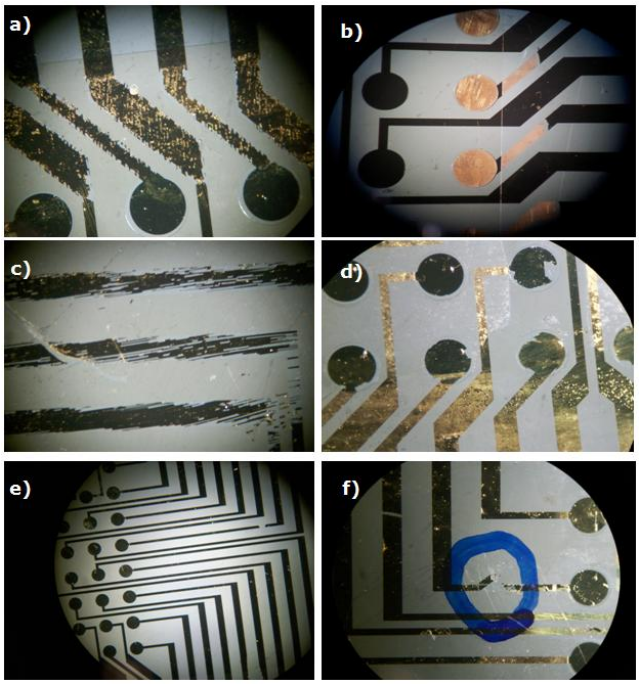

Figure 4.8: Damages after electrochemical measurements. a); b); c); d) reticulated marks on passivated gold. e) and f) Gold paths disruptions

4.5 Electrochemical array characterization

4.5.1 SAM immobilization in closed chamber

The closed chamber concept is referred to the protocol in which the bioreceptors are immobilized on the array and the subsequent steps were done under flow with the cell closed. The biosensor building block characterization was done layer by layer added. This experiments set were performed to observe the electrochemical response of each adlayer. All measures were done without any redox solution, sowith NaCl 10 mM in the electrochemical cell to discard possible masking of peaks from undesired molecules. The CV parameters were the next; potential range from -0.1 to +0.8 V with a scan rate of 0.05 mV/s. It should be noted that all these tests were performed for all other capture probes individually. The surface modification protocol has a sequence of steps;the first one was the bare gold surface characterization to assure a clean platform. The second step was the MalPEG disulfide (thiolated linker) layer immobilization. Then, the capture probe was attached and characterized. In addition, the free gold surfaces and the unreacted maleimide groups were fully covered to avoid NSA with MCH.Finally, the ferrocene labeled target DNA was injected into the cell to obtain a duplex formation and its

subsequent electrochemical detection. After each immobilization steps, a cleaning procedure was done. The CV characterization was carried out after each adlayer also; we wanted to test that none of the added reagents could give a redox response competing with the target DNA redox labeled.

Figure 4.9 shows the electrochemical behavior observed from each adlayer. We can note the difference between the layers without redox molecule within its interface. From those results we can assure that, none of the added reagents in the biosensor gives a redox signal. The duplex formation labelled with ferrocene was detected and confirm us the well performance of the array.

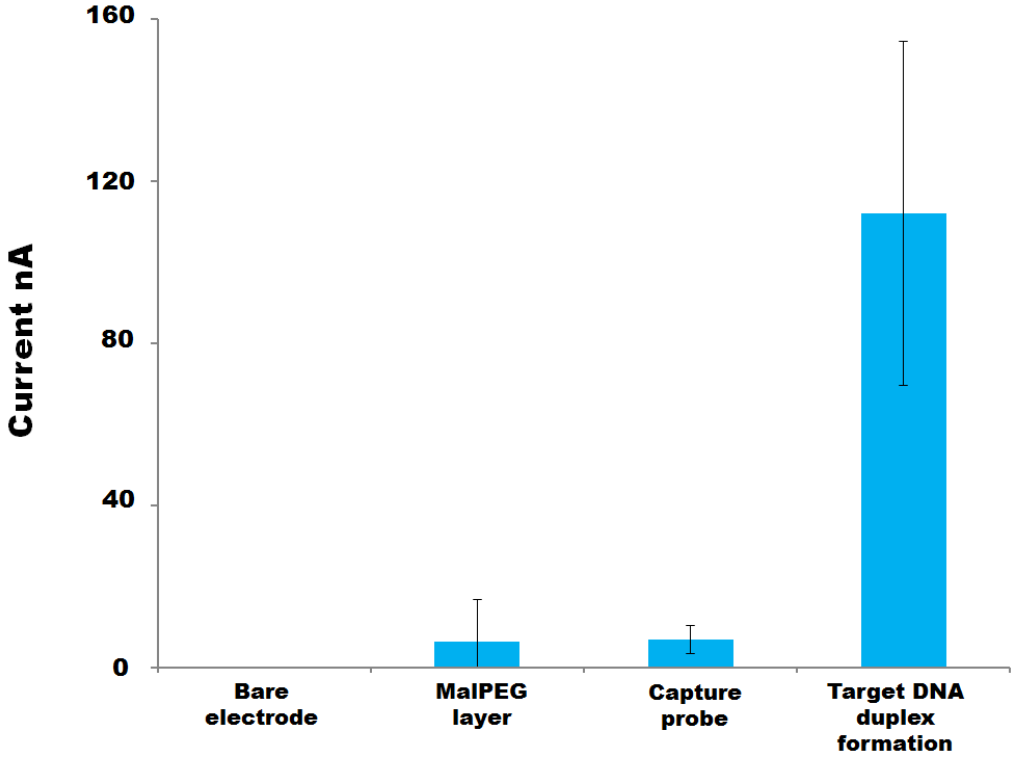

Figure 4.9: CV current obtained from adlayer in the electrochemical characterization

4.5.2 SAM immobilization in open chamber

Next experiments were performed with the microfluidic chamber opened in order to have the flexibility of performing distinct hybridization assays in the same array. Meanwhile in closed chamber strategy, the SAM composition has tobe the same for all gold electrodes in the array.

To start taking advantage of this feature in the next experiments we analyzed the NSA on gold sensors, and the specificity of DNA duplex formation. For this purpose three different controls were done; one without CPs immobilized (MalPEG + MCH +

Target DNA), another with a mutated CP with the sequence of one of the others target that will be detected in the multiarray (MalPEG + MCP + MCH + Target DNA). Both controls are to test the unselective hybridization of the ferrocene amplified target and the adsorption of the other molecules that could give electrochemical signal. The last control was focused in the detection of the signal from remaining ferrocene-labeled primers that could left over after PCR amplification. For this purpose, a CP with the primer sequence was used, (MalPEG + CPPr + MCH + Target DNA). The last sample is the positive assay that hybridizes with the complementary CP the target DNA (MalPEG + CCP + MCH + Target DNA). These four different modifications of the MalPEG SAM are shows in figure 4.10, where 16 gold electrodes for each modification were used.

In this section applies to mention that the target solution is a mixture of amplified DNA and PCR reagents, wherein besides the target DNA, one of the primers is labeled with ferrocene also.

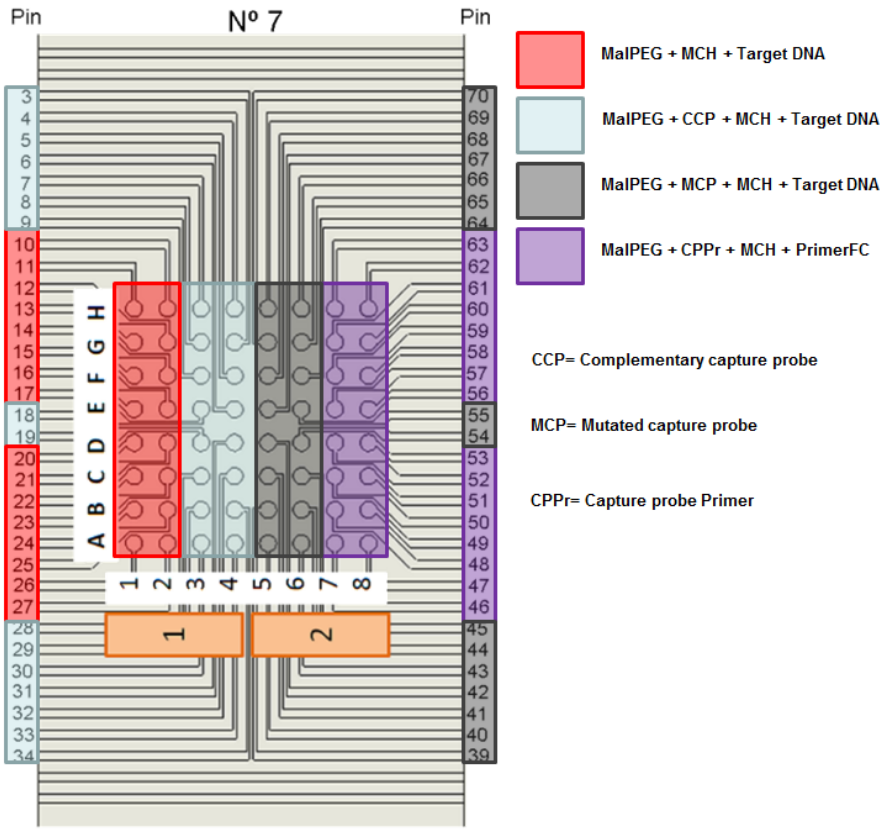

Figure 4.10: Different functionalization to determine NSA (red area), target DNA specificity (gray area), redox ferrocene behavior (purple area),and normal hybridization (blue area)

To immobilize the distinct SAMs in open chamber the protocol involved next steps. For each immobilization, a micropipette was used and the contained solution was dripped manually and carefully on the respective gold electrodes. For MalPEG layer, which was common to all SAMs, a drop was placed on the entire electrodes array. This incubation was left for two hours. Then a cleaning step was performed. The second layer was different for each area on the array. The respective molecules were immobilized in small volumes that were placed dropwise in each area of the spots, and left to react with maleimide for 1 hour.

In case of (MalPEG + MCH + Target DNA), lacking of CP layer, the respective electrodes were covered with Tris buffer solution. The following immobilizations (MCH and target DNA) were common to all SAMs, so for next steps the hybridization cell was sealed. Thereby the immobilization of these layers was made by fluidic filling. Each immobilization lasted 1 hour. Like even, between each immobilization a cleaning step was performed.

4.5.2.1 Positive control

The SAM immobilization with the complementary CP of the target DNA was our positive control. This control is generally used to compare the expected response with changes in other controls. In figure 4.11, we can see the electrochemical measurement after each adlayer. The ferrocene peak detection is notorious in the increase of current observed at 0.65 V (green line); this is an indicative of a correct hybridization event.

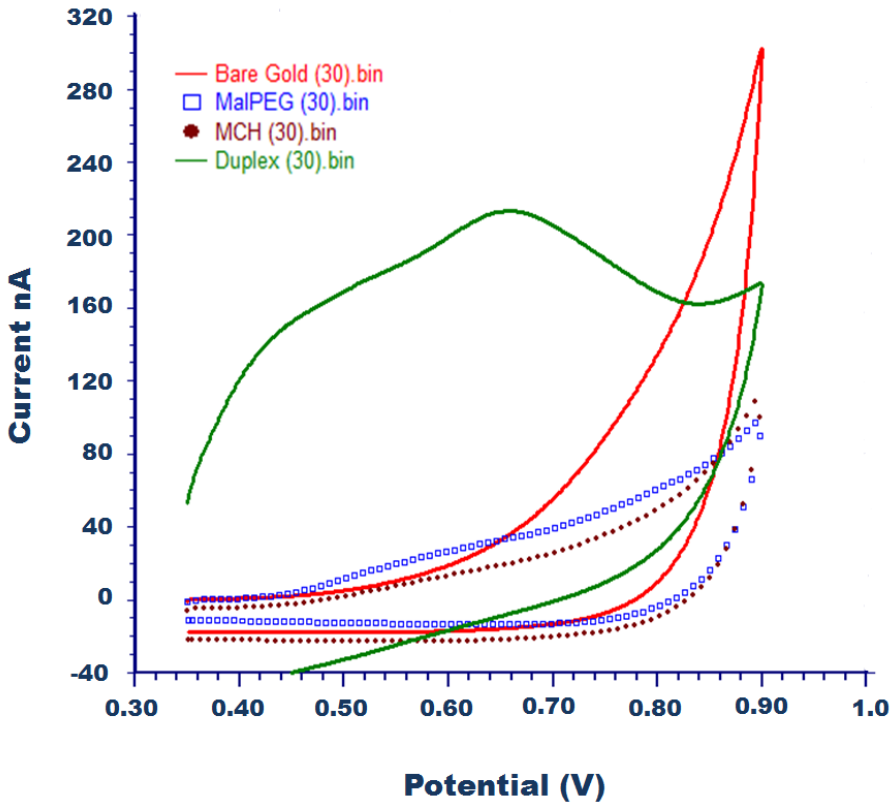

Figure 4.11: Electrochemical response of each adlayer in the same electrode (number 30). Bare gold (red line), MalPEG layer (blue line), CP-MCH layer (brown line), and duplex formation (green line)

One thing that is noticeable from the initial trials was the redox behavior of the ferrocene molecule. In literature, the oxidation peak of this molecule with a 20-mer oligo conjugated is located approximately at 0.1 V. However, our target DNA has 106 mer and the electronic transfer is different from the short 20 mer synthetic DNA target reported. The simple fact that the DNA strand that we use is longer than reported in literature implies a much higher density of negative charge on the surface. This higher density is due to the polyelectrolytic nature of DNA and its known negative charge density. The anion accumulation near the interface of the gold surface slows down the electron transport and decreases the reversibility of the redox ferrocene process, also the higher distance where is found the ferrocene in our system respect to the electrode, slow down the electron transport. During our experimental sets measured, the ferrocene oxidation peak appeared at 0.75 V. This value is closer to helical peptides ferrocene labelled with similar length used in other studies and reported in literature [228-231]. The similarities can be seen in figure 4.12.

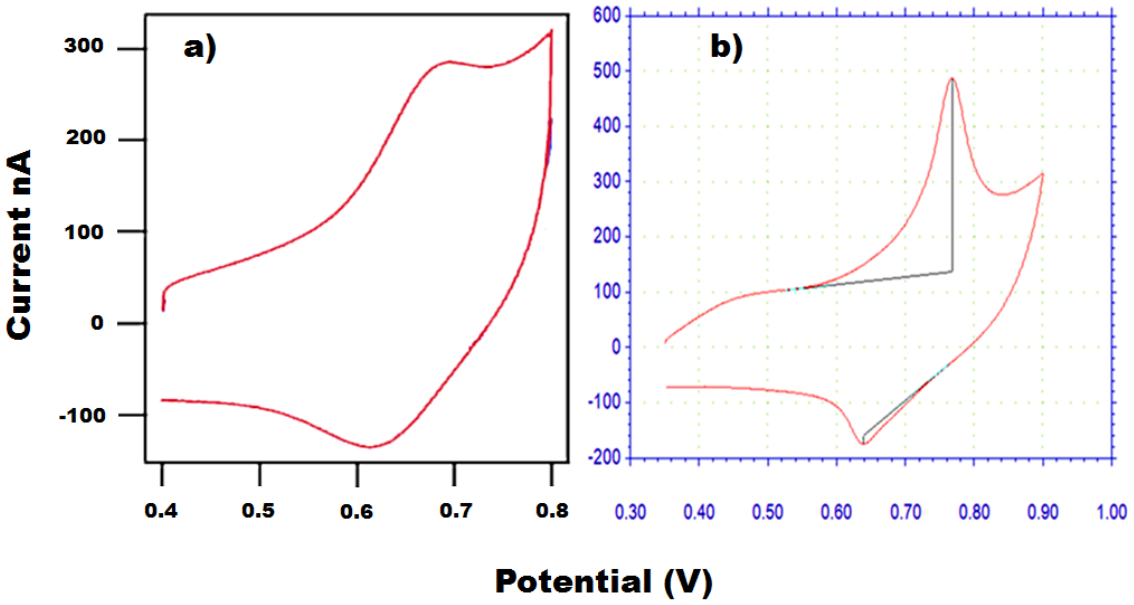

Figure 4.12: CV from different ferrocene platforms, a) helical peptides and b) our developed sensor

After many optimizations and experiments, the electrochemical detection protocol was established. We perform a cyclic voltammetry technique in NaCl 10 μM at a scan rate 0.05 V/s, from 0.3 V to 0.9 V. For electrochemical measurements analysis, we take the values of cationic ip from each measurement.

4.5.2.2 Controls comparison

The comparison between the different controls gives us more clues about the performance of our platform, which are summarized in figure 4.13. Regarding the NSA control (no CP control), we observed low current, so we could consider that the PEG and MHC molecules carry out their role as antifouling agents.

The mutated CP control vs positive control comparison allows us to infer the correct configuration of the CP sequence on the maleimide layer and the good selectivity of the hybridization, comparing with the control without CP signal. Probably the sensor surface covered with a negatively charged non-complementary NSA; prevent better the NSA of other DNA molecules, due to charge repulsion.

We can also affirm that the spacing between CP molecules is sufficient to allow the formation of the complementary duplex. This control also allows establishing the high specificity of the selected capture probe sequence.

The complementary CP and CP primer control comparison assays, let us dismiss the idea that the "free" ferrocene labeled primers remaining from the PCR and contained in the same solution that our target DNA, can interfere in the electrochemical detection signal of duplex.

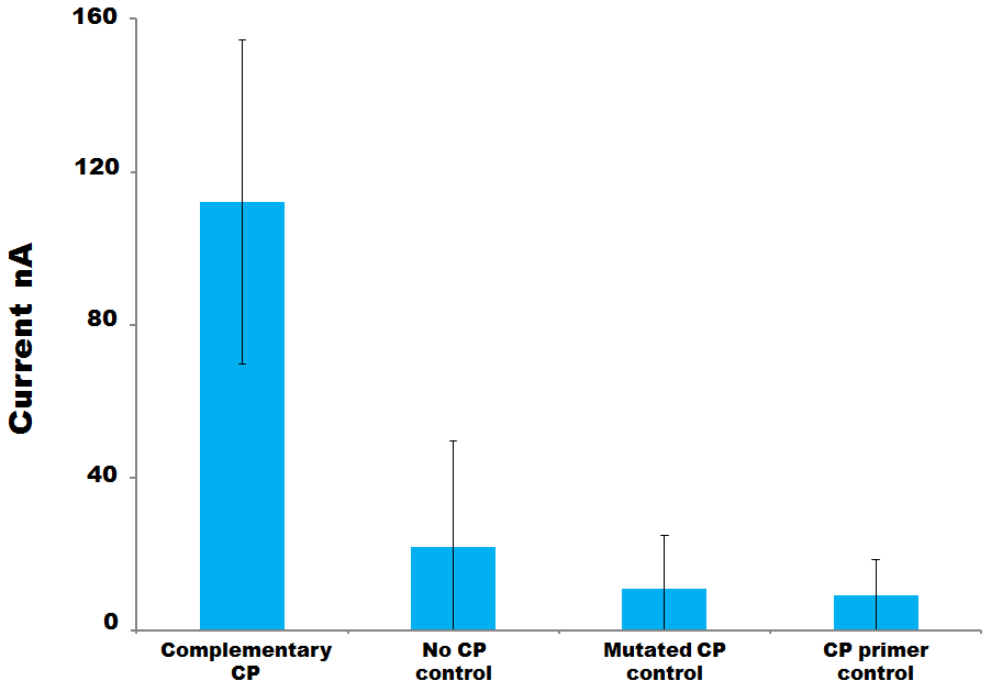

Figure 4.13: CV electrochemical responses of the controls immobilized in the biosensor (open chamber)

4.6 Limit of detection (LOD)

Once both; the array functionality with the electrochemical detection of DNA duplex was established and the manual immobilization protocol was optimized, our next step was to determine the minimum amount of DNA that we could detect in the array. To achieve this, different number of DNA copies before PCR amplification procedure were taken and amplified, following the same protocol. The initial DNA copies numbers of Diana 4 were, 100000, 500000, 100000, 50000, 10000, 5000, 1000, and 50. The amplification cycles were standardized in 30 for all experiments. The idea was to obtain several post-PCR solutions with different initial copies of PCR amplified target DNA. Then three arrays were immobilized following the scheme in figure 4.14, for reproducibility studies.

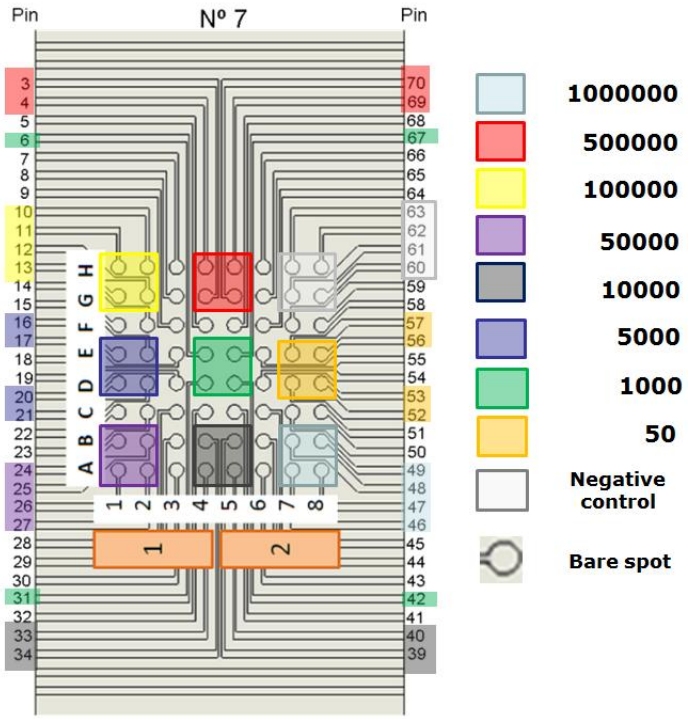

Figure 4.14: Array functionalization scheme for different DNA concentrations

The different steps for biosensor immobilization were made manually layer by layer in an open chamber. The results obtained of these trials to find the LOD can be seen in figure 4.15. Fifty initial copies of DNA for PCR amplification were not enough for being detected with the good sensitivity of electrochemical detection. However, no problems for detection of subsequent concentrations was encountered which show good reproducibility. The higher concentrations (1000000; 500000) showed much more irreproducibility. Maybe due to surface saturation of DNA strands, this may interfere with the transport of electrons. Other possible reasons can be an irreproducible amplification during the PCR cycles, due to DNA strand saturation. The 100000 experimental sets had a strange behavior, being its electrochemical signal lower than expected but with good reproducibility. This made us to think that perhaps this concentration would be the saturation point of the system, affecting on the PCR amplification and/or in the electron transport. Regarding other concentrations, we can say that the reproducibility was lower and the detection signal was acceptable. Our detection limit was quite low; 1000 initial copies of DNA before the PCR amplification process. However, because our system uses multiple capture probes, with different targets length, for the next optimization we decided to take the 50000 initial DNA copies concentration due to its low irreproducibility and high signal detection.

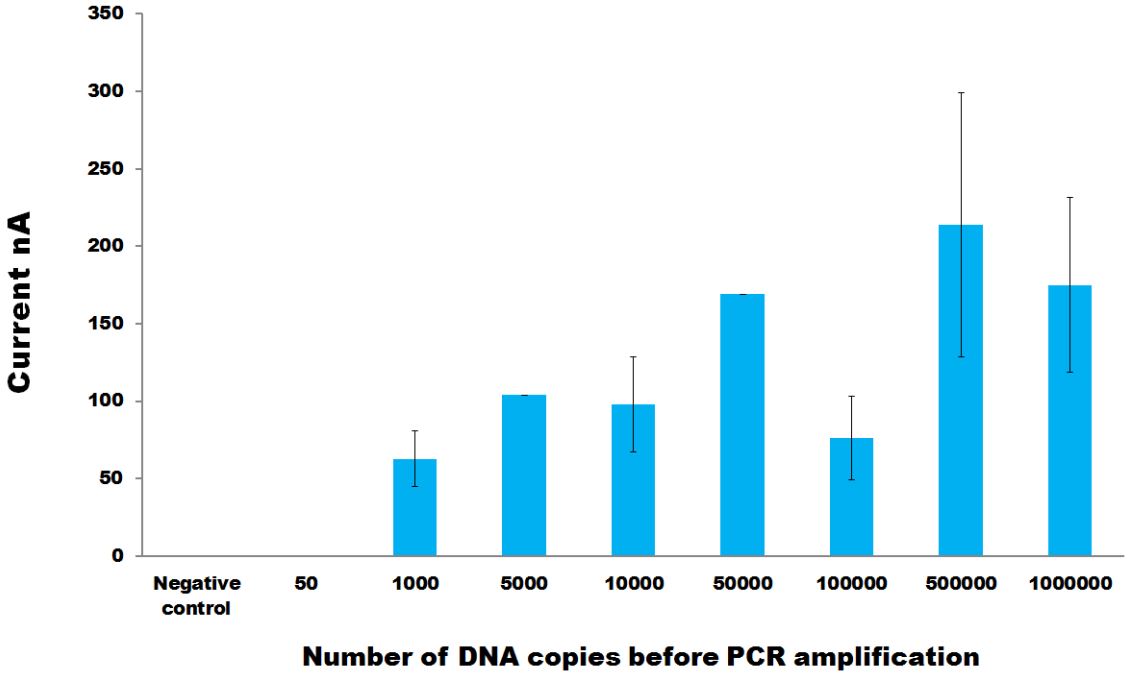

Figure 4.15: CV electrochemical response for different DNA concentrations

4.7 Crossreactivity test

Having established the ideal working concentration of initial target DNA copies, the next step was to test the crossreactivity between two of the target that will be detected in the final array. In the final prototype for cancer detection 14 different CPs will be immobilized on the array, for the detection of 14 different targets DNA labelled with ferrocene. The objectives of these experiments are two, to determine whether the SAM works fine for other capture probes with longer targets and to establish possible cross-reactions between different targets and immobilized capture probes on the array. The capture probe of target DNA Diana 8 was randomly chosen for these experiments.

The array immobilization experiments sets is show in figure 4.16, were was tested the next systems; SAM with CP Diana 4 and SAM with CP Diana 8 were hybridized with target Diana 8 and target Diana 4 respectively; with these two systems we established the possible crossreactivity between these two DNA targets. In other words, we probed the non-specificity between these DNA targets. Other two systems with CP Diana 4 and CP Diana 8 were hybridized with its respective target DNA; these experiments give us information about the correct MalPEG SAM behavior for different capture probes. A set of measurements with mutated target

(a synthetic ferrocene-labelled ssDNA external to the project) and negative control without CP incubated with target DNA Diana 4 would strengthen our study of the capture probes specificity.

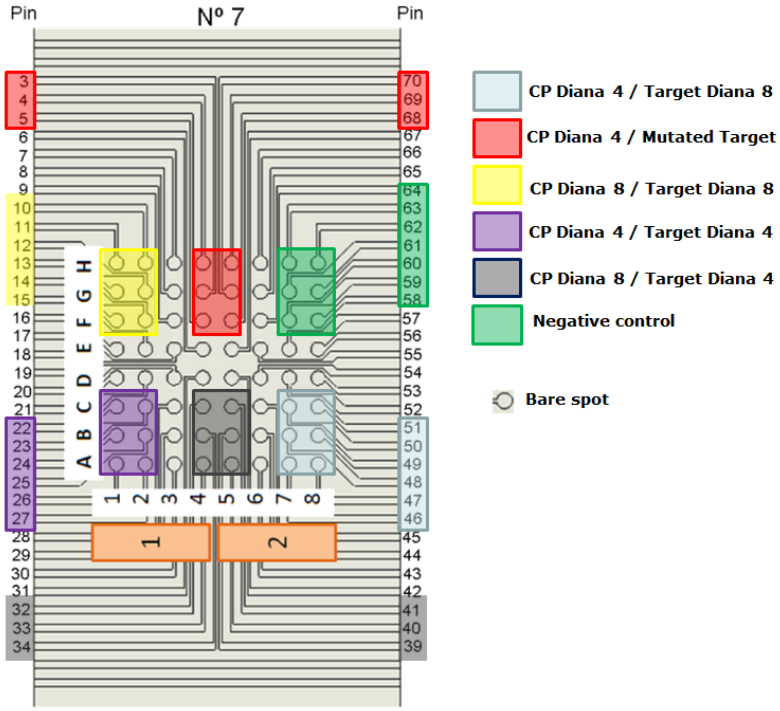

Figure 4.16: Array functionalization scheme for crossreactivity test

Regarding the duplex formation detection with different capture probes and its respective target DNA, we obtained good results, figure 4.17 shows those responses. As in previous experiments, this test was performed in triplicate, to test the reproducibility of the responses. We detected hybridization event in each one of the capture probes tested, Diana 4 and Diana 8. However, some differences were observed in the current obtained from the two systems. These variabilities could be understood due to its DNA structural differences.

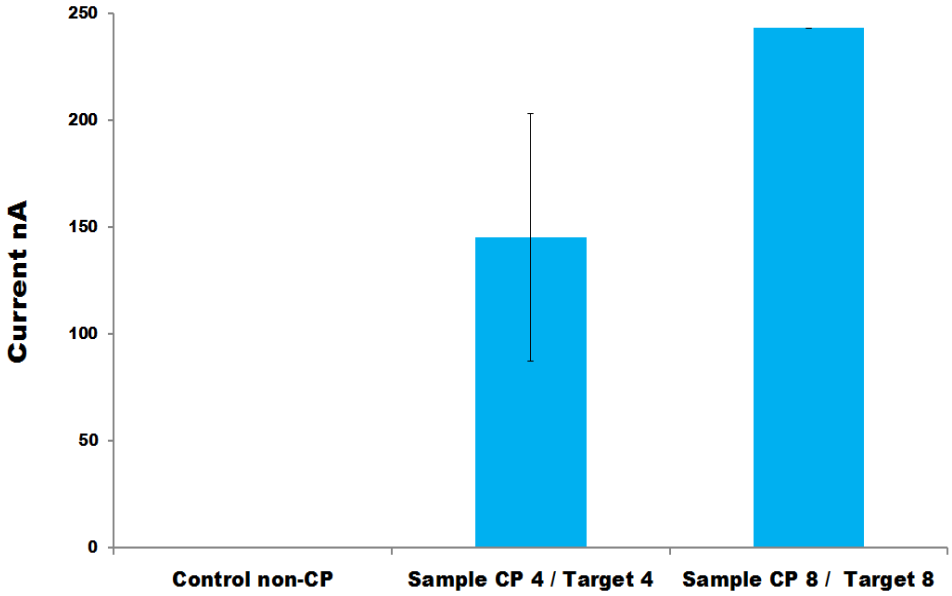

Figure 4.17: Diana 4 and Diana 8 electrochemical detection signals

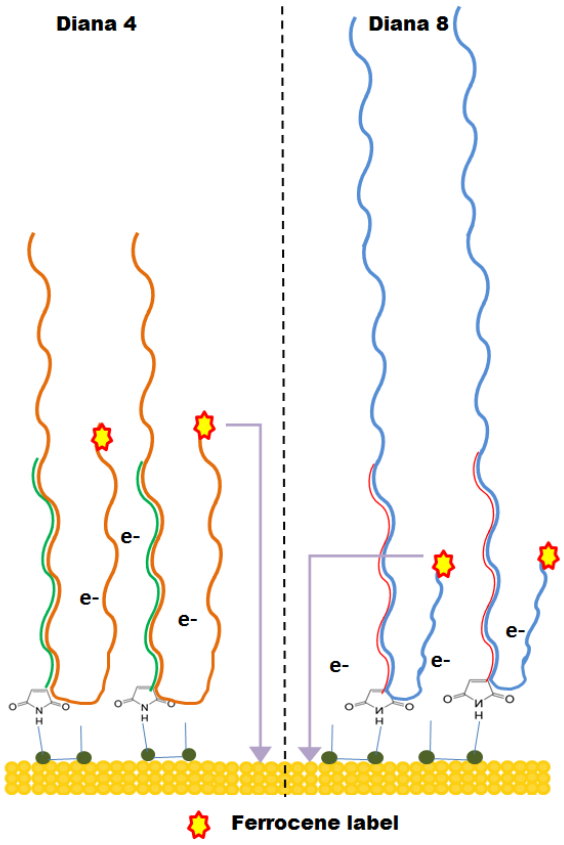

Figure 4.18: Structural differences during the hybridization event to Diana 4 and Diana 8, the purple arrows indicates the distance of ferrocene label to surface

The higher signal and reproducibility corresponding to the hybridization detection of target DNA 8 comparing with target DNA 4. Taking into consideration the two structures of the target 4 and 8 after hybridization (figure 4.18), the longer sequence of target 8 could make think in a more difficult hybridization, but there is another important factor in the hybridizationdetection that is the position of ferrocene. In the target 8 hybridization, the ferroceneis found in a shorter distance from the electrode andthe lower packing density of the DNA strand on gold surface in this case would facilitate the electron transport. Therefore, in this case, this configurational change allows that the current obtained in this system is higher.

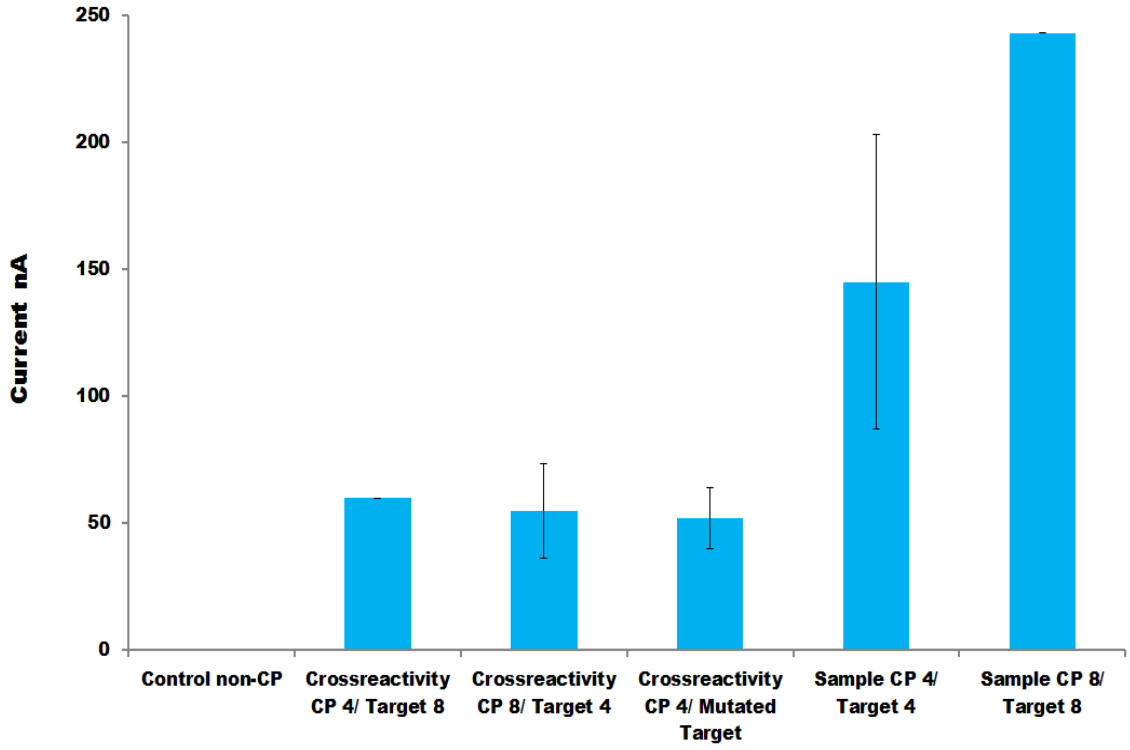

Figure 4.19: Summary of multiprobe functionalization test

Having a look in the crossreactivity response observed in the control (figure 4.19), the non-specificity of the target DNA Diana 4 over mutated CP and CP 8 and viceversa were giving the same current. These controls current were about 3 times lower than Diana 4, which show the lower response and about 4 times lower than Diana 8, which makes this crossreactivity clearly different from the positive signals.

4.8 Electrochemical signal amplification

Despite the excellent results of ferrocene as redox label on these targets, during the trial conducted with longer targets that have the complementary CP sequence farthest of the ends, its behavior was unpredictable. In some target, the signals obtained were too low and another was very irreproducible, the explanations of these responses could be several[232-239], however the figure 4.20 schematizes some hypotheses that were proposed. The main reason that may have influenced was probably a deficit in the electrons transport due to the conformational changes of the DNA strands during the hybridization. Some targets are too long and its hybridization is difficult, moreover a higher number of basesimplicate a higher steric hindrances as well as higher charge density on the surface sensor.

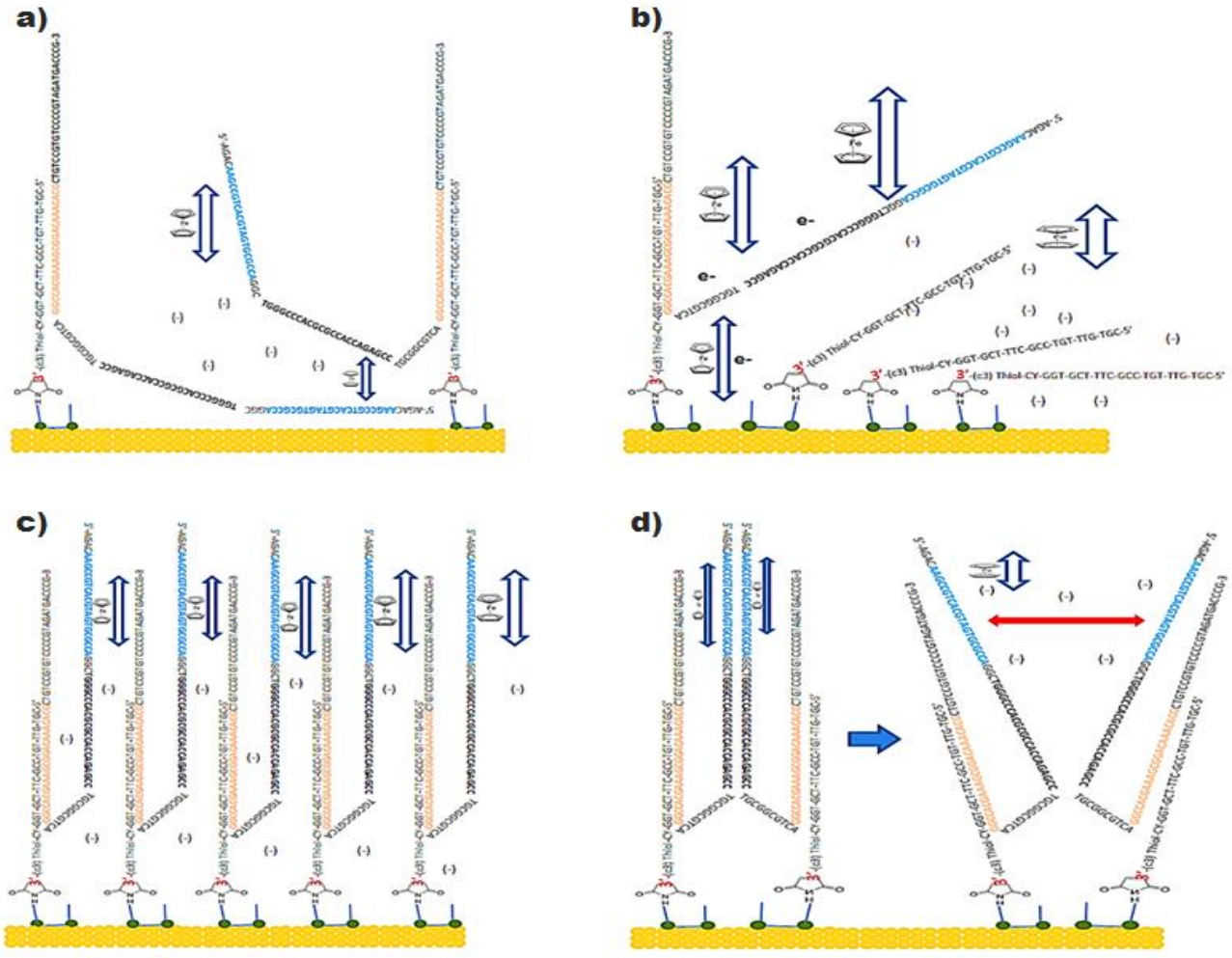

Figure 4.20:Possible hybridization kinds and its subsequent problems in longer target DNAs, a) lower hybridization events, b) free CP due to electronegative tilts of closer segments of target DNA, c) accumulation of negative charges on the sensor surface because a high density of DNA strands and d) steric hindrances due to spatial conformations

Because the large differences between the currents obtained with different DNA targets, a different label to targets was proposed. The idea was to obtain similar electrochemical responses in all targets tested. However, a direct label with other redox molecule will give the same problems that the ferrocene. It was necessary to look for an electrochemical diffusional mediated system to avoid the distance effects with the electrode and redox molecules that produce more amounts of electrons for each label to amplify the current and reduce the irreproducibility. In this way, the biotin-streptavidin-horseradish peroxidase (HRP) complex was proposed. Unlike that the ferrocene system, wherein the detection was directly due to the redox nature of the molecule itself, these complex requires three steps to be activated. During the PCR amplification instead of to use ferrocene-labeled primers, biotin-labeled primers were used to obtain fromPCR amplification biotin-labeled targets (figure 4.21). After of the hybridization in the sensor surface, the second step consists in the incubation of the streptavidin-HRP complex for15 minutes to bind on the biotin withthe target DNA. This enzymatic complex (biotin-streptavidin-HRP) has higher specificity. The last step was to introduce in the system a mix of tetramethylbenzidine (TMB) and hydrogen peroxide (H_2O_2) in 1:1 ratio. This solution is preincubated on the biosensor surface t for 10 minutes, to produce with the catalytic effect of peroxidase high amount of electronsbefore the electrochemical reading.

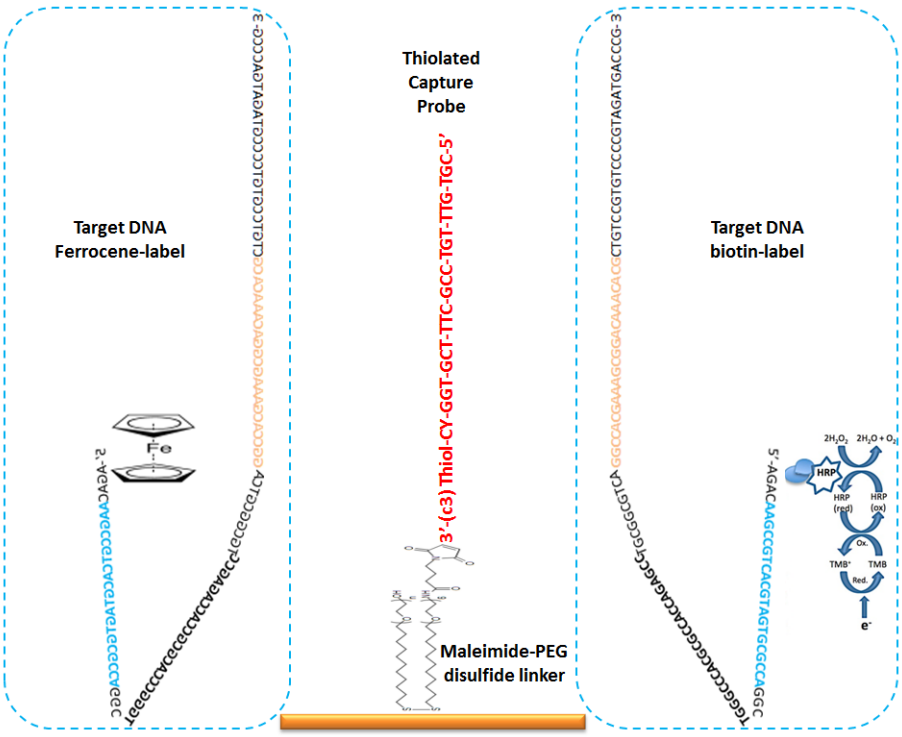

Figure 4.21: Target DNA labels (left) ferrocene (right) biotin, the label position into the target sequence is the same indistinctly of the system

This lapse is enough to initiate the redox reaction between the HRP and H_2O_2, releasing water and oxygen and reducing TMB on the electrode surface (figure 4.22). This reaction is time dependent due to ithas a limiting agent, the peroxide, but it has high concentration to avoid its consumption. This reaction was detected by chronoamperometry since it is much faster that CV and permits the correct measurements of all sensors with few time.

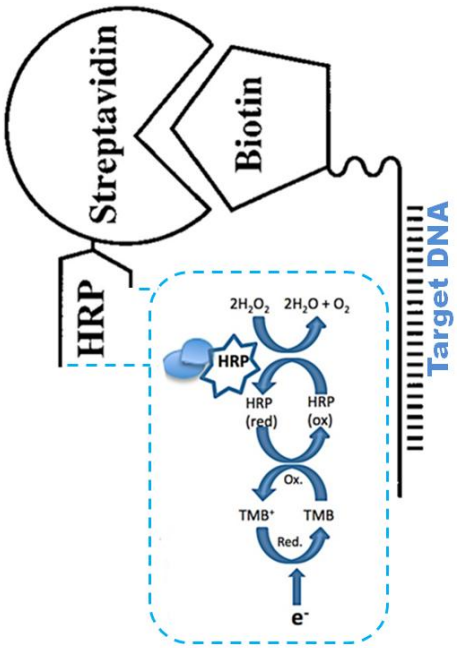

Figure 4.22: Biotin label and its complex redox scheme

4.9 Thermal stability of MalPEG-CP interface

As mentioned above, the presented electrochemical DNA array will be integrated in a LOC in a sandwich format with a mini-PCR. The work was conducted in parallel, with theother research groups mentioned before, and we tested each development, component or improvement directly in the array.

The mini-PCR arrangement involves a peltier mechanism that works as thermocycler for the different PCR amplification processes. In the final architecture

of the device this peltier is closer to the electrodes matrix. This means that abrupt temperature changes during PCR amplification can affect the stability of the immobilized monolayers of biomolecules on gold electrodes.

We begin to notice this effect when we incorporated the hybridization process with the thermocycler system. During the hybridization, the inner temperature of the chamber must be 59°C to facilitate the duplex formation. However, the PCR amplification steps require higher temperatures for de-hybridization (95ºC) and polymerization (72ºC). The heat transfer between materials may produce a heating on the electrochemical chamber, and depends on the applied temperature, it may affect the thiol-gold breaking bonds and so the bioreceptors desorption.

To test the thermal stability of MalPEG-CP SAM we performed a set of SPR experiments that included different temperatures post MalPEG immobilization.

The main goal was to determinate a possible desorption of molecules regarding temperature. In this way, we follow the optimized protocol and we immobilized a MalPEG interface for two hours, then, we link up this linker with the CP and we blocked with MCH for one hour.

Afterward, it was incorporated the target DNA labeled with biotin and incubated for 1 hour, with its subsequent incubation for one hour with streptavidin-HRP. Between each step, we performed a washing step. The electrochemical readouts were done with a mixture of TMB and H_2O_2 following the protocol explained in previous section.

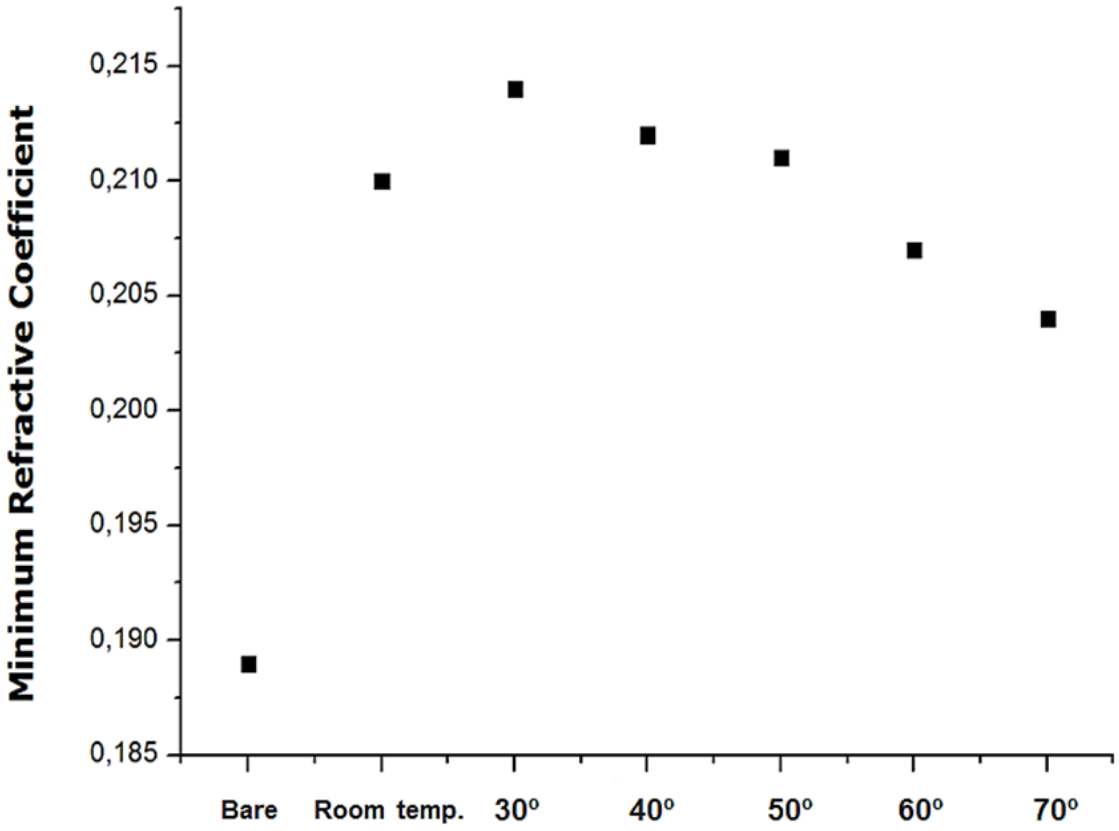

Figure 4.23: SPR minimum refractive coefficient of MalPEG after each indicated temperature

Figure 4.23 summarized the behavior of the MalPEG SAM under different temperatures. We can see the loss of reflectivity when the temperature was increased up to 50ºC. These results clearly show desorption of molecules on the gold surface. Some groups has studied the single thiol gold bound stability with temperature, considering that at temperatures higher than 60 occurs the breaking of this bound in spherical gold nanoparticles [240].

Several results of these experiments arose. The hybridization temperature was reduced from 59 ºC to 37 °C degrees lower than the temperature of the initial protocol to avoid desorption problems. Also, the structure of the cartridge sandwich was redesigned. Initially the layer where the array was patterned was directly touching the PCR cell and it was interchanged by the RE/CE layer in order to left more far the WEs layer from the Peltier.

4.10 Hybridization conditions optimization

4.10.1 Hybridization study

Thermal tests of the hybridization were done this time with controls to ensure that the reduction of the hybridization temperature is not affecting the selectivity of the biosensor. The systems tested were; SAM without CP as negative control, normal SAM with complementary CP Diana 4 as positive control, SAM with mutated CP as mutated control, and a SAM with a CP of other DNA target as crossreactivity control. Figure 4.24 show the results obtained at 37ºC and 59ºC. The duplex formation in the positive control was favored at 37ºC; the current obtained was 1.6 time higher, with better reproducibility. Also, the mutated control was benefited by the lower temperature. Regarding negative and crossreactivity controls, the NSA it does not change.

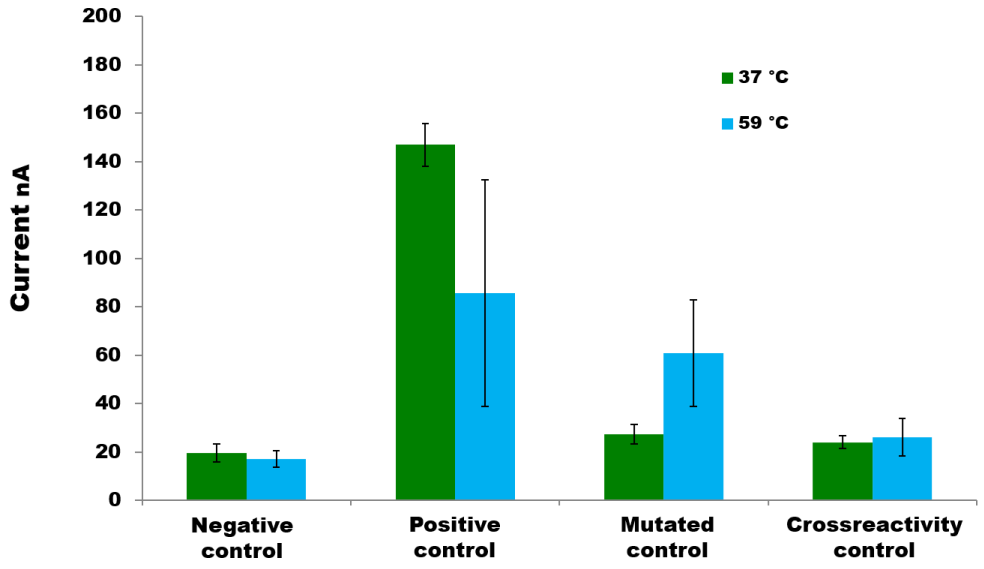

Figure 4.24: Hybridization temperature optimization

4.10.2 Interface composition test

In order to optimize the new platform based on HRP detection instead of ferrocene, the configurations of the biosensor interface was also studied, since the way of detection is very different from a direct electron transfer of ferrocene, to a diffusional mediation with HRP, and so the interface may affect a lot in the biosensors performance. Experiments with LAM molecule compared with disulfide MalPEG was tested again. The objective was to determine if disulfide MalPEG

molecule was still the best thiolated linker of the capture probe on gold surface, be recalled that the concentrations used during this trials were the same that the established in chapter two. The two molecules were tested with biotin-labeled PCR amplified target 4, the experimental sets with target 4CP are de positive control, with non-complementary CP are the controls 1, and without CP are the controls 2. In the results showed in figure 4.25, we find that the maleimide disulfide was still the best option as can be appreciated. These outcomes may be due to the structural differences of the two linkers. In the case of LAM o unique PEG branch is immobilized for each linker molecule, meanwhile disulfide MalPEG has two. Thus, MalPEG is covering better the biosensor surface with PEG molecule, which helps in the reduction of NSA. Moreover, the second PEG branch in the disulfide, kept a distance between CPs that may help in the reduction of steric hindrances during the hybridization of the biotin-labeled target DNA, improving both the efficiency of the duplex formation and the electron transfer process.

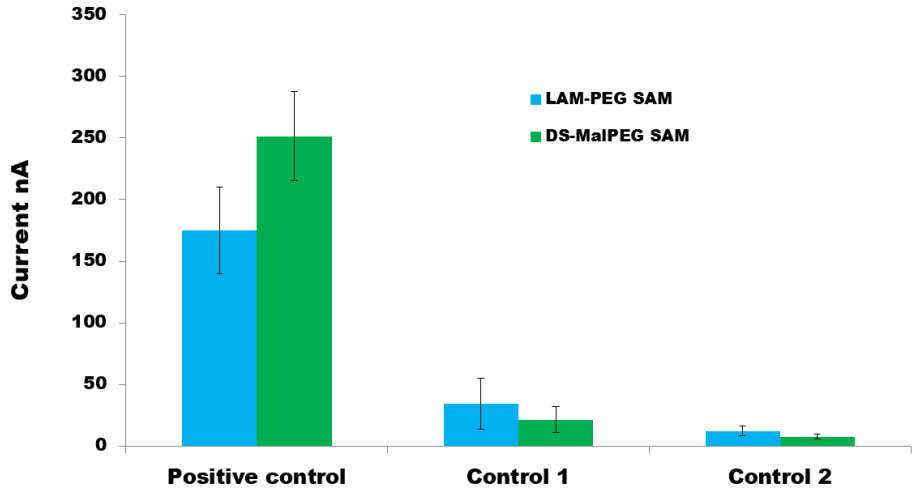

Figure 4.25: Thiolated linker comparison, LAM (lipoic acid maleimide), DS (disulfide MalPEG)

4.10.3 Ratio MalPEG/CP optimization

To follow with the biosensing interface optimization, test of different ratio of MalPEG:CP concentrations were performed. First the MalPEG concentration was tested under fixed CP concentration of 10 μM, the negative control was, as even, a system without CP. Figure 4.26 shows the ratios of MalPEG in μM tested and its corresponding electrochemical detection.

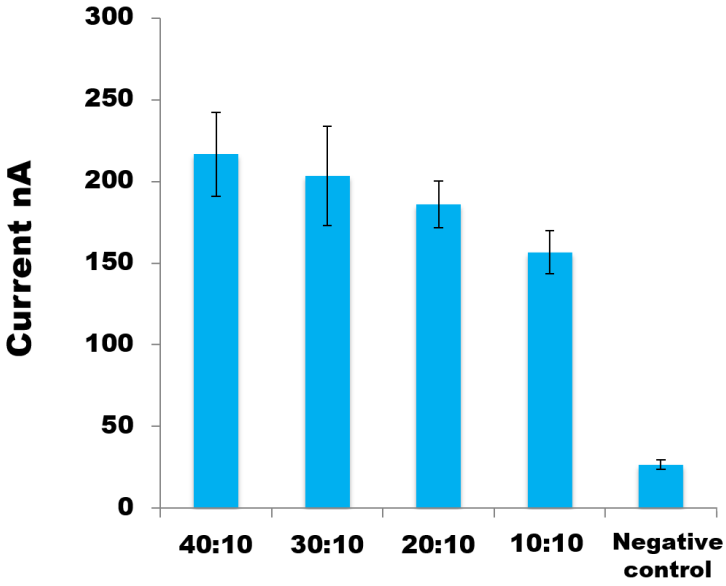

Figure 4.26: Different MalPEG concentration (μM) with CP fixed concentration at 10 μM

An increasing trend of the current is observed in the results, when the MalPEG concentration rises up. The values of 40 μM and 30 μM where the ones chosen for being tested with different concentration of CP. Figure 4.27 summarizes the experiments sets with fixed MalPEG concentrations at 40 and 30 μM and with different CP concentrations; 10, 20, 30, 40, 50, and 60 μM.

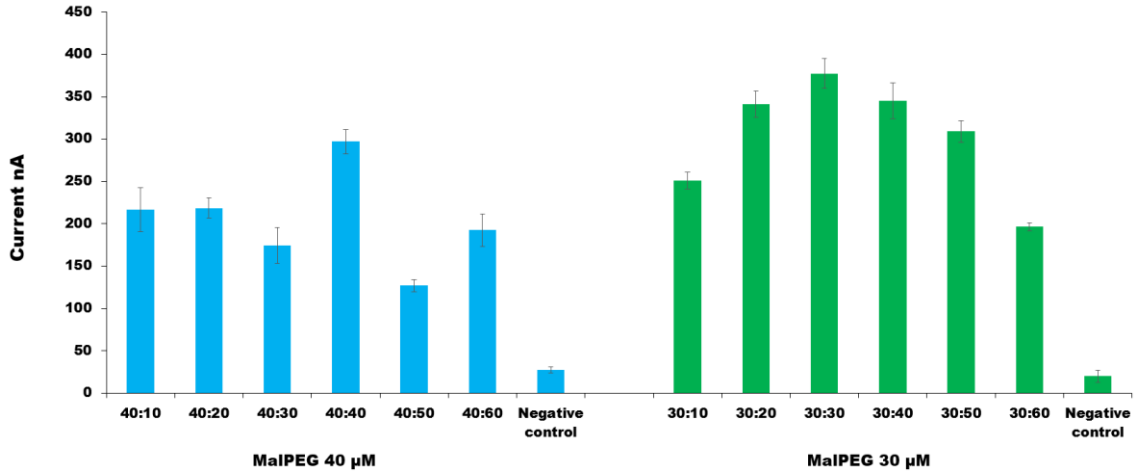

Figure 4.27: Different CP concentrations with MalPEG fixed concentration at 40 μM (blue) and at 30 μM (green)

As a clear differences from the previous results at different concentrations of MalPEG, where a clear decreasing trend was observed, in the case of different CPs concentrations a Gaussian tendency is observed in MalPEG fixed concentration at 30 μM. However, in both fixed concentrations the maximum value is characteristic of the ratio 1:1 of MalPEG:CP. Finally, the ratio 30:30 was chosen to optimize the biosensor in the next experiments due to its high signal between all systems tested.

4.10.4 Crossreactivity test

We continued testing all probes on the array in order to detect the behavior of each one and to establish possible crossreactivity with other CPs. Several experiments were performed and each time that a new improvements in the platform arrived, was tested with the new SAM on the array. In figures 4.28 and 4.29, we can see some electrochemical results obtained during the development of the project. Is notorious the low cross-reactivity between the distinct CP.

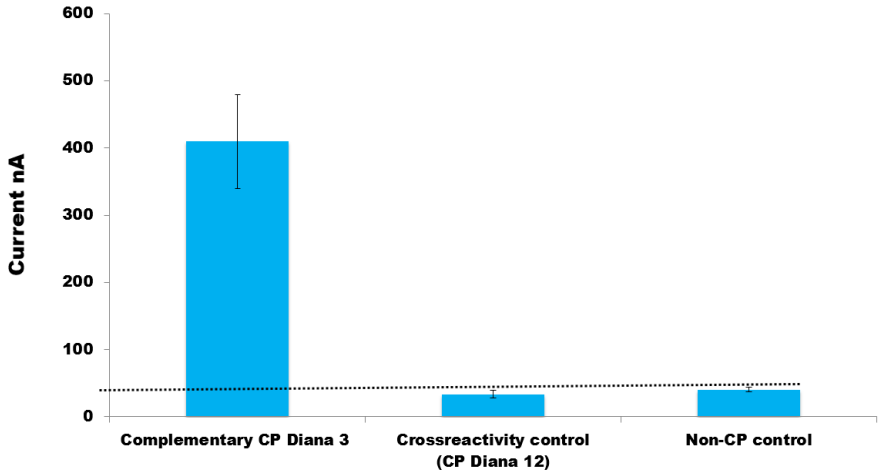

Figure 4.28: Target DNA hybridization detection of Diana 3

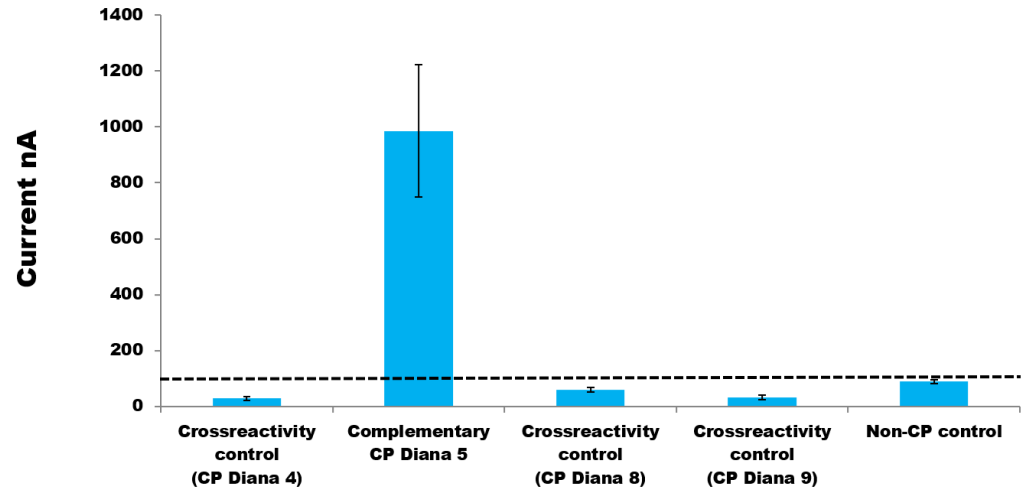

Figure 4.29: Target DNA hybridization detection of Diana 5

A summary of hybridization detection results of each CP tested and its crossreactivity with some of the CPs is shown in figures 4.30 and 4.31. An excellent behavior in general is observed. The difference in the intensity of the signal is due to several factors such as the length of the respective target DNA that affects on the hybridization efficiency and the electrochemical readout. Another possible factor is the PCR amplification efficiency, which is also dependent on the DNA target length where the longer DNA strands are more difficult to amplify.

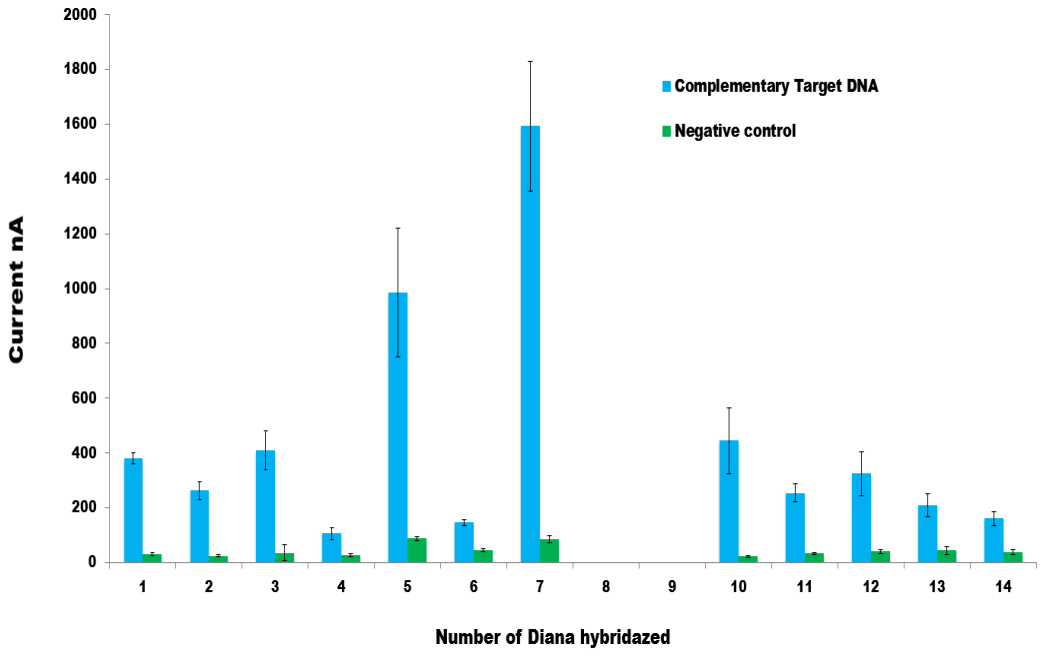

Figure 4.30: Summary of electrochemical results for all CPs

Regarding the cross-reactivity, we can see in figure 4.31, the low interference between each DNA target and the non-complementary CPs.

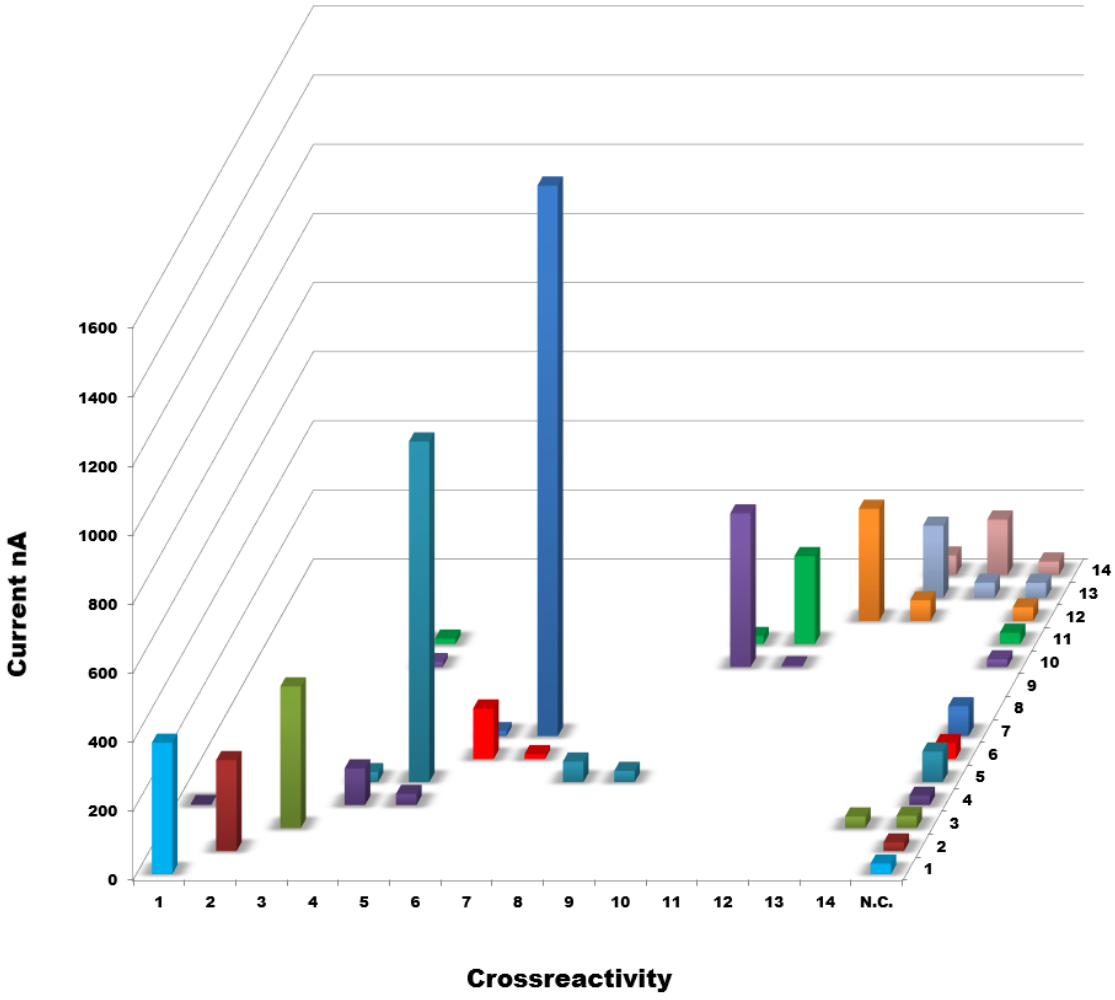

Figure 4.31: Crossreactivity of the different Diana tested

4.11 Summary

The electrochemical characterization of the gold array integrated into the cartridge,initially found several problems that were solved,like thickness of gold film, forthe manufacturing of the array.The gold WE surface manually and automatically functionalized with the nanoplotter with the optimized interface. ,

Crossreactivity with other CPs in the array and NSA and positive controls were tested, giving good electrochemical results. However, due to the lower signal presented in some targets, the electrochemical amplification method was changed from a ferrocene label to an enzymatic HRPlabel. In this way, the target DNA wasnot label with ferrocene, but with biotin to label it with streptavidin-HRP. The advantage of this change of label is the higher, fasterand more reproducibleresponse, but with a negative counterpart of having more steps and reagents into the system.Because of this change, the ratios between the components of the SAM were changed and optimized again to exclude future inconveniences and improve signal.

4.12References

228. Watanabe, J., T. Morita, and S. Kimura, *Effects of dipole moment, linkers, and chromophores at side chains on long-range electron transfer through helical peptides.* The journal of physical chemistry. B, 2005. **109**(30): p. 14416-14425.
229. Morita, T. and S. Kimura, *Long-range electron transfer over 4 nm governed by an inelastic hopping mechanism in self-assembled monolayers of helical peptides.* Journal of the American Chemical Society, 2003. **125**(29): p. 8732-8733.
230. Takeda, K., T. Morita, and S. Kimura, *Effects of monolayer structures on long-range electron transfer in helical peptide monolayer.* The journal of physical chemistry. B, 2008. **112**(40): p. 12840-12850.
231. Kai, M., et al., *Distance dependence of long-range electron transfer through helical peptides.* Journal of peptide science : an official publication of the European Peptide Society, 2008. **14**(2): p. 192-202.
232. Giese, B., *Long-distance charge transport in DNA: the hopping mechanism.* Accounts of chemical research, 2000. **33**(9): p. 631-636.
233. Hüsken, N., et al., *Impact of single basepair mismatches on electron-transfer processes at Fc-PNA·DNA modified gold surfaces.* Chemphyschem : a European journal of chemical physics and physical chemistry, 2012. **13**(1): p. 131-139.
234. Tao, N.J., *Electron transport in molecular junctions.* Nature nanotechnology, 2006. **1**(3): p. 173-181.

235. Anne, A. and C. Demaille, *Electron transport by molecular motion of redox-DNA strands: unexpectedly slow rotational dynamics of 20-mer ds-DNA chains end-grafted onto surfaces via C6 linkers.* Journal of the American Chemical Society, 2008. **130**(30): p. 9812-9823.
236. Bumm, L.A., J.J. Arnold, and T.D. Dunbar…, *Electron transfer through organic molecules.* The Journal of …, 1999.
237. Giese, B., *Long-distance electron transfer through DNA.* Annual review of biochemistry, 2002. **71**: p. 51-70.
238. Giese, B., *Electron transfer in DNA.* Current opinion in chemical biology, 2002. **6**(5): p. 612-618.
239. Sun, P. and M.V. Mirkin, *Kinetics of electron-transfer reactions at nanoelectrodes.* Analytical chemistry, 2006. **78**(18): p. 6526-6534.
240. Li, F., et al., *Thermal Stability of DNA Functionalized Gold Nanoparticles.* Bioconjugate chemistry, 2013. **24**(11): p. 1790-1797.

Chapter 5

5.1 Conclusions

The constant search for methods and alternatives for DNA detection and the need for many applications of portable and low cost devices has popularized the integrated systems of sample analysis. Today, we found in the market several kinds of LOCs for this purpose. Most of them use optical detection techniques, making expensive and impractical mass adoption of these technologies in clinical laboratories. For these reasons, the incorporation of electrochemical techniques for DNA detection has become not only an excellent tool but also the future of these portable devices.

This work presents the development of a new platform in multiprobe LOC electrochemical DNA detection. This prototype has been focused in its final commercial application for cancer detection in the framework of an industrial project joined with abiotech company. The nanostructured distribution of the biomolecules on the biosensor surface is one of the main features that affects in the successful of DNA biosensor performance. The self-assembly of this bioreceptors is the principal tool used for its attachment and distribution on the surface. Many self-assembling materials, such as thiols and dithiols, are of particular interest due to its ability to anchor on metal surfaces. The easy formation of stable heterogeneous structures is in many points of view, one of the biggest attractive of self-assembled monolayers. Their great number of applications, ranging from the stabilization of many nanostructures and nano-objects through the surfaces functionalization to their interaction with biological molecules like DNA, SAMs made the best bioinorganic platform in biosensors. Multiple studies have characterized gold-sulfhydryl links as distribution geometry between the molecules assembled.In addition, there are data about the molecular orientation, packing density, and molecular adsorption patterns of SAM among other things. However, these studies have been mainly based in thiol-gold interaction leaving aside other types of sulfhydryl groups, like the disulfides and lipoic acid derivate linkers used in this work.

Our goal in this project, in first place, was to establish the optimal conditions that maximize the hybridization efficiency and subsequent detection of specific target DNA, amplified by PCR. In this way, we compared the behavior of three different SAMs in single gold chips; a SH-DNA/MCH mixed monolayer (thiol-based SAM), a HO-EG6-C11-S-S-C11-EG6-NHCO-Maleimide-SH-DNA monolayer (MalPEG-based

SAM) and finally a lipoic acid derivate with maleimide-SH-DNA monolayer (LAM-PEG based SAM). The results show that the MalPEG SAM offers the best conditions for the detection, with better sensitivity and selectivity of the different DNA targets. Techniques such as XPS, SPR, and CV electrochemical technique were used for both; determining the SAM structure and measure the hybridization efficiency. The different characterization of phases during the dynamic chemisorption of gold-thiol bond helps us to improve the distribution geometry of functionalized thiol domains on gold. Moreover, the modification of the gold surface through annealing showed great advantages for the electrochemical detection of target DNA. However, due to the low cost nature of the end cartridge and the characteristics of the materials used, it was not possible to apply this technique in the cartridge array of 64 electrodes.

The electrochemical array for DNA detection was integrated in a LOC with a mini-PCR chamber for the amplification of the DNA sample in a portable and low cost device. For this purpose, it was fabricated a cartridge in a sandwich format that integrates both chambers. The original model of the cartridge configuration consisted of seven layers, containing within these layers two with electrodes; one with the counter and reference electrodes serigraphed and another with a64 working electrodes array, fabricated in gold by photolithography.

Some challenges were solved like; leaks, deformation by heat, and chemical or physical degradation of the material, among others. In addition, the technique used to join the layers of sandwich not gives the expected results. For these reasons, some layers were redesigned and/or made of other materials obtaining finally an efficient cartridge for the purpose of the project.

Regarding the functionalization of the integrated array both, the automatic immobilization by plotterand manualincubation, showed a correct behavior and it coulddetected the target DNA without mishap. Because of the multi array configurations, the crossreactivity and NSA was deeply tested and was done in parallel with the positive controls. The functionalization with multiple capture probes was successful, giving good electrochemical results. However, in order to improve the reproducibility and sensitivity ofthe electrochemical results, there was a change in the redox label in the biosensor. The hybridization signal was amplified by changing the label of the target DNA from the redox ferrocene molecule to a more efficient electrocatalyticenzyme complex.

The integration of the central automatized unit, the PCR thermocycler, the microfluidic cartridge, the confinement of the liquids into the cartridge chambers, andthe integration of the electrochemical biosensor arrayare still in process.

Chapter 6

Resumen en español

6.1 Introducción

El presente trabajo de tesis doctoral está enmarcado en el proyecto de investigación y desarrollo (I+D) conjunto entre la empresa privada de biotecnología de diagnóstico molecular Genómica S.A.U., el Instituto de Bioingeniería de Cataluña (IBEC), la Universidad de Barcelona y la empresa privada alemana ChipShop Microfluidics.

El objetivo principal del proyecto es la fabricación, puesta en marcha y comercialización de un dispositivo de diagnóstico temprano para detección de secuencias de ADN involucradas con el cáncer. El dispositivo multisistema, o *lab-on-a-chip* (LOC), está conformado por una unidad central de automatización (UCA), un sistema de Peltier como elemento de control térmico que hacen parte de un sistema en miniatura de amplificación de ADN o reacción en cadena de polimerasa (mini-PCR) y una plataforma de biosensado (*cartridge*) compuesta por una matriz o array electroquímico y un sistema fluídico tipo *loop* con múltiples compartimentos para confinación de líquidos. Cada grupo se encarga de una parte del desarrollo del proyecto y paralelamente se integran algunos sistemas para su optimización.

6.2 Monocapa autoensamblada

El objetivo de ésta tesis fue la creación, caracterización y optimización de la plataforma de reconocimiento bioquímico entre dos hebras de ADN sencillas de longitudes disímiles pero con algunas secuencias complementarias, para la posterior detección electroquímica de un evento de hibridación entre éstas, y su integración en el cartridge. Para la creación de ésta plataforma, se optó por utilizar una monocapa autoensamblada (SAM) de tioles como interfaz de bioreconocimiento de las 14 secuencias de ADN que hacen parte del proyecto. Durante la optimización de esta interfaz se utilizaron chips de oro individuales así como varias moléculas para la inmovilización de las sondas de captura, siendo elegidas tres: una molécula de disulfuro con dos brazos de poli etilenglicol (PEG) y un grupo malaimida en el extremo de uno de ellos. Este enlazador (o MalPEG *linker*) reacciona con la superficie de oro debido a la interacción dativa entre los átomos de azufre del disulfuro y los átomos de oro de la superficie de los chips. Al mismo

tiempo, el grupo malaimida reacciona con el grupo tiol de la sonda de captura, inmovilizándola. Los grupos PEG funcionan como *antifouling.* La siguiente molécula es la primera hebra de ADN, que trabaja como sonda de captura (CP) de la segunda hebra de ADN (ADN objetivo) y está inmovilizada sobre el chip de oro gracias al *linker*. La tercera molécula es el mercaptohexanol (MCH) que hace las veces de agente *antifouling*-reforzando la labor de los grupos PEG-y agente bloqueante de grupos malaimida que no reaccionaron con el CP. Las tres moléculas una vez inmovilizadas sobre la superficie de oro, conforman el biosensor electroquímico.

Para establecer los ratios entre las tres moléculas anteriores se realizaron una serie de pruebas con técnicas como: la resonancia de plasmones superficiales (SPR) y la voltametría cíclica (CV). Además, se caracterizó la formación de la SAM mediante análisis de componentes químicos por espectroscopia de fotoelectrones emitidos por rayos X (XPS) despuésde cada capa de molécula incubada. La detección electroquímica de la hibridación de ADN es posible debido al marcaje redox con la molécula de ferroceno que tiene la hebra de ADN objetivo en su secuencia y que es introducido por medio de una amplificación por PCR. Despuésde múltiples experimentos y controles de adsorción no específica (NSA) así como de reactividad cruzada, los ratios finales optimizados en los chips de oro de los componentes de la SAM fueron 20 µM de MalPEG: 10 µM de CP. El mercaptohexanol fue estandarizado a 10 µM.

6.3 Celda electroquímica

Durante la fabricación del cartucho electroquímico se presentaron algunos problemas durante la fusión de capas así como de respuesta al estrés de algunos materiales. Debido a esto, rediseño de patrones como también introducción de nuevos materiales fueron llevados a cabo. El uso de distintas técnicas de microfabricación también fue necesario durante el ensamblaje.

El cartridge está dividido en dos bloques principales, el bloque de biosensadoelectroquímico y el bloque de PCR. El bloque electroquímico está compuesto de 4 capas que juntas conforman una celda electroquímica de tres tipo de electrodos el de trabajo, el auxiliar y el de referencia. Así, la capa I está hecha de una ciclo-olefina (COP) y contiene un array electroquímico fotolitografiado de 64 sensores de oro que funcionan como electrodos de trabajo o *working electrodes*

(WE) y que contienen la superficie de oro que va ser funcionalizada con la SAM del apartado anterior. Además, cada uno de los sensores tiene una pista de oro que termina en un lado de la capa y que sirven como conexión entre el *cartridge* y el potenciostato. La capa II es una película fotolitografiada, de resina SU8, sobre la capa I que define el área de los sensores de oro que debe ser funcionalizada y que aísla la superficie de oro de las pistas. La capa III es una adhesivo doble cara que posee un agujero hexagonal que trabaja como cámara de hibridación. Esta capa une las capas I y II con la capa IV sellando la celda electroquímica. La capa IV de COP tiene impresos, por medio de *screen printing*, los electrodos de referencia (RE) y auxiliar (CE) en Ag/AgCl y carbono respectivamente. La conexión entre estos dos electrodos y sus respectivas pistas de oro, para que tengan un punto de conexión con el potenciostato, está hecha a través de un canal microfluídico vertical que se rellena de una resina conductora de plata durante el ensamblaje del bloque. Esta capa también posee dos orificios que hacen las veces de entrada y salida de líquidos de la celda electroquímica.

En lo que concierne al bloque de PCR, éste tuvo un cambio de diseño estructural con respecto a la idea original. Se pasó de un sistema de tres capas de COP (capa IV, capa V y capa VI) con una celda de PCR tipo hexagonal, a una pieza mecanizada del mismo material con un canal microfluídico tipo*loop* de solo dos capas, la que posee el canal y la que lo sella. La función de este bloque es el de contener las soluciones durante los procesos de amplificación de ADN por medio de la mini-PCR. Está en contacto directo con la Peltier y está comunicado con el bloque electroquímico por medio de canales fluídicos verticales. La unión de los bloques se realiza a través de una técnica que involucra una modificación en la superficie del COP y posteriores procesos de unión por presión y temperatura.

6.4 Integración de la biointerfaz de sensado en la celda electroquímico

La integración de la SAM optimizada en los chips de oro y el cartridge electroquímico, se realizó a través de dos formas; la primera de ellas fue un goteo por etapas, y por micropipeta, de las soluciones que contenían los componentes de la SAM sobre cada una de los 64 sensores de oro. La segunda forma fue hacer

exactamente lo mismo pero de forma automatizada con un nanoploter, para mayor control en volúmenes cobertura y tiempos de incubación. Los mayores problemas durante estos ensayos de integración radicaron en la baja señal electroquímica obtenida en algunos DNA objetivos. En ensayos tempranos se utilizó la molécula de ferroceno como marcaje pero, debido a estos resultados con algunos ADN objetivos, fue remplazado por la molécula biotina, cuya función es enlazar al sistema de sensado un complejo enzimático con mayor eficiencia en el transporte de electrones. Este complejo enzimático comprende la unión de la estreptavidina-HRP (horseradish peroxidase) a la biotina, es altamente específico y amplifica la señal de un evento de hibridación mucho más que la molécula de ferroceno. Para éste último sistema de marcaje y después de varios controles de NSA y de reactividad cruzada sobre el biosensor electroquímico, las concentraciones optimizadas finales de los componentes de la SAM son de 30 μM tanto de *linker* como de CP. Con respecto al MCH se estandarizó en 100 μM. Estas nuevas relaciones ofrecen excelentes resultados electroquímicos en los distintos ADN objetivos que han sido probados.

6.5 Conclusiones

La elección de una monocapa autoensamblada como plataforma de anclaje de las sondas de captura sobre la superficie del oro, por medio de un *linker* MalPEG, fue acertada. Es un método eficaz para la posterior hibridación y detección de un ADN objetivo convirtiendo a esta SAM en una excelente interfaz de biosensado.

La combinación de técnicas y materiales de fabricación para una configuración en sándwich de los bloques constitutivos del cartridge, resultó satisfactoria; disminuyendo al máximo las fugas de líquido, las deformaciones por calor y el desgaste por uso.

La integración de la interfaz de bioreconocimiento al array electroquímico, supuso cambios tanto en los ratios de los componentes de la SAM como del marcaje redox de las hebras de ADN objetivos. Los diferentes procesos de fabricación de los sensores de oro entre los chips sencillos y el array de 64 electrodos, así como los cambios de substrato entre ellos, fueron la causa más posible para una menor señal de detección de la hibridación. Sin embargo, los nuevos ratios de los componentes

constitutivos y la incorporación del sistema enzimático redox solvento sin mayores complicaciones este problema.